

One of Everything: The Breakthrough Listen *Exotica Catalog*

BRIAN C. LACKI,¹ BRYAN BRZYCKI,² STEVE CROFT,² DANIEL CZECH,² DAVID DEBOER,² JULIA DEMARINES,²
VISHAL GAJJAR,² HOWARD ISAACSON,^{2,3} MATT LEBOFKY,² DAVID H. E. MACMAHON,⁴ DANNY C. PRICE,^{2,5}
SOFIA Z. SHEIKH,² ANDREW P. V. SIEMION,^{2,6,7,8} JAMIE DREW,⁹ AND S. PETE WORDEN⁹

¹*Breakthrough Listen, Department of Astronomy, University of California Berkeley, Berkeley CA 94720*

²*Department of Astronomy, University of California Berkeley, Berkeley CA 94720*

³*University of Southern Queensland, Toowoomba, QLD 4350, Australia*

⁴*Radio Astronomy Laboratory, University of California, Berkeley, CA 94720, USA*

⁵*Centre for Astrophysics & Supercomputing, Swinburne University of Technology, Hawthorn, VIC 3122, Australia*

⁶*SETI Institute, Mountain View, California*

⁷*University of Manchester, Department of Physics and Astronomy*

⁸*University of Malta, Institute of Space Sciences and Astronomy*

⁹*The Breakthrough Initiatives, NASA Research Park, Bld. 18, Moffett Field, CA, 94035, USA*

ABSTRACT

We present Breakthrough Listen’s “Exotica” Catalog as the centerpiece of our efforts to expand the diversity of targets surveyed in the Search for Extraterrestrial Intelligence (SETI). As motivation, we introduce the concept of survey breadth, the diversity of objects observed during a program. Several reasons for pursuing a broad program are given, including increasing the chance of a positive result in SETI, commensal astrophysics, and characterizing systematics. The *Exotica Catalog* is an 865 entry collection of 737 distinct targets intended to include “one of everything” in astronomy. It contains four samples: the Prototype sample, with an archetype of every known major type of non-transient celestial object; the Superlative sample of objects with the most extreme properties; the Anomaly sample of enigmatic targets that are in some way unexplained; and the Control sample with sources not expected to produce positive results. As far as we are aware, this is the first object list in recent times with the purpose of spanning the breadth of astrophysics. We share it with the community in hopes that it can guide treasury surveys and as a general reference work. Accompanying the catalog is extensive discussion of classification of objects and a new classification system for anomalies. We discuss how we intend to proceed with observations in the catalog, contrast it with our extant Exotica efforts, and suggest similar tactics may be applied to other programs.

Keywords: Search for extraterrestrial intelligence — Classification systems — Celestial objects catalogs — Philosophy of astronomy — Astrobiology

1. INTRODUCTION

Breakthrough Listen is a ten year program to conduct the deepest surveys for extraterrestrial intelligence (ETI) in the radio and optical domains (Worden et al. 2017). The core of the program is a deep search for artificial radio emission from over a thousand nearby stars and galaxies (Isaacson et al. 2017, hereafter I17; see also Enriquez et al. 2017; Price et al. 2020 for results), and commensal studies of a million more stars in the Galaxy

(Worden et al. 2017). It joins other programs in the Search for Extraterrestrial Intelligence (SETI), most of which have also focused on nearby stars (Tarter 2001). But where should we look for ETIs? Indeed, how should we look for new phenomena of any kind?

Serendipity is a key ingredient in the discovery of most new types of phenomena and extraordinary new objects (Harwit 1981; Dick 2013; Wilkinson 2016). From

Ceres¹ to pulsars, from the cosmic microwave background (CMB) to gamma-ray bursts (GRBs), the majority of unknown phenomena have been found by observers that were not explicitly looking for them.² Historically, theory has rarely driven these findings.³ Instead, they frequently come about by new regions of parameter space being opened by new instruments and telescopes (Harwit 1981).

Other discoveries – like the moons of Mars or Cepheid variables in external galaxies – were delayed because no thorough observations were carried out on the targets (Hall 1878; Dick 2013). The pattern persists to this day. Because ultracompact dwarf galaxies have characteristics that fall in the cracks between other galaxies and globular clusters, they were only recognized recently despite being easily visible on images for decades (Sandoval et al. 2015). Of relevance to SETI, hot Jupiters were speculated about in the 1950s (Struve 1952), but they were not discovered until 1995 in part because no one systematically looked for them (for further context, see Mayor & Queloz 2012; Walker 2012; Cenadelli & Bernagozzi 2015). This may have delayed by years the understanding that exoplanets are not extremely rare, one of the factors in the widely-used Drake Equation in SETI relating the number of ETIs to evolutionary probabilities and their lifespan (Drake 1962).

Despite searches spanning several decades, no compelling evidence for ETIs has been found by the SETI community to date (e.g., Horowitz & Sagan 1993; Grifith et al. 2015; Pinchuk et al. 2019; Lipman et al. 2019; Price et al. 2020; Sheikh et al. 2020). The continuing lack of a discovery among SETI efforts looking for various technosignatures is sometimes called the Great Si-

lence (Brin 1983). If at least some ETIs are willing and capable of expanding across interstellar space, a bolder interpretation of the null results is popularly referred to as the Fermi Paradox, the unexpected lack of any obvious technosignatures in the Solar System (Cirkovic 2009).⁴ Although the simplest resolution may be that we are alone in the local Universe (Hart 1975; Wesson 1990), and others question whether we should expect to have detected technosignatures yet (Tarter 2001; Wright et al. 2018), many have suggested that ETIs are actually abundant but we are simply looking in the wrong places for them (e.g., Corbet 1997; Ćirković & Bradbury 2006; Davies 2010; Di Stefano & Ray 2016; Benford 2019; Gertz 2019). It is very difficult to detect a society of similar power and technology as our own through the traditional methods of narrowband radio searches unless it makes intentional broadcasts (Forgan & Nichol 2011). But like hot Jupiters, might there be easy discoveries in SETI that we keep missing because we keep looking in the wrong ways or at the wrong places?

Considerations like these in astrophysics have inspired efforts to accelerate serendipity, by expanding the region of parameter space explored by instruments (c.f., Harwit 1984; Djorgovski et al. 2001; Cordes 2006; Djorgovski et al. 2013). This approach has been highlighted in SETI to gauge the progress of the search (Wright et al. 2018; Davenport 2019; see also Sheikh 2019).⁵ Breakthrough Listen harnesses expanding capabilities in several dimensions. In radio, Breakthrough Listen has developed a unique backend, already implemented on the Green Bank Telescope (MacMahon et al. 2018) and the CSIRO Parkes telescope (Price et al. 2018), and more are being installed on MeerKAT (an array described in Jonas 2009). These allow for an unprecedented frequency coverage at high spectral and temporal resolution. In optical, Breakthrough Listen continues to use the Automated Planet Finder (APF; Vogt et al. 2014) for high spectral resolution observations of stars in hopes of spotting laser emission (e.g., Lipman et al. 2019), and we have partnered with the VERITAS gamma-ray tele-

¹ A planet between Mars and Jupiter was “predicted” by the Titius-Bode Law. Interestingly, in September 1800, a group of astronomers colloquially known as the “Cosmic Police” chose twenty-four astronomers to search for this planet. Giuseppe Piazzi was among the twenty-four selected, but did not know this when he discovered Ceres serendipitously during the construction of a star catalog in January 1801 (Cunningham et al. 2011).

² For discussion of the discovery of Ceres, Cunningham et al. 2011; the discovery of pulsars, reported in Hewish et al. 1968, is recounted in Bell Burnell 1977; the CMB is reported as unexpected noise in Penzias & Wilson 1965; Klebesadel et al. 1973 presents the discovery of GRBs by the *Vela* satellites, designed to watch for nuclear weapon tests in violation of treaty.

³ Among the rare exceptions are the discovery of radio emission from interstellar HI (Ewen & Purcell 1951) and molecules (Weinreb et al. 1963), small Kuiper belt objects (Jewitt & Luu 1993), and binary black hole mergers (Abbott et al. 2016). The CMB was almost found by a dedicated experiment (Dicke et al. 1965), but Penzias & Wilson (1965) discovered it instead before the results came in. The discovery of Neptune – not a new type of object but certainly significant – was driven by theoretical calculations of its perturbations on Uranus (Galle 1846; Airy 1846).

⁴ The accuracy of the name “Fermi Paradox” is disputed by Gray (2015); Cirkovic (2018) on the other hand applies the term to all of the Great Silence.

⁵ We should be careful not to equate parameter space volume to survey value or the probability of discovery, however. The volume depends on parameterization (for example, vastly different volumes are found when substituting wavelength for frequency). The more general notion of *measure* on parameter space is more appropriate; these include Bayesian probability distributions (c.f., Lacki 2016a). A suitable measure avoids the apparent problem that current SETI efforts are worth $\sim 10^{-20}$ the value of an ETI discovery noted by Wright et al. 2018; current and past SETI efforts do have significant value.

scope (Very Energetic Radiation Imaging Telescope Array System; Weekes et al. 2002) for its sensitivity to extremely short optical pulses (Abeysekara et al. 2016). But we can also consider exploring observational parameter space too, by expanding our strategies for where and when to look.

This paper presents our motivations and initial selection and strategies for exotic targets. The centerpiece is a broad catalog of targets, most unlike those previously covered by SETI, that we intend to observe over the coming years. Although I17 already included a broad range of stellar and galaxy types, the *Exotica Catalog*'s aim is to include “one of everything” to ensure that we are not missing some obvious technosignatures. Also among the targets are extreme examples of cosmic phenomena, to cover the full range of environments, and mysterious anomalies that might yield interesting results if examined closely. In addition, we describe our other efforts to expand SETI in unconventional directions and to enhance our primary scientific results with campaigns observing selected classes of interesting targets. In these efforts, we seek evidence for both ETIs and new astrophysical phenomena.

We present this catalog in hopes that it aids in other searches for unexpected phenomena. A program of observing as wide a range of targets as possible does not need to be restricted to SETI, or to radio and optical wavelengths. Any new facility across the spectrum might benefit by doing a treasury survey using a catalog based off or inspired by this one.

The paper has the following structure. We discuss basic concepts motivating exotica observations and the Catalog in Section 2. A brief overview of the division of the Catalog into four samples is presented in Section 3. The next four sections each describe the construction and principles behind each of these samples: the Prototype sample in Section 4, the Superlative sample in Section 5, the Anomaly sample in Section 6, and the Control sample in Section 7. We discuss the properties of the *Exotica Catalog* and its planned supplementary materials in Section 8. Section 9 discusses the need for wide-field surveys to fully span the breadth of astrophysics. We discuss possible strategies for the Catalog and other exotica efforts in Section 10. Section 11 is a summary of the paper. A series of appendices presents the entries in each sample: Prototypes in Appendix A, with discussion of classification; Superlatives in Appendix B; Anomalies in Appendix C; and Controls in Appendix D. Appendix E presents the full unified Catalog, with notes on data sources used.

2. CONCEPTS

2.1. Breadth, depth, and count

Each astronomical survey on a given instrument makes trade-offs. To illustrate the differences of our programs, we distinguish between three measures of the extent of a targeted survey of individual axes. The program must balance the variety of observed object types, the number of each observed type of object, and how long to spend observing each individual object. We call these three dimensions breadth, count, and depth, respectively. These three quantities can be loosely thought of as three different dimensions of parameter space, and a survey searches a bounded volume within that space, as depicted in Figure 1. A program can emphasize extent along one dimension over another, but because of limited observational resources, it cannot cover the entire realm of possibilities.

The reader should be cautioned, however, that Figure 1 is not literal. Each “dimension” can itself be multi-valent (for example, increasing depth by increasing integration time versus cadence versus frequency coverage) and thus could actually be represented as a subspace with many dimensions (as in Harwit 1984; Djorgovski et al. 2013; Wright et al. 2018). Our emphasis here is evaluating target selection of a survey rather than its effectiveness for a given target (see also Sheikh 2019). Note also that breadth and count apply more to targeted surveys rather than wide-field surveys, which may be better parameterized with sky area (c.f., Djorgovski et al. 2013).

Breadth, count, and depth each emphasize different levels of confidence in our ideas about for where we can make desired discoveries. If we are very confident that a phenomenon, such as ETIs, are very common around a particular kind of object, like G dwarfs, we should push for high depth. Depth is essential when we are sure the signals will be faint, since shallow observations cannot then be successful. If instead we believe that a phenomenon is very rare, but are still sure of the environments that generate it, then we should aim to examine a large number of objects, in hopes that some of its signatures will turn out to be bright. Finally, if we have no idea where we are likely to find a phenomenon, it makes sense to have a broad survey. After all, we do not want to keep missing something otherwise obvious because we never happen to look. Shifting our emphasis from depth to count to breadth allows for increasing levels of serendipity.

The guiding assumption of many previous SETI efforts has been that ETIs are likely to live around sunlike stars and are not vastly more powerful than our own. This kind of technological society is the only one known to exist (e.g., Sagan et al. 1993), and a conservative approach

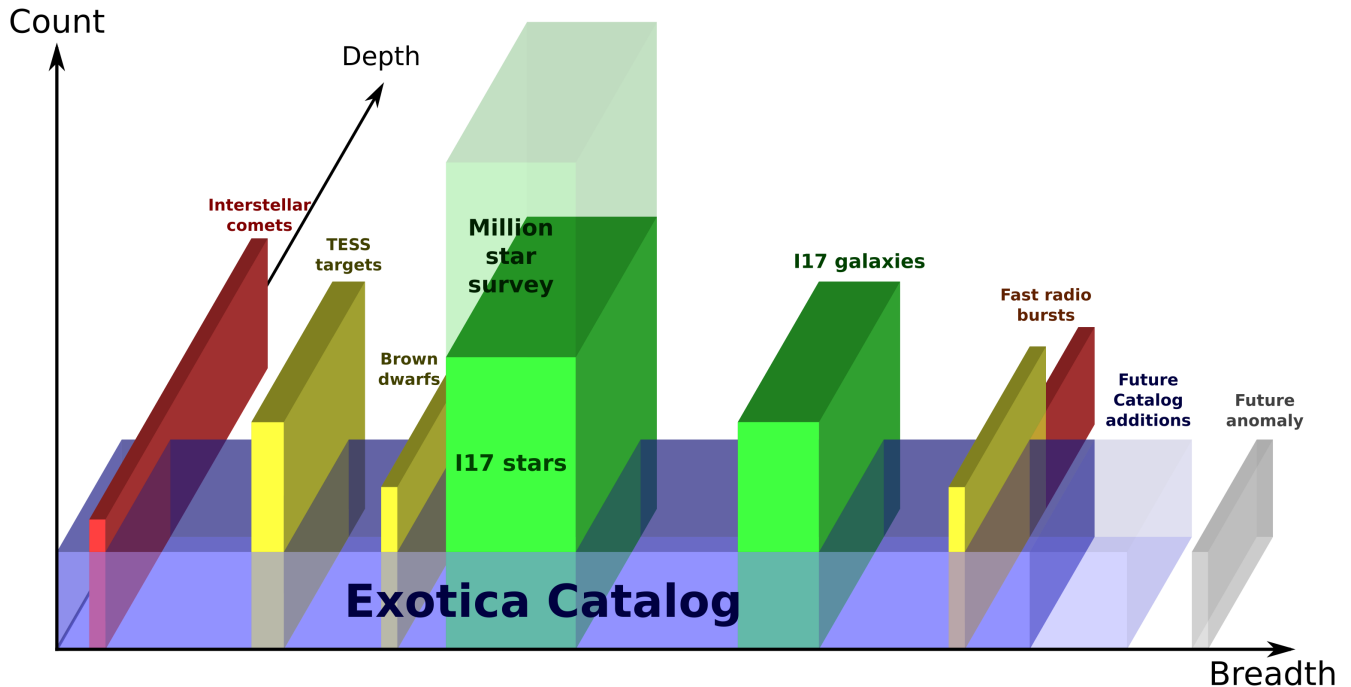


Figure 1. A cartoon of the three directions of target selection and the relative advantages of Breakthrough Listen’s primary programs observing stars and galaxies (green), a survey of the Breakthrough Listen *Exotica Catalog* (blue), and some example campaigns. Previous SETI surveys have generally aimed for depth, achieving strong limits for a small number of similar targets, or high-count, achieving modest limits for a large number of similar targets. Other exotica efforts can be high-depth (red) or high-count (gold) campaigns, but observations of the *Exotica Catalog* will be broad, achieving modest limits on a small number each of a wide variety of targets. Future discoveries may be added to a later version of the catalog (pale blue), or prompt new campaigns that we cannot yet plan for (grey).

minimizes the amount of speculation piled upon the hypotheses that ETIs are common and that they broadcast brightly enough to be detected. Some surveys have gone for the deep approach by examining a few nearby stars with high sensitivity (as in Rampadarath et al. 2012). Drake’s equation implies that it’s unlikely for a given star to be inhabited now, unless the ETIs persist for billions of years or has interstellar travel. For this reason, a common SETI approach is to examine a large number of sunlike stars, as with the HabCat of Project Phoenix (Turnbull & Tarter 2003).

Few SETI surveys have sought to examine a broad range of possible habitats. An important exception to this are the all-sky surveys, as done with Big Ear (Dixon 1985) or META (Horowitz & Sagan 1993). In a way, all-sky surveys allow for the ultimate breadth and count because they observe everything in the sky. Even if a new phenomenon is completely unknown, an all-sky survey has a chance to pick it up. In order to accomplish this, however, they tend to have a very small depth. The limited number of SETI surveys of external galaxies may be considered broad to the extent the target galaxies presumably include all kinds of stellar and planetary phenomena, although the diversity of galaxies itself is

usually limited (Shostak et al. 1996; Gray & Mooley 2017). As far as targeted surveys go, Harp et al. (2018) is one of the few recent efforts that emphasize breadth; their targets included quasars, masers, pulsars, supernova remnants, and an Earth-Sun Lagrange point.

Surveys are constrained by the cost and ease of access to facilities. Breakthrough Listen has unprecedented access to powerful instruments for SETI purposes, allowing our program to stretch out in all three directions. Our main efforts so far have concentrated on the nearby stars and galaxies listed in I17. This is a relatively broad catalog in SETI terms, including stars of spectral type from B to M and class from dwarfs to giants, as well as galaxies with a wide range of luminosities and morphologies. Our reach will be expanded immensely by our upcoming million star survey with MeerKAT, a commensal effort that will achieve the largest count of a targeted SETI search. Nonetheless, its breadth is limited because the types sampled are not too rare, unconventional, or extreme: there are no X-ray binaries or blazars in the I17 sample, for example.

To supplement the large but finite extent of I17 (green boxes in Figure 1), we have engaged in several additional programs that can extend along any of the three

dimensions. In some cases (yellow boxes), we have effectively appended an object class to I17 by observing a number of examples, as with brown dwarfs (Price et al. 2020). In others, we have focused intently on a single extraordinary object to a high depth (red boxes), as in our studies of the repeating FRB 121102 (Gajjar et al. 2018). To these efforts, we now add the *Exotica Catalog* (blue box), an effort to cover the full range of known astrophysical phenomena. The broadness of this catalog is unprecedented in targeted SETI, with only all-sky surveys being even less biased. Given how little we know about ETI prevalence, forms, technology, and motivations, we believe that efforts along all three dimensions are necessary.

2.2. Core motivations for an exotica SETI program

We have several motivations in mind for observing exotic targets, and these have informed the kind of catalogs we have created:

- *Motivation I*: constraining the possibility of different kinds of intelligence living in non-Earthly habitats. Speculations about exotic habitats in the literature include: life living on habitable icy worlds around red giants (Lorenz et al. 1997; Lopez et al. 2005; Ramirez & Kaltenegger 2016), inside large carbonaceous asteroids (Abramov & Mojszsis 2011), in Kuiper Belts (Dyson 2003), inside rogue planets (Stevenson 1999; Abbot & Switzer 2011), or in the atmospheres of gas giants and brown dwarfs (Sagan & Salpeter 1976; Sagan 1994; Yates et al. 2017). Exotic life may be based on alternate biochemistries (Baross et al. 2007).

Intelligence does not need to be native to unusual habitats, as some locations may draw ETIs from their homeworlds for reasons of energy collection, curiosity, or isolation. Some phenomena might be modulated or harnessed to act as beacons (e.g., Cordes 1993; Learned et al. 2008; Chennaman-galam et al. 2015). The postbiological universe paradigm also suggests that a spacefaring intelligence could be very different from its biological origins, with very different needs (Scheffer 1994; Dick 2003). The practicality of some kinds of megastructures may depend on their environment or the phenomenon they are harnessing (Semiz & Oğur 2015; Osmanov 2016). Thus, there could be inhabited environments that seem inhospitable to us, like the central engine of an AGN or the outskirts of a galaxy (some examples include Dyson 1963; Ćirković & Bradbury 2006; Vidal 2011; Inoue & Yokoo 2011; Lingam & Loeb 2020). This goal mo-

tivates us to examine a wide variety of phenomena, both typical and extreme examples.

- *Motivation II*: constraining the possibility that some astrophysical phenomena or objects are themselves artificial, a possibility suggested at least as early as the 1960s by Kardashev (1964). Blue straggler stars and fast radio bursts are examples of classes posited as engineered in the literature (Beech 1990; Lingam & Loeb 2017). Not just entire source classes, but individual mysterious objects or small subclasses might be artificial as well. Examples of these anomalies include Boyajian’s Star and Przybylsky’s Star (Wright et al. 2016) and Hoag’s Object (Voros 2014). Although non-artificial explanations are far likelier and frequently plentiful, there is a small chance that we are throwing away evidence of ETIs that is staring us in the face because it does not fit our preconceptions (e.g., Ćirković 2018). This goal motivates us to examine rare, unusual subtypes of astronomical phenomena, as well as anomalous sources that defy explanation.
- *Motivation III*: constraining the possibility that some natural phenomena mimic ETIs. Pulsars were briefly if unseriously considered possible contenders for alien signals because of their regular radio signals (for a historical perspective on the SETI context, see Penny 2013). The Astropulse survey seeks nanosecond long radio pulses from ETIs (Siemion et al. 2010), but brief pulses are known to be generated by the Crab Pulsar (Hankins et al. 2003), and it’s possible that evaporating primordial black holes and relativistic fireballs produce similar signals (Rees 1977; Thompson 2017). Thus, we want to deliberately seek out objects that are likely to generate unusual signals naturally. This goal motivates us to examine extreme objects with nonthermal emission mechanisms.
- *Motivation IV*: using the unique Breakthrough Listen instrumentation for general astrophysical interest. Previous efforts along these lines include our observations of fast radio bursts (Gajjar et al. 2018; Price et al. 2019a). This goal motivates us to examine a wide range of sources, not just stars and galaxies that are hospitable to life.
- *Motivation V*: constraining the possibility that some unexpected systematics generate false positives for ETIs. These might include instrumental problems, problems with analysis, or especially

radio frequency interference (RFI). A claimed detection of an ETI, or even an unusual natural phenomenon, will lead to considerable skepticism. By conducting observations where we expect nothing at all, we learn about the behavior of the instrument system. This goal motivates us to examine empty spots on the sky, or unphysical “sources” like the zenith.

2.3. Campaigns and catalogs

Previously we have focused on targets classes that are typical of SETI, for which the nearest members were well-known. In contrast, exotica include the more dynamic side of astrophysics. The list of known astrophysical phenomena, and proposed links between them and ETIs, is always growing. Some of the phenomena that fall under the auspice of exotica include violent and energetic objects that emit bright transients, like pulsars and active galactic nuclei. Others are very faint or small, so faint that new nearby examples are constantly being discovered, like the coolest brown dwarfs and ultrafaint galaxies. Either way, a program that observes exotica for SETI reasons needs to be more flexible than one that observes nearby stars and galaxies.

Breakthrough Listen has two basic approaches to observe exotic objects. The first is a series of short *campaigns*, each dedicated to a particular object or object class. If someone proposes a phenomenon is actually artificial or claims detection of ETIs, we follow up on it by observing it. By focusing on just a few objects each, these campaigns allow us to peer deeply to lower flux levels, constraining transmitters with lower equivalent isotropic radiated power (EIRP).⁶ Unlike the catalogs of stars and galaxies, these programs are developed as new opportunities and discoveries arise, a more dynamic approach than having a fixed catalog. Some examples are discussed in Section 10.2.

The second is a *catalog* of “exotic” objects, including those that are extreme or interesting from an astrophysical perspective, and those that are just unusual to typical SETI searches. The catalog is a wide mix of objects, but with few members of each type: it is more broad than deep. On the other hand, the *Exotica Catalog* is intended to be a more permanent fixture of Breakthrough Listen. Nonetheless, we anticipate revisions and additions as further new phenomena are discovered and classified.

⁶ EIRP is the luminosity of an isotropically radiating object at the same distance and with the same flux as a source.

3. THE *EXOTICA CATALOG*: SURVEYING THE BREADTH OF ASTROPHYSICAL PHENOMENA

To address the core motivations (Section 2.2), the *Exotica Catalog* has four parts:

- A Prototype sample including one of each type of astrophysical phenomenon (Motivations I and IV). We emphasize the inclusion of many types of energetic and extreme objects like neutron stars (Motivations II and III), but many quiescent examples are included too.
- A Superlative sample that includes objects of known subtypes but that are on the tail ends of the distribution of some properties, to better span the range of objects in the Universe (Motivations I, II, and IV).
- An Anomaly sample that includes inexplicable sources noted in the literature (Motivations II, III, and IV). A subsample includes previously published ETI candidates (Motivations I, II, and III).
- A Control sample that includes “sources” that are unphysical, like the zenith, or objects that have been revealed to be mundane or nonexistent. These targets will help us get a better handle on systematics (Motivation V).

In addition, we plan on doing occasional pointings at random positions on the sky. That will ensure we do not miss any completely unknown phenomenon because we are looking at known objects, allowing a non-biased sample of the sky (Motivation I). Postbiological ETIs living in interstellar space are a possible example of a hostless phenomenon.

4. THE PROTOTYPE SAMPLE: A TREASURY SURVEY

The Prototype Sample is the largest portion of the full *Exotica Catalog*. The objects and source classes are listed in Table A1 in Appendix A.

4.1. Classification of objects

The Prototypes form the bulk of the *Exotica Catalog*, and represent our effort to have “one of everything”. The range of things we would like includes both long-lived objects and localized phenomena. To build this catalog, we need some classification system to enumerate the different kinds of things. We start with a high-level classification system with 13 main categories listed in Table 1. These categories have extremely different evolutionary mechanisms and power sources, and they

might each have a chapter in an undergraduate textbook or have an entire advanced textbook to themselves. Nonetheless, they are narrower than the three “kingdoms” proposed by Dick (2013). In analogy with the “kingdoms”, we call these categories *phyla*, emphasizing both the shared fundamental traits and the vast diversity within them, and allowing for higher level “root” categories.⁷

ETIs would probably need distinct engineering methods to harness members of different phyla. They span the Kardashev (1964) (K64) scale, which groups technological ETIs broadly by the amount of power they consume. On the K64 scale, Type I ETIs harness the amount of power available on a planet, Type II ETIs harness the power available from a sun, and Type III ETIs harness the power available from a galaxy, with proposed extensions to allow for levels beyond the range I–III and fractional levels. The power usage increases by a factor of order ten billion between each K64 level. Table 1 gives a very rough estimation of the K64 rating available in each phylum.

There are edge cases like brown dwarfs that might fit in several categories, which we have placed according to convention or our judgement. To the natural categories we have added *technology*. Human artifacts in space are part of the optical and radio sky, and are thus part of the astrophysical landscape now. Our primary aim in SETI is to find other examples of this category. We have also added a category for reference points not corresponding to any physical points. Transients are also discussed separately (Section 4.3).

The phyla, while covering the breadth of astrophysics, are too coarse to form an exhaustive Prototype list by themselves. Obviously, hugely different possibilities for habitability and exploitation exist for an asymptotic giant branch (AGB) star and a red dwarf, for example, or a white dwarf and a black hole. Thus, we have broken down these categories into much more fine-grained types for the Prototype catalog. Some formal classification schemes already exist in the literature, most notably Harwit (1984) and Dick (2013). There are also three classification systems designed as metadata for organizing the literature that nonetheless have played a huge role in astronomical research: the old AAS jour-

nal keyword list⁸, Simbad’s object classification system (described in Wenger et al. 2000), and most recently the Unified Astronomy Thesaurus (Frey & Accomazzi 2018).⁹

We found none exactly fit our needs, usually being too coarse-grained in most respects (e.g., not emphasizing the great differences between interacting and detached binary stars), or too detailed for a subset of phenomena (e.g., the many narrow types of dwarf novae). Nevertheless, these systems did serve to ensure coverage of the gamut of astronomical objects. To supplement these classification systems, we consulted review articles and textbooks, which frequently describe classification systems used for particular types of astrophysical phenomena, and how they are distinguished. Discovery papers announcing new classes of phenomena also are useful for assembling a list of classes.

Astrophysical phenomena can be classified according to a wide range of characteristics. An object’s composition, evolution, environment, and kinematics could all affect their attractiveness as a habitat for ETIs, or indicate new phenomena at work. Some examples include asteroids, which may be classified according to orbit or composition. We therefore included several overlapping classification systems. Some Prototypes do double duty, acting as representative examples of several of these overlapping classes, to help keep the number of objects manageable.

Some classes of objects are excluded, usually because they are too impractical to observe. These included diffuse “objects” like the interstellar medium as a whole and very large structures like the Fermi Bubbles (Su et al. 2010). In addition, we required classes to have at least one example that was fairly well established to serve as the Prototype. For example, carbon planets, open cluster remnants, and dark matter minihalos are omitted because there have no confirmed examples.

Although our goal is to have “one of everything” for the Prototype catalog, our focus is not entirely even. We cannot be entirely consistent about how fine-grained each category is, as it relies on subjective judgements about how to distinguish types. We have included finer subclasses when they may be relevant to SETI. Among these are the non-interacting double degenerate binary stars, which have been proposed as possible “gravitational engines” (Dyson 1963). We also included some subclasses because their members have unusual properties that might indicate or motivate ETI presence. Hy-

⁷ Of course, the use of “phylum” does not imply a biological relationship in terms of inheritance from a common ancestor. Instead the term refers more to the older usage of morphological similarities. Nor do the phyla necessarily fit in a tree-like hierarchy within Dick (2013)’s kingdoms as zoological phyla generally do: arguably stellar groups and the ISM straddle his Stellar and Galactic kingdoms.

⁸ <https://journals.aas.org/keywords-2013/>

⁹ Hosted at <http://astrothesaurus.org/blog/>. We consulted version 3.1.0 during the writing of this paper.

Table 1. Phyla of astronomical phenomena: a high-level classification system used in the *Exotica Catalog*

K64 Rating	Phylum	Characteristics	Example
$\frac{1}{2}$	Minor bodies	Solid, small, typically irregular shape, modification mostly from cratering after initial ^{26}Al differentiation	1I/'Oumuamua
I	Solid planetoids	Hydrostatic equilibrium; solid; round; geology plays key role in interior evolution; fluids in form of thin atmosphere and liquid ocean	Titan
I	Giant planets	Hydrostatic equilibrium; fluids dominate mass and evolution; large; typically high internal heat luminosity; formation by gas accretion on to solid core	Jupiter
II	Stars	Hydrostatic equilibrium; plasma; powered by nuclear fusion or sometimes gravitational collapse; no solid cores; includes brown dwarfs and protostars by convention	Sun
II	Collapsed stars	Supported by degeneracy pressure if at all; luminosity from release of stored thermal, rotational, or magnetic energy	Sirius B
$\text{II}\frac{1}{2}$	Interacting binary stars	Evolution of component stars affected by mass transfer; substantial luminosity from accretion, surface nuclear burning, or shocked outflow; often compact object is mass recipient	SS 433
$\text{II}\frac{1}{2}$	Nebulae and ISM	Diffuse gases and plasmas; includes flows of matter to/from stars and diffuse galaxy; generally not self-bound	Orion GMC
$\text{II}\frac{1}{2}$	Stellar groups	Gravitationally bound collections of stars, which do not otherwise interact for the most part; little to no dark matter	47 Tuc
III	Galaxies	Gravitationally bound, dominated by dark matter; generally contain vast numbers of stars, gas, and possibly a central black hole; gravitationally bound	Milky Way
III	Active galactic nuclei	Powered by accretion onto a supermassive black hole; includes gas flows on and off SMBH, frequently with jets and particle-filled bubbles	Cygnus A
III	Galaxy associations	Dark matter dominates internal gravitation; gravitationally bound collections of galaxies and intracluster medium	Virgo Cluster
$\text{III}\frac{1}{2}$	Large-scale structures	Unbound or loosely bound structures on \gg Mpc scales; includes high-order arrangements of galaxies and diffuse gas (IGM); non-virialized	Shapley Supercluster
Any	Technology	Structures built intentionally, frequently for processing of matter, energy, and information; so far only known to exist on/near Earth	<i>Voyager 1</i>
...	Reference	Sky locations only important relative to observer	Solar antipoint

NOTE—The “phyla” are used to group objects in the Prototype and Superlative samples by shared physical traits. From a SETI perspective, they indicate the need for very different techniques necessary for astroengineering, as reflected in the amount of used power measured by the Kardashev (1964) scale rating of on left.

pervelocity stars, for example, might be good places for ETIs interested in extragalactic travel to settle. A couple of large classes that lie on a continuum of properties, namely main sequence stars and disk galaxies, have been broken up to ensure good coverage over the possible range of environments they can host.

To complete a broad census of the cosmos, we also consider the possibility that habitability changes with cosmic time (c.f., Loeb et al. 2016). Luminous AGNs, explosive transients, and galaxies with immense star-formation rates and chaotic morphology were more prevalent at high redshift (e.g., Elmegreen et al. 2005; Madau & Dickinson 2014), with unknown effects on the evolution of ETIs and their technological capabilities (for additional speculation on some of these effects, see Annis 1999a; Ćirković & Vukotić 2008; Gowanlock 2016; Lingam et al. 2019). We partly mitigate the sensitivity losses over the vast luminosity distances by selecting gravitationally lensed galaxies. Our EIRP sensitivity will thus be boosted by about an order of magnitude. There is also the potential for gravitational microlensing from foreground objects, which has been known to

magnify individual $z \gtrsim 1$ stars by over a thousand (Kelly et al. 2018), allowing us to achieve better EIRP limits for small high- z populations.

4.2. Prototype selection

Each class’s Prototype is selected to be a fairly typical example, even if the object type itself is unusual. When available, we generally pick objects that are well-studied and explicitly called a “prototype”, “archetype”, “benchmark”, or something similar, like the “prototypical” starburst M82 (e.g., Seaquist & Odegard 1991; Leroy et al. 2015). This will provide us the greatest context if we discover something. However, because Breakthrough Listen has unique capabilities, these observations will not be redundant with previous studies.

Although not directly referred as such, stars have prototypes in the form of spectral standard stars, which we have used when practical. Classes of variable stars (including interacting binaries, like cataclysmic variables) are named after well-known examples, and we generally adopt the eponymous object as the Prototype. In two cases, we substituted another object if it is much

closer and well-studied: TW Hydrae for T Tauri stars (Zuckerman & Song 2004), and AG Car for S Dor-type Luminous Blue Variables (Groh et al. 2009).

A principle we adopted, especially when explicit prototypes are lacking, is to use objects with high citation counts, which we take as a proxy for how well studied an object is. We adopted this criterion by either selecting nearby objects filtered by object type in Simbad, or by viewing the objects in a prominent catalog for a type in Simbad (Wenger et al. 2000). Then we sorted by number of citations, and examined a few objects with the highest citation count. We are mindful that well-cited objects may be particularly well studied because they host a rarer phenomenon or are anomalous rather than representative.¹⁰

A final consideration is that we pick objects that are easy to observe and set meaningful limits on. Nearby objects are generally preferred. Not only are they usually well-studied and well-known, but in a survey with limited integration time, we set tighter limits on novel signals from nearby objects. We also try to pick Prototypes that have already been observed by Breakthrough Listen as part of its nearby stars and nearby galaxy programs, or other campaigns. Since these have been selected by distance, already observed objects also tend to be nearby and frequently have high citation rates anyway.

4.3. The challenge of transients

Among the panoply of celestial phenomena, transients pose special challenges for any attempt to observe “one of everything”. Of course, everything in astronomy is transient on some scale: the planets, stars, galaxies, and black holes will all disperse over the next 10^{200} yr (Adams & Laughlin 1997); life, intelligence, and technology too all are expected to perish in a Λ CDM universe (Krauss & Starkman 2000). Transients here has an observer-relative definition, referring to objects that evolve in some way, typically brightness, on a timescale comparable to or shorter than the observing program. The importance of transients to our understanding of the cosmos has been recognized in the past few decades, and the past few years have seen a huge growth in detection capabilities and characterization, from radio (e.g., with the SETI-oriented Allen Telescope Array: Croft et al. 2011; Siemion et al. 2012; see also Murphy et al. (2017); CHIME/FRB Collaboration et al. (2018) for other recent examples) to optical (e.g., Law et al. 2015;

Chambers et al. 2016), X-rays (e.g., Matsuoka et al. 2009; Krimm et al. 2013), gamma-rays (e.g., Ackermann et al. 2016; Abdalla et al. 2019), neutrinos (e.g., Adrián-Martínez et al. 2016; Aartsen et al. 2017), and gravitational waves (e.g., Abbott et al. 2019a,b).

Classes of transient events already number in the dozens, with a variety listed in Table A2. They span all of the electromagnetic spectrum and all messengers, all timescales from nanoseconds to decades and longer, and occur among most of the phyla, including some more properly considered Anomalies (Section 6). Although some are mundane visual effects, like eclipses, others contribute profoundly to cosmic evolution, like the r -process element birthsites in supernovae and neutron star mergers. We excluded in Table A2 those phenomena that induce only small variability (e.g., planetary transits), or are continuously ongoing rather than episodic (e.g., variable stars).

If there were no constraints on observations, we would like to observe at least one of each of the transient classes in Table A2. This follows from a broad-minded perspective on the possible forms of ETIs. Both known and hypothetical transients have been studied as possible technosignatures. More speculatively, conceivably some ETIs live on a completely different timescale than humans: perhaps whole societies of rapidly evolving artificial intelligences or neutron star life rise and fall in moments (c.f., Forward 1980). Practical considerations make observing every known transient class in the table impossible. The most important reason for the difficulty is that we have to be pointing the telescope at the right point on the sky when the transient occurs. In order to detect a member of a rare transient class, we would either have to commit our facilities to staring and waiting for an event, or use facilities that observe much of the sky. Future wide-field instruments could be helpful (Section 9). Although there is no such facility in radio above 1 GHz or optical associated with Breakthrough Listen, we have pilot programs with the low-frequency facilities LOFAR (LOW-Frequency ARray; van Haarlem et al. 2013) and MWA (Murchinson Widefield Array; Tingay et al. 2013) with wide-field capabilities.

Some transients repeat. These are listed in the first two sections of the Table. The hosts of repeating transients in Table A2 represent object types in their own right listed in the *Exotica Catalog*. A few transients occur at predictable times since their timing is the result of orbital motion: these include the periodic comets and OJ 287’s flares. We may schedule observations during examples of predicted transients, as resources permit. Most are unpredictable, though, so simply knowing where they happen is of little help in ensuring a tran-

¹⁰ For example, ω Cen is one of the most cited “globular clusters” but likely is a dwarf galaxy nucleus; Cen A may be the most cited lenticular galaxy, but is not representative.

sient is observed. We would need to rely on alerts, and observations of the event itself will be dependent on our access to the facilities.

Other transients occur only once, at least on human timescales, as listed in the second section of Table A2. With these, we not only are unable to schedule observations of a transient example, we generally cannot study the pre-transient progenitor.¹¹ Any hope of observing them requires an alert and a flexible observing schedule. While we may learn of an ongoing transient event through Astronomer’s Telegrams (Rutledge 1998)¹² and Gamma-ray Coordinates Network (GCN) circulars¹³, we cannot guarantee that we will be able to slot in observations in time. Furthermore, some transients are so short lived – minutes or less – that they would be over by the time we received any alert. If the event occurs in the field-of-view of a radio telescope with a ring buffer, a trigger or prompt alert can allow us to beamform on it using temporarily stored voltages in the buffer (e.g., Wilkinson et al. 2004). Otherwise, we can only hope to observe the aftereffects of these short-lived transients. It is also possible short-lived transients are technosignatures of a larger ETI society that is still observable after the event itself is over. Hence, we include anomalous transients as objects in their own right in the Anomaly sample (Section 6).

Finally, a few transients are common enough that they invariably will occur during our observations, as listed in the final part of the table. Since these are generally not coming from the sources we are interested in observing, they in fact have the opposite problem of most transients: they are a form of interference that we cannot avoid even though we want to.

5. THE SUPERLATIVE SAMPLE

The Superlative sample expands the reach of the *Exotica Catalog* survey across a wider range of parameter space. These are objects that are among the most extreme in at least one major physical property, the record-breakers. Perhaps ETIs, or unusual natural phenomena, are biased to very atypical examples of space objects, like the hottest planets, the lowest mass stars, or the richest galaxy clusters. Extreme physical properties can also be a sign of different evolutionary histories or even new subtypes of phenomena. For example, pulsars with very short rotation periods are the result of a

mass transfer phase during their evolution (Alpar et al. 1982). Table B1 in Appendix B lists the members of the Superlative sample, and the ways they are superlative.

5.1. Classification and Superlatives

Classification is an important factor in determining whether an object is really a superlative at the tail end of its class’s properties, the prototype of a new class, or even a unique anomaly. In astronomy, some kinds of objects fall on a continuum in terms of properties, but are conventionally delineated by an arbitrarily chosen range. An example is the spectral type of a star: there is a continuous range of temperature, but the boundaries of the spectral types themselves do not directly map onto different evolutionary trajectories or habitability. Objects at the boundary of these classes have no special significance. We thus focus on the superlatives of easily distinguishable classes. Thus, we give superlatives for the phyla (Section 4.1), which is our coarsest level of classification. We include superlatives for some intermediate level classes, particularly within the Solar System and by distinguishing white dwarfs, neutron stars, and black holes. Yet even the use of phyla does not completely solve the problem of overlapping categories. The smallest sub-brown dwarfs have the same mass as the biggest giant planets (as is the case for the coldest “star” listed); galaxies overlap with stellar associations, with globular clusters forming a continuum with ultra-compact dwarf galaxies.

An object may have properties that are so outstanding that we consider it an Anomaly. The basic distinction we make is that a Superlative should still be clearly a member of its class, governed by the same physical processes. Superlatives are drawn for the tail of a class’s distribution, while Anomalies appear to lie far outside it, often inexplicably so.

5.2. Properties considered: Superlative in what way?

An object can stand out in one of many possible quantities. In principle, there are hundreds: the abundance of every element, absolute magnitude in every possible filter band or frequency, quantities describing internal structure, and velocities in different frames are all possibilities.

Additionally, we could take advantage of known empirical relations between quantities, and include outliers from these relations as “superlative”. These superlatives with respect to relations can actually indicate new object classes: objects lying far off the stellar main sequence are the giants and white dwarfs, both fundamentally different from dwarf stars, for example.

There are a great many such relations, however. Considering all observables or physical properties in a high-

¹¹ For example, if some peculiar supernovae actually herald the self-destruction of a Type II ETI, it would be too late to detect them once the supernova went off.

¹² <http://www.astronomerstelegram.org/>

¹³ https://gcn.gsfc.nasa.gov/gcn3_archive.html

dimensional parameter space, objects generally fall into “clouds” surrounding manifolds in that space (Djorgovski et al. 2013).¹⁴ The “superlatives” would be all of the objects forming the boundary of that cloud, lying the furthest away from the manifold. Indeed, searching for such outliers is one proposed method to search for new phenomena (Djorgovski et al. 2001). The number of possible combinations of variables is vast, each corresponding to one small piece of the boundary, and we conceivably could include them all. It is impractical to select and observe all such objects.

We avoid proliferation by focusing on a small number of quantities that describe the basic properties of objects, which usually apply to most to all the phyla. We consider the basic characteristics to be *size*, quantified by radius and mass; *composition*, quantified by density and metallicity; and *energetics*, quantified by bolometric luminosity and temperature. When appropriate, mainly for objects with well-characterized orbits like planets, we include *kinematics* or *position*, quantified by space velocity and orbital semi-major axis and/or period. Finally, we include *era*, in the form of ages for planets and stars, and redshift for larger or brighter objects like galaxies. Some additional properties are included for certain object classes when they fundamentally regulate an object’s behavior and are easy to find in the literature. For planets, we also consider some basic characteristics of the host star (mass, luminosity, surface temperature, and metallicity). Magnetic fields and rotation periods are included for neutron stars.

5.3. Finding Superlatives in the literature

We used several methods to try to find Superlative objects. Starting a search for a Superlative involves reading through literature (generally as part of the Prototype and Anomaly search) and being alert for mentions of record-breaking objects. Sometimes the search started outside the peer-reviewed literature. Wikipedia maintains several lists of Superlative objects¹⁵; although

we do not consider its entries as final, the objects it lists are generally among the most extreme, providing a place to start, and it includes links to relevant papers. Sorting major catalogs on VizieR¹⁶ (Ochsenbein et al. 2000) or exoplanet.eu¹⁷ (Schneider et al. 2011) by key quantities also gave us candidates. When we find a paper describing a candidate Superlative, we look at citing papers in the Astrophysical Data System (ADS; Kurtz et al. 2000), as anything that supersedes the object is likely to cite the previous record holder. We also look for papers describing previous record holders, and the papers that cite those, especially if the Superlative’s measurements are uncertain.

Ideally, we wish to use objects that are explicitly described as being superlative in some regard in the literature. These can be announced by papers in journals like *Nature* or *Science*.¹⁸ In other cases, the record may not be heralded prominently as the subject of a paper, but we found it mentioned in a paper while searching for Prototypes or Anomalies: the most massive supercluster (Shapley), for example (Kocevski & Ebeling 2006, while researching the Great Attractor). Review papers or compendiums sometimes highlight objects that are outliers and can be useful in this regard.¹⁹

Many cases are less certain. Papers sometimes proclaim the extraordinary nature of an object without explicitly stating it is superlative. One case is the Superlative R136 a1 is noted to have an extraordinary mass ($\sim 300 M_{\odot}$), the highest in recent literature, without being explicitly said to be the most massive known star (Crowther et al. 2010).

Sometimes it seems that no one keeps track of certain extremes, and measurements may not be all that reliable. While there are many cases of extremely low metallicity stars or galaxies being touted (e.g., for Superlatives in our catalog, Caffau et al. 2011; Keller et al. 2014; Simon et al. 2015; Izotov et al. 2018), few papers describe very high metallicity stars or galaxies (a few exceptions are Trevisan et al. 2011; Do et al. 2018), and none proclaim a single Superlative. As we do

¹⁴ Djorgovski et al. (2013) calls these spaces Measurement Parameter Spaces and Physical Parameter Spaces, and differentiates them from the Observable Parameter Spaces that include the “Cosmic Haystack” discussed in SETI.

¹⁵ These lists and others are themselves listed at https://en.wikipedia.org/wiki/Lists_of_astronomical_objects. Examples include the “List of exceptional asteroids” (https://en.wikipedia.org/wiki/List_of_exceptional_asteroids), the “List of most luminous stars” (https://en.wikipedia.org/wiki/List_of_most_luminous_stars), the “List of largest galaxies” (https://en.wikipedia.org/wiki/List_of_largest_galaxies; note it is not on the meta-list) and the “List of most distant astronomical objects” (https://en.wikipedia.org/wiki/List_of_the_most_distant_astronomical_objects).

¹⁶ <http://vizier.u-strasbg.fr/>

¹⁷ <http://exoplanet.eu/catalog/>

¹⁸ For example: the hottest planet (Gaudi et al. 2017), the star with the shortest Galactic orbital period (Meyer et al. 2012), and the most distant quasar (Bañados et al. 2018). In other journals, the lowest albedo exoplanet (Kipping & Spiegel 2011), the slowest spinning radio pulsar (Tan et al. 2018), and the densest galaxy (Sandoval et al. 2015).

¹⁹ As when Lattimer (2019) mentions the possibility that black widow neutron stars are the most massive; MACS J0717.5+34 as having the brightest radio halo in van Weeren et al. (2019); 65 UMa as being a rare septuplet system in Tokovinin (2018).

want to include a superlative high metallicity star, we looked through several catalogs listing stellar metallicities: Cayrel de Strobel et al. (2001), Hypatia (Hinkel et al. 2014), Bensby et al. (2014), PASTEL (Soubiran et al. 2016), CATSUP (Hinkel et al. 2017), PTPS (Dekaszymankiewicz et al. 2018), and Aguilera-Gómez et al. (2018). These often gave contradictory measurements; a star that is the highest metallicity in one is relatively normal in another. In this case, we looked for a star that was frequently among the highest metallicities, and reliably supersolar metallicity, settling on 14 Her (Gonzalez et al. 1999 comments on its high metallicity explicitly, supporting its selection). As our goal is to sample the range of astrophysical phenomena, we thus prefer reliable outliers over including the most extreme objects with unreliable measurements. Very large catalogs often include these extreme superlatives, but do not comment on them. For example, PASTEL contains dozens of stars listed with $[\text{Fe}/\text{H}] > +1.0$, although these results are not replicated in other catalogs. We disregard these cases as likely being due to model inadequacies or measurement errors.

Some superlatives are not included at all. This is particularly the case when one class blends into another and the superlative depends simply on where the boundary is set, with many objects lying upon the border consistent with measurement errors. The most massive planet and the least massive brown dwarf are excluded superlatives for this reason (see the extensive discussion of the issue of classification in Dick 2013).

Of course, we cannot guarantee that the Superlatives listed here are literally the most record-breaking objects in the Universe. New record breakers are being discovered all the time. We expect to update the list as these are discovered.

6. THE ANOMALY SAMPLE

Anomalies are phenomena with observable properties that do not easily fit into current theories, not even roughly. Upon discovery, they frequently spur theorists to develop many new hypotheses and explore new mechanisms that might operate in the Universe (as happened with gamma-ray bursts and continues to happen with fast radio bursts; Nemiroff 1994; Platts et al. 2019). Wild early speculation about alien engineering also tends to be associated with Anomalies, although to-date natural explanations have been eventually found. Nonetheless, it has often been encouraged to look at Anomalies for ETIs and any distinct signs of alien intelligence will be an Anomaly upon discovery (Djorgovski 2000; Davies 2010). Examining these anomalies does not only have to reflect a belief that they are alien engineer-

ing. Anomalies may also induce natural phenomena that mimic ETIs and are interesting in that regard (Motivation III). By examining these anomalies, we get a better sense of what to expect from the non-ETI Universe, and a better sense of what isn't normal. Thus the presence of an object in the Anomaly sample is *not* a statement of belief about artificiality; many of the objects are clearly natural if unusual, like Iapetus.

The targets in our Anomaly sample are listed in Tables C1 and C2 in Appendix C.

6.1. Types of Anomalies

We use a supplementary classification scheme for Anomalies that group them by the nature of their anomalousness.²⁰ Our hope is that it will aid both further searches for anomalies in diverse datasets and inspire new ideas about technosignatures (for example, as Class I or V anomalies).

This system has six classes.

- Class 0 objects are those that are not anomalous from an astrophysical point of view, although they can be exotic in terms of SETI. We define Class 0 anomalies as a likely member of a known, explained population even if classification is ambiguous, with no evidence for unknown phenomena at work. Almost all of the Prototypes and Superlatives fall in Class 0. An object can still have ambiguous classification without actually being mysterious; Pluto in the early 2000s was Class 0. Alternatively, an object that is mysterious because of multiple good explanations remains Class 0: IRAS 19312+1950 may be either a young star or an AGB, but seems readily explainable (Nakashima et al. 2011; Cordiner et al. 2016).
- Class I anomalies are likely members of a known, explained population, with normal intrinsic properties, but located in an anomalous environment or context. In other words, the object itself is not mysterious, only where it is. This also includes objects with inexplicable kinematics. Hot Jupiters were Class I anomalies until it was understood that gas giants could migrate (Mayor & Queloz 1995; Guillot et al. 1996).
- Class II anomalies are likely members of a known, explained class, but whose properties quantitatively fall far outside the usual distribution. Class

²⁰ For previous anomaly classification schemes, see Cordes (2006) and Norris (2017).

II anomalies are qualitatively similar to other objects of the same type. Millisecond pulsars, for a short time after discovery, were Class II because of their extreme spin (Backer et al. 1982). Candidate megastructures identified by infrared emission in excess of the expected value (as identified by the far-infrared radio correlation of galaxies, for example; Garrett 2015; Zackrisson et al. 2015) or abnormally faint optical emission (Annis 1999b; Zackrisson et al. 2018) are examples in a SETI context.

- Class III anomalies are likely members of a known, explained class, but displaying a qualitatively new and unexplained phenomenon. These phenomena are something that do not even happen around other members of the class. Saturn’s rings are a classical example, as their nature as debris belts took centuries to understand despite Saturn clearly being a planet (Dick 2013). Candidate SETI signals found in targeted surveys of nearby stars through the traditional methods of ultranarrowband radio emission or nanosecond optical pulses would be Class III anomalies.
- Class IV anomalies are those of an unexplained or unknown phenomenon class. They may be identified only in one waveband, without counterparts in any others. Current explanations generally have plausibility issues. Many of the famous discoveries of the past century were originally Class IV anomalies: among them, Galactic synchrotron emission (Jansky 1933), quasars (Schmidt 1963), pulsars (Hewish et al. 1968), gamma-ray bursts (Klebesadel et al. 1973; Nemiroff 1994), and now fast radio bursts (Lorimer et al. 2007; Platts et al. 2019). They are, however, relatively rare. Candidate SETI signals found in wide-field surveys are frequently Class IV, including the Wow! signal (Dixon 1985; Gray & Ellingsen 2002).
- Class V anomalies are objects or phenomena that appear to defy known laws of physics, whether the object itself is identifiable or not. These are extremely rare. In very special cases they may herald an upheaval in our understanding, as the Galilean satellites did, but usually they are simply in error (e.g., the notorious case of candidate superluminal neutrinos in an early version of Adam et al. 2012, which was a non-localized Class V anomaly).

These classes, all else being equal, roughly increase in order of mysteriousness. Judgements about the classification of an anomaly will vary with new data and

different emphasis. For example, in the 18th century, was Saturn a planet with the anomalous feature of rings (Class III), or were the rings themselves an anomalous object (Class IV)? Other considerations are whether an Anomaly has some theoretical explanation, if a problematic one, and the confidence that the anomaly is real. We list those with partial or possible explanations as Class 0/ x in Table C1 (where x is in the range I–V) and avoid those whose existence has been rejected.

6.2. Collecting Anomalies

The search for Anomalies in the literature is even more associative and subjective than finding Prototypes and Superlatives. While there is plenty of discussion of mysterious classes of objects like FRBs, to our knowledge, there hasn’t been an attempt to create a list of anomalous objects. An Anomaly might consist of a single object or event that doesn’t attract a lot of outside attention, especially if it is poorly characterized.

A few Anomalies are well known in the SETI literature, including KIC 8462852 (Boyajian et al. 2016; Wright et al. 2016; Abeysekara et al. 2016; Wright 2018a; Lipman et al. 2019) and 1I/’Oumuamua (Bialy & Loeb 2018; Enriquez et al. 2018; Tingay et al. 2018b; ’Oumuamua ISSI Team et al. 2019). The abundance pattern of Przybylski’s star, particularly the possible presence of short-lived radioisotopes (Cowley et al. 2004; Bidelman 2005; Gopka et al. 2008), has been informally discussed online as a possible technosignature (c.f., Whitmire & Wright 1980).²¹ Others were known to us through general knowledge (e.g., the CMB cold spot, Cruz et al. 2005). Still other anomalies were found using the help of Astrophysical Data System, particularly while looking at citations and references to evaluate an object (ADS; Kurtz et al. 2000). Papers that identify Anomalies frequently cite previous (explained or unexplained) Anomalies.²² Papers about Anomalies can cite well-known review articles or compendiums specifically so they can situate or differentiate their mysterious object from mundane phenomena.²³

The process was mainly serendipitous, however. We did search ADS for terms like “anomalous”, “mysterious”, “enigmatic”, and “unusual”, although they tended to mostly turn up papers that were about relatively nor-

²¹ See <https://sites.psu.edu/astrowright/2017/03/15/przybylskis-star-i-whats-that/> and subsequent articles in the series.

²² Vinkó et al. (2015) on “Dougie” citing Cenko et al. (2013) on PTF11agg; Saito et al. (2019) about VVV-WIT-07 citing Boyajian et al. (2016) on KIC 8462852.

²³ Moskovitz et al. (2008) on (10537) 1991 RY₁₆ citing Bus & Binzel (2002) on asteroid spectral classification.

mal objects.²⁴ Those papers were mainly about minor puzzles that we do not consider inexplicable enough to rise to Anomaly status, although this is a subjective judgement. We also had to ignore object classes with “anomalous” in the name, such as Anomalous X-ray Pulsars. Similar searches on the Astronomer’s Telegram archives netted several examples.²⁵ Papers about recently identified mysterious objects appear in arXiv²⁶ or journals like *Nature* and *Science*, where they garner attention.²⁷

Transients are frequently unexplained upon discovery, and they are well-represented in the sample. Even though the events themselves are over, anomalous transients may hypothetically be technosignatures of K64 Type II–III ETIs. We may then hypothesize there to be other technosignatures – and other Anomalies – coming from these societies, which would share the same field as the transients themselves did. As a very speculative example, perhaps the large early-type galaxy M86 is one such location, as it hosts two Anomalous X-ray transients.²⁸

For this present catalog, we had to search for Anomalies through a literature scan. There is great interest in searching for anomalous signals in instrumental data with machine learning (e.g., [Baron & Poznanski 2017](#); [Solarz et al. 2017](#); [Giles & Walkowicz 2019](#)), however. In the coming years, these automated efforts will likely flag new objects with unusual properties that can be added to future versions of the *Exotica Catalog* ([Zhang et al. 2019](#)).

6.3. Previous SETI candidates

A special subset of Anomalies, one especially relevant for Breakthrough Listen, are those identified by other SETI programs. Signals identifiable as technosignatures essentially have to be anomalies, otherwise they could always be given a more mundane explanation and it would not be effective as a SETI search. Indeed, the Earth, or the Solar System, would appear to be a Class III anomaly to radio astronomers with sensitive enough telescopes, due to its unnatural narrowband radio emission.

²⁴ For a success, [Demers & Battinelli \(2001\)](#) refers to the apparent “hole” in UMi dSph as an “enigma”.

²⁵ ASASSN-V J060000.76-310027.83 via [Way et al. \(2019a\)](#); ASASSN-V J190917.06+182837.36 via [Way et al. \(2019b\)](#); DDE 168 via [Denisenko \(2019\)](#).

²⁶ [Santerne et al. \(2019\)](#) on HIP 41378 f.

²⁷ [De Luca et al. \(2006\)](#) on RCW 106; historically, [Schmidt \(1963\)](#) on 3C 273, for example.

²⁸ XRT 000519 and M86 tULX-1.

Candidate signals identified by other SETI searches are included in the subcatalog listed in Table C2. These include suggestions of narrowband radio emission ([Dixon 1985](#); [Blair et al. 1992](#); [Horowitz & Sagan 1993](#); [Colomb et al. 1995](#); [Bowyer et al. 2016](#); [Pinchuk et al. 2019](#)), nanosecond-duration optical pulses ([Howard et al. 2004](#)), optical spectral features consistent with picosecond-cadence pulses ([Borra & Trottier 2016](#)), infrared excesses compatible with waste heat from megastuctures ([Carrigan 2009](#); [Griffith et al. 2015](#); [Garrett 2015](#); [Lacki 2016b](#)), and one example of an apparently vanished star ([Villarroel et al. 2016](#)). Most of the non-SETI Anomalies are not single-instance transients, and therefore their anomalous natures can be confirmed by independent groups. The SETI candidates have a more uncertain existence, though, and may turn out to be mundane (e.g., RFI).

Despite not widely being considered strong evidence, we include them because they match previous specific predictions about technosignatures. In addition, Breakthrough Listen has followed up on claimed SETI candidates in the past, to-date verifying none ([Enriquez et al. 2018](#); [Isaacson et al. 2019](#)). Finally, the wide variety of technosignatures covered helps ameliorate the difficulty of learning about anomalies with unfamiliar techniques or subfields. When a great many candidate ETIs are given, we include only a few examples, chosen according to the brightness of the stellar host ([Borra & Trottier 2016](#)), the evaluated quality of the candidate ([Howard et al. 2004](#); [Carrigan 2009](#); [Griffith et al. 2015](#); [Zackrisson et al. 2015](#)), or the signal-to-noise ratio of the event ([Horowitz & Sagan 1993](#); [Colomb et al. 1995](#); [Bowyer et al. 2016](#)).

7. THE CONTROL SAMPLE

The final group of targets are those we observe with the expectation of *not* observing anything new. Instead, they provide a baseline set of observations for comparison with any positive detection of a new phenomenon, a control sample for the SETI experiment. If some subtle systematic or source of interference is generating false positives, it should eventually show up during observations of appropriately chosen control sources. We could thus rule out the false positive by comparison with the results of the Control sample.

7.1. The Control sample

The first part of the Control sample is along the lines of the other samples, a list of astrophysical targets (Table D1 in Appendix D). These are targets that were once thought to represent a new or anomalous phenomenon but that turned out to have very mundane explanations.

We can simulate our response to transients or the discovery of an anomaly by looking at purported transients that turned out to be banal.

As an example, Bailes et al. (1991) reported the first discovered pulsar planet around PSR B1829-10. If Breakthrough Listen had been operating in 1991, we surely would have scheduled a rapid campaign to observe PSR B1829-10, similar to our campaigns observing 1I/'Oumuamua and FRB121102, because it was among the first exoplanets reported in the literature. A year later, however, the same authors traced the pulsar timing signal to an error in the treatment of Earth's orbit (Lyne & Bailes 1992). We would have acquired deep radio observations of a planet that turned out not to exist. Any detection would likely have been the result of an error in our analysis, or perhaps have come from the pulsar itself.

Because of limited data and the difficulties of interpretation, there have been many mistaken claims in astronomy. We chose the objects and phenomena in Table D1 on a few principles. First, there should be consensus that the claimed discovery was in fact in error, preferably by the authors themselves. Second, most of the claimed discoveries should have appeared to be confident enough to have provided a strong impetus for observations. Most appeared in the peer-reviewed literature, although KIC 5520878 was explained in the same paper that reported it (Hippke et al. 2015). An exception is GRB 090709A: although a claimed 8 second quasiperiodicity was not published in a peer-reviewed journal (see de Luca et al. 2010; Cenko et al. 2010), it was reported in several GCNs by multiple groups, drawing interest to it (Markwardt et al. 2009; Golenetskii et al. 2009; Gotz et al. 2009; Ohno et al. 2009). Third, we avoided picking bright or exceptional sources, where we might expect new phenomena, in favor of non-existent or anonymous targets. An example of a source we excluded is the X-ray binary Cygnus X-3, which was widely considered to be a brilliant TeV–EeV gamma-ray and cosmic ray source in the 1980s before the early detections lost credibility (Chardin & Gerbier 1989; see also Archambault et al. 2013 and references therein for recent gamma-ray observations). Similarly, we excluded Barnard's Star, a nearby star that had two candidate exoplanets in the 1960s–1970s (van de Kamp 1963; Choi et al. 2013), because it actually does have a planet, albeit one much smaller, listed as a Prototype (Ribas et al. 2018). Fourth, sky coordinates needed to be reported, which prevented us from including perytons, seeming atmospheric radio transients later explained as RFI from a microwave oven (Petroff et al. 2015).

Our inclusion of a target in the Control sample is not meant to disparage the claimants. Science has a long history of observational errors, some of which have prompted deeper studies that in turn revealed real phenomena. The mistaken discovery of planets around PSR B1829-10 encouraged the announcement of the actual first pulsar planets around PSR B1257+12 (Wolszczan & Frail 1992; Wolszczan 2012). The retraction then encouraged careful scrutiny of PSR B1257+12's planets, building a more solid case for their existence. The apparent discovery also prompted theoretical work into the origins of pulsar planets. Another early exoplanet announcement was HD 114762 B, an apparent warm super-Jupiter detected by the radial velocity method (Latham et al. 1989). In a case of terrible luck, this real object has in recent years been shown to be a red dwarf orbiting HD 114762 in a nearly face-on orbit (Kiefer 2019).²⁹ Yet it turns out there really are warm and hot gas giants, including those much bigger than Jupiter, and they really could be detected through the radial velocity method, in defiance of the expectations of the time (Latham 2012; Cenadelli & Bernagozzi 2015). Discoveries like these can open conceptual spaces, unexplored possibilities that were simply not thought of before. In other cases, a purported anomaly can be studied well enough that it becomes the prototype of an object class. This has happened with NGC 1277, a prototypical red nugget galaxy studied because of the now-disputed extreme mass of its central black hole (Trujillo et al. 2014).

7.2. *Could we just look at “empty” regions of the sky?*

Even with the Control sample, there is a danger that we could observe something real. HD 117043 probably does not have potassium flares (Wing et al. 1967), but for all we know it does have a planet with ETIs; it's even one of the I17 sample stars. Likewise, PSR B1829-10 is a real radio pulsar, even if it does not host planets (Lyne & Bailes 1992). Most of these are relatively distant, so only a very bright ETI signal would be discovered, but it remains a possibility. Only the Perseus Flasher is believed to be not astronomical at all (Schaefer et al. 1987; Borovicka & Hudec 1989).

A more stringent set of Control sources would be to look at empty places on the sky with no objects at all. This is often not actually possible, though. A famous example is the Hubble Deep Field, chosen to be away

²⁹ Interestingly, HD 114762 was originally viewed as a Control source, because it was thought that no actual planet could be massive and close enough to be detected around it, according to Cenadelli & Bernagozzi (2015). The possibility that some Control sources may themselves turn out to be interesting is discussed in the next section.

from any known bright sources, which has thousands of galaxies (Williams et al. 1996). The beam size of the GBT at 1 GHz is about $9'$, which would cover thousands of galaxies and trillions of extragalactic planets, and only one would need to send a bright broadcast in our direction.

At high frequency, radio beam sizes are smaller. It could be possible to slip a beam between known all stars and galaxies near 100 GHz with GBT, or 10 GHz with one kilometer baselines using MeerKAT. Even this would not guarantee the non-existence of ETIs within the main beam. Red dwarfs, brown dwarfs, and white dwarfs would generally not be detectable from many kiloparsecs away and might exist in the beam, although hard limits on their abundance on sightlines towards the Magellanic Clouds have been set with microlensing surveys (e.g., Tisserand et al. 2007). But for all we know, some ETIs actually exist in the depths of interstellar space, away from all stars (Ćirković & Bradbury 2006). Perhaps they broadcast from starships (e.g., Messerschmitt 2015), or ride along ubiquitous interstellar objects like 'Oumuamua. Thus, there is no place on the sky that can be guaranteed to be free of ETIs. The main utility of looking at “empty” sky regions as a control is to limit the prevalence of relatively faint signals from nearby, known objects.

7.3. *Unphysical targets*

The ultimate Control source is one that cannot possibly be an actual source at all. Then if we do observe what looks like an ETI signal, we can be quite sure it is some systematic issue, whether instrumental or caused by interference. An unreal source can be simulated by selecting an unphysical trajectory for where the telescope is pointed, and then treating the output data as if it came from a single location on the sky. Sources outside of the Solar System near the celestial equator are bound to rise in the east and set on the west like all other non-circumpolar sidereal sources; to do otherwise would be to violate causality. Even within the Solar System, the motion of objects is constrained.

As an example, consider the zenith as a “source”. It is a very special point from the viewpoint of the observer, convenient and easily attention-grabbing. But practically speaking, the zenith actually sweeps out a band on the sky. No distant source beyond one light day could remain at the zenith because of causality. Unless the observatory is on the equator, no object in Earth orbit would remain at the zenith. Any such beacon would have to be both nearby and would require expensive, power-intensive maneuvers. Furthermore, the zenith’s sightline depends on the *specific* location of the

observatory, an improbable coincidence unless the makers mapped the Earth thoroughly, recognized radio telescopes, and somehow determined which ones were doing SETI. If needed, other possible unreal sources abound by choosing other implausible tracking trajectories: we could track faux “targets” that rise in the west and set in the east, that rise in the north and set in the south or vice-versa, that move along circles of constant sky altitude as if we were at a pole, or jitter randomly on the sky.

The GBT and Parkes are able to stare at fixed altitude-azimuth positions to conduct drift scan surveys of the sky. It is also possible to do raster scan surveys where the telescope is tracked along “impossible” paths to map the sky quickly. The key difference is that we would analyze the data not as a scan moving across the sky, but as if the telescope’s celestial coordinates were fixed: we would look for signals that persist for the entire “observation” instead of rising and falling as the beam sweeps over them. We must also be aware that signals might spill in from the sidelobes of the beam.

We will not usually have control over where the dishes of MeerKAT are pointed. Nonetheless, we do have the power to electronically beamform within the primary field of view. We could move one commensal beam to a new random location in the field every millisecond, making jumps that are about a degree long in an instant. No celestial source could follow such a trajectory.

The use of “fake sources” is closely related to our extant techniques to constrain RFI in our radio observations. Bright RFI from elsewhere in the sky can impinge on the detector through the dish’s sidelobes. During observations, we employ an ABABAB (or ABACAD) strategy: we spend five minutes pointed at a target and then move to look at a different target for five minutes. We alternate between on- and off-target five-minute pointings for a total of three each. Signals that are detected through the sidelobes will appear in both the ON- and OFF-pointings, whereas a genuine signal that is not exceedingly bright will disappear in the OFF-pointings (Enriquez et al. 2017; Price et al. 2020). The advantage of using scans as “sources” compared to ON/OFF strategies is that we will be able to constrain systematic issues that persist for only a few seconds. A somewhat related strategy is possible on Parkes, where the multibeam receiver points at seven sky locations si-

multaneously. Interference coming in from the sidelobes will appear in several beams at once.³⁰

Analyzing the faux sources will require some updating of our metadata and software. In addition, the unphysicality of the simulated “sources” depend on their movement on the sky, which only is significant if the signals are prolonged. Thus, they are no better than the Control sample or random sky locations in looking for false positives in pulse searches. Other facilities interested in using the *Exotica Catalog* may not even have the capability to do raster scans. For these reasons, we maintain the Control sample as an easy to implement check for systematics.

7.4. *Technological sources: looking for trouble*

A final set of objects that could act as a check are the technology Prototypes (listed at the end of Table A1). Technology, particularly RFI, is the biggest source of false positives in SETI. Our observations of the technology Prototypes should build a small library of RFI for comparison with potential ETI candidates. Indeed, we already have serendipitous observations at the GBT that could contribute to such a library, including from GPS and Iridium satellites. Unlike the other Controls, when we look where we expect to see no signals, with these Prototypes, we are looking where we do expect to see a signal, one that confounds our other observations, to better understand our systematics.

Not all technological RFI can be studied in this manner, though. Aircraft and ground transmitters would not be covered by these observations. Nonetheless, satellites remain one of the biggest contaminants, and are likely to become much worse with the launch of Internet satellite constellations.

8. DISCUSSION OF THE FULL *EXOTICA CATALOG*

8.1. *Target demographics*

The full *Exotica Catalog* contains over eight hundred entries and more than seven hundred distinct targets. It is about one-third of the size of the I17 nearby stars and galaxies catalog, and thus observing all objects would represent a significant effort on our part. The targets are distributed across both hemispheres on the sky, with concentrations in Cygnus and the *Kepler* field within it, the Galactic Center and the inner Galactic Plane,

the Large Magellanic Cloud, and around the Virgo (and Coma) Cluster (Figure 2). The breakdown of the different catalogs into samples, into phyla, and objects we have already observed is given in Table 2.

Over 150 ($\sim 21\%$) distinct targets are in what Dick (2013) calls the Kingdom of the Planets: the minor bodies, the solid planetoids, and the giant planets. Two of the most important properties of these bodies – mass and stellar insolation – are plotted in Figure 3. The giant planets span over a factor of 100,000 in insolation (~ 20 in temperature for a constant albedo), and the solid planets span nearly as large of a range. The giant planets cover a full range of masses from super-Jovian to Neptunian and insulations from $\gtrsim 1,000$ Earth to 0.001 Earth. The solid planetoids we have chosen cover the range of temperate to hot temperatures and sub-Earths to super-Earths, with a tail of low-mass cold planetoids from the dwarf planets and large moons in the Solar System. Minor bodies, almost all from the Solar System, cover temperate to cold environments and a factor of over ten billion in mass.

The *Exotica Catalog* will allow us to conduct a thorough initial reconnaissance of the Solar System. All of the major planets³¹, all IAU-recognized dwarf planets, and most of the larger moons³² are included. But an even greater coverage of the Solar System comes from the inclusion of the minor bodies, which form the third-largest phylum in the *Exotica Catalog* ($\sim 12\%$). There are a great many minor body Prototypes, which comes from the use of fine types. This is partly because minor bodies form a large population that can be well-studied in the Solar System, but we include them also to ensure we examine objects from every region of the Solar System. The importance for SETI is the possibility of ETI probes in the Solar System, which may have gone unnoticed (Papagiannis 1978; Freitas 1985; Gertz 2016; Benford 2019; see also Wright 2018b; Schmidt & Frank 2019 for more extreme possibilities). Their radio presence will begin to be constrained with *Exotica Catalog* observations.

The phylum most represented in the final catalog is stars, with over 150 distinct targets ($\sim 21\%$). This is partly driven by the fine classifications we use in the Prototypes catalog, particularly with the main sequence divided into narrow spectral subtypes. The fact that we have already observed most of the main sequence Prototypes allow us this luxury, since we will not need to

³⁰ Sometimes, a bright celestial source can appear in multiple beams: the Lorimer et al. (2007) burst was detected in three beams through their sidelobes. Nonetheless, it was not detected in all of the beams simultaneously, allowing it to be localized to a position clearly in the sky.

³¹ In Saturn’s case, through its rings, which surround the planet.

³² The Moon, the Galilean satellites, all of the large Saturn moons except Dione and Rhea, Miranda around Uranus, Triton around Neptune, and Charon around Pluto.

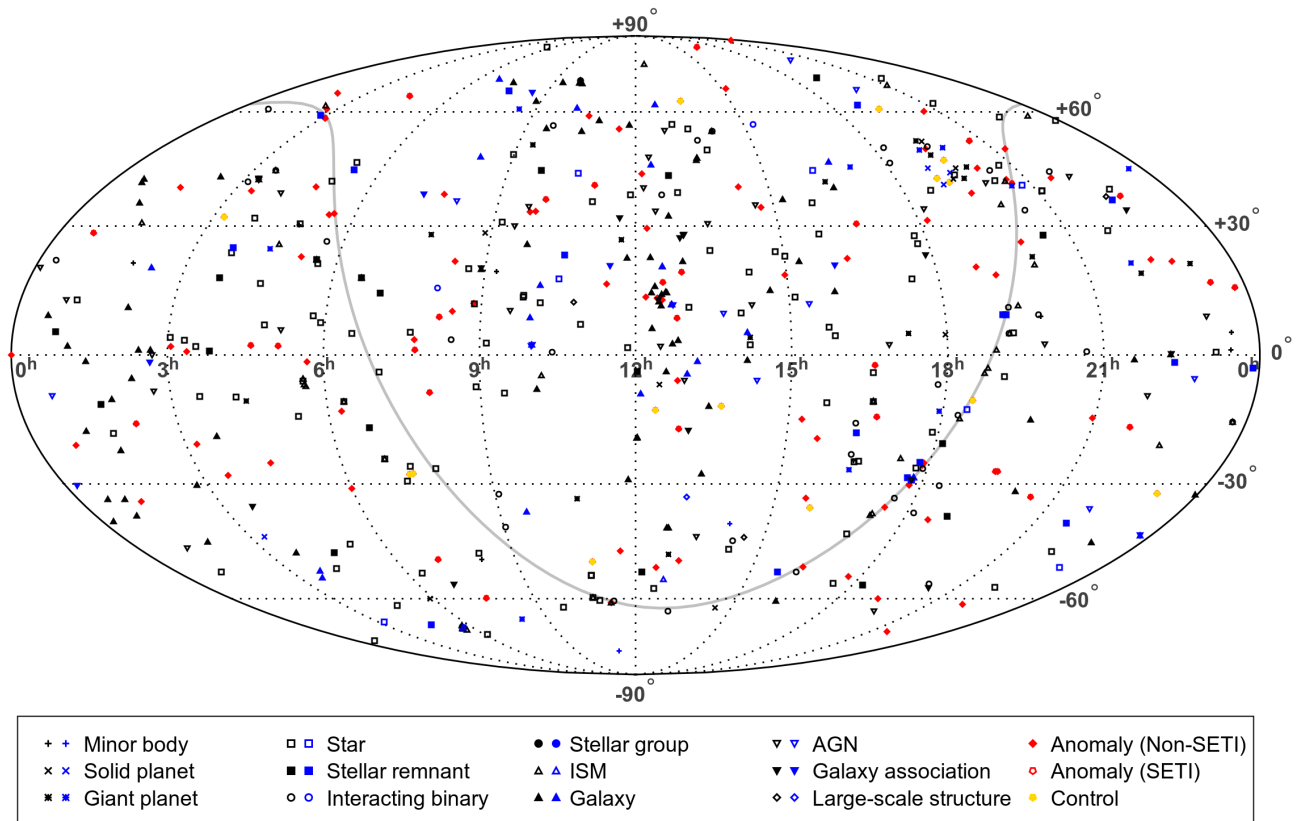


Figure 2. Map of objects in the *Exotica Catalog* in equatorial coordinates. Each phylum is given its own symbol, with Prototypes in black and Superlatives in blue. Anomalies are plotted in red and Control sources in gold. The plane of the Milky Way is shown as the grey curve.

repeat most of those observations (Enriquez et al. 2017; Price et al. 2020). Yet the stars also include a number of types not at all represented in I17. We see this in Figure 4, the color-magnitude diagram (CMD) and Hertzsprung-Russel (HR) diagram of stars in the *Exotica Catalog*. The *Exotica Catalog* expands the coverage of Breakthrough Listen to include supergiants and hypergiants at the top of the diagram, a region of parameter space entirely missed by the I17 sample. O dwarfs are finally covered as well. Sprinkled around the diagram are some unusual stellar types that result from binary evolution, which swell the ranks of stars in the Prototypes sample. Among them are the hot subdwarfs (sdB and sdO), which sit in between the white dwarfs and hot main sequence on the left of Figure 4. The *Exotica Catalog* also includes some star types that are unusual in ways other than where they sit on the HR diagram, like hypervelocity stars. Not shown in the color-magnitude diagram are brown dwarfs, mostly invisible in optical light, which supplement the ones observed in Price et al. (2020).

Collapsed stars and interacting binary stars are smaller phyla, each with about forty-five objects ($\sim 6\%$).

Collapsed stars have relatively few entries in the Prototypes sample – they broadly fall into white dwarfs, neutron stars, and the hard-to-observe black holes – but the compact objects power a rich variety of interacting binary stars. There are also about as many Superlative collapsed stars as Prototypical ones, especially since the well-studied pulsars allow for precise studies of their properties. The *Exotica Catalog* includes five symbiotic systems, twelve cataclysmic variables and related white-dwarf powered binaries, and twenty X-ray binaries. These sources have been practically ignored in SETI, but they are among the most powerful and dynamic objects in our Galaxy and others. Including them allows us to start probing the idea that they draw energy-hungry ETIs. These extreme objects are also good bets to look for other new astrophysical phenomena. A few more collapsed stars in detached binaries reside among the stellar associations.

Stellar groups and the ISM are also smaller phyla ($\sim 6\%$). Even within the Galaxy, the simple open/globular cluster divide is supplemented by division of the globulars into distinct populations and the inclusion of Superlative clusters. Observations of other galaxies have

Table 2. *Exotica Catalog Summary*

Property	Prototypes	Superlatives	Anomalies		Control	Total
			Non-SETI	SETI		
Entries	540	177	98	36	14	865
Distinct	488	147	89	33	14	737
...Minor body	73	13	6	0	0	88
...Solid planetoid	27	21	2	2	0	37
...Giant planet	18	12	2	0	0	31
...Star	108	15	19	13	4	152
...Collapsed star	23	21	4	0	1	45
...Interacting binary star	42	3	0	0	0	44
...Stellar group	26	15	8	1	1	48
...ISM	39	6	1	0	0	45
...Galaxy	79	22	3	10	0	113
...AGN	33	12	7	0	0	52
...Galaxy association	14	9	0	0	1	23
...LSS	3	1	1	0	0	5
...Technology	15	0	0	0	0	15
...Unknown	0	0	39	9	0	47
...Not real	1	0	0	0	6	7
...Other	0	1	0	0	1	2
Solar System	96	26	5	0	0	112
Sidereal	392	121	84	33	14	625
I17 stars	39	2	1	1	1	44
I17 galaxies	15	0	1	0	0	16
Other BL observed	2	1	3	1	0	5
New targets	432	144	84	31	13	672

NOTE—Entries that are cross-listed in two different phyla are counted in the number of distinct targets in each phylum.

revealed star clusters different from those in the Galaxy, and have identified a number of Superlative clusters with densities and masses far more extreme than anything nearby. To these are added detached stellar multiples and unbound stellar associations. The ISM includes a panoply of clouds in different phases and on different scales. Because of its diffuse nature, though, some of its most important features cannot be divided into discrete targets or are not practical to observe, particularly large structures of hot gas like the Local Bubble (Snowden et al. 1990). A variety of energetic phenomena drive a similar variety of expanding bubbles. We note the inclusion of cosmic ray ISM features, particularly the Cygnus Cocoon (Ackermann et al. 2011).

Galaxies form the second largest phylum ($\sim 15\%$). Even though we use a relatively coarse division along the Hubble (1926) “tuning fork”, they are supplemented by a rich variety of subtle morphological features (Buta et al. 2015) and peculiar galaxies (c.f., Arp 1966). In fact, about one-fifth of the galaxy prototypes simply cover disk galaxy morphologies, such as lenses and rings. Just as some abnormal stellar types are the result of binary interactions, we have peculiar galaxy types from their own interactions. High redshift galaxies only in-

crease the panoply, as do the technosignature candidates identified by previous SETI studies.

Figure 5 summarizes their gross properties, mass and color. Included galaxies span a factor of $\sim 10^{10}$ in stellar mass. In terms of gross properties, I17 samples much of the same parameter space, and in fact includes many more faint red (dwarf spheroidal) galaxies. Note however that we were unable to find data to plot certain extreme dwarf galaxies like Segue 1, which are far smaller than the ones in I17. We also are excited by the outliers in the CMD, particularly IC 1101 (red circled dot at far right), the Leoncino dwarf (black cross-dot at lower left), and NGC 4650A (isolated black dot at lower right). More profound differences are visible in the mass-SFR diagram, where highly star-forming galaxies stand out with respect to the I17 sample, particularly those at high redshift (open circles) and dwarf starbursts (purple dots at center-left), as does Coma P (circled blue dot in lower-left) and the Leoncino dwarf. These are entirely new regions of parameter space to SETI.

Active galactic nuclei ($\sim 7\%$) and galaxy associations ($\sim 3\%$) are among the smaller phyla. We might have gone with finer AGN classifications, with Padovani et al. (2017) noting several dozen types posited over the years,

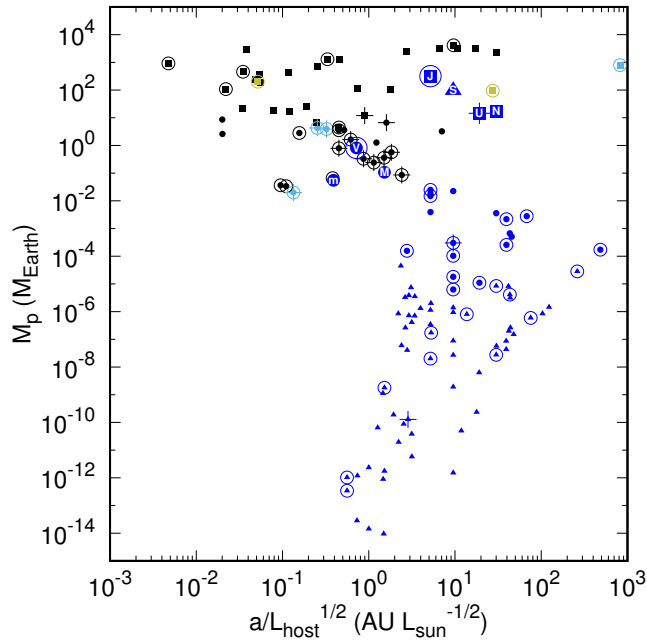


Figure 3. Diagram of planetary mass and stellar insolation for planets in the *Exotica Catalog*. Solar System bodies are marked in deep blue, those around stellar remnants in sky blue, and those around protostars in gold. Minor bodies (including planets hosting ring systems) are denoted by triangles, solid planetoids by circles, and giant planets by squares. Bodies in the Superlative sample are marked by a ring around them, and those in the Anomaly sample are marked by an overlaid cross.

but as per [Padovani et al. \(2017\)](#), we did not wish to cloud the Prototypes list with a menagerie of mostly overlapping types. On the other hand, galaxy associations have a richer (if small) representation than might have been expected. A galaxy cluster, being virialized, can support some intriguing phenomena in its intra-cluster medium. Superlative galaxy associations almost match the number of Prototypes, and include several rich galaxy clusters, which are unexplored in SETI.

The smallest phylum is large scale structure ($< 1\%$). Its variety is limited because it has only begun to form. Furthermore, superclusters, walls, and voids have poorly defined boundaries and cover vast areas on the sky, and are excluded similarly to much of the ISM and IGM. We do include the Great Attractor, formerly a striking anomaly, in the form of the Laniakea basin of attraction ([Tully et al. 2014](#)). Also included is the superlative Shapley Supercluster, the densest and richest region in the local Universe. This supercluster is a massive collection of rich galaxy clusters, and has bound a region over 10 Mpc in radius; its gravitational pull actually entirely subsumes the flow from the Great Attractor ([Kocevski & Ebeling 2006](#); [Chon et al. 2015](#); [Hoffman et al. 2017](#)). It

is an exceptional place for aspiring Kardashev Type IV ETIs, and it will evolve into one of the most outstanding “island universes” as the accelerating cosmic evolution cuts off long-distance travel over the next trillion years ([Heyl 2005](#)).

Finally, about seventy ($\sim 10\%$) targets stand apart from the conventional astrophysical phenomena. Two thirds of them ($\sim 6\%$ of the catalog) are unidentified, consisting of both SETI-related and non-SETI related Anomalies. Another fifth, in the unique phylum of technology, consists of our own technosignatures, which we may someday extend with non-Earthly examples. Nine spurious and miscellaneous targets complete the Catalog.

Further discussion of specific issues in classification are in the Appendices [A](#) (Prototype), [B](#) (Superlative), [C](#) (Anomaly), and [D](#) (Control). More extensive notes on the entries in the catalog and their selection will be available online.³³

We note that the entries in the catalog are not all independent entities. Some are collective objects that contain other entries in the catalog, or are “siblings” in the same cluster. In addition, some “new” objects in the *Exotica Catalog* are related to objects in the I17 catalog. Examples include the several objects located in the Virgo Cluster, which itself is a Prototype. In these cases, one observation may actually cover several objects, and they can be treated as all one object. [Table E3](#) lists these relationships.

8.2. Catalog presentation

The objects in the catalog are listed in [Table E1](#) (targets within the Solar System) and [Table E2](#) (sidereal targets outside the Solar System). Each distinct source has been assigned a unique identifier of the form **XNNN**, where **X** is an abbreviation standing for the first sample the object belongs to (“P” for Prototypes, followed by “S” for Superlatives, “A” for non-SETI Anomalies, “E” for ETI candidate Anomalies, and “C” for Controls). These tables also include basic data about the sources, with references discussed in [Appendix E.1](#).

In addition, we will host an online database on the *Exotica Catalog* sources. The database will include detailed notes motivating our selection of a particular object, links to the object on Simbad or other databases, and references for the object and its type.

9. ALL-SKY AND RANDOM SURVEYS

The least biased strategy of when and where to look is to look everywhere all the time, with an all-sky sur-

³³ <http://seti.berkeley.edu/exotica>

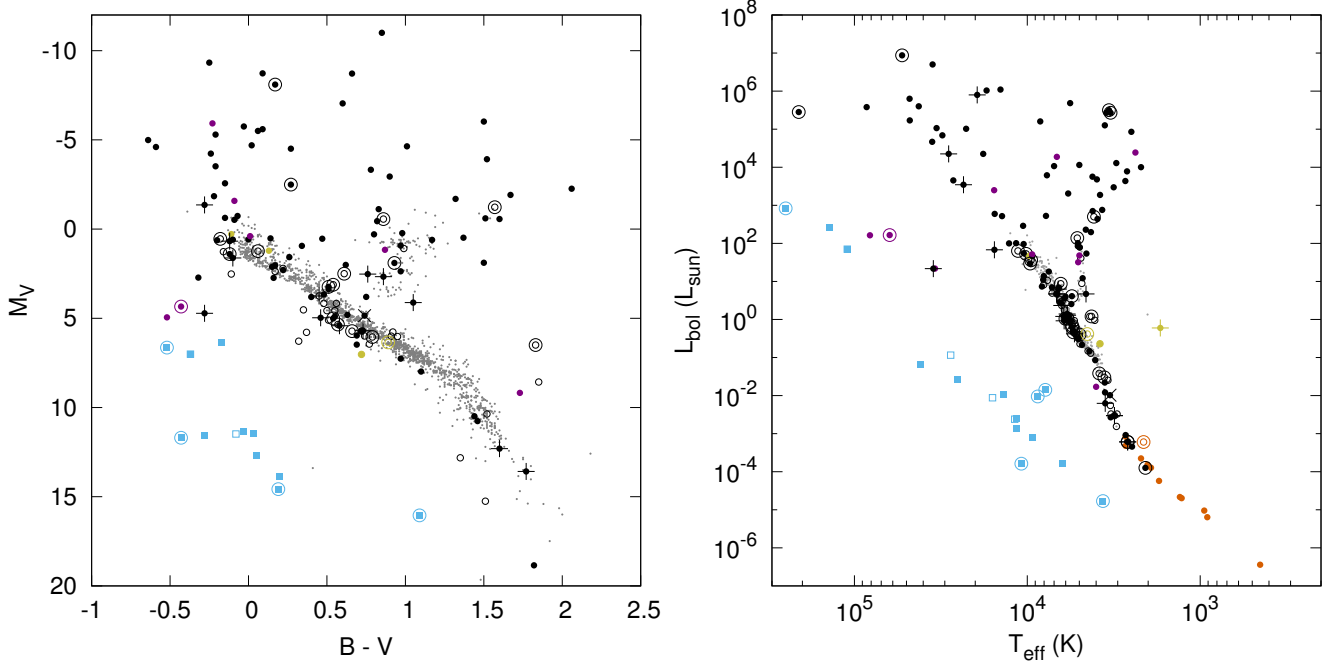


Figure 4. Color-magnitude (left) and HR (right) diagram of stars (circles) and white dwarfs (sky blue squares) in the *Exotica Catalog*. Protostars and pre-MS stars are colored gold, brown dwarfs are dark orange, and post-interaction stars are dark violet. The hosts of exoplanets are also included as open circles (stars) or open squares (white dwarfs). Stars in I17 are shown as grey dots. Superlatives and Anomalies sources are marked as in Figure 3.

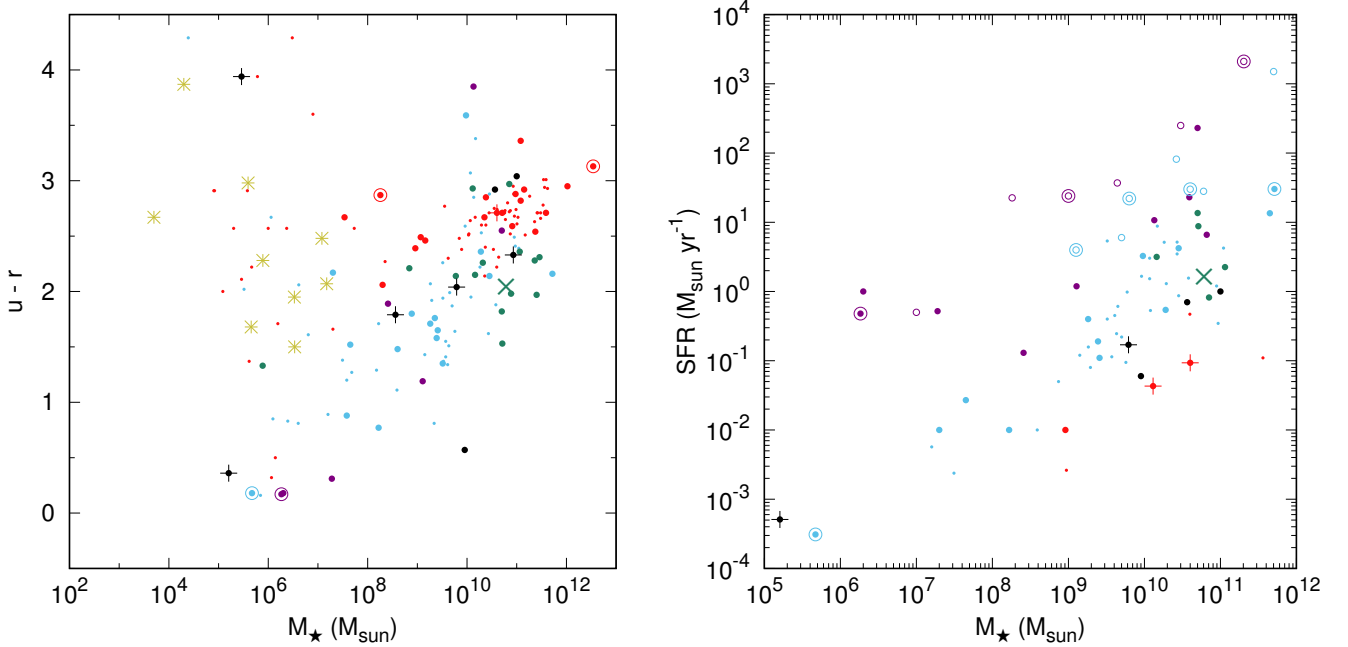


Figure 5. Mass-color (left) and Mass-SFR (right) diagram of galaxies in the *Exotica Catalog* for which we could find or derive data. Galaxies classified as quiescent are shown in red, Green Valley galaxies in dark teal, main sequence galaxies in sky blue, and starbursts in dark violet. Samples are marked as in Figure 3. Galaxies in other categories are classified according to morphological type, with the remainders in black. We also show I17 galaxies as small dots, and the Milky Way as the big teal X. For the mass-color diagram, we include star clusters as gold asterisks, but exclude galaxies with $z \geq 0.1$ due to k -correction effects. High-redshift galaxies are included in the mass-SFR diagram: those with $z < 0.5$ are marked with filled dots, and those with $z \geq 0.5$ are marked with open circles.

vey. Even if ETIs inhabit objects we haven’t even detected yet, we would still be able to see their activities. Similarly, we would be able to look for natural objects that are completely unanticipated in our current paradigms (Wilkinson 2016). Since the sky has already been mapped across the spectrum, such unanticipated sources either are intermittent, very faint, or are unrecognized in current data sets.

The need for all-sky all-the-time surveys has been recognized in SETI and other fields of astronomy. Ideally, we would be able to keep the data permanently from such sources. This would both allow us to do searches for precursors when an anomalous event is triggered, or to find anomalies years later in re-analyses. At present, no radio SETI facility exists with all these capabilities, despite the strong possibility that any “beacons” have a very low duty cycle to conserve energy. In the future, dipole arrays may be constructed to fulfill this purpose (Garrett et al. 2017). In the optical and the near-infrared, the Pano-SETI experiment aims to monitor several steradians instantaneously for short pulses (Cosens et al. 2018). Outside of SETI, there are multiple instruments with wide-field high-cadence capabilities in the optical (Law et al. 2015), X-rays (Krimm et al. 2013), gamma-rays (Atwood et al. 2009; Abeysekara et al. 2017), neutrinos (Aartsen et al. 2017), and gravitational waves (Abbott et al. 2019a).

Wide-field facilities allow us to set meaningful constraints on unanticipated events at the present. Very wide-field capabilities are already granted by LOFAR and MWA (e.g., Tingay et al. 2016, 2018a), and have been used for serendipitous constraints (Tingay et al. 2018b). MeerKAT, an array of 64 dishes of aperture 13.5 meters, will allow us to synthesize dozens of commensal beams within the relatively large primary field of view. It will be possible to devote one beam to painting the entire primary dish field over and over, a miniature wide-field survey that is open to finding truly unknown sources at unknown locations. The Breakthrough Listen backend will also perform incoherent summing of the dish voltages during observations. Despite having less sensitivity (S_ν larger by a factor of 8), the entire primary dish beam is covered, an instantaneous field thousands of times larger than a single synthesized beam. The incoherent summing will be our first steps towards all-sky surveys, which have the maximal breadth allowed. Because it needs to observe the extended Cherenkov light of air showers produced by gamma-rays, VERITAS always has a relatively wide field-of-view (Weekes et al. 2002). However, neither telescope’s pointings are uniformly distributed across the sky.

A more limited unbiased search that is possible even on narrow field of view telescopes is to point at random targets on the sky. Some completely random positions on the celestial sphere can be added as a supplement to the *Exotica Catalog*; they may be observed like any other target or with long integration times as a “pencil beam” survey to achieve sensitivity to faint flux levels or very intermittent sources. This will also be possible with MeerKAT, which will perform long targeted observations of some sky regions during its nominal science operations. We could devote synthesized beams to a random point in the dish field to do a pencil beam survey with every observation.

The final possibility – that anomalies already are present in extant datasets – calls for keeping data until such time as innovative analyses can find them. There has been plenty of precedent for this scenario: the long-term variability of Boyajian’s Star was recovered in *Kepler* data (Montet & Simon 2016); the Lorimer burst, the first reported FRB, happened in 2001 but was not reported until Lorimer et al. (2007); the first ANITA upwards neutrino shower was not reported for three years after its detection (Gorham et al. 2018). Breakthrough Listen is devoted to making its data publically available in accessible formats (Lebofsky et al. 2019). Moreover, on the analysis side, we are pursuing research in using machine learning to classify signals and look for anomalies (e.g., Zhang et al. 2019). These have the potential of evading our biases.

10. EXOTICA EFFORTS AND BREAKTHROUGH LISTEN

As noted in Section 2.3, Breakthrough Listen’s exotica efforts will include both observations of the targets in the Catalog and a flexible series of campaigns. In this section, we briefly discuss our engagement with exotica with both approaches.

10.1. Strategy for observing the Exotica Catalog

The full *Exotica Catalog* includes over seven hundred distinct sources, nearly 40% of the number of targets in the I17 list. Priority is given to the I17 targets, however, with the *Exotica Catalog* nominally getting $\lesssim 10\%$ of telescope time. This is especially a problem since many of the sources are extended. An additional constraint is disk space, which prohibits keeping the raw voltages from radio observations of the entire Catalog. We present some strategies for dealing with these issues, which may be useful to other programs aiming to observe the *Exotica Catalog*.

The core of our strategy is to develop a prioritization system for the targets. With GBT, Parkes, and APF, we

are free to select targets without the constraints of commensal observing. Furthermore, the GBT has a number of frequency bands to observe in, and we can choose which ones to emphasize. Thus, we do not need to carry out the full suite of observations we perform on the I17 stars and galaxies, and conversely we can spend more time on high-priority targets. Table 3 breaks down the radio data products for one possible prioritization plan, as might be implemented on the GBT. If all objects and all bands are observed with this plan, the *Exotica Catalog* would take ~ 800 hr to observe and would generate ~ 1.8 PB of data (~ 1.5 PB of filterbank files). For comparison, the $\sim 1,700$ stars in the I17 catalog observed in all bands would take $\sim 8,000$ hr and would generate 14 PB of data. The amount of time spent at each rank is 150–300 hr. Restricting our *Exotica Catalog* efforts to the low- and mid-frequency bands observed in Price et al. (2020) would roughly halve the observing time, mostly spent on low priority targets.

As yet, prioritization is subjective. We intend to favor extreme phenomena: those with high luminosities and nonthermal emission across the spectrum. These are more likely to display new astrophysical phenomena. Higher luminosities also make them better suited for modulation as beacons by ETIs. Thus, we will include proportionally more pulsars, interacting binaries, and AGNs. We specifically will put maximum priority on the primary calibrators at radio frequencies and high energies: Cygnus A and the Crab Nebula, respectively (Perley & Butler 2017; Kirsner et al. 2005). The Crab Nebula specifically is known to flare (Wilson-Hodge et al. 2011; Tavani et al. 2011; Abdo et al. 2011). Another thing we have in mind is to achieve the widest breadth in astrophysical environments and object type. We will assign high-to-maximal priority to at least one object of every phylum priority list. We also intend to prioritize Superlatives with extreme luminosities and several Anomalies.

The APF is capable of collecting high resolution spectra of exotica targets. Target acquisition is challenging for targets fainter than $V \sim 12$ and those with large motions across the sky. As such, we expect to only be able to observe a limited subset of the catalog. Such a search for narrow wavelength signals would be different than that in Lipman et al. (2019) since the targets are producing almost no astrophysical optical signal.

Our time on MeerKAT and VERITAS is commensal; thus, we will be unable to choose where the telescopes are pointed or prioritize different targets. Some of the Southern targets are likely to be primary-user targets of MeerKAT during its nominal observations. In these cases, we will be able to re-use the primary synthesized

beam data for our observations. Others will likely enter the field of view during large sky area surveys. Additionally, Breakthrough Listen’s backend will allow us to form dozens of commensal beams within the dish field of view. While most of these beams will be dedicated to the one million star effort of Breakthrough Listen, several will typically be available for exotica observing efforts. From time to time, we may substitute a suitable object in the MeerKAT field for a given Prototype by using supplementary catalogs. VERITAS has a wide field of view, with diameter of several degrees (Weekes et al. 2002). Many of the objects in the *Exotica Catalog* have been primary targets of VERITAS. Others are clustered near the targets, like M81 and NGC 3077 near M82 (VERITAS Collaboration et al. 2009), or the galaxies in the Virgo and Perseus Clusters (Acciari et al. 2008, 2009). Thus, for many of the Northern *Exotica Catalog* targets, it will simply be a matter of collecting VERITAS’s commensal observations and organizing them.

The large angular extent of many of the objects in the catalog pose another challenge, especially in high-frequency radio observations where the beams of the telescopes are very small. It would be impractical to map the full extent of the sources with the GBT and Parkes. For the low priority sources, we will observe only the core or flux peak of the target, as a proxy for the potential for activity. There will be additional pointings for higher priority sources, resource permitting, generally including two at the ends of the semimajor axis. In some cases where there are multiple well-defined interesting spots, we will target these (e.g., the hotspots of radio galaxies). Parkes’ multibeam receiver will also be useful, since it covers seven times the sky area, although its frequency range is limited. The electronic beamforming capabilities of MeerKAT will afford us more flexibility; we will be able to dedicate a synthesized beam to “painting” the entire primary field of view, allowing us to construct low sensitivity maps. The APF’s nominal field of view of 1 square arcsecond will limit its use for extended exotica objects. VERITAS should be able to observe all but the largest targets in their entirety at any given moment.

Another part of our strategy will be to opportunistically take advantage of available time. As we complete observations of the I17 sample with our main radio facilities, the GBT and Parkes, more time will be freed up for exotica. Another tactic is to make use of the ON/OFF strategies we use to constrain RFI: we can use an exotica source as an OFF-source during observations of a program star or vice-versa, whereas previously we have used stars. The OFF observations themselves can be used for technosignature searches, using the ON-observations to

Table 3. Example prioritization system

Rank	Count	Total data	Filterbank products	Raw voltages	Observed bands	Extended target strategy
Maximal	12	~ 0.6 PB	3 × 5 min ABACAD	5 min in a low-, medium-, and high- ν bands for at least one pointing	All	~ 5 pointings, including core and axes
High	30	~ 0.4 PB	3 × 5 min ABACAD	1 min in medium-frequency band for one pointing	All (one pointing), three (other pointings)	~ 3 pointings
Medium	60	~ 0.3 PB	3 × 5 min ABACAD	None	Three	~ 3 pointings
Low	~ 600	~ 0.5 PB	As available	None	Single	1 pointing

NOTE—The ABACAD (and related ABABAB) strategies) involve pointing the telescope on- and then off- target to constrain RFI; see [Price et al. \(2020\)](#) for further information. The data rates assume that half the objects at each rank are extended, for an order-of-magnitude estimate.

check for RFI ([Price et al. 2020](#)). Additionally, the remaining GBT observations are mostly at high frequency, and are sensitive to the weather. When weather conditions preclude high frequency observations, we can observe exotica sources at low frequency. A similar strategy may be employed at other facilities, perhaps taking advantage of time when the Moon is up for at least the brighter sources.

Finally, some of the targets in the *Exotica Catalog* have already been observed as part of previous studies. These will not need to be re-observed. This too could be adapted to other facilities, adapting the catalog to include sources that have already been covered.

10.2. *Exotica campaigns and Breakthrough Listen*

Several focused programs to observe unusual classes of objects have been completed, and more are ongoing. These single- or few-target campaigns are complementary to both our primary high-count effort in observing stars and galaxies over a hundred nearby galaxies and also the high-breadth catalog. These have included:

- *Interstellar asteroids: A test case for SETI* – The interstellar objects 1I/'Oumuamua (['Oumuamua ISSI Team et al. 2019](#)) and 2I/Borisov ([Guzik et al. 2020](#)) were observed by us as they passed through the Solar System. Starfaring ETIs might very slowly diffuse through the galaxy by hitching rides on comets. More pragmatically, our observing campaigns for 1I/'Oumuamua and 2I/Borisov act as rehearsals if a convincing ETI probe is detected. The 'Oumuamua observations included two hours each in L, S, C, and X-bands, allowing us to cover the entire rotation cycle of the object to an EIRP sensitivity of 0.08 W, comparable to some Bluetooth or WiFi transmitters ([Enriquez et al. 2018](#)). We also observe Solar System asteroids that have been postulated to be captured interstellar objects, the first being the observation

of (514107) 2015 BZ₅₀₉ on Parkes for ten minutes of total integration ([Price et al. 2019b](#)). These observations are being supplemented by observations of other candidate captured interstellar objects, effectively adding a new class of objects to the Breakthrough Listen program.

- *FRB 121102 and other FRBs: Transient astrophysics* – The Breakthrough Listen backend can also be applied to phenomena thought to be natural. In [Gajjar et al. \(2018\)](#), we observed the repeating FRB 121102 with the backend on the GBT for an entire hour. On average, one burst was detected every three minutes, achieving the highest frequency detections of the anomalous object; we also independently confirmed the high rotation measure discovered by [Michilli et al. \(2018\)](#). The long time devoted to these observations allowed us to observe and characterize many bursts, which would not have been possible with a five minute observing time. This highlights the advantage of the flexible nature of campaigns, allowing us to achieve high depth. The backend of Parkes was able to record a real-time fast radio burst, FRB 180301, in commensal mode ([Price et al. 2019a](#)). Significantly, we were able to capture raw voltages on this anomalous object, greatly increasing the analysis possibilities. We expect to observe other FRBs in the future.
- *Ultracool dwarfs: Extending I17* – We have devoted time to specifically observe five nearby ultracool dwarfs of spectral types late M to early Y with Parkes, as reported by [Price et al. \(2020\)](#). The observations of each object was otherwise similar to those of the stars in the catalog. The purpose of these observations was to extend the completeness of I17, effectively supplementing it with a new object type. In the future, it might be possible to

further increase the I17 catalog’s breadth by running short campaigns on other object classes, such as nearby white dwarfs (c.f., [Gertz 2019](#)).

- *SETI campaigns on stars: Following up on SETI candidates* – Campaigns have also been undertaken on the facilities to test claims of technosignatures. [Borra & Trottier \(2016\)](#) reported the existence of a spectral comb in the Sloan spectra of dozens of Sun-like stars, which they interpreted as resulting from coherent pulses repeating on picosecond timescales. The two brightest of these stars were observed with the APF, but no signs of a spectral comb were found in the spectra ([Isaacson et al. 2019](#)). Other campaigns to follow up on individual objects that have been noted by SETI researchers include optical observations of Boyajian’s Star with VERITAS ([Lipman et al. 2019](#)), radio observations of the Random Transiter ([Brzycki et al. 2019](#)), and radio follow up of an ETI candidate signal from Ross 128 ([Enriquez et al. 2019](#)). These observations were scheduled rapidly, within four days for Ross 128. With campaigns, new high-priority targets can be followed up rapidly, without waiting for the catalog to be updated.

These efforts demonstrate the uses of campaigns to supplement the *Exotica Catalog*: (1) rapid follow-up of new and time-sensitive discoveries; (2) deep observations of high-priority targets; (3) supplementing the primary program to expand its breadth; and (4) moderate count programs of unconventional targets. These advantages should apply to other programs as well.

11. SUMMARY

Breakthrough Listen intends to spend $\sim 10\%$ of its observing time on exotic objects. There are many reasons to search for technological intelligence in unconventional places. Unearthlike or nonbiological entities will not be constrained to live in Earthly habitats hospitable to lifeforms like us. It is also conceivable that some kinds of seemingly natural phenomena are the result of alien engineering. Yet there are good motivations for observing unusual objects even if ETIs cannot possibly live there. Extreme, energetic objects are more likely to produce unusual signals, particularly transients, that might be confused with artificial signals. Breakthrough Listen has unique instrumentation, and observation of a broad range of objects would benefit the general astronomy community. Finally, there could be unaccounted for systematic errors in our systems that give false positives. Observing exotic objects and empty regions on the sky allow us to constrain these possibilities.

Whereas the nearby star and galaxy catalogs aim for depth and high count, efforts to look for exotica can be more broad, trying to peek at everything that might be interesting. Breakthrough Listen’s approach to exotica is twofold. First, from time to time, we have dedicated programs that observe one to a few objects of one class. Although we sample only a few types of object this way, these types are very diverse. Efforts include observations of the interstellar minor body ‘Oumuamua, and the repeating fast radio burst FRB 121102. By focusing these efforts on just a few objects, we can achieve deep sensitivity with the long integration times devoted to them.

The other prong is the *Exotica Catalog*, which is the main focus of this paper. The *Exotica Catalog* aims to achieve the widest possible breadth, including the most diverse range of celestial phenomena possible. The catalog itself contains four samples:

- The Prototype sample includes an archetypal object of each type of astrophysical phenomenon.
- The Superlative sample list record-breaking objects with the most extreme values of basic properties like mass.
- The Anomaly sample contains objects and phenomena that are inexplicable by current theories, including candidate positive events from other SETI efforts.
- A small Control sample includes objects once thought to be anomalous or noteworthy but that turned out to be banal or non-existent, and will be used as a check on systematics and to rehearse observations.

There are 737 objects in the total *Exotica Catalog*, which are sorted into different levels of priority. About a dozen sources will be observed with maximum priority and will include raw voltage data in multiple bands. Most will be low priority and will be observed as allowed by time.

We hope that the *Exotica Catalog* will prove useful to other efforts, both within SETI and outside it, in characterizing the whole panoply of objects in the known Universe.

ACKNOWLEDGMENTS

Breakthrough Listen is managed by the Breakthrough Initiatives, sponsored by the Breakthrough Prize Foundation.

This work would not have been possible without the extensive use of a number of online databases. It has made thorough use of the SIMBAD database, the VizieR catalogue access tool, and the cross-match service XMatch, all operated at CDS, Strasbourg, France. We have also benefited immensely from the NASA Astrophysics Data System Bibliographic Services and the arXiv preprint server. This research has made use of the NASA/IPAC Extragalactic Database, which is funded by the National Aeronautics and Space Administration and operated by the California Institute of Technology.

APPENDIX

A. THE PROTOTYPE SAMPLE

A.1. *Minor bodies*

We classify Solar System minor bodies according to both orbital family and composition, with a small number of additional subtypes. Minor bodies of specific compositions might be selected by ETIs for mining (c.f., Papagiannis 1978). From a SETI perspective, orbital families might be targeted by ETI probes to provide a unique vantage point on bodies like the Earth, or because they are dynamically stable for long periods of time and could accumulate a large number of artifacts (e.g., Benford 2019). There is a large overlap in some cases (as in DeMeo & Carry 2014), as with the E-belt and E-type asteroids, for which we use the same Prototype.

For asteroids, our spectral-type system is largely taken from Tholen (1984) (see also Tedesco et al. 1989). We selected those types considered the most significant by Tholen (1984), adding those unique to one or a few members. Some intermediate classes that blend into larger “complexes” in the more recent Bus & Binzel (2002) taxonomy were omitted. In choosing the Prototypes, we were guided by the classifications of Tholen (1984), Tedesco et al. (1989), and Bus & Binzel (2002).

The comet orbital classifications were informed by Levison (1996).

“Icy bodies” refer to outer Solar System bodies beyond the Jupiter Trojans that are not comets. The spectral type system is that of Barucci et al. (2005) and Fulchignoni et al. (2008), with the latter guiding our Prototype selection. The division into orbital groups is based on the system in Gladman et al. (2008), which we consulted especially when selecting Scattered Disk and Detached objects. We aimed to select Prototypes that are almost certainly minor bodies and not dwarf planets, as indicated by a “probably not dwarf planet” designation on Mike Brown’s website.³⁴

The small classification system for satellites into regular, irregular, and “collisional shards” in Burns (1986) informs our classification.

Hughes et al. (2018) informed our grouping of debris disks into cold, warm, and hot/exozodis.

A.2. *Solid planetoids*

Planets were classed according to size and stellar insolation. *Kepler* result papers classifies planets by radius into: Earths ($< 1.25 R_{\oplus}$), Super-Earths ($1.25\text{--}2 R_{\oplus}$), Neptunes ($2\text{--}6 R_{\oplus}$), Jupiters ($6\text{--}15 R_{\oplus}$), and non-planetary ($> 15 R_{\oplus}$) (Borucki et al. 2011; Batalha et al. 2013). We adjusted this scheme by: (1) setting the boundary between solid super-Earths and giant Neptunes at $1.5 R_{\oplus}$, except when density is known (Rogers 2015; Fulton et al. 2017); (2) adding a sub-Earth category for radii $< 0.75 R_{\oplus}$ to cover planets like Mars where the habitability prospects are likely different (e.g., Wordsworth 2016); (3) using the Weiss & Marcy (2014) relation to translate the radii categories into mass categories when no radius is available, using the mean $\sin i$ of $\pi/4$ as a guide. The mass categories for solid planetoids are sub-Earths ($\lesssim 0.4 M_{\oplus}$), Earth ($\sim 0.4\text{--}2 M_{\oplus}$), and super-Earths ($\sim 2\text{--}4.5 M_{\oplus}$, unless densities are known).

We use the terms “hot”, “warm”, “temperate”, and “cold” to group by insolation. Cold planets are outside the conventional habitable zone (roughly taken to be $\lesssim 0.25$ Earth), temperate planets are within the conventional habitable zone ($\sim 0.25\text{--}2$ Earth), warm planets are interior to the habitable zone but with insulations $\lesssim 100$ Earth, and hot planets have insulations $\gtrsim 100$ Earth. The distinction between “warm” and “hot” carries over from the giant planets, where warm planets around Sunlike stars are defined by period or semimajor axis (Dong et al. 2014; Huang et al. 2016; Petrovich & Tremaine 2016).

Dwarf planets in the Solar System are classed according to the spectral type and orbit, similarly to minor bodies (Appendix A.1).

We added a “geological” classification intended to very roughly sample the diversity of surface environments and histories in the Solar System, excluding the Earth itself.

A.3. *Giant planets*

Giant planets are classed according to insolation and size (see Appendix A.2). Where possible we use densities to distinguish between ice giants and gas giants. We also added a “Superjovian” category to cover a better range of

³⁴ <http://web.gps.caltech.edu/~mbrown/dps.html>

planetary masses. In the literature, the minimum mass for “superjovians” has been defined as 1, 3, and 5 M_J (Clanton & Gaudi 2014; Johnson et al. 2009; Currie et al. 2014). We arbitrarily are guided by a threshold of $\sim 3 M_J$, and allow $M \sin i$ values of 2–10 M_J .

A.4. Stars

Our estimation is that the major distinction between different types of stars is based on evolutionary stage and stellar mass.

Low mass protostars and pre-main sequence stars are classed numerically in the literature as 0, I, II, and III according to obscuration, where II and III correspond to T Tauri stages (Lada 1987). We retain the distinction between class 0 and 1 protostars and T Tauri stars. High mass protostars are given their own categories.

Sub-brown dwarfs are too small to have fused deuterium but are believed to have formed similarly to stars (Caballero 2018).

Brown dwarfs and main sequence (MS) stars are classed by Harvard spectral type. Each spectral type is divided into early (0-3), mid (4-6), and late (7+) subdivisions. Where possible we chose spectral standards as Prototypes (Morgan & Keenan 1973; Kirkpatrick et al. 1991; Walborn et al. 2002; Kirkpatrick 2005; Burgasser et al. 2006). We also favored stars in I17, because we have already observed a wide range of B through mid-M dwarfs. For brown dwarfs, we also tried to choose those with a mass that was clearly below the hydrogen-burning limit.

Covering post-MS evolution is more complicated. Stars that are actually in distinct evolutionary stages can appear on the same place in the HR diagram, such as the red giant branch and the asymptotic giant branch. To start, we divided post-MS stars into mass groups with qualitatively different evolution:

- *Very low mass stars* (initial mass $\lesssim 0.2 M_\odot$) are not predicted to have a red giant phase, but no isolated post-MS examples are known (Laughlin et al. 1997)
- *Low mass stars* (initial mass $\sim 0.2\text{--}2.2 M_\odot$) pass through a red giant branch (RGB) phase terminating in a degenerate helium flash. The RGB star rapidly ($\ll 10^6$ yr) transitions to a Core Helium Burning (CHeB) phase before ascending the Asymptotic Giant Branch (AGB). The ultimate remnant is a CO white dwarf.
- *Intermediate mass stars* (initial mass $\sim 2.2\text{--}7 M_\odot$) ascend the RGB but do not have a helium flash, settle gradually into the CHeB phase, possibly executing a “blue loop”, before ascending the AGB. The ultimate remnant is a CO white dwarf (Karakas & Lattanzio 2014).
- *Transitional mass stars*³⁵ (initial mass $\sim 7\text{--}11 M_\odot$) proceed similarly to the intermediate mass stars until the end of the AGB phase, whereupon they begin carbon burning as a super-AGB phase. Those with lower mass end as an ONeMg white dwarf, while larger ones may undergo electron capture supernovae and possibly leave behind neutron stars (Karakas & Lattanzio 2014; Woosley & Heger 2015; Jones et al. 2016). The division between these two fates is not precisely known, so we do not make the distinction.
- *Massive stars* (initial mass $\sim 11\text{--}40 M_\odot$) undergo later stages of core nuclear burning. They switch between being red and blue supergiants during these later stages (Gordon & Humphreys 2019). They may have pronounced mass loss that transforms them into Wolf-Rayet stars (Clark et al. 2012). Massive stars end with a core collapse leaving behind a neutron star or black hole (Heger et al. 2003).
- *Very massive stars* (initial mass $\gtrsim 40 M_\odot$) leave the main sequence but are unable to become red supergiants. They instead become blue supergiants and blue hypergiants, generally suffering extreme mass loss and becoming Wolf-Rayet stars (Clark et al. 2012). The stellar remnant is a black hole or nothing at all (Heger et al. 2003).

ETIs living around stars in different groups would face different challenges when adapting to post-MS evolution (for example, the post-helium flash contraction would require large-scale migration over just a few millennia to remain in the habitable zone). For low- and intermediate-mass stars, we preferred to use *Gaia* benchmark stars with well-determined masses (Heiter et al. 2015).

³⁵ This term does not appear in the literature; we use it to indicate they have characteristics similar to smaller intermediate mass stars (no core collapse supernova) and massive stars (later stages of nuclear burning, possible neutron star remnants). Karakas & Lattanzio (2014) calls these stars mid- and upper-intermediate mass stars.

The evolutionary stages are supplemented with stars with atypical characteristics, including chemically peculiar stars, Be stars with decretion disks, pulsar-like stars, Population II stars, and a small collection of pulsational variables. Peculiar stars that are the result of stellar mergers are emphasized because of their diverse and unique evolutionary histories (e.g., [Jeffery 2008](#); [Heber 2016](#)).

A.5. *Collapsed stars*

These are divided into white dwarfs, neutron stars, and black holes.

White dwarfs are mainly grouped according to mass ([Liebert et al. 2005](#)), with supplemental subtypes based on evolutionary, composition, magnetic, variability, or spectral characteristics.

Neutron stars are grouped primarily by their rotation rate and magnetic field. These parameters also control the emission we observe and are related to evolutionary state (e.g., [Alpar et al. 1982](#); [Olausen & Kaspi 2014](#)).

Black holes are grouped by detection method. Only a few detached black holes are known, constraining our choice of Prototypes.

A.6. *Interacting binary stars*

We group interacting binary stars powered by accretion by the nature of the mass donor and that of the recipient:

- *Semidetached and contact binaries* – both components are stars.
- *Symbiotic stars* – donor is a giant, recipient is a small early-type star or a white dwarf ([Belczyński et al. 2000](#)).
- *Cataclysmic variables (CVs)* – donor is a late-type dwarf star, recipient is a white dwarf. They are further divided by variability/eruption characteristics ([Osaki 1996](#); [Schaefer 2010](#)) and white dwarf magnetic field interaction with the accretion disk ([Patterson 1994](#)). Closely related are the AM CVn binaries, where the donor is a helium star or white dwarf, and the close binary supersoft sources where the donor is a higher mass subgiant ([Kahabka & van den Heuvel 1997](#)).
- *X-ray binaries* – The recipient is a neutron star or black hole. They are further divided based on the mass of the donor (low mass or high mass), and still further by the mode of mass transfer and other characteristics (see especially [Reig 2011](#); [Kaaret et al. 2017](#)).

In a few cases, stellar outflows rather than accretion dominates the system. These include systems where shocks dominate the luminosity, and the spider pulsars where a formerly-accreting neutron star ablates its companion (e.g., [Dubus 2013](#); [Roberts 2013](#)).

A.7. *Stellar associations*

We include non-interacting binary and multiple stars with other stellar associations like star clusters. As in [Eggleton & Tokovinin \(2008\)](#), they are distinguished from clusters by their hierarchical organization. Binary systems are well represented in the I17 catalog, and we do not try to capture all combinations of stellar types or separations. We specifically include double degenerate systems, which are not included by I17, and have the potential to be sites of ETI activity ([Dyson 1963](#)).

Globular clusters are classified according to the orbit classification of [Mackey & van den Bergh \(2005\)](#); additional subtypes are based on internal structure and luminosity. Other stellar clusters are divided into massive super star clusters, nuclear clusters (including former nuclei of dwarf galaxies), and open star clusters.

Some unbound stellar associations are also included, when well-studied examples were not too large on the sky to be practically observed.

A.8. *Interstellar medium and nebulae*

The interstellar medium (ISM) as a whole has a complicated turbulent structure, although it is classically divided into hot, warm, and cool and cold phases (e.g., [Cox 2005](#)). Some structures in the interstellar medium are too large to practically study with our facilities: the hot ISM, the loops, the warm ionized medium, and so on. In terms of the general ISM, we focus on molecular clouds and HII regions, which are relatively compact. These are classed according to column density into translucent and dark clouds, with the dark clouds further divided by scale. Molecular clouds

have self-similar structure, and although they are sometimes labelled as complexes, clouds, clumps, and cores in the literature, the divisions are arbitrary (see Wu et al. 2010). HII regions formed within the molecular clouds are also included and likewise grouped by density/size (Habing & Israel 1979).

Most of the entries in this phylum are structures produced by outflows from central engines and their interaction with the general ISM. These are grouped according to the nature of the central engine.

Additionally, we include a bubble of cosmic rays to represent the nonthermal ISM, and two circumgalactic medium clouds that we judged practical to observe.

A.9. Galaxies

We regard the fundamental distinction between galaxies as based on their specific star-formation rate (sSFR), the ratio of star-formation rate and stellar mass. There is a natural division in this parameter plane that is robust out to high redshift into quiescent galaxies, intermediate galaxies, “main sequence” star-forming galaxies, and starbursts (Brinchmann et al. 2004; Elbaz et al. 2011; Speagle et al. 2014; Renzini & Peng 2015). The first three categories translate into different features on a color-magnitude diagram: the red sequence, green valley, and blue cloud, respectively (e.g., Strateva et al. 2001; Wyder et al. 2007). The abundance of phenomena that might affect galactic habitability or could be used for astroengineering, like core collapse supernovae, is tied to sSFR. At low redshift, quiescent galaxies are associated with early-type morphologies (ellipticals, spheroidals, and lenticulars), while main sequence galaxies are associated with late-type morphologies (late-type spirals and irregulars), but the correlation is not exact and we specifically include outliers as subtypes. At redshift 0, there is also a correlation with environment, with quiescent galaxies more often located in clusters, although we again include outliers.

Among the quiescent galaxies, there appears to be a robust division of most large ellipticals into two types: boxy/cored and disk/coreless. The division is based on surface brightness profiles, shape, and X-ray emission (Kormendy et al. 2009). Small early-type galaxies tend to be divided into high-density compact galaxies and low-density dwarf galaxies. There is a vigorous debate in the literature about which are more likely to be the analogs of large ellipticals, and which form a separate sequence (e.g., Graham & Guzmán 2003; Kormendy & Bender 2012). Dwarf quiescent galaxies are arbitrarily divided into dwarf elliptical, spheroidal, and ultrafaint simply to cover a full range in mass.

Green valley galaxies are a heterogeneous class, and are here classed mainly by the mode of their passage through the “valley” (Salim 2014; Schawinski et al. 2014).

The blue main sequence galaxies are very diverse. Note the characteristic sSFR decreases with time since the Big Bang (Speagle et al. 2014): a galaxy that would be classified as main sequence at $z \sim 2$ would be considered a starburst now. In the present-day Universe, these are classified coarsely by morphology (see below for discussion of fine morphology types), with a few subtypes each of late spirals and irregulars. We chose Prototypes mainly based on having consistent morphological types between de Vaucouleurs et al. (1991), Karachentsev et al. (2013), Ann et al. (2015), and Buta et al. (2015).

High-redshift star-forming galaxies have been classified mainly by spectrophotometric characteristics (e.g., BzK galaxies satisfy certain criteria in $(B - z)$ and $(z - K)$ colors). These subtypes can include both main sequence and true starburst galaxies. Our choice of Prototypes is constricted by the need for them to be gravitationally lensed to boost our sensitivity. In some cases we were unable to find a likely candidate of a common class of high-redshift galaxies (particularly, no lensed main sequence Lyman- α emitters or main sequence Lyman Break Galaxies).

Starbursts are those galaxies with sSFRs significantly above the typical sSFR of star-forming galaxies at their redshift (Elbaz et al. 2011). We group them into nuclear starbursts occurring in the centers of larger galaxies, and dwarf starbursts occurring in small galaxies. We also specifically include some relatively nearby starbursts noted to have properties analogous to high- z galaxies, in addition to some lensed starbursts at high redshift, to further constrain the possibility that habitability evolves with time.

Disturbed galaxies broadly fall into three types: the ring galaxies (which themselves have diverse origins), interacting galaxies, and galaxies affected by ram pressure stripping in an intracluster medium.

We add a catchall class of “morphological subtypes”, which includes examples of galaxies hosting many kinds of features, particularly those found in galactic disks. There are many morphological classification schemes for disk galaxies. The basic sequence from early to late types is universal (e.g., Hubble 1926) and is included in the previous classes. In many traditional systems, the disk galaxies are classified by the strengths of their bar patterns (de Vaucouleurs et al. 1991; Graham 2019). van den Bergh (1976) instead classifies them according to the prominence of their arms from

spirals to “anemic” galaxies to lenticulars (Kormendy & Bender 2012). Spiral arms themselves come in a great many varieties, from grand design to flocculent varieties (Elmegreen & Elmegreen 1982). Added to this are many other obvious morphological features in disk galaxies: rings, pseudo-rings, lenses, plumes, and more, all with a number of variants (Buta et al. 2015). Each feature adds another dimension to parameter space. The resultant morphological types are lengthy and can vary from paper to paper. To avoid combinatorial explosion, we just have a list of possible features (see Buta et al. 2015, for detailed discussion of these features). Some galaxies here are Prototypes for several types to minimize the number of galaxies observed. Prototypes are chosen by their classification in Comerón et al. (2014) and Buta et al. (2015), especially if they are given as explicit examples of a morphology in Table 1 of Buta et al. (2015).

Finally, we include two types of galaxies defined by their extreme density environments, and a satellite galaxy.

A.10. AGNs

There are a plethora of classification schemes for AGNs, as reviewed in Padovani et al. (2017). We use a canonical division of AGNs into the major divisions of LINERs, Seyferts, radio galaxies, quasars, and blazars as the foundation (e.g., Peterson 1997). Except for LINERs, these are further subdivided into the common categories inspired by optical and radio characteristics (as in Osterbrock 1977; Fanaroff & Riley 1974; Kellermann et al. 1989; Ghisellini et al. 2011, respectively). These main object types represent different luminosities, radio-loudness, and viewing angle, with some admitted overlap between the classes (Urry & Padovani 1995; Padovani et al. 2017).

Additional classes were added to cover objects with unusual spectral or morphological features, or the presence of multiple supermassive black holes.

A few auxiliary objects related to AGNs have also been included: megamasers and AGN relics (voorwerps and fossil AGNs).

A.11. Galaxy associations

Galaxy associations are mainly classified by richness, from isolated pairs of galaxies through groups and clusters. Only compact and “fossil” groups are included due to practicality considerations, as neither is vastly larger than a galaxy (Hickson 1993). A very simple galaxy cluster classification scheme is used, based on relative symmetry and richness (compare with the more elaborate systems in Bahcall 1977). A high-redshift protocluster, a grouping which has not yet virialized at the time of observation, is in the sample.

To the structures themselves, we also included examples of features in the intracluster medium (ICM) of galaxy clusters, both thermal and nonthermal (e.g., Markevitch & Vikhlinin 2007; van Weeren et al. 2019).

A.11.1. Large-scale structures

Most large-scale structures are too diffuse and large to observe practically. The included “attractor” and “repeller” points are not physical objects, but instead indicate local sinks and sources in the peculiar velocity of galaxies. They do roughly correspond to a dense group of clusters and a void, respectively (Hoffman et al. 2017), and may draw the attention of ETIs as special places.

A.11.2. Technology

Which active satellites are available for observation will depend on new launches and re-entries. Although we list some major classes of satellite, the selection of sources will be opportunistic.

A.11.3. Not real

We include the Solar antipoint as a “source” because of its special significance in SETI. The Earth transits the Sun as seen by observers at stars in this direction. It has been suggested that ETIs that observe Earth transits would be especially motivated to broadcast in our direction because they know a habitable planet exists; furthermore, the transit itself can be used for synchronization (Shostak 2004; Heller & Pudritz 2016; Sheikh et al. 2020).

Table A1. Prototype Sample

Type	Subtype	Prototype	ID	Solar?
------	---------	-----------	----	--------

Table A1 continued

Table A1 (*continued*)

Type	Subtype	Prototype	ID	Solar?
Minor body				
Asteroid	A-type	446 Aeternitas	P001	✓
	C-type	52 Europa	P002	✓
	D-type	624 Hektor	P003	✓
	E-type	434 Hungaria	P004	✓
	M-type	16 Psyche	P005	✓
	O-type	3628 Božněmcová	P006	✓
	P-type	420 Bertholda	P007	✓
	Q-type	1862 Apollo	P008	✓
	R-type	349 Dembowska	P009	✓
	S-type	15 Eunomia	P010	✓
	T-type	233 Asterope	P011	✓
	V-type	4 Vesta	P012	✓
	Binary (double)	90 Antiope	P013	✓
	Mercury-crossers	3200 Phaethon	P014	✓
	Vatira	2020 AV ₂	P015	✓
	Venus co-orbital	(322756) 2001 CK ₃₂	P016	✓
	Atira	163693 Atira	P017	✓
	Aten	3753 Cruithne	P018	✓
	Arjuna	1991 VG	P019	✓
	Apollo	1862 Apollo	P008	✓
	Earth Trojan	2010 TK ₇	P020	✓
	Earth horseshoe	3753 Cruithne	P018	✓
	Earth quasisatellite	(469219) Kamo'oalewa	P021	✓
	Earth Kozai librator	4660 Nereus	P022	✓
	Amor	433 Eros	P023	✓
	Mars Trojan	5261 Eureka	P024	✓
	Hungaria	434 Hungaria	P004	✓
	Flora	8 Flora	P025	✓
	Main Belt Zone I	4 Vesta	P012	✓
	Phocaea	25 Phocaea	P026	✓
	Main Belt Zone II	15 Eunomia	P010	✓
	Main Belt Zone III	52 Europa	P002	✓
Cybele	65 Cybele	P027	✓	
Hilda	153 Hilda	P028	✓	
Jupiter Trojan	624 Hektor	P003	✓	
Comet	Active	1P/Halley	P029	✓
	Manx	C/2014 S3 (PAN-STARRS)	P030	✓
	Extinct (Damocloid)	5335 Damocles	P031	✓
	Falling evaporating bodies	β Pic	P032	✓
	Encke-type	2P/Encke	P033	✓
	Main belt comet	133P/Elst-Pizarro	P034	✓
	Jupiter-family	9P/Tempel 1	P035	✓
	Chiron-type	95P/Chiron	P036	✓
	Halley-type	1P/Halley	P029	✓
	Long-period	153P/Ikeya-Zhang	P037	✓
	Icy bodies	BB-type	(24835) 1995 SM ₅₅	P038
BR-type		(15788) 1993 SB	P039	✓
IR-type		(385185) 1993 RO	P040	✓
RR-type		15760 Albion	P041	✓
Binary		79360 Sila-Nunam	P042	✓
Centaur		2060 Chiron	P036	✓
Uranus Trojan	2011 QF ₉₉	P043	✓	

Table A1 *continued*

Table A1 (*continued*)

Type	Subtype	Prototype	ID	Solar?
	Neptune Trojan	2001 QR ₃₂₂	P044	✓
	Plutino	(385185) 1993 RO	P040	✓
	Cold classical KBO	15760 Albion	P041	✓
	Hot classical KBO	(523899) 1997 CV ₂₉	P045	✓
	Haumea family	(24835) 1995 SM ₅₅	P038	✓
	Twotino	(20161) 1996 TR ₆₆	P046	✓
	Scattered disk object	(91554) 1999 RZ ₂₁₅	P047	✓
	Extended disk object	(181902) 1999 RD ₂₁₅	P048	✓
Satellite	Rocky	Phobos	P049	✓
	Icy	Amalthea	P050	✓
	Egg	Methone	P051	✓
	Collisional shard	Amalthea	P050	✓
	Irregular (prograde)	Himalia	P052	✓
	Irregular (retrograde)	Phoebe	P053	✓
	Trojan	Helene	P054	✓
	Co-orbital	Epimetheus	P055	✓
	Temporary Earth minimoon	2006 RH ₁₂₀	P056	✓
	Shepherd moon	Prometheus	P057	✓
	Chaotic rotator	Hyperion	P058	✓
Planetesimals	White dwarf bodies	WD 1145+017	P059	
Circumplanetary bodies	Planetary rings	Saturn	P060	✓
Interstellar	Comet	2I/Borisov	P061	✓
	'Oumuamua-type	1I/'Oumuamua	P062	✓
Protoplanetary disk		TW Hya	P063	
	Dippers	EPIC 203937317	P064	
Transitional disk		GM Aur	P065	
Debris disk	Cold (Kuiper-analog)	τ Cet	P066	
	Warm (asteroidal)	κ Psc	P067	
	Hot (exozodi)	Altair	P068	
	Extreme	NGC 2547 ID8	P069	
	Planetary collision	BD+20 307	P070	
	Post-stellar (rejuvenated)	NGC 7293 central star	P071	
	Post-stellar (tidal disruption)	G29-38	P072	
	Post-stellar (evaporation)	WD J0914+1914	P073	
Solid planetoid				
Planet	Mercury (warm)	Mercury	P074	✓
	Supermercury	K2-229 b	P075	
	Sub-Earth (temperate)	Mars	P076	✓
	Sub-Earth (warm)	Mercury	P074	✓
	Sub-Earth (hot)	Kepler 444 d	P077	
	Earth (temperate)	Proxima b	P078	
	Earth (warm)	Venus	P079	✓
	Earth (hot)	Kepler 78 b	P080	
	Superearth (cold)	Barnard's star b	P081	
	Superearth (temperate)	LHS 1140 b	P082	
	Superearth (warm)	HD 40307 f	P083	
	Superearth (hot)	55 Cnc e	P084	
Disintegrating planet		KIC 12557548 b	P085	
Pulsar planet		PSR B1257+12 ABC	P086	
Dwarf planet	C-complex	1 Ceres	P087	✓
	BB-type	136199 Eris	P088	✓
	BR-type	134340 Pluto	P089	✓
	RR-type	90377 Sedna	P090	✓

Table A1 *continued*

Table A1 (*continued*)

Type	Subtype	Prototype	ID	Solar?
	Main asteroid belt	1 Ceres	P087	✓
	Plutino	134340 Pluto	P089	✓
	Hot classical KBO	136472 Makemake	P091	✓
	Haumea family	136108 Haumea	P092	✓
	Detached object	90377 Sedna	P090	✓
Satellite	Rocky	Moon	P093	✓
	Icy	Titan	P094	✓
	Retrograde	Triton	P095	✓
	Resonant chain	Europa	P096	✓
Geological classifications	Primordial	Callisto	P097	✓
	Inactive	Ganymede	P098	✓
	Solar	Triton	P095	✓
	Convective	134340 Pluto	P089	✓
	Hydrological	Titan	P094	✓
	Stagnant lid	Venus	P079	✓
	Tectonic	Europa	P096	✓
	Cryovolcanic	Enceladus	P099	✓
	Volcanic	Io	P100	✓
Giant planet				
Ice giant	Cold Neptune	Neptune	P101	✓
	Temperate Neptune	Kepler 22 b	P102	
	Warm Neptune	GJ 436 b	P103	
	Hot Neptune	HATS-P-26 b	P104	
	Mini-Neptune	GJ 1214 b	P105	
Gas giant	Cold Jupiter	Jupiter	P106	✓
	Temperate Jupiter	HD 93083 b	P107	
	Warm Jupiter	HATS-17 b	P108	
	Hot Jupiter	HD 189733 b	P109	
	Inflated	HD 209458 b	P110	
	Gas Neptune	Kepler 18 d	P111	
	Circumbinary	Kepler 16 b	P112	
	Post main sequence host	Kepler 56 bc	P113	
Superjovian	Cold super-Jovian	HR 8799 bcde	P114	
	Temperate super-Jovian	HD 28185 b	P115	
	Warm super-Jovian	HD 80606 b	P116	
	Hot super-Jovian	HD 147506 b	P117	
	Giant host	Pollux b	P118	
Star				
Protostars	Class 0	IRAS 16293-2422	P119	
	Class I	Elias 29	P120	
	High mass	IRAS 20126+4104	P121	
Pre-main sequence	T Tauri	TW Hya	P063	
	Herbig Ae/Be	AB Aur	P122	
	FU Orionis	FU Ori	P123	
Sub-brown dwarf	Early Y	WISE J085510.83-071442.5	P124	
Brown dwarf	Early Y	WISE J071322.55-291751.9	P125	
	Late T	2MASSI J0415195-093506	P126	
	Mid T	ϵ Ind Bb	P127	
	Early T	Luhman 16B	P128	
	Late L	Luhman 16A	P129	
	Mid L	HD 130948BC	P130	

Table A1 *continued*

Table A1 (*continued*)

Type	Subtype	Prototype	ID	Solar?
Main sequence	Early L	2MASSI J1506544+132106	P131	
	M	PPL 15	P132	
	Early L	2MASS J0523-1403	P133	
	Late M	VB 10	P134	
	Mid M	Wolf 359	P135	
	Early M	HD 95735	P136	
	Late K	61 Cyg B	P137	
	Mid K	61 Cyg A	P138	
	Early K	ϵ Eri	P139	
	Late G	τ Cet	P066	
	Mid G	κ_1 Cet	P140	
	Early G	Sun	P141	✓
	Late F	β Vir	P142	
	Mid F	π_3 Ori	P143	
	Early F	78 UMa	P144	
	Late A	α Cep	P145	
	Mid A	Alcor	P146	
	Early A	Vega	P147	
	Late B	λ Aql	P148	
	Mid B	α Gru	P149	
Early B	η UMa	P150		
Late O	10 Lac	P151		
Mid O	HD 46150	P152		
Early O	HD 64568	P153		
Low mass subgiants	K	κ CrB	P154	
	G	μ Her	P155	
	F	Procyon	P156	
	A	ι UMa	P157	
Low mass RGB	M	γ Cru	P158	
	Late K	Aldebaran	P159	
Low mass CHeB	Early K	Arcturus	P160	
	Red clump	α Ser	P161	
	Red horizontal branch	BD +17 3248	P162	
	RR Lyrae	RR Lyr	P163	
	Blue horizontal branch	HD 161817	P164	
Low-intermediate mass AGB	M	R Dor	P165	
	S (intrinsic)	RS Cnc	P166	
	C	IRC +10216	P167	
	OH/IR	IRC +10011	P168	
Low-mid mass post-AGB	Post-AGB	HD 44179	P169	
	Final flash	V4334 Sgr	P170	
Intermediate mass subgiant	B	Regulus	P171	
Intermediate mass RGB	K	α Hya	P172	
	M	α Cet	P173	
Intermediate mass giant	K supergiant	ζ Aur	P174	
	G giant	ϵ Vir	P175	
Intermediate mass CHeB	Red clump	Capella Aa	P176	
	Blue loop	δ Cep	P177	
	Classical Cepheid	δ Cep	P177	
	K supergiant	β Ara	P178	
Transitional mass giant	G supergiant	1 Car	P179	
	AF supergiant	Canopus	P180	
	Super-AGB	MSX SMC 055	P181	
Massive post-MS	OB giant	ι Ori	P182	

Table A1 *continued*

Table A1 (*continued*)

Type	Subtype	Prototype	ID	Solar?
	Blue (B) supergiant	ζ Per	P183	
	White (BA) supergiant	Deneb	P184	
	Red supergiant	Betelgeuse	P185	
	Yellow hypergiant	ρ Cas	P186	
	Cool hypergiant	VY CMa	P187	
Wolf-Rayet	WR N	EZ CMa	P188	
	WR C	γ_2 Vel	P189	
	WR O	WR 102	P190	
Very massive post-MS	B hypergiant	ζ_1 Sco	P191	
	LBV (S Dor type)	AG Car	P192	
	LBV (η Car type)	η Car	P193	
Chemically peculiar	Non-magnetic	ϵ Ser	P194	
	Magnetic	α_2 CVn	P195	
Extreme rotation	Classical Be	ζ Tau	P196	
Stellar pulsar	Ultracool pulsar	TVLM 513-46546	P197	
	mCP pulsar	CU Vir	P198	
Population II brown dwarf	sdL	2MASS J0532+8246	P199	
Population II subdwarf	sdM	Kaptyen's Star	P200	
	sdK	Groombridge 1830	P201	
	sdG	BD -00 4470	P202	
	sdF	HD 84937	P203	
Population II subgiant		HD 140283	P204	
Extremely metal poor		HD 122563	P205	
	CEMP (intrinsic)	HE 0107-5240	P206	
Pulsational variable	Long-period variable	Mira A	P207	
	Instability strip	δ Cep	P177	
	Early-type pulsator	β Cep	P208	
	Non-radial pulsator	γ Dor	P209	
Flare star	dMe	UV Cet	P210	
Post-merger/interaction	Luminous red nova	V838 Mon	P211	
	Yellow straggler	M67-S1236	P212	
	FK Com	FK Com	P213	
	R CrB	R CrB	P214	
	Extreme helium	HD 124448	P215	
	Blue straggler	40 Cancri	P216	
	Hot subdwarf (sdB)	HD 149382	P217	
	Hot subdwarf (sdO)	BD+28 4211	P218	
	Dwarf carbon	G77-61	P219	
High velocity	Runaway	ζ Oph	P220	
	Hyperrunaway (Ia SN)	HD 271791	P221	
	Hypervelocity (SMBH)	HVS 1	P222	
Collapsed star				
White dwarf	Extremely low mass	NLTT 11748	P223	
	Low mass	LAWD 32	P224	
	Typical mass	van Maanen 2	P225	
	Massive	Sirius B	P226	
	Ultramassive	GD50	P227	
	Central star of PN	NGC 7293*	P071	
	Pre-white dwarf	PG 1159-035	P228	
	ONeMg	QU Vul	P229	
	Magnetic	Grw +70°8247	P230	
	Pulsating	ZZ Cet	P231	
	Blackbody	Ton 124	P232	

Table A1 *continued*

Table A1 (*continued*)

Type	Subtype	Prototype	ID	Solar?	
Neutron star	Compact central object	1E 1207.4-5209	P233		
	Radio-quiet pulsar	Geminga	P234		
	Radio-loud pulsar	Crab pulsar	P235		
	Optical pulsar	Crab pulsar	P235		
	Magnetar (radio quiet)	SGR 1806-20	P236		
	Magnetar (fast radio burster)	SGR 1935+2154	P237		
	Rotating radio transient	PSR B0656+14	P238		
	X-ray dim isolated NS	RX J1856.5-3754	P239		
Black hole	Millisecond pulsar	PSR J0437-4715	P240		
	Accreting	Cygnus X-1	P241		
	Detached	QV Tel Ab	P242		
	Failed SN	NGC 6946-BH1	P243		
Interacting binary star					
Semidetached	Algol-type	Algol	P244		
Contact binary	Shallow overcontact	W UMa	P245		
	Deep overcontact	FG Hya	P246		
Symbiotic star	OO Aql	OO Aql	P247		
	S-type	CH Cyg	P248		
	D-type	R Aqr	P249		
	Weakly symbiotic	Mira	P207		
	Symbiotic nova	RR Tel	P250		
	Supersoft source (symbiotic)	RR Tel	P250		
Cataclysmic variable	Symbiotic recurrent nova	RS Oph	P251		
	Dwarf nova	SS Cyg	P252		
	Novalike variable	UX UMa	P253		
	Recurrent nova (CV)	T Pyx	P254		
	Old classical nova	GK Per	P255		
	Intermediate polar	DQ Her	P256		
	IP propeller	AE Aqr	P257		
	Polar	AM Her	P258		
	CV pulsar	AR Sco	P259		
	AM CVn binary		AM CVn	P260	
Close binary SSS		QR And	P261		
Neutron star X-ray binary	Z source	Sco X-1	P262		
	Atoll source	4U 1608-52	P263		
	Type II burster	4U 1730-335	P264		
	Ultracompact LMXB	4U 1820-303	P265		
	Accreting millisecond pulsar	SAX J1808.4-3658	P266		
	Transitional millisecond pulsar	PSR J1023+0038	P267		
	Be/X-ray binary (HMXB, NS)	A 0535+26	P268		
	Classical supergiant HMXB (NS)	Vela X-1	P269		
	Roche-lobe overflow HMXB (NS)	Cen X-3	P270		
	Black hole XRB	Black hole LMXB	V404 Cyg	P271	
		Be/X-ray binary (BH)	MCW 656	P272	
		Supergiant HMXB (BH)	Cyg X-1	P241	
Microquasar	Microquasar	GRS 1915+105	P273		
Supercritical XRB	Faint supercritical	SS433	P274		
	Non-pulsating ULX	M82 X-1	P275		
	Supersoft ULX	M101 ULX-1	P276		
	Ultraluminous X-ray pulsar	M82 X-2	P277		
	Indeterminate XRB	γ Cas	γ Cas	P278	
	Superfast X-ray transient	IGR J17544-2619	P279		
Outflow interaction binary	Colliding wind binary	WR 140	P280		

Table A1 *continued*

Table A1 (*continued*)

Type	Subtype	Prototype	ID	Solar?
Spider pulsar	Pulsar wind gamma-ray binary	PSR B1259-63	P281	
	Black widow	PSR B1957+20	P282	
	Redback	PSR J1023+0038	P267	
	Huntsman	PSR J1417-4402	P283	
Stellar group				
Detached binaries	Star-star	α Cen AB	P284	
	Multiple protostar	T Tau	P285	
	Brown dwarf-brown dwarf	Luhman 16	P286	
	White dwarf-white dwarf	WD 0135-052	P287	
	Neutron star-planet mass object	PSR J1719-1438	P288	
	Neutron star-white dwarf	PSR J0437-4715	P240	
	Neutron star-neutron star	PSR B1913+16	P289	
	Chromospherically active binary	RS CVn	P290	
	Eclipsing binary star	YY Gem	P291	
	Eclipsing disk	ϵ Aur	P292	
	Eclipsing binary pulsar	PSR J0737-3039	P293	
	Self-lensing binary	KIC 8145411	P294	
	Open star cluster	Young	IC 2391	P295
Old		M67	P296	
Super star cluster		Westerlund 1	P297	
Globular cluster	Bulge-disk	47 Tuc	P298	
	Young halo	M15	P299	
	Old halo	NGC 6752	P300	
	Core-cusp	M15	P299	
	Extended	M31-EC4	P301	
	Ultrafaint	Palomar 1	P302	
Nuclear cluster		Central Cluster	P303	
	Stripped nucleus	ω Cen	P304	
R association		CMa R1	P305	
OB association	Compact	Cyg OB2	P306	
	Scaled	NGC 604	P307	
	Jet induced	Cen A Outer Filament	P308	
ISM				
Diffuse molecular cloud	Translucent sightline	ζ Oph cloud	P309	
	Photodissociation region	NGC 7023	P310	
Dark molecular cloud	Giant molecular cloud	Orion A	P311	
	Infrared dark cloud	G028.37+00.07	P312	
	Dark cloud	TMC-1	P313	
	Starless core	Barnard 68	P314	
	Hot core	Orion hot core	P315	
	Reflection nebula	NGC 7023	P310	
HI supershell		Sextans A hole	P316	
Star-forming HII regions	Classical HII region	M42	P317	
	Ultracompact	W3(OH)	P318	
	Giant	NGC 3603	P319	
Star-formation maser regions	Maser region	W3(OH)	P318	
	OH megamaser	Arp 220	P320	
Protostellar outflow	Herbig-Haro Object	HH 1	P321	
	Extended Green Object	EGO G16.59-0.05	P322	
Stellar bowshock nebula		ζ Oph bow shock	P323	
Proto-planetary nebula		Red Rectangle nebula	P324	

Table A1 *continued*

Table A1 (*continued*)

Type	Subtype	Prototype	ID	Solar?
Planetary nebula	Elliptical	Helix Nebula	P325	
	Bipolar/multipolar	NGC 6302	P326	
Massive star ejecta	Post-RSG shell	IRC +10420	P327	
	LBV shell	Homunculus Nebula	P328	
Supernova remnant	Wolf-Rayet bubble	S 308	P329	
	Shell	Cas A	P330	
	Composite	Kes 75	P331	
	Mixed-morphology	W44	P332	
Pulsar wind nebula	Young	SN 1987A	P333	
	Plerion	Crab nebula	P334	
	Bow shock	PSR B1957+20 bow shock	P335	
Symbiotic nebula	TeV halo	Geminga halo	P336	
		R Aqr nebula	P337	
Nova remnant		GK Per shell	P338	
SSS nebula		CAL 83 nebula	P339	
XRB nebula	X-ray binary bow shock nebula	SAX J1712.6-3739 nebula	P340	
	X-ray binary bubble	Cygnus X-1 shell	P341	
	X-ray ionized X-ray binary nebula	N159F	P342	
	ULX nebula	W50	P343	
Nonthermal bubble	Cosmic ray cocoon	Cygnus Cocoon	P344	
Circumgalactic medium	Compact high velocity cloud	HVC 125+41-208	P345	
	Lyman α blob	SSA22a-LAB01	P346	
Galaxy				
Quiescent (Red)	cD	NGC 6166	P347	
	Boxy/cored elliptical	NGC 4636	P348	
	Disky/coreless elliptical	M59	P349	
	Field elliptical	NGC 821	P350	
	Lenticular	NGC 3115	P351	
	Passive spiral	NGC 4260	P352	
	Compact elliptical	M32	P353	
	UltraCompact Dwarf	NGC 4656 UCD-1	P354	
	Dwarf elliptical	NGC 205	P355	
	Dwarf spheroidal	Sculptor dSph	P356	
	Ultrafaint dwarf	UMa II	P357	
	Dwarf S0	NGC 4431	P358	
	Relic red nugget	NGC 1277	P359	
	Red nugget	MRG-M0150	P360	
Green Valley	Large quiescent (high-z)	MRG-M0138	P361	
	Post-starburst	IC 976	P362	
	Extended star-formation	NGC 404	P363	
	Sa-Sab spiral	M81	P364	
	Sb-Sbc spiral	M100	P365	
	Dwarf Sa-Sb spiral	D563-4	P366	
	Edge-on Sa-Sb spiral	NGC 891	P367	
Main sequence (blue)	Dwarf transitional	Phoenix dwarf	P368	
	Star-forming elliptical	NGC 5173	P369	
	Blue cored dwarf elliptical	IC 225	P370	
	Sc-Scd spiral	M101	P371	
	Sd-Sdm spiral	NGC 300	P372	
	Sm spiral	NGC 55	P373	
	Dwarf Sc-Sd spiral	NGC 4701	P374	
Super spiral	SS 16	P375		
	Cluster late spiral	M99	P376	

Table A1 *continued*

Table A1 (*continued*)

Type	Subtype	Prototype	ID	Solar?
	Edge-on late spiral	NGC 4631	P377	
	Irregular (dE/Magellanic-size)	NGC 6822	P378	
	Irregular (dSph-size)	IC 1613	P379	
	Amorphous	NGC 3077	P380	
	LIRG ($z \sim 1$)	SGAS J143845.1+145407	P381	
	Spiral galaxy ($z \sim 1.5$)	Sp1149 (A1)	P382	
	BzK-type ULIRG ($z \sim 1.5$)	A68-HLS115	P383	
	Submillimeter galaxy (MS, high- z)	HLock-01 (R)	P384	
Starburst	Infrared-transparent nuclear	M82	P385	
	Blackbody nuclear	Arp 220	P320	
	Lyman Break Analog	Arp 236	P386	
	Blue compact dwarf	I Zwicky 18	P387	
	Ultracompact blue dwarf	POX 186	P388	
	Lyman α Emitter ($z \sim 0$)	Haro 2	P389	
	Green pea	NGC 2366	P390	
	Dwarf starburst ($z \sim 3$)	ID11	P391	
	Lyman α Emitter (SB, $z \sim 2$)	SL2S J02176-0513	P392	
	Lyman Break Galaxy (SB, $z \sim 3$)	cB 58	P393	
	Submillimeter galaxy (SB, high- z)	SMM J2135-0102	P394	
	Jet induced starburst	Minkowski's Object	P395	
Low surface brightness	Giant	Malin 1	P396	
	Red UltraDiffuse Galaxy	VCC 1287	P397	
	Blue UltraDiffuse Galaxy	UGC 2162	P398	
	Almost dark	HI 1232+20	P399	
Disturbed	Collisional ring	Cartwheel	P400	
	Polar ring	NGC 4650A	P401	
	Hoag-like ring	Hoag's Object	P402	
	Interacting	M51a/b	P403	
	Major merger	Antennae	P404	
	Tidal dwarf	Antenna TDG	P405	
	Dumbbell galaxy	3C 75	P406	
	Jellyfish	ESO 137-001	P407	
	Fireball tail	IC 3418	P408	
Morphological subtypes	Grand design spiral	M51a	P409	
	Flocculent spiral	NGC 7793	P410	
	Leading spiral arms	NGC 4622	P411	
	Anemic spiral	M91	P412	
	Nuclear ring morphology	NGC 1097	P413	
	Nuclear lens morphology	M64	P414	
	Barlens morphology	NGC 2787	P415	
	Strong bar morphology	NGC 1365	P416	
	x_1 ring morphology	NGC 6012	P417	
	Inner ring morphology	NGC 1433	P418	
	Plume morphology	NGC 1433	P418	
	Outer lens morphology	NGC 2787	P415	
	Outer pseudoring morphology	NGC 1365	P416	
	Outer Lindblad ring	NGC 5101	P419	
	Double outer ring	NGC 3898	P420	
	Counterrotating disks	M64	P414	
	Superthin disk	UGC 7321	P421	
	Shell galaxy	NGC 3923	P422	
	Rectangular galaxy	LEDA 074886	P423	
Environmental classification	Void galaxy	KK 246	P424	
	Brightest cluster galaxy	NGC 6166	P347	

Table A1 *continued*

Table A1 (*continued*)

Type	Subtype	Prototype	ID	Solar?
	Satellite galaxy	NGC 205	P355	
AGN				
Intermediate Mass BH	Hyperluminous X-ray source	ESO 243-49 HLX1	P425	
Low luminosity	Quiescent	Sgr A*	P426	
	LINER (AGN-powered)	NGC 1052	P427	
XBONG	Dwarf Seyfert	NGC 4395	P428	
		NGC 4686	P429	
Seyfert	Seyfert 1	NGC 7469	P430	
	Seyfert 2	NGC 1068	P431	
Radio galaxy	Starburst/Seyfert composite	NGC 1068	P431	
	Narrow line Seyfert 1	I Zwicky 1	P432	
	FR 0	NGC 2911	P433	
	FR I	Centaurus A	P434	
	FR II	Cygnus A	P435	
	Head-tail radio galaxy	NGC 1265	P436	
	X-shaped radio galaxy	3C 403	P437	
Quasar	Compact Steep Spectrum	3C 286	P438	
	GHz Peaked Source	PKS 1934-638	P439	
	Radio loud	3C 273	P440	
	Radio quiet	Mrk 335	P441	
	Broad Absorption Line	Cloverleaf quasar	P442	
	Weak line	PHL 1811	P443	
	Blazar	BL Lac	BL Lac	P444
Dust-obscured galaxy (AGN)	Flat Spectrum Radio Quasar (blazar)	3C 279	P445	
	Neutrino blazar	TXS 0506+056	P446	
	Power-law DOG	SST24 J143644.2+350627	P447	
Water megamaser AGN	Hot DOG	WISE 1814+3412	P448	
	Disk megamaser	NGC 4258	P449	
Changing look	Jet-driven megamaser	NGC 1052	P427	
	Optical	NGC 4151	P450	
Offset	X-ray	NGC 1365	P416	
	Wandering	ESO 243-49 HLX1	P425	
Multiple AGN	Dual AGN	NGC 6240	P451	
	Binary AGN	0402+379	P452	
	Interacting SMBH binary	OJ 287	P453	
	Merging jets dual AGN	3C 75	P406	
Remnant	Voorwerp	Hanny's Voorwerp	P454	
	Radio fossil	B2 0924+30	P455	
Galaxy association				
Binary galaxy		Arp 294	P456	
Dwarf galaxy association		UGCA 319/320	P457	
Galaxy group	Compact	Stephan's Quintet	P458	
	Fossil	NGC 6482	P459	
Galaxy cluster	Galaxy interaction shock	Stephan's Quintet	P458	
	Regular	Fornax Cluster	P460	
	Irregular	Virgo Cluster	P461	
	Poor	Fornax Cluster	P460	
	Rich	Coma Cluster	P462	
	Cool core	Perseus Cluster	P463	
Protocluster	Merging	Bullet Cluster	P464	
		SSA22	P465	

Table A1 *continued*

Table A1 (*continued*)

Type	Subtype	Prototype	ID	Solar?
Intracluster medium	Cold front	Abell 3667	P466	
	Shock front	Bullet Cluster	P464	
	X-ray cavities	Perseus Cluster	P463	
Nonthermal ICM	Giant radio halo	Coma C	P467	
	Radio minihalo	NGC 1275 minihalo	P468	
	Radio relic	1253+275	P469	
LSS				
Intergalactic medium	Giant HI ring	Leo Ring	P470	
Gravitational basin	Attractor	Laniakea (Great) attractor	P471	
	Repeller	Dipole repeller	P472	
Technology				
Space station	Space station	ISS	P473	✓
Satellite	Navigation satellite	TBD	P474	✓
	Communications satellite	TBD	P475	✓
	Amateur radio satellite	TBD	P476	✓
	Earth observation radar satellite	TBD	P477	✓
	Weather satellite	TBD	P478	✓
	Space telescope	TBD	P479	✓
Spacecraft	Space probe	<i>Voyager 1</i>	P480	✓
	Solar sail	<i>Light-Sail 2</i>	P481	✓
Passive structure	Radar calibration target	LCS-1	P482	✓
Space debris	Derelict satellite	Vanguard I	P483	✓
	Rocket booster	TBD	P484	✓
	Dipole clump	1963-014G	P485	✓
	NaK coolant droplets	Cosmos 860 coolant (1976-103G)	P486	✓
	Car	Tesla Roadster	P487	✓
Not real				
Solar System		Solar antipoint	P488	✓

NOTE—**Solar?** – ✓ if object is in or passed through Solar System and listed in Table E1; otherwise listed in Table E2.

References for Table A2 are given in the full online appendices.³⁶

Table A2. Properties of transient phenomena

Phylum	Type	Example host	Host ID	Duration	Recurrence	Emission	Ref
Periodic and predictable transients							
Minor body	Periodic comets	1P/Halley	P029	Weeks–Months	Years–Centuries	O	
	Stellar occultation	Milliseconds–Minutes	Infrequent	O	
Solid planetoid	Total solar eclipse	Sun/Moon	P141/P093	Minutes	Decades	O	
	Lunar eclipse	Moon	P093	Hours	Months	O	
	Lunar/planetary occultation (ingress/egress)	Moon/Aldebaran	P093/P159	Milliseconds	Infrequent	O	

Table A2 *continued*

³⁶ <http://seti.berkeley.edu/exotica>.

Table A2 (continued)

Phylum	Type	Example host	Host ID	Duration	Recurrence	Emission	Ref
Collapsed star	Pulsar pulse	Crab Pulsar	P235	Milliseconds	Milliseconds–Seconds	RIOX γ	1
Stellar group	Binary eclipse	YY Gem	P291	\gtrsim Minutes	\gtrsim Minutes	O	2
	Disk-star eclipse	ϵ Aur	P292	Years	Decades	OI	3
Active galactic nucleus	Binary SMBH flare	OJ 287	P453	Days	Years	O	4
	Quasiperiodic eruption	GSN 069	A043	Hour	Hours	O	5
Anomaly	Periodic FRB	FRB 180916.J0158+65	A063	Milliseconds	Hours	R	6
Unpredictable repeating transients with known hosts							
Solid planetoid	Lightning	Earth	...	Milliseconds	Minutes	RO	
Stars	Solar radio bursts	Sun	P141	Milliseconds–Hours	Multiscale	R	7
	M dwarf flare	UV Cet	P210	Minutes–Hours	Multiscale	ROUX	8
	Superflare	Groombridge 1830	P201	Minutes–Hours	Centuries	ROUX	9
	Yellow hypergiant eruption	ρ Cas	P186	Years	Decades	O	10
	LBV giant eruption	η Car	P193	Years	Centuries	IO	11
	R CrB dip	R CrB	P214	Weeks	Years	O	12
Compact stellar remnants	Pulsar nanoshots	Crab Pulsar	P235	Nanoseconds	Frequent	R	13
	Giant pulse	Crab Pulsar	P235	Milliseconds	Minutes	R	14
	Magnetar flares	SGR 1806+20	P236	Seconds–Minutes	Years	X γ	15
	Magnetar afterglow	SGR 1806+20	P236	Week	Years	R	16
Interacting binary stars	RRAT	PSR B0656+14	P238	Milliseconds	Minutes–Hours	R	17
	Symbiotic slow nova	RR Tel	P250	Decades	>Decades	O	18
	Symbiotic recurrent nova	RS Oph	P251	Weeks	Decades	O γ	19
	Dwarf nova	SS Cyg	P252	Days–Weeks	Weeks–Years	O	20
	Recurrent nova (CV)	T Pyx	P254	Week–Months	Decades	ROX	21
	Type I X-ray burst	4U 1608-52	P263	Seconds–Minutes	Minutes–Hours	X	22
	Type II X-ray burst	4U 1730-335	P264	Seconds	Seconds–Hour	X	23
	X-ray nova	V404 Cyg	P271	Minutes	Multiscale	OX γ	24
	Supergiant fast X-ray transient	IGR J17544-2619	P279	Hours–Days	Months–Year	X	25
	Plasma lensed pulsar pulse	PSR B1957+20	P282	Seconds	Hours	R	26
ISM	Maser flare	W49(N)	S081	\gtrsim Days	Multiscale	R	27
	Pulsar wind nebula flare	Crab Nebula	P334	Days	Months	γ	28
Active galactic nucleus	Quiescent flares	Sgr A*	P426	Minutes–Hours	Hours–Days	RIX	29
	Extreme γ -ray blazar flare	3C 279	P445	Hours–Days	Months	X γ	30
Anomaly	Neutrino blazar flare	TXS 0506+056	P446	Months	Years	ν	31
	Radio burster	GCRT J1745-3009	A061	Minutes–Hour	\gtrsim Hour	R	32
	Repeating FRB	FRB 121102	A062	Milliseconds	Minute–Hours	R	33
Transients that occur once or very rarely per object, or with unknown recurrence							
Minor bodies	Meteor	Seconds	...	RO	
	Giant comet eruption	17P/Holmes	A011	Weeks	...	O	34
Stars	Hyperbolic comet	2I/Borisov	P061	Weeks–Months	...	O	35
	FU Ori outburst	FU Ori	P123	Years–Century	...	O	36
	Microlensing event ¹	Days	...	O	37

Table A2 continued

Table A2 (*continued*)

Phylum	Type	Example host	Host ID	Duration	Recurrence	Emission	Ref
Compact stellar remnants	Core collapse neutrino flash	SN 1987A	P333	Seconds	...	ν	38
	Supernova breakout	shock XRT080109	...	Minutes–Hours	...	OX	39
	Core collapse supernova	SN 1987A	P333	Weeks	...	OUX	40
	Radio supernova	SN 1993J	... ²	Weeks–Months	...	R	41
	Superluminous Type I	Super-nova SN 2005ap	...	Weeks	...	O	42
	Superluminous Type II	Super-nova SN 2006gy	...	Months	...	OX	43
	Failed supernova	NGC 6946-BH 1	P243	~Year	...	O	44
	Long-soft GRB	GRB 030329	...	Seconds	...	X γ	45
	GRB X-ray flare	GRB 050502B	...	Minutes	...	X	46
	Long-soft afterglow	GRB GRB 030329	...	Hours–Days	...	RIOUX	47
Interacting binary stars	Magnetar FRB	SGR 1935+2154	P237	Milliseconds	...	R	48
	Luminous red nova	V838 Mon	P211	Weeks–Months	...	IO	49
	Nova	GK Per	P255	Weeks	>Decades	RIOUX γ	50
	Nova supersoft phase	X-ray V1974 Cyg (1992)	...	Year	...	X	51
	Type Ia supernova	SN 2014j	... ³	Weeks	...	IOU	52
	Type Iax supernova	SN 2002cx	...	Weeks	...	O	53
	Type .Ia supernova	SN 2010X	...	Days	...	O	54
	Neutron star merger	GW170817	...	Milliseconds–Second	...	$\gamma\mathcal{G}$	55
	Kilonova	GW170817	...	Days	...	IOU	56
	Black hole merger	GW150914	...	Seconds	...	\mathcal{G}	57
ISM	Extreme scattering event	scattering QSO 0954+658 sightline	...	Months	...	R	58
AGN	Tidal disruption event	TDE1	...	Months	Millennia	OU	59
		NGC 5905	...	Months	Millennia	X	60
	Jetted tidal disruption event	Swift J164449.31573451	...	Days	Millennia	RIOX γ	61
Anomaly	Optical spike	Spikey	A042	Days	Years?	O	62
	Unexplained transients	radio RT 19920826	A060 ⁴	Seconds–Decades	...	R	63
	Unexplained transient	infrared VVV-WIT-002	A064	Months?	...	I	64
	Intermediate red transient	luminosity SN 2008S	A069	Months	...	IOU	65
	Ca-rich gap transient	PTF 09dav	A070	Week	...	O	66
	Fast transients	blue optical AT 2018cow	A071 ⁵	Days	...	RIOUX	67
	ASASSN -15lh	ASASSN -15lh	A024	Years	...	OUX	68
	Unexplained very fast X-ray transients	XRT 000519	A073 ⁶	Minutes	...	X	69
	Ultraluminous transients	X-ray CXOU J124839.0054750	A075 ⁷	Hours–Years	...	X	70
	Galactic gamma-ray transient	long-soft Swift J195509.6+261406	A077	Seconds	...	O γ	71
Ubiquitous transients							
ISM	Cosmic ray shower	Nanoseconds	Ubiquitous	RO γ <i>ei</i>	
Technology	Radio interference	frequency	Minutes	Ubiquitous	R
	Satellite glints	Milliseconds–Seconds	Frequent	O

Table A2 *continued*

Table A2 (*continued*)

Phylum	Type	Example host	Host ID	Duration	Recurrence	Emission	Ref
--------	------	--------------	---------	----------	------------	----------	-----

NOTE—**Duration** – Order-of-magnitude timescale for rise and fall of transient.

Recurrence – Order-of-magnitude time between transients emitted by host.

Emission – R: radio; I: infrared; O: optical; U: ultraviolet; X: X-rays; γ : gamma-rays; ν : neutrinos; \mathcal{G} : gravitational waves; e : high-energy electrons; i : high-energy ions.

¹ Microlensing of a star in the galaxy Sp1149 (A1) (P382) by stars in a foreground lens galaxy has been observed.

² The host galaxy of SN 1993J is M81 (P364).

³ The host galaxy of SN 2014j is M82 (P385).

⁴ For additional examples, A054–A059.

⁵ See also Dougie (A072).

⁶ See also CDF-S XT1 (A074).

⁷ See also M86 tULX-1 (A076).

B. THE SUPERLATIVE SAMPLE

Table B1. Superlative catalog: Sidereal targets

Type	Property	Value	Superlative	ID	Solar?	Ref
Minor body						
All minor bodies	α_G^V (darkest)	$0.027_{-0.007}^{+0.006}$	1173 Anchises	S001	✓	1
	α_G^V (brightest)	$0.76_{0.45}^{+0.18} - 0.88_{-0.06}^{+0.15}$	(55636) 2002 TX ₃₀₀	S002	✓	2
	M_{host} (smallest)	$8_{-3}^{+7} M_J$	Cha 110913-773444	S003		3
Interplanetary minor bodies	a (closest)	0.5553 ± 0.0002 AU	2019 LF ₆	S004	✓	4
	Q (closest)	0.65377 ± 0.00012 AU	2020 AV ₂	P015	✓	5
	q (furthest)	80.424 AU	2012 VP ₁₁₃	S005	✓	6
		55.846 AU	2014 FZ ₇₁	S006	✓	...
Minor satellites	R (largest)	210 km	Proteus	S007	✓	7
	a (closest)	9.376 Mm	Phobos	P049	✓	...
	a (furthest)	49 Gm	Neso	S008	✓	...
	a/R_p (smallest)	1.79	Metis	S009	✓	...
Planetary rings	M_{host} (smallest)	$\sim 8 \times 10^{-7} M_{\oplus}$	2060 Chiron	P036	✓	8
	M_{host} (largest)	$\sim 14\text{--}26 M_J$	1SWASP J140752.03-394415.1 b	S010		9
	R (smallest)	324 km	2060 Chiron	P036	✓	10
	R (largest)	~ 27 Gm	1SWASP J140752.03-394415.1 b	S010		11
Solid planetoid						
Solid planetoids	M (smallest)	$6.3 \times 10^{-6} M_{\oplus}$	Mimas	S011	✓	...
	R (smallest)	198 km	Mimas	S011	✓	...
	α_G (darkest)	0.05	Iapetus	S012	✓	...
		0.09	1 Ceres	P087	✓	...
	α_G (brightest)	1.3	Enceladus	P099	✓	...
Major satellites	M (largest)	$0.0248 M_{\oplus}$	Ganymede	P098	✓	...
	R (largest)	2,631 km	Ganymede	P098	✓	...
	ρ (lowest)	0.973 g cm^{-3}	Tethys	S013	✓	...
	ρ (highest)	3.528 g cm^{-3}	Io	P100	✓	...
	$M_{\text{moon}}/M_{\text{host}}$ (smallest)	6.60×10^{-8}	Mimas	S011	✓	...
	$M_{\text{moon}}/M_{\text{host}}$ (largest)	0.122	Charon	S014	✓	12

Table B1 *continued*

Table B1 (*continued*)

Type	Property	Value	Superlative	ID	Solar?	Ref
Dwarf planets	$M_{\text{moon}}/M_{\text{host}}$ (largest, planet)	0.0123	Moon	P093	✓	...
	a (closest)	19.6 Mm	Charon	S014	✓	13
	a (closest, planet)	129.9 Mm	Miranda	S015	✓	...
	a (furthest)	3.56 Gm	Iapetus	S012	✓	...
	M (smallest)	0.000157 M_{\oplus}	1 Ceres	P087	✓	...
	M (largest)	0.0028 M_{\oplus}	136199 Eris	P088	✓	14
	R (smallest)	939.4 km	1 Ceres	P087	✓	15
	R (largest)	1188.3 km	134340 Pluto	P089	✓	16
	a (closest)	2.768 AU	1 Ceres	P087	✓	...
	a (furthest)	67.86 AU	136199 Eris	P088	✓	...
Solid planets		484.4 AU	90377 Sedna	P090	✓	...
	M (smallest)	0.022 M_{\oplus}	PSR 1257+12 A	P086		17
	M (smallest, non-PSR host)	0.067 M_{\oplus}	Kepler 138b	S016		18
	R (smallest)	$0.303^{+0.053}_{-0.073} R_{\oplus}$	Kepler 37b	S017		19
	α_G (brightest)	0.65	Venus	P079	✓	...
	t (oldest)	11.0 ± 0.8 Gyr	Kepler 444	P077		20
		$\sim 12\text{--}13$ Gyr	82 Eri	S018		21
	P (shortest)	4.25 hr	KOI 1843.03	S019		22
	N_{planet} (most)	7	TRAPPIST-1	S020		23
	M_{host} (smallest, star)	$0.086 \pm 0.008 M_{\odot}$	TRAPPIST-1	S020		24
Giant planet						
Giant planets	R (biggest, $< 1 M_J$)	$22.9^{+1.1}_{-0.8} R_{\oplus}$	HAT-P-67 b	S021		25
	ρ (lowest)	$0.034^{+0.069}_{-0.019} \text{ g cm}^{-3}$	Kepler 51 c	S022		26
	T (hottest)	4,600 K	KELT 9 b	S023		27
	α_G (darkest)	0.025–0.05	TRES-2 b	S024		28
	α_G (brightest)	0.52	Jupiter	P106	✓	...
	t (youngest)	2 Myr	V830 Tau b	S025		29
	t (oldest)	12.7 Gyr	PSR B1620-26 b	S026		30
	M_{host} (largest)	2.8 M_{\odot}	κ And b	S027		31
		1.6–3.2 M_{\odot}	σ UMa b	S028		32
	L_{host} (brightest)	610 L_{\odot}	HD 208527b	S029		33
	T_{host} (hottest)	$11,327^{+421}_{-44} \text{ K}$	κ And	S027		34
		$10,170 \pm 450 \text{ K}$	KELT 9 b	S023		35
	a (furthest)	2,500 AU	GJ 3483 B	S030		36
	a (furthest, $< 1 M_J$)	137 AU	HD 163269 b	S031		37
	Star					
Sub-brown dwarfs	T_{eff} (coldest)	225–260 K	WISE J085510.83-071442.5	P124		38
Stars	M (largest)	$265^{+80}_{-35}\text{--}315^{+60}_{-15} M_{\odot}$	R136 a1	S032		39
	L (faintest)	0.00013 L_{\odot}	2MASS J0523-1403	P133		40
	L (brightest)	$8.7^{+2.0}_{-1.6} \times 10^6 M_{\odot}$	R136 a1	S032		41
	R (smallest)	$0.086 \pm 0.003 R_{\odot}$	2MASS J0523-1403	P133		42
		0.11 R_{\odot}	Feige 34	S033		43
	R (largest)	5 – 13 AU	NML Cyg	S034		44
		$8 \pm 1 \text{ AU}$	UY Sct	S035		45
	T_{eff} (coldest)	$2,074 \pm 21 \text{ K}$	2MASS J0523-1403	P133		46
	T_{eff} (hottest)	210,000 K	WR 102	P190		47
	t (oldest)	12–14 Gyr	HD 140283	P204		48
	[Fe/H] (poorest)	< -7.1	SMSS J0313-6708	S036		49
	[Fe/H] (richest)	~ 0.5	14 Her	S037		50
	[C/H] (lowest)	< -4.3	SDSS J102915+172927	S038		51

Table B1 *continued*

Table B1 (*continued*)

Type	Property	Value	Superlative	ID	Solar?	Ref
	v (fastest)	$12,000 \text{ km s}^{-1}$	S0-16	S039		52
	v (fastest, unbound)	$1,755 \pm 50 \text{ km s}^{-1}$	S5-HVS1	S040		53
	P_{SMBH} (shortest)	11.5 yr	S0-102	S041		54
	q_{SMBH} (closest)	$45 \pm 16 \text{ AU}$	S0-16	S039		55
Collapsed star						
White dwarfs	M (smallest)	$0.16 M_{\odot}$	SDSS J222859.93+362359.6	S042		56
		$0.13\text{--}0.16 M_{\odot}$	NLTT 11748	P223		57
	M (largest)	$1.36\text{--}1.37 M_{\odot}$	U Sco	S043		58
	M (largest, non-interacting)	$1.310\text{--}1.335 M_{\odot}$	LHS 4033	S044		59
	T_{eff} (coldest)	$< 3,000 \text{ K}$	PSR J2222-0137b	S045		60
	T_{eff} (hottest)	$250,000 \text{ K}$	RX J0439.8-6809	S046		61
	B (strongest)	$0.5\text{--}1 \text{ GG}$	PG 1031+234	S047		62
	t (oldest)	11.5 Gyr	WD 0346+246	S048		63
	v (fastest)	$\sim 2,400 \text{ km s}^{-1}$	D6-3	S049		64
	Neutron stars	M (smallest)	$1.02 \pm 0.17 M_{\odot}$	4U 1538-522	S050	
M (largest)		$2.14_{-0.09}^{+0.10} M_{\odot}$	MSP J0740+6620	S051		66
		$2.40 \pm 0.12 M_{\odot}$	PSR B1957+20	P282		67
L_{rot} (brightest)		$130,000 L_{\odot}$	PSR J0537-6910	S052		68
L_{rot} (dimmiest)		$6.8 \times 10^{-6} L_{\odot}$	PSR J2144-3933	S053		69
T_{eff} (coldest)		$< 42,000 \text{ K}$	PSR J2144-3933	S053		70
P_{rot} (fastest)		0.89 ms	XTE J1739-285	S054		71
P_{rot} (slowest)		$36,200 \pm 110 \text{ s}$	AX J1910.7+0917	S055		72
B (strongest)		0.70 PG	SGR 1900+14	S056		73
t (youngest)		33 yr (2020)	NS 1987A	S057		74
Radio pulsars	P_{rot} (fastest)	1.397 ms	PSR J1748-2446ad	S058		75
	P_{rot} (fastest, unrecycled)	16.11 ms	PSR J0537-6910	S052		76
	P_{rot} (slowest)	23.5 s	PSR J0250+5854	S059		77
Black holes	M (smallest)	$3.3_{-0.7}^{+2.8} M_{\odot}$	2MASS J05215658+4359220	S060		78
Interacting binary star						
Interacting binaries	P (shortest)	$321.25 \pm 0.25 \text{ s}$	HM Cnc	S061		79
	EIRP (brightest)	$\sim (0.7\text{--}6) \times 10^7 L_{\odot}$	NGC 5907 ULX	S062		80
Stellar association						
ISM						
ISM	T (coldest)	$0.3\text{--}2 \text{ K}$	Boomerang Nebula	S077		81
Giant molecular clouds	M (largest, Galactic)	$8 \times 10^6 M_{\odot}$	Sgr B2	S078		82
Hot cores	M (largest)	$9,000 M_{\odot}$	Sgr B2(N) AN01	S079		83
HII regions	$L_{\text{H}\alpha}$ (brightest)	$(1.3\text{--}3.9) \times 10^6 L_{\odot}$	30 Dor	S080		84
	R (biggest)	$\sim 200 \text{ pc}$	NGC 604	P307		85
Maser regions	EIRP $_{\text{H}_2\text{O}}$ (brightest, Galactic)	$\sim 1 L_{\odot}$	W49N	S081		86
Galaxy						
Galaxies	$M_{1/2}$ (smallest)	$< 1.5 \times 10^5 M_{\odot}$	Segue 2	S082		87
	M_{\star} (smallest)	$600_{-105}^{+115}\text{--}1,300_{-200}^{+200} M_{\odot}$	Segue 1	S083		88
	M_{\star} (largest)	$(1\text{--}4) \times 10^{12} L_{\odot}$	IC 1101	S084		89
		$(2\text{--}6) \times 10^{12} L_{\odot}$	OGC 21	S085		90

Table B1 (*continued*)

Table B1 (*continued*)

Type	Property	Value	Superlative	ID	Solar?	Ref
	R _{max} (biggest)	610 kpc	IC 1101	S084		91
		960 kpc	LEDA 088678	S086		92
	R _{eff} (biggest)	146 kpc (halo)	IC 1101	S084		93
	Σ (largest)	$9.4 \times 10^{10} M_{\odot} \text{ kpc}^{-2}$	M59-UCD3	S087		94
	L _* (faintest)	$335_{-185}^{+235} L_{\odot}$	Segue 1	S083		95
	L _* (brightest)	$(3.6 \pm 0.3) \times 10^{13} L_{\odot}$	SPT 0346-52	S088		96
		$(4.9 \pm 1.0) \times 10^{13} L_{\odot}$	WISE J101326.25+611220.1	S089		97
	μ (faintest)	$31.9 \text{ mag arcsec}^{-2}$	Antlia 2	S090		98
	[Fe/H] (poorest)	-2.65 ± 0.07	Reticulum II	S091		99
	z (furthest)	$11.09_{-0.12}^{+0.08}$	GN-z11	S092		100
		10.7–11.1	MACS0647-JD	S093		101
Quiescent galaxies	L _V (brightest)	$1.1 \times 10^{12} L_{\odot}$	IC 1101	S084		102
	z (furthest)	3.717	ZF-COSMOS-20115	S094		103
Star-forming galaxies	SFR (highest)	$3,600 \pm 300 M_{\odot} \text{ yr}^{-1}$	SPT 0346-52	S088		104
	R _{eff} (smallest)	$\sim 166 \pm 54 \text{ pc}$	POX 186	P388		105
	M _{gas} /M _*	35–475	AGC 229385	S095		106
	12 + log O/H (poorest)	6.98 ± 0.02	J0811+4730	S096		107
	EIRP _{OH} (brightest)	13,000 L _⊙	IRAS 14070+0525	S097		108
Spiral galaxies	M _* (largest)	$\sim 1.4 \times 10^{12} M_{\odot}$	SS 14	S098		109
	R _{max} (largest)	67 kpc	SS 03	S099		110
	z (furthest)	2.54	A1689B11	S100		111
Lensed galaxies	ℳ (greatest)	$(60\text{--}65) \pm 20$	SPT-CLJ2344-4243 Arc	S101		112
		$\sim 80 \pm 10$	The Snake	S102		113
AGN						
AGNs	M _{SMBH} (smallest)	$5 \times 10^4 M_{\odot}$	RGG 118	S103		114
	M _{SMBH} (largest)	$(4.0 \pm 0.8) \times 10^{10} M_{\odot}$	Holm 15A	S104		115
		$(4\text{--}10) \times 10^{10} M_{\odot}$	IC 1101	S084		116
	L (brightest)	$8.5 \times 10^{14} L_{\odot}$	HS 1946+7658	S105		117
		$6.95 \times 10^{14} L_{\odot}$	SMSS 2157-36	S106		118
	L _{IR} (brightest)	$(1.2\text{--}3.6) \times 10^{14} L_{\odot}$	WISE 2246-0526	S107		119
	M _{host} (smallest)	$(1.2 \pm 0.4) \times 10^8 M_{\odot}$	M60-UCD1	S108		120
	M _{SMBH} /M _{host} (largest)	$0.175_{-0.088}^{+0.26}$	M60-UCD1	S108		121
	z (furthest)	7.54	J1342+0928	S110		122
Lensed AGNs	ℳ (greatest)	~ 173	CLASH B1938+666	S111		123
		~ 159	COSMOS 5921+0638	S112		124
Radio lobes	2R (largest)	4.7 Mpc	J1420-0545	S113		125
Water megamasers	EIRP (brightest)	23,000 L _⊙	J0804+3607	S114		126
Galaxy association						
Galaxy groups	ρ (densest)	$\sim 2 M_{\odot} \text{ pc}^{-3}$	HCG 54	S115		127
		$\sim 0.3 M_{\odot} \text{ pc}^{-3}$	Seyfert's Sextet	S116		128
Galaxy clusters	M (largest)	$(2.93_{-0.32}^{+0.36}\text{--}3.4_{-0.4}^{+0.4}) \times 10^{15} M_{\odot}$	Abell 370	S117		129
	M (largest, z > 0.5)	$\sim (2.8 \pm 0.4) \times 10^{15} M_{\odot}$	MACS J0717.5+34	S118		130
	ℛ (richest)	5	Abell 665	S119		131
	L _X (brightest)	$2.14_{-0.05}^{+0.03} \times 10^{12} L_{\odot}$	Phoenix Cluster	S120		132
	T _{ICM} (hottest)	$17.4 \pm 2.5 \text{ keV}$	Bullet Cluster	P464		133
	z (furthest, X-ray)	2.506	CL J1001+0220	S121		134
Radio halos	L _{1.4 GHz} (brightest)	$0.26\text{--}0.4 L_{\odot} \text{ Hz}^{-1}$	MACS J0717.5+34	S118		135
Radio relics	L _{1.4 GHz} (brightest)	$0.13 L_{\odot} \text{ Hz}^{-1}$	MACS J0717.5+34	S118		136

Table B1 *continued*

Table B1 (*continued*)

Type	Property	Value	Superlative	ID	Solar?	Ref
Protoclusters	z (furthest)	8.38	A2744z8OD	S122		137
LSS						
Galaxy superclusters	M (largest)	$\sim (2-7) \times 10^{16} M_{\odot}$	Shapley Supercluster	S123		138

NOTE—**Quantities** – $12 + \log O/H$: abundance of oxygen relative to hydrogen; a : orbital semimajor axis; α_G : geometric albedo; α_V^G : geometric albedo (V-band); B : magnetic field strength; $[C/H]$: \log_{10} abundance of carbon with respect to Solar composition; EIRP: effective isotropic radiation power; EIRP $_{H_2O}$: EIRP of maser in water emission line; EIRP $_{OH}$: EIRP of maser in OH emission line; $[Fe/H]$: \log_{10} abundance of iron with respect to Solar composition; L: object luminosity; $L_{1.4\text{ GHz}}$: luminosity at 1.4 GHz; $L_{H\alpha}$: luminosity of H α emission line; L_{host} : luminosity of host star; L_{IR} : infrared luminosity; L_{rot} : estimated spin-down power of pulsar; L_V : luminosity in V-band; L_X : X-ray luminosity; M: object mass; $M_{1/2}$: mass within half-light radius; M_{SMBH} : mass of galaxy’s central black hole; M_{gas} : gas mass of galaxy; M_{host} : mass of host galaxy; M_{host^*} : mass of host star; $M_{\text{host}^{\text{planet}}}$: mass of host planet; M_{moon} : mass of satellite; $M_2 \sin i$: minimum mass of secondary (less massive) object in system as determined by radial velocity method; M_* : stellar mass of galaxy; M_V : absolute magnitude in V-band; \mathcal{M} : magnification by gravitational lens; μ : surface brightness; N_{planet} : number of planets of given phylum in stellar system; N_* : number of stars in system; N_{tier} : number of hierarchical levels in multiple star system; P : orbital period; P_{SMBH} : orbital period around host galaxy’s central black hole; P_{rot} : rotation period; q : pericenter; q_{SMBH} : pericenter of orbit around host galaxy’s central black hole; Q : apocenter; R: object radius; R_{eff} : effective (half-light) radius of system; R_p : radius of host planet; R_{max} : full radius of entire object; \mathcal{R} : richness of galaxy cluster; ρ : density; SFR: star-formation rate; t : age; T: object surface temperature; T_{eff} : effective temperature; T_{host} : effective temperature of host star; T_{ICM} : temperature of intracluster medium; v : speed; z : redshift.

Solar? – \checkmark if object is in or passed through Solar System and listed in Table E1; otherwise listed in Table E2.

References—(1) Horner et al. (2012); (2) Elliot et al. (2010); (3) Vilenius et al. (2018); (3) Luhman et al. (2005); (4) de la Fuente Marcos & de la Fuente Marcos (2019); (5) Greenstreet (2020); de la Fuente Marcos & de la Fuente Marcos (2020); (6) Trujillo & Sheppard (2014); (7) Croft (1992); (8) Ortiz et al. (2015); (9) Kenworthy et al. (2015); (10) Ortiz et al. (2015); (11) Mamajek et al. (2012); (12) Stern et al. (2018); (13) Stern et al. (2018); (14) Brown & Schaller (2007); (15) Russell et al. (2016); (16) Stern et al. (2018); (17) Schneider et al. (2011); (18) Schneider et al. (2011); (19) Barclay et al. (2013); (20) Campante et al. (2015); (21) Buldgen et al. (2019); (21) Bernkopf et al. (2012); (22) Ofir & Dreizler (2013); Rappaport et al. (2013); (23) Gillon et al. (2017); (24) Gonzales et al. (2019); (25) Zhou et al. (2017); (26) Libby-Roberts et al. (2020); Piro & Vissapragada (2020); (27) Gaudi et al. (2017); (28) Kipping & Spiegel (2011); Angerhausen et al. (2015); Esteves et al. (2015); (29) Donati et al. (2016); (30) Sigurdsson & Thorsett (2005); (31) Currie et al. (2018); (32) Sato et al. (2007); (32) Andreasen et al. (2017); Stock et al. (2018); (33) Lee et al. (2013); (34) Currie et al. (2018); (35) Gaudi et al. (2017); (36) Rodriguez et al. (2011); (37) Teague et al. (2018); (38) Luhman (2014); (39) Crowther et al. (2016); (40) Dieterich et al. (2014); (41) Crowther et al. (2016); (42) Dieterich et al. (2014); (43) La Palombara et al. (2019); (44) Wing (2009); Zhang et al. (2012); (45) Wittkowski et al. (2017); (46) Dieterich et al. (2014); (47) Trammer et al. (2015); (48) Bond et al. (2013); VandenBerg et al. (2014); Creevey et al. (2015); Sahlholdt et al. (2019); (49) Keller et al. (2014); (50) Gonzalez et al. (1999); Feltzing & Gonzalez (2001); Taylor (2006); Soubiran et al. (2016); Hinkel et al. (2017); Caffau et al. (2019); (51) Caffau et al. (2011); (52) Ghez et al. (2005); Chu et al. (2018); (53) Koposov et al. (2020); (54) Meyer et al. (2012); (55) Ghez et al. (2005); (56) Hermes et al. (2013); (57) Kaplan et al. (2014a); (58) Hachisu & Kato (2001); Shara et al. (2018); (59) Dahn et al. (2004); (60) Kaplan et al. (2014b); (61) Werner & Rauch (2015); (62) Schmidt et al. (1986); Wickramasinghe & Ferrario (2000); (63) Kilic et al. (2012); (64) Shen et al. (2018); (65) Falanga et al. (2015); (66) Cromartie et al. (2020); (67) van Kerkwijk et al. (2011); (68) Marshall et al. (1998); (69) Tiengo et al. (2011); (70) Guillot et al. (2019); (71) Kaaret et al. (2007); (72) Sidoli et al. (2017); (73) Olausen & Kaspi (2014); (74) Cigan et al. (2019); Page et al. (2020); (75) Hessels et al. (2006); (76) Andersson et al. (2018); (77) Tan et al. (2018); (78) Thompson et al. (2019); (79) Israel et al. (2002); (80) Israel et al. (2017); Song et al. (2020); (81) Sahai & Nyman (1997); Bohigas (2017); (82) Schmiedeke et al. (2016); (83) Sánchez-Monge et al. (2017); (84) Kennicutt & Hodge (1986); Relaño & Kennicutt (2009); Crowther (2019); (85) Melnick (1980); Maíz-Apellániz et al. (2004); Tachihara et al. (2018); Crowther (2019); (86) Lo (2005); (87) Kirby et al. (2013); (88) Geha et al. (2009); Martin et al. (2008); (89) Loubser & Sánchez-Blázquez (2011); Dullo et al. (1991); (90) Ogle et al. (2019); (91) Uson et al. (1991); (92) Gonzalez et al. (2000); (93) Dullo et al. (2017); (94) Liu et al. (2015); (95) Martin et al. (2008); Geha et al. (2009); Simon (2019); (96) Ma et al. (2016); Litke et al. (2019); (97) Toba et al. (2020); (98) Torrealba et al. (2019); (99) Simon et al. (2015); (100) Oesch et al. (2016); (101) Coe et al. (2013); Chan et al. (2017); Lam et al. (2019); (102) Uson et al. (1991); Dullo et al. (2017); (103) Glazebrook et al. (2017); Schreiber et al. (2018); (104) Ma et al. (2016); (105) Guseva et al. (2004); (106) Janowiecki et al. (2015); Ball et al. (2018); (107) Izotov et al. (2018); (108) Baan et al. (1992); Pihlström et al. (2005); (109) Ogle et al. (2016, 2019); (110) Ogle et al. (2016); (111) Yuan et al. (2017); (112) Bayliss et al. (2020); (113) Ebeling et al. (2009); (114) Baldassare et al. (2015); (115) Mehrhan et al. (2019); (116) Dullo et al. (2017); (117) Hagen et al. (1992); (118) Wolf et al. (2018); (119) Fan et al. (2018); Tsai et al. (2018); (120) Seth et al. (2014); (121) Seth et al. (2014); (122) Bañados et al. (2018); (123) Barvainis & Ivison (2002); (124) Anguita et al. (2009); (125) Machalski et al. (2008); (126) Barvainis & Antonucci (2005); (127) Hickson et al. (1992); (128) Hickson et al. (1992); Durbala et al. (2008); (129) Broadhurst et al. (2008); Umetsu et al. (2011); (130) Medezinski et al. (2013); (131) Abell et al. (1989); (132) McDonald et al. (2012); (133) Tucker et al. (1998); (134) Wang et al. (2016); (135) Bonafede et al. (2009); Pandey-Pommier et al. (2013); (136) van Weeren et al. (2009); (137) Ishigaki et al. (2016); Laporte et al. (2017); (138) Bardelli et al. (1994); Proust et al. (2006); Chon et al. (2015)

C. THE ANOMALY SAMPLE

Table C1. Anomalies (Non-SETI) catalog

Type	Description	Anomaly	Class	ID	Solar?	Ref
Class I						
Pulsar planets	Unknown formation mechanism, rare for PSR	PSR B1257+12	I (III)	P086		1

Table C1 *continued*

Table C1 (*continued*)

Type	Description	Anomaly	Class	ID	Solar?	Ref	
Paradoxical ELM WDs	ELM white dwarf in too wide binary to be formed	KIC 8145411	I	P294		2	
Peripheral MSP binaries	MSP-WD binary unexpectedly at edge of globular	HE 0430-2457	I	A001		3	
		PSR J1911-5958A	I	A002		4	
Nuclear cluster stars	PSR-star binary at edge of globular cluster	PSR J1740-5340	I	A003		5	
		Stars in hostile Galactic Center environment, where tides could prevent star formation	S0-2	I	A004		6
Nuclear subcluster	Apparent extremely dense star subcluster within inner parsec, possibly within tidal disruption limit	IRS 16C	I	A005		7	
		IRS 16E	I	S066		8	
Nuclear cluster clouds	Oddly compact Galactic Center cloud	G2	I/IV	A006		9	
Displaced supernova	Core collapse supernova well beyond host galaxy's plane	ASASSN -14jb	0/I	A007		10	
Hypervelocity globular cluster	Intergalactic globular cluster with peculiar velocity $\sim 1,000 \text{ km s}^{-1}$	HVGC-1	I	A008		11	
Peculiar offset AGNs	AGNs with offsets in location and velocity from galactic center, possible recoiling SMBHs	3C 186	0/I	A009		12	
		SDSS J113323.97+550415.9	0/I/IV	A010		13	
Class II							
Extreme comet outburst	Unexplained brightening by factor 10^6	17P/Holmes	0/II	A011	✓	14	
Underheated ice giant	Unexplained low heat flux	Uranus	0/II	A012	✓	15	
Super-puffs	Planets with unexplained, extremely low density	HIP 41378f	II	A013		16	
Anomalous abundance star	Unexplained rare-earth and radioactive elements	Przybylski's Star	II	A014		17	
		Abnormally high Be abundance	HD 106038	0/II	A015		18
		Unusual high abundances of some elements	HD 135485	II	A016		19
		Star with abnormal abundances	LS IV-14 116	II	A017		20
Red straggler (subsubgiant)	Stars redder than MS, below subgiant branch	M67-S1063	II	A018		21	
		Unexplained red straggler companion to PSR	PSR J1740-5340	0/II	A003		22
Bloatars	Luminous stars with $T \sim 2,000 \text{ K}$	[SBD2011] 5	II	A019		23	
Kilosecond pulsar	Unexplained 7 hr rotation period	1E 1613-5055	II	A020		24	
Paradoxical WD binary	WD-WD binary, older WD also more massive	DWD HS 2220+2146	II	A021		25	
Overmassive SMBH	Lies far off correlations	NGC 1277*	0/II	A022		26	
		Was 49b	II	A023		27	
Hyperluminous SN/TDE	Abnormally bright TDE or possibly SLSN	ASASSN -15lh	0/II	A024		28	

Table C1 *continued*

Table C1 (continued)

Type	Description	Anomaly	Class	ID	Solar?	Ref
CMB Cold Spot	Unusually extreme temperature fluctuation in CMB	CMB Cold Spot	II	A025		29
Class III						
(10537) 1991 RY ₁₆	Asteroid with unusual spectrum in sparse region of MBA, no sign of parent collisional family	(10537) 1991 RY ₁₆	0/III (+ I)	A026	✓	30
Unexplained geology	Ridge encircles moon, formation unclear	Iapetus	III	S012	✓	31
Anomalous interstellar object	Non-gravitational accelerations, claimed unusual shapes	1I/'Oumuamua	0/III + 0/III	P062	✓	32
Anomalous transits	Deep aperiodic eclipses	Boyajian's Star	0/III	A027		33
	Random transiter	HD 139139	III	A028		34
	Mysterious eclipses	VVV-WIT-07	III	A029		35
	Star with fading and brightening episodes	ASASSN-V J060000.76-310027.83	III	A030		36
Anomalous spectrum star	Red dwarf with WD-like excess emission and Na absorption lines	WISEA 0615-1247	III	A031		37
Anomalous variable star	Star with abnormal variability	LS IV-14 116	III	A017		38
Anomalous dimming stars	Unexplained decadal variability	Boyajian's Star	III	A027		39
	Unusually dimming star	ASASSN-V J190917.06+182837.36	III	A032		40
		ASASSN-V J213939.3-702817.4	III	A033		41
	Vanishing supergiants	NGC 6946-BH1 NGC 3021-CANDIDATE 1	0/III 0/III	P243 A034		42 43
Anomalous stellar outburst	Unexplained FU Ori-like outburst	PTF 14jg	0/III	A035		44
Complex magnetic star	Young star with unusually complex magnetic field geometry and decadal rotational variability	Landstreet's Star	0/III	A036		45
Anomalous stellar flare star	Host of stellar flares with unidentified spectral lines	YZ CMi	III	A037		46
Fast radio burster	Magnetar that emitted brilliant millisecond radio transient	SGR 1935+2154	III	P237		47
Anomalous eclipsing WD/MSP	MSP-WD binary with strange light curve	PSR J1911-5958A	III	A002		48
Red flaring CVs/YSOs		DDE 168	III/IV	A038		49
Galactic hole	Possible void in center of galaxy or other substructure	UMi dSph	III	A039		50
	Anomalous multi-kpc void to one side of galaxy, apparently not due to SF	NGC 247	III/IV	A040		51
Variable galaxy	Dwarf galaxy hosts unknown transient, also seems to change in position or morphology over decades	Leoncino Dwarf	III/IV/V	A041		52
Anomalous flaring AGN	AGN with days-long symmetric burst in optical light curve, possible self-lensing SMBH binary	Spikey	0/III	A042		53

Table C1 continued

Table C1 (*continued*)

Type		Description	Anomaly	Class	ID	Solar?	Ref
Quasi-periodic AGN	erupting	AGN with hour-long X-ray flares, occur on regular (several hour) basis	GSN 069	III	A043		54
Coherently AGN	variable	Coherent picosecond optical variability from AGN	MCG+00-09-070	III	A044		55
Class IV							
Unidentified sources	radio	Bright radio source with possible unidentified optical counterpart	3C 141	IV	A045		56
		Bright radio source with no counterparts	3C 125	IV	A046		57
			3C 431	IV	A047		58
			PMN J1751-2524	IV	A048		59
Radio filament		Unexplained narrow synchrotron-emitting filaments	Galactic Center Radio Arc	IV	A049		60
Unidentified source	γ -ray	Unassociated GeV gamma-ray source off Galactic Plane	3FGL J1539.2-3324	0/IV	A050		61
			3FGL J1231.6-5113	IV	A051		62
Dark accelerator		Unassociated TeV gamma-ray source near Galactic Plane	TeV J2032+4130	0/IV	A052		63
			HESS J1745-303	IV	A053		64
Unidentified transient	radio	Sub-minute duration low frequency radio transient	LWAT 171018	IV	A054		65
		Minute duration low frequency radio transient	ILT J225347+862146	IV	A055		66
		Long duration low frequency radio transient	TGSSADR J183304.4-384046	IV	A056		67
		Multi-hour low frequency radio transient	J103916.2+585124	IV	A057		68
		Multi-day radio transient	WJN J1443+3439	IV	A058		69
		Decade-long radio transient	FIRST J141918.9+394036	0/IV	A059		70
		5 GHz radio transient	RT 19920826	IV	A060		71
Radio burster		Several > 1 Jy radio bursts from inner Galaxy	GCRT J1745-3009	IV	A061		72
Repeating FRB		Unexplained aperiodic millisecond radio transients	FRB 121102	IV (III)	A062		73
Periodic FRB		Unexplained, periodic millisecond radio transients	FRB 180916.J0158+65	IV	A063		74
Unidentified transient	NIR	Possible recurrent NIR transient	VVV-WIT-02	IV	A064		75
Unidentified transient	optical	Possible minutes-long recurrent OT	OTS 1809+31	IV	A065		76
		Pseudo-afterglow	PTF 11agg	0/II/IV	A066		77
		Flaring red object	MASTER OT J051515.25+223945.7	IV	A067		78
		Red point source appearing in one epoch of optical images	USNO-B1.0 1084-0241525	IV	A068		79
		Intermediate luminosity red transient	SN 2008S	IV	A069		80
		Ca-rich gap transient	PTF 09dav	IV	A070		81
		Fast blue UV-optical transients	AT 2018cow	IV	A071		82

Table C1 *continued*

Table C1 (*continued*)

Type	Description	Anomaly	Class	ID	Solar?	Ref
Unidentified transient	X-ray	Unexplained minutes-long X-ray transients	Dougie	0/IV	A072	83
			XRT 000519	IV	A073	84
			CDF-S XT1	IV	A074	85
			Ultraluminous minute-long X-ray transient	IV	A075	86
			Ultraluminous years-long X-ray transient	IV	A076	87
Unidentified transient	γ -ray	Galactic long GRB-like transient with rapid (< 1 s) optical flaring	Swift J195509.6+261406	IV	A077	88
Neutrino coincidence		Coincidence of several neutrinos detected by IceCube	IceCube neutrino multiplet	0/IV	A078	89
Class V						
Impossible eclipsing star	“Impossible” eclipsing triple star with eclipses that cannot be fit	KIC 2856960	0/V	A079		90
ANITA upwards showers	EeV neutrino candidates impossibly propagating through Earth	AAE-061228	V	A080		91
		AAE-141220	V	A081		92
		AAC-150108	V	A082		93

NOTE—**Class** – classification according to scheme in Section 6.1. A “0” in the class indicates the existence of a partial explanation. **Solar?** – \checkmark if object is in or passed through Solar System and listed in Table E1; otherwise listed in Table E2.

References—(1) Wolszczan & Frail (1992); Phinney & Hansen (1993); Podsiadlowski (1993); (2) Masuda et al. (2019); (3) Vos et al. (2018); (4) Cocozza et al. (2006); (5) Orosz & van Kerkwijk (2003); (6) Ghez et al. (2003); Habibi et al. (2017); (7) Paumard et al. (2006); (8) Paumard et al. (2006); Fritz et al. (2010); Wang et al. (2020); (9) Gillessen et al. (2012); Phifer et al. (2013); Plewa et al. (2017); (10) Meza et al. (2019); (11) Caldwell et al. (2014); (12) Chiaberge et al. (2017, 2018); (13) Koss et al. (2014); Stanek et al. (2019); Pursimo et al. (2019); (14) Montalto et al. (2008); Reach et al. (2010); Hsieh et al. (2010); (15) Pearl et al. (1990); (16) Santerne et al. (2019); (17) Przybylski (1961); Cowley et al. (2004); Bidelman (2005); Gopka et al. (2008); (18) Smiljanic et al. (2008); Hansen et al. (2017); (19) Trundle et al. (2001); (20) Naslim et al. (2011); (21) Mathieu et al. (2003); (22) Orosz & van Kerkwijk (2003); Mucciarelli et al. (2013); (23) Spezzi et al. (2011); (24) De Luca et al. (2006); (25) Andrews et al. (2016); (26) van den Bosch et al. (2012); Graham et al. (2016); (27) Secrest et al. (2017); (28) Dong et al. (2016); Leloudas et al. (2016); (29) Cruz et al. (2005, 2008); Szapudi et al. (2015); (30) Moskovitz et al. (2008); (31) Porco et al. (2005); (32) Meech et al. (2017); Micheli et al. (2018); ‘Oumuamua ISSI Team et al. (2019); (33) Boyajian et al. (2016); Wright & Sigurdsson (2016); Boyajian et al. (2018); (34) Rappaport et al. (2019); (35) Saito et al. (2019); (36) Way et al. (2019a); Sokolovsky et al. (2019); (37) Fajardo-Acosta et al. (2016); (38) Green et al. (2011); Randall et al. (2015); (39) Schaefer (2016); Montet & Simon (2016); Wright & Sigurdsson (2016); Hippke & Angerhausen (2018); (40) Way et al. (2019b); (41) Jayasinghe et al. (2019); (42) Gerke et al. (2015); Adams et al. (2017); (43) Reynolds et al. (2015); (44) Hillenbrand et al. (2019); (45) Mikulášek et al. (2019); (46) Haisch & Glampapa (1985); (47) Scholz & Chime/Frb Collaboration (2020); Bochenek et al. (2020); (48) Cocozza et al. (2006); (49) Denisenko (2019); (50) Demers & Battinelli (2001); Bellazzini et al. (2002); (51) Wagner-Kaiser et al. (2014); (52) Filho & Sánchez Almeida (2018); (53) Smith et al. (2018); Hu et al. (2020); (54) Miniutti et al. (2019); (55) Borra (2013); (56) Martel et al. (1998); Maselli et al. (2016); (57) Maselli et al. (2016); (58) Maselli et al. (2016); (59) Titov et al. (2011); (60) Yusef-Zadeh et al. (1984); Anantharamaiah et al. (1991); (61) Massaro et al. (2015); Salvetti et al. (2017); (62) Acero et al. (2013); Massaro et al. (2015); (63) Aharonian et al. (2002, 2008); Aliu et al. (2014); (64) Aharonian et al. (2008); Hayakawa et al. (2012); Hui et al. (2016); (65) Varghese et al. (2019); (66) Stewart et al. (2016); (67) Murphy et al. (2017); (68) Jaeger et al. (2012); (69) Niinuma et al. (2007); Aoki et al. (2014); (70) Law et al. (2018); Marcote et al. (2019); (71) Bower et al. (2007); Frail et al. (2012); (72) Hyman et al. (2005); Roy et al. (2010); (73) Spitler et al. (2016); Chatterjee et al. (2017); (74) The CHIME/FRB Collaboration et al. (2020); Marcote et al. (2020); (75) Dekany et al. (2014); (76) Hudec et al. (1990); (77) Cenko et al. (2013); (78) Balanutsa et al. (2015); (79) Villarroel et al. (2016, 2020); (80) Prieto et al. (2008); (81) Sullivan et al. (2011); Kasliwal et al. (2012); (82) Prentice et al. (2018); (83) Vinkó et al. (2015); (84) Jonker et al. (2013); (85) Bauer et al. (2017); (86) Sivakoff et al. (2005); (87) van Haften et al. (2019); (88) Kasliwal et al. (2008); Stefanescu et al. (2008); Castro-Tirado et al. (2008); (89) Icecube Collaboration et al. (2017); (90) Marsh et al. (2014); Wright et al. (2016); (91) Gorham et al. (2018); (92) Gorham et al. (2018); (93) Aartsen et al. (2020)

Table C2. Anomalies (SETI) catalog

Type	Description	Program	Candidate	Class	ID
Class II					

Table C2 *continued*

Table C2 (*continued*)

Type	Description	Program	Candidate	Class	ID		
IR excess stars	MIR-bright star	C09	IRAS 16466-1406	I	E001		
		C09	IRAS 20331+4024	II	E002		
		C09	IRAS 20369+5131	II	E003		
IR excess galaxies	MIR-bright star cluster	\hat{G}	IRAS 04287+6444	0/II	E004		
	Microwave-excess star	L16	UW CMi	0/II	E005		
	MIR-bright galaxy	\hat{G}	WISE J224436.12+372533.6	II	E006		
	MIR-radio correlation outlier	Ga15	UGC 3097	II	E007		
			NGC 814	II	E008		
			ESO 400-28	II	E009		
			MCG+02-60-017	II	E010		
Abnormally faint star	Luminosity discrepant with spectral type	Z18	TYC 6111-1162-1	0/II	E011		
Underluminous galaxy	Disk galaxies too faint for Tully-Fisher relation	Z15	UGC 5394	II	E012		
			NGC 4502	II	E013		
			NGC 4698	II	E014		
			IC 3877	II	E015		
			AGC 470027	II	E016		
Class III							
Narrowband radio star	Narrowband radio emission from star	B92	HR 6171	III	E017		
		SERENDIP III	GJ 1019	III	E018		
			GJ 299	III	E019		
			P19	LHS 1140 (1.728 GHz)	0/III	P082	
Optical pulse star	Nanosecond optical pulses from star	Harvard OSETI	TRAPPIST-1 (1.153 GHz)	0/III	S020		
			HD 220077	0/III	E020		
			HIP 107359	0/III	E021		
Coherently variable star	Coherent picosecond optical variability from star	BT16	TYC 3010-1024-1	III	E022		
Class IV							
Narrowband radio source	Narrowband transient	Big Ear	Wow! Signal (A)	IV	E023		
			Wow! Signal (B)	IV	E024		
		SERENDIP III	Narrowband radio source	5.13h +2.1	IV	E025	
			Ultra-narrowband radio emission	META	08.00h -08.50	IV	E026
					03.10h +58.0	IV	E027
Unidentified IR source	Unidentified MIR candidate galaxies	META II	11.03.91	IV	E028		
		\hat{G}	WISE 0735-5946	IV	E029		
		\hat{G}	IRAS 16329+8252	IV	E030		
Vanishing star-like source	Apparent star disappearing between archival images	V16	USNO-B1.0 1084-0241525	IV	A068		

NOTE—All sources in this sample are sidereal.

References—BT16: Borra & Trottier (2016); C09: Carrigan (2009); \hat{G} : Griffith et al. (2015); L16: Lacki (2016b); META: Horowitz & Sagan (1993); META-II: Colomb et al. (1995); P19: Pinchuk et al. (2019); SERENDIP-III: Bowyer et al. (2016); V16: Villarroel et al. (2016); Z15: Zackrisson et al. (2015); Z18: Zackrisson et al. (2018)

D. THE CONTROL SAMPLE

Table D1. Control catalog

Object	Original explanation	Class	Ref	Current explanation	Ref	ID
CSL-1	Cosmic string as gravitational lens	III	1	Galaxy pair	2	C001
GRB 090709A	GRB with 8 sec periodicity	III	3	GRB with no periodicity	4	C002
GW100916 (A)	First BH merger observed in gravitational waves	0	5	Blind injection	6	C003
GW100916 (B)		0	7		8	C004
HD 117043	Potassium line-emitting stellar flares	III	9	Matches in observatory	10	C005
HIP 114176	Nearby star	0	11	Scattered light	12	C006
KIC 5520878	RR Lyr with prime number oscillation period ratios	0/III	13	Two period variability	14	C007
KIC 9832227	Imminent stellar merger and LRN	0	15	Triple stellar system with W UMa-type binary, timing typo	16	C008
KOI 6705.01	Variable Moon-sized transiter	III	17	Detector problem	18	C009
Perseus Flasher	Bright optical short transients	IV	19	Satellite glints or physiological response	20	C010
PSR B1829-10	First exoplanet discovered	I/III	21	Pulsar timing correction error	22	C011
OT 060420	Naked-eye optical transient	IV	23	CR hit coincidence	24	C012
SSSPM J1549-3544	Candidate nearest white dwarf	0	25	Distant halo star	26	C013
Swift Trigger 954840	Gamma-ray burst	0	27	Statistical fluctuation	28	C014

NOTE—All sources in this sample are sidereal.

References—(1): Sazhin et al. (2003); (2): Agol et al. (2006); (3): Markwardt et al. (2009); Golenetskii et al. (2009); Gotz et al. (2009); (4): Luca et al. (2010); Cenko et al. (2010); (5): Evans et al. (2012); (6): Evans et al. (2012); (7): Evans et al. (2012); (8): Evans et al. (2012); (9): Barbier & Morguleff (1962); (10): Wing et al. (1967); (11): Perryman et al. (1997); (12): Perryman et al. (1997); (13): Hippke et al. (2015); (14): Hippke et al. (2015); (15): Molnar et al. (2017); (16): Socia et al. (2018); Kovacs et al. (2019); (17): Coughlin et al. (2016); (18): Gaidos et al. (2016); Coughlin et al. (2016); (19): Katz et al. (1986); (20): Halliday et al. (1987); Corso et al. (1987); Maley (1987); Schaefer et al. (1987); Borovicka & Hudec (1989); (21): Bailes et al. (1991); (22): Lyne & Bailes (1992); (23): Shamir & Nemiroff (2006); (24): Shamir & Nemiroff (2006); Smette (2006); Nemiroff & Shamir (2006); (25): Scholz et al. (2004); (26): Farihi et al. (2005); (27): Lipunov et al. (2020); (28): Gropp et al. (2020)

E. THE FULL *EXOTICA* CATALOG

E.1. Notes on data sources

Much of the data used in Figures 3–5 comes from papers on individual sources on the literature. Some general sources we used are listed here; further specific references are listed in the full online appendices using the keys in Tables E1 and E2.³⁷

For Solar System bodies, we consulted the Jet Propulsion Laboratory’s Solar System Dynamics pages³⁸, particularly the Small Solar System Browser³⁹. When masses were unavailable, we estimated them by assuming that objects interior to Jupiter had density 3 g cm^{-3} and the rest had density 2 g cm^{-3} .

We relied on Simbad data for the bulk of Table E2. Stellar data was partly based on *Gaia* distances, colors, and extinctions (Gaia Collaboration et al. 2018); extinctions from Savage et al. (1985) and Gudennavar et al. (2012); PASTEL effective temperatures and surface gravities (Soubiran et al. 2016); *Hipparcos* photometry and distances (Perryman et al. 1997); and individualized references. For the I17 stars plotted in Figure 4, it was impractical to find individualized sources; we supplemented with data from Holmberg et al. (2007), Takeda et al. (2007), CATSUP (Hinkel et al. 2017), and Swihart et al. (2017). Frequently, we had to calculate the luminosity and/or surface temperature from other quantities (mass, radius, bolometric flux, angular size, and distance).

Galaxy data was partly based on NED redshifts and photometry from 2MASS (Skrutskie et al. 2006), de Vaucouleurs et al. (1991), and Data Releases 9 and 12 of the Sloan Digital Sky Survey (Ahn et al. 2012; Alam et al. 2015). For I17 galaxies, we relied mainly on the B-band magnitudes in I17 itself and the photometry in Mateo (1998). Because photometry in u and r bands was frequently unavailable, we relied heavily on the color transformations of Blanton & Roweis (2007), Jester et al. (2005), and Lupton’s equations⁴⁰ to derive the approximate colors for use in Figure 5. Redshifts were converted to luminosity distances assuming $H_0 = 70 \text{ km s}^{-1} \text{ Mpc}^{-1}$, $\Omega_m = 0.3$, and $\Omega_\Lambda = 0.7$. In some cases, the stellar mass was calculated from K_s absolute magnitudes using the conversion of Cappellari (2013). I17

³⁷ Hosted at <http://seti.berkeley.edu/exotica>.

³⁸ <https://ssd.jpl.nasa.gov/>

³⁹ <https://ssd.jpl.nasa.gov/sbdb.cgi>

⁴⁰ As presented at <http://classic.sdss.org/dr6/algorithms/sdssUBVRITransform.html>.

galaxy star-formation rates were largely calculated from GALEX ultraviolet and IRAS total infrared luminosities (Bai et al. 2015; Sanders et al. 2003), using the corrections of Hao et al. (2011), with additional data from Licquia et al. (2015), Jarrett et al. (2019), and McConnachie (2012).

E.2. Tables of the catalog

Table E1. The *Exotica Catalog*: Solar System targets

ID	Name	Samples	Phyla	Primary	a	e	i	a_{\odot}	MOID $_{\oplus}$	Θ	Ref
								(AU)	(AU)		
P001	446 Aeternitas	P	Minor body	Sun	2.79 AU	0.126	10.62	2.79	1.45	...	
P002	52 Europa	P	Minor body	Sun	3.09 AU	0.110	7.48	3.09	1.77	0.2''	
P003	624 Hektor	P	Minor body	Sun	5.26 AU	0.023	18.16	5.26	4.15	...	
P004	434 Hungaria	P	Minor body	Sun	1.94 AU	0.074	22.51	1.94	0.83	...	
P005	16 Psyche	P	Minor body	Sun	2.92 AU	0.134	3.10	2.92	1.54	0.2''	
P006	3628 Božněmcová	P	Minor body	Sun	2.54 AU	0.297	6.88	2.54	0.78	...	
P007	420 Bertholda	P	Minor body	Sun	3.41 AU	0.030	6.69	3.41	2.33	...	
P008	1862 Apollo	P	Minor body	Sun	1.47 AU	0.560	6.35	1.47	0.03	...	
P009	349 Dembowska	P	Minor body	Sun	2.92 AU	0.092	8.25	2.92	1.66	0.1''	
P010	15 Eunomia	P	Minor body	Sun	2.64 AU	0.186	11.75	2.64	1.19	0.3''	
P011	233 Asterope	P	Minor body	Sun	2.66 AU	0.099	7.69	2.66	1.40	...	
P012	4 Vesta	P	Minor body	Sun	2.36 AU	0.089	7.14	2.36	1.14	0.6''	
P013	90 Antiope	P	Minor body	Sun	3.15 AU	0.166	2.21	3.15	1.61	...	
P014	3200 Phaethon	P	Minor body	Sun	1.27 AU	0.890	22.26	1.27	0.02	0.4''	
P015	2020 AV ₂	PS	Minor body	Sun	0.56 AU	0.177	15.87	0.56	0.35	...	
P016	(322756) 2001 CK ₃₂	P	Minor body	Sun	0.73 AU	0.383	8.13	0.73	0.08	...	
P017	163693 Atira	P	Minor body	Sun	0.74 AU	0.322	25.62	0.74	0.21	...	
P018	3753 Cruithne	P	Minor body	Sun	1.00 AU	0.515	19.81	1.00	0.07	...	
P019	1991 VG	P	Minor body	Sun	1.03 AU	0.052	1.43	1.03	0.00	...	
P020	2010 TK ₇	P	Minor body	Sun	1.00 AU	0.190	20.90	1.00	0.08	...	
P021	(469219) Kamo'oalewa	P	Minor body	Sun	1.00 AU	0.103	7.79	1.00	0.03	...	
P022	4660 Nereus	P	Minor body	Sun	1.49 AU	0.360	1.43	1.49	0.00	0.1''	
P023	433 Eros	P	Minor body	Sun	1.46 AU	0.223	10.83	1.46	0.15	0.2''	
P024	5261 Eureka	P	Minor body	Sun	1.52 AU	0.065	20.28	1.52	0.50	...	
P025	8 Flora	P	Minor body	Sun	2.20 AU	0.156	5.89	2.20	0.88	0.2''	
P026	25 Phocaea	P	Minor body	Sun	2.40 AU	0.255	21.61	2.40	0.92	...	
P027	65 Cybele	P	Minor body	Sun	3.42 AU	0.112	3.56	3.42	2.03	0.2''	
P028	153 Hilda	P	Minor body	Sun	3.98 AU	0.140	7.82	3.98	2.41	...	
P029	1P/Halley	P	Minor body	Sun	17.83 AU	0.967	162.26	17.83	0.06	0.2''	
P030	C/2014 S3 (PAN-STARRS)	P	Minor body	Sun	90.46 AU	0.977	169.32	90.46	1.09	...	
P031	5335 Damocles	P	Minor body	Sun	11.84 AU	0.866	61.60	11.84	0.61	...	
P033	2P/Encke	P	Minor body	Sun	2.22 AU	0.848	11.78	2.22	0.17	...	
P034	133P/Elst-Pizzaro	P	Minor body	Sun	3.16 AU	0.157	1.39	3.16	1.65	...	
P035	9P/Tempel 1	P	Minor body	Sun	3.15 AU	0.510	10.47	3.15	0.53	...	
P036	95P/Chiron	PS	Minor body	Sun	13.69 AU	0.379	6.94	13.69	7.50	...	
P037	153P/Ikeya-Zhang	P	Minor body	Sun	51.21 AU	0.990	28.12	51.21	0.33	...	
P038	(24835) 1995 SM ₅₅	P	Minor body	Sun	41.66 AU	0.101	27.04	41.66	36.60	...	
P039	(15788) 1993 SB	P	Minor body	Sun	39.15 AU	0.317	1.94	39.15	25.80	...	
P040	(385185) 1993 RO	P	Minor body	Sun	39.23 AU	0.199	3.71	39.23	30.40	...	
P041	15760 Albion	P	Minor body	Sun	43.93 AU	0.071	2.18	43.93	39.80	...	
P042	79360 Sila-Nunam	P	Minor body	Sun	43.64 AU	0.009	2.26	43.64	42.30	...	
P043	2011 QF ₉₉	P	Minor body	Sun	19.04 AU	0.175	10.82	19.04	14.70	...	
P044	2001 QR ₃₂₂	P	Minor body	Sun	30.23 AU	0.031	1.32	30.23	28.30	...	

Table E1 continued

Table E1 (continued)

ID	Name	Samples	Phyla	Primary	a	e	i	a_{\odot}	MOID $_{\oplus}$	Θ	Ref
								(AU)	(AU)		
P045	(523899) 1997 CV ₂₉	P	Minor body	Sun	42.06 AU	0.043	8.04	42.06	39.30	...	
P046	(20161) 1996 TR ₆₆	P	Minor body	Sun	47.96 AU	0.401	12.40	47.96	27.70	...	
P047	(91554) 1999 RZ ₂₁₅	P	Minor body	Sun	103.40 AU	0.701	25.46	103.4	29.90	...	1
P048	(181902) 1999 RD ₂₁₅	P	Minor body	Sun	123.24 AU	0.696	25.94	123.24	36.60	...	2
P049	Phobos	PS	Minor body	Mars	9.376 Mm	0.015	1.08	1.52	0.52	...	
P050	Amalthea	P	Minor body	Jupiter	181.4 Mm	0.003	0.38	5.20	4.20	...	
P051	Methone	P	Minor body	Saturn	194.4 Mm	0.000	0.01	9.54	8.54	...	
P052	Himalia	P	Minor body	Jupiter	11.46 Gm	0.159	28.61	5.20	4.20	...	
P053	Phoebe	P	Minor body	Saturn	12.95 Gm	0.163	175.24	9.54	8.54	...	
P054	Helene	P	Minor body	Saturn	377.4 Mm	0.000	0.21	9.54	8.54	...	
P055	Epimetheus	P	Minor body	Saturn	151.4 Mm	0.016	0.35	9.54	8.54	...	
P056	2006 RH ₁₂₀	P	Minor body	Sun	1.00 AU	0.035	1.09	1.00	0.00	...	3
P057	Prometheus	P	Minor body	Saturn	139.4 Mm	0.0022	0.007	9.54	8.54	...	
P058	Hyperion	P	Minor body	Saturn	1.501 Gm	0.023	0.62	9.54	8.54	...	
P060	Saturn	P	Minor body	Sun	9.54 AU	0.054	2.49	9.54	8.54	18.8''	
P061	2I/Borisov	P	Minor body	Sun	-0.85 AU	3.356	44.05	-0.85	1.09	...	
P062	1I/'Oumuamua	PA	Minor body	Sun	-1.27 AU	1.201	122.74	-1.27	0.10	...	
P074	Mercury	P	Solid planetoid	Sun	0.39 AU	0.206	7.00	0.39	0.61	11.0''	
P076	Mars	P	Solid planetoid	Sun	1.52 AU	0.093	1.85	1.52	0.52	18.0''	
P079	Venus	PS	Solid planetoid	Sun	0.72 AU	0.007	3.39	0.72	0.28	59.6''	
P087	1 Ceres	PS	Solid planetoid	Sun	2.77 AU	0.076	10.59	2.77	1.59	0.8''	
P088	136199 Eris	PS	Solid planetoid	Sun	67.86 AU	0.436	44.04	67.86	37.30	...	4
P089	134340 Pluto	PS	Solid planetoid	Sun	39.45 AU	0.250	17.09	39.45	28.60	0.1''	
P090	90377 Sedna	PS	Solid planetoid	Sun	484.44 AU	0.843	11.93	484.44	75.30	...	5
P091	136472 Makemake	P	Solid planetoid	Sun	45.43 AU	0.161	28.98	45.43	37.20	...	
P092	136108 Haumea	P	Solid planetoid	Sun	43.18 AU	0.195	28.21	43.18	33.80	...	6
P093	Moon	PS	Solid planetoid	Earth	384.4 Mm	0.055	5.16	0.00	0.00	31.1'	
P094	Titan	P	Solid planetoid	Saturn	1.222 Gm	0.029	0.31	9.54	8.54	0.8''	
P095	Triton	P	Solid planetoid	Neptune	354.8 Mm	0.000	156.87	30.07	29.10	0.1''	
P096	Europa	P	Solid planetoid	Jupiter	671.1 Mm	0.009	0.47	5.20	4.20	1.0''	
P097	Callisto	P	Solid planetoid	Jupiter	1.883 Gm	0.007	0.19	5.20	4.20	1.6''	
P098	Ganymede	PS	Solid planetoid	Jupiter	1.070 Gm	0.001	0.18	5.20	4.20	1.7''	
P099	Enceladus	PS	Solid planetoid	Saturn	238.0 Mm	0.000	0.00	9.54	8.54	...	
P100	Io	PS	Solid planetoid	Jupiter	421.8 Mm	0.004	0.04	5.20	4.20	1.2''	
P101	Neptune	P	Giant planet	Sun	30.07 AU	0.009	1.77	30.07	29.10	2.3''	
P106	Jupiter	PS	Giant planet	Sun	5.20 AU	0.048	1.30	5.20	4.20	45.9''	
P141	Sun	P	Star	Milky Way	8 kpc	0.00	1.00	32.0'	
P473	ISS	P	Technology	Earth	1.00	0.00	...	
P474	TBD	P	Technology	Earth	1.00	0.00	...	
P475	TBD	P	Technology	Earth	1.00	0.00	...	
P476	TBD	P	Technology	Earth	1.00	0.00	...	
P477	TBD	P	Technology	Earth	1.00	0.00	...	
P478	TBD	P	Technology	Earth	1.00	0.00	...	
P479	TBD	P	Technology	Earth	1.00	0.00	...	
P480	<i>Voyager 1</i>	P	Technology	Milky Way	0.00	...	
P481	<i>Light-Sail 2</i>	P	Technology	Earth	1.00	0.00	...	
P482	LCS-1	P	Technology	Earth	1.00	0.00	...	
P483	Vanguard I	P	Technology	Earth	1.00	0.00	...	
P484	TBD	P	Technology	Earth	0.00	...	
P485	1963-014G	P	Technology	Earth	1.00	0.00	...	
P486	Cosmos 860 coolant (1976-103G)	P	Technology	Earth	1.00	0.00	...	

Table E1 continued

Table E1 (*continued*)

ID	Name	Samples	Phyla	Primary	a	e	i	a_{\odot}	MOID $_{\oplus}$	Θ	Ref
								(AU)	(AU)		
P487	Tesla Roadster	P	Technology	Sun	1.33 AU	0.259	1.09	1.33	0.33	...	
P488	Solar antipoint	P	Not real	(Sun)	0.00	...	
S001	1173 Anchises	S	Minor body	Sun	5.29 AU	0.139	6.92	5.29	3.55	...	
S002	(55636) 2002 TX ₃₀₀	S	Minor body	Sun	43.27 AU	0.126	25.83	43.27	36.80	...	7
S004	2019 LF ₆	S	Minor body	Sun	0.56 AU	0.429	29.51	0.56	0.26	...	
S005	2012 VP ₁₁₃	S	Minor body	Sun	261.49 AU	0.693	24.11	261.49	79.50	...	
S006	2014 FZ ₇₁	S	Minor body	Sun	75.41 AU	0.259	25.52	75.41	74.40	...	8
S007	Proteus	S	Minor body	Neptune	117.6 Mm	0.001	0.08	30.07	29.10	...	
S008	Neso	S	Minor body	Neptune	50.26 Gm	0.424	131.27	30.07	29.10	...	
S009	Metis	S	Minor body	Jupiter	128.0 Mm	0.001	0.02	5.20	4.20	...	
S011	Mimas	S	Solid planetoid	Saturn	185.5 Mm	0.020	1.57	9.54	8.54	...	
S012	Iapetus	SA	Solid planetoid	Saturn	3.561 Gm	0.029	8.30	9.54	8.54	0.2''	
S013	Tethys	S	Solid planetoid	Saturn	294.7 Mm	0.000	1.09	9.54	8.54	0.2''	
S014	Charon	S	Solid planetoid	Pluto	19.59 Mm	0.000	0.08	39.48	38.50	...	
S015	Miranda	S	Solid planetoid	Uranus	129.9 Mm	0.001	4.34	19.19	18.20	...	
A011	17P/Holmes	A	Minor body	Sun	3.62 AU	0.432	19.09	3.62	1.06	...	
A012	Uranus	A	Giant planet	Sun	19.19 AU	0.047	0.77	19.19	18.20	3.8''	
A026	(10537) 1991 RY ₁₆	A	Minor body	Sun	2.85 AU	0.071	7.26	2.85	1.63	...	

NOTE—**Samples** – All samples a target is in. P: Prototype, S: Superlative, A: non-SETI Anomaly, E: SETI Anomaly, C: Control.

Primary – Name of body the target orbits.

a , e , i – Semimajor axis, eccentricity, inclination of target's orbit around body's primary, respectively.

a_{\odot} – Semimajor axis of target's or primary's orbit around Sun.

MOID $_{\oplus}$ – Minimum orbital intersection distance with Earth's orbit.

Θ – Maximum angular size of body, as calculated from radius and MOID $_{\oplus}$.

Table E2. *The Exotica Catalog: Sidereal targets*

ID	Name	Samples	Phyla	RA	Dec	D_L^{eff}	μ_{α}	μ_{δ}	Θ	I17?	Refs
P032	β Pic	P	Minor body	5:47:17.1	-51:03:59	19.8 pc	4.7	83.1	...	✓	1
P059	WD 1145+017	P	Minor body	11:48:33.6	+1:28:59	141.7 pc	-43.7	-4.1	...		2
P063	TW Hya	P	Minor body, Star	11:01:51.9	-34:42:17	60.1 pc	-68.4	-14.0	...		3
P064	EPIC 203937317	P	Minor body	16:26:17.1	-24:20:22	134.3 pc	-6.6	-27.1	...		4
P065	GM Aur	P	Minor body	4:55:11.0	+30:21:59	159.6 pc	3.9	-24.5	...		5
P066	τ Cet	P	Minor body, Star	1:44:04.1	-15:56:15	3.6 pc	-1721.0	854.2	...	✓	6
P067	κ Psc	P	Minor body	23:26:56.0	+1:15:20	48.9 pc	87.1	-95.7	...	✓	7
P068	Altair	P	Minor body	19:50:47.0	+8:52:06	5.1 pc	536.2	385.3	...	✓	8
P069	NGC 2547 ID8	P	Minor body	8:09:02.5	-48:58:17	360.9 pc	-12.1	9.9	...		9
P070	BD+20 307	P	Minor body	1:54:50.3	+21:18:22	120.0 pc	38.8	-22.6	...		9
P071	NGC 7293 central star	P	Minor body, Collapsed star	22:29:38.5	-20:50:14	201.0 pc	38.9	-3.4	...		10
P072	G29-38	P	Minor body	23:28:47.6	+5:14:54	13.6 pc	-398.2	-266.7	...		11
P073	WD J0914+1914	P	Minor body	9:14:05.3	+19:14:12	443.0 pc	-1.2	-11.6	...		12
P075	K2-229 b	P	Solid planetoid	12:27:29.6	-6:43:19	102.8 pc	-80.9	7.4	...		13, 14
P077	Kepler 444 d	PS	Solid planetoid	19:19:00.5	+41:38:05	36.5 pc	94.7	-632.2	...		15, 16
P078	Proxima b	P	Solid planetoid	14:29:42.9	-62:40:46	1.3 pc	-3781.3	769.8	...	✓	17, 18
P080	Kepler 78 b	P	Solid planetoid	19:34:58.0	+44:26:54	124.8 pc	38.1	-16.1	...		19
P081	Barnard's star b	P	Solid planetoid	17:57:48.5	+4:41:36	1.8 pc	-802.8	10363.0	...	✓	20, 21

Table E2 *continued*

Table E2 (continued)

ID	Name	Samples	Phyla	RA	Dec	D_L^{eff}	μ_α	μ_δ	Θ	I17?	Refs
P082	LHS 1140 b	PE	Solid planetoid, Star	0:44:59.3	-15:16:18	15.0 pc	317.6	-596.6	...		22, 23
P083	HD 40307 f	P	Solid planetoid	5:54:04.2	-60:01:24	12.9 pc	-52.4	-60.2	...		24, 25
P084	55 Cnc e	P	Solid planetoid	8:52:35.8	+28:19:51	12.6 pc	-485.9	-233.7	...	✓	26, 27
P085	KIC 12557548 b	P	Solid planetoid	19:23:51.9	+51:30:17	618.5 pc	0.3	11.1	...		28
P086	PSR B1257+12 ABC	PSA	Solid planetoid	13:00:03.1	+12:40:55	600.0 pc	46.4	-84.9	...		29
P102	Kepler 22 b	P	Giant planet	19:16:52.2	+47:53:04	195.7 pc	-39.7	-66.7	...		30
P103	GJ 436 b	P	Giant planet	11:42:11.1	+26:42:24	9.8 pc	895.0	-814.0	...		31, 32, 33
P104	HATS-P-26 b	P	Giant planet	14:12:37.5	+4:03:36	142.4 pc	37.8	-142.9	...		34
P105	GJ 1214 b	P	Giant planet	17:15:18.9	+4:57:50	14.6 pc	580.4	-749.6	...		35, 36
P107	HD 93083 b	P	Giant planet	10:44:20.9	-33:34:37	28.5 pc	-92.7	-152.2	...		37, 38, 39
P108	HATS-17 b	P	Giant planet	12:48:45.5	-47:36:49	404.6 pc	-32.1	2.8	...		40, 41
P109	HD 189733 b	P	Giant planet	20:00:43.7	+22:42:39	19.8 pc	-3.3	-250.2	...	✓	42, 43
P110	HD 209458 b	P	Giant planet	22:03:10.8	+18:53:04	48.4 pc	29.6	-17.9	...		44, 45
P111	Kepler 18 d	P	Giant planet	19:52:19.1	+44:44:47	438.5 pc	-1.4	-20.3	...		46, 47
P112	Kepler 16 b	P	Giant planet	19:16:18.2	+51:45:27	75.2 pc	14.0	-48.6	...		48, 49
P113	Kepler 56 bc	P	Giant planet	19:35:02.0	+41:52:19	936.9 pc	-6.7	-12.0	...		50, 51
P114	HR 8799 bcde	P	Giant planet	23:07:28.7	+21:08:03	41.3 pc	108.3	-49.5	...	✓	52, 53
P115	HD 28185 b	P	Giant planet	4:26:26.3	-10:33:03	39.4 pc	84.1	-59.8	...		54, 55
P116	HD 80606 b	P	Giant planet	9:22:37.6	+50:36:13	66.6 pc	55.9	10.3	...		56, 57
P117	HD 147506 b	P	Giant planet	16:20:36.4	+41:02:53	128.2 pc	-10.3	-29.2	...		58, 59
P118	Pollux b	P	Giant planet	7:45:18.9	+28:01:34	10.4 pc	-626.5	-45.8	...	✓	60, 61, 62
P119	IRAS 16293-2422	P	Star	16:32:22.6	-24:28:32	120.0 pc		63, 64
P120	Elias 29	P	Star	16:27:09.4	-24:37:19	120.0 pc		65
P121	IRAS 20126+4104	P	Star	20:14:25.9	+41:13:37	1.4 kpc	-3.9	-4.6	...		
P122	AB Aur	P	Star	4:55:45.8	+30:33:04	162.9 pc	3.9	-24.1	...		66
P123	FU Ori	P	Star	5:45:22.4	+9:04:12	416.2 pc	2.2	-2.8	...		
P124	WISE J085510.83-071442.5	PS	Star	8:55:10.8	-7:14:42	2.2 pc	-4800.0	500.0	...		67, 68
P125	WISE J071322.55-291751.9	P	Star	7:13:22.6	-29:17:52	9.9 pc	341.1	-411.1	...		69
P126	2MASSI J0415195-093506	P	Star	4:15:19.5	-9:35:07	5.6 pc	2193.0	527.0	...		70
P127	ϵ Ind Bb	P	Star	22:04:10.5	-56:46:58	3.6 pc	3955.6	-2464.3	...		71
P128	Luhman 16B	P	Star	10:49:18.9	-53:19:09	2.0 pc		72, 73
P129	Luhman 16A	P	Star	10:49:19.0	-53:19:10	2.0 pc		74, 75
P130	HD 130948BC	P	Star	14:50:16.0	+23:54:42	17.9 pc	144.7	32.4	...	✓	76
P131	2MASSI J1506544+132106	P	Star	15:06:54.3	+13:21:06	11.7 pc	-1071.0	-11.9	...		

Table E2 continued

Table E2 (continued)

ID	Name	Samples	Phyla	RA	Dec	D_L^{eff}	μ_α	μ_δ	Θ	I17?	Refs
P132	PPL 15	P	Star	3:48:04.7	+23:39:30	142.1 pc	18.8	-45.5	...		77
P133	2MASS J0523-1403	PS	Star	5:23:38.2	-14:03:02	12.8 pc	107.3	160.9	...		78
P134	VB 10	P	Star	19:16:57.6	+5:09:02	5.9 pc	-598.2	-1365.3	...		79, 80
P135	Wolf 359	P	Star	10:56:28.8	+7:00:52	2.0 pc	-3808.1	-2692.6	...	✓	81
P136	HD 95735	P	Star	11:03:20.2	+35:58:12	2.5 pc	-580.3	-4765.9	...	✓	82
P137	61 Cyg B	P	Star	21:06:55.3	+38:44:31	3.5 pc	4105.8	3155.8	...	✓	83
P138	61 Cyg A	P	Star	21:06:53.9	+38:44:58	3.5 pc	4164.2	3250.0	...	✓	84
P139	ϵ Eri	P	Star	3:32:55.8	-9:27:30	3.2 pc	-975.2	19.5	...	✓	85
P140	κ_1 Cet	P	Star	3:19:21.7	+3:22:13	9.1 pc	269.3	93.8	...	✓	86
P142	β Vir	P	Star	11:50:41.7	+1:45:53	11.1 pc	740.2	-270.4	...	✓	87
P143	π_3 Ori	P	Star	4:49:50.4	+6:57:41	8.0 pc	464.1	11.2	...	✓	88
P144	78 UMa	P	Star	13:00:43.7	+56:21:59	25.4 pc	107.9	2.0	...	✓	89
P145	α Cep	P	Star	21:18:34.8	+62:35:08	15.0 pc	150.6	49.1	...	✓	90
P146	Alcor	P	Star	13:25:13.5	+54:59:17	24.7 pc	120.2	-16.0	...	✓	91
P147	Vega	P	Star	18:36:56.3	+38:47:01	7.7 pc	200.9	286.2	...	✓	92
P148	λ Aql	P	Star	19:06:14.9	-4:52:57	37.0 pc	-20.1	-89.1	...	✓	93
P149	α Gru	P	Star	22:08:14.0	-46:57:40	31.0 pc	126.7	-147.5	...	✓	94
P150	η UMa	P	Star	13:47:32.4	+49:18:48	31.9 pc	-121.2	-14.9	...	✓	95
P151	10 Lac	P	Star	22:39:15.7	+39:03:01	358.7 pc	-0.3	-5.5	...		96
P152	HD 46150	P	Star	6:31:55.5	+4:56:34	1.5 kpc	-2.1	-0.6	...		97
P153	HD 64568	P	Star	7:53:38.2	-26:14:03	7.1 kpc	-0.6	3.8	...		98
P154	κ CrB	P	Star	15:51:13.9	+35:39:27	30.1 pc	-8.8	-347.8	...		99, 100
P155	μ Her	P	Star	17:46:27.5	+27:43:14	8.4 pc	-291.7	-749.6	...	✓	101
P156	Procyon	P	Star	7:39:18.1	+5:13:30	3.5 pc	-714.6	-1036.8	...	✓	102
P157	ι UMa	P	Star	8:59:12.5	+48:02:31	14.5 pc	-441.3	-215.3	...	✓	103
P158	γ Cru	P	Star	12:31:10.0	-57:06:48	27.2 pc	28.2	-265.1	...	✓	104
P159	Aldebaran	P	Star	4:35:55.2	+16:30:33	20.4 pc	63.5	-188.9	...	✓	105
P160	Arcturus	P	Star	14:15:39.7	+19:10:57	11.3 pc	-1093.4	-2000.1	...	✓	106
P161	α Ser	P	Star	15:44:16.1	+6:25:32	25.4 pc	133.8	44.8	...	✓	107
P162	BD +17 3248	P	Star	17:28:14.5	+17:30:36	819.1 pc	-47.7	-22.4	...		108
P163	RR Lyr	P	Star	19:25:27.9	+42:47:04	265.2 pc	-109.1	-195.5	...		109, 110
P164	HD 161817	P	Star	17:46:40.6	+25:44:57	187.8 pc	-37.7	-43.6	...		111
P165	R Dor	P	Star	4:36:45.6	-62:04:38	54.6 pc	-69.4	-75.8	...		112
P166	RS Cnc	P	Star	9:10:38.8	+30:57:47	143.5 pc	-11.1	-33.4	...		113
P167	IRC +10216	P	Star	9:47:57.4	+13:16:44	92.7 pc	33.8	10.0	...		114
P168	IRC +10011	P	Star	1:06:26.0	+12:35:53	500.0 pc		115, 116
P169	HD 44179	P	Star	6:19:58.2	-10:38:15	440.5 pc	-6.5	-22.7	...		117
P170	V4334 Sgr	P	Star	17:52:32.7	-17:41:08	2.9 kpc		118
P171	Regulus	P	Star	10:08:22.3	+11:58:02	23.8 pc	-248.7	5.6	...	✓	119
P172	α Hya	P	Star	9:27:35.2	-8:39:31	55.3 pc	-15.2	34.4	...		120
P173	α Cet	P	Star	3:02:16.8	+4:05:23	76.4 pc	-10.4	-76.8	...		121, 122
P174	ζ Aur	P	Star	5:02:28.7	+41:04:33	241.0 pc	9.4	-20.7	...		123
P175	ϵ Vir	P	Star	13:02:10.6	+10:57:33	32.7 pc	-273.8	20.0	...	✓	124
P176	Capella Aa	P	Star	5:16:41.4	+45:59:53	13.0 pc	75.2	-426.9	...		125
P177	δ Cep	P	Star	22:29:10.3	+58:24:55	244.0 pc	15.3	3.5	...		126
P178	β Ara	P	Star	17:25:18.0	-55:31:48	198.0 pc	-8.5	-25.2	...		127
P179	1 Car	P	Star	9:45:14.8	-62:30:28	478.5 pc	-12.9	8.2	...		128
P180	Canopus	P	Star	6:23:57.1	-52:41:44	94.8 pc	19.9	23.2	...		129
P181	MSX SMC 055	P	Star	0:50:07.2	-73:31:25	61.9 kpc		130, 131
P182	ι Ori	P	Star	5:35:26.0	-5:54:36	714.3 pc	1.4	-0.5	...		132

Table E2 continued

Table E2 (continued)

ID	Name	Samples	Phyla	RA	Dec	D_L^{eff}	μ_α	μ_δ	Θ	I17?	Refs
P183	ζ Per	P	Star	3:54:07.9	+31:53:01	400.0 pc	5.8	-9.9	...		133
P184	Deneb	P	Star	20:41:25.9	+45:16:49	432.9 pc	2.0	1.9	...		134
P185	Betelgeuse	P	Star	5:55:10.3	+7:24:25	152.7 pc	27.5	11.3	...		135
P186	ρ Cas	P	Star	23:54:23.0	+57:29:58	1.1 kpc	-5.4	-2.6	...		136
P187	VY CMa	P	Star	7:22:58.3	-25:46:03	1.2 kpc	5.7	-6.8	...		137, 138, 139
P188	EZ CMa	P	Star	6:54:13.0	-23:55:42	838.0 pc	-4.4	2.9	...		140, 141
P189	γ_2 Vel	P	Star	8:09:32.0	-47:20:12	157.0 pc	-6.1	10.4	...		142
P190	WR 102	PS	Star	17:45:47.5	-26:10:27	2.9 kpc	0.9	-0.2	...		143
P191	ζ_1 Sco	P	Star	16:53:59.7	-42:21:43	1.6 kpc	0.0	-2.9	...		144
P192	AG Car	P	Star	10:56:11.6	-60:27:13	1.3 kpc	-4.7	1.9	...		145
P193	η Car	P	Star	10:45:03.5	-59:41:04	2.4 kpc	-11.0	4.1	...		146, 147, 148
P194	ϵ Ser	P	Star	15:50:49.0	+4:28:40	20.8 pc	128.2	62.2	...		149
P195	α_2 CVn	P	Star	12:56:01.7	+38:19:06	35.2 pc	-235.1	53.5	...	✓	150
P196	ζ Tau	P	Star	5:37:38.7	+21:08:33	136.4 pc	1.8	-20.1	...		151
P197	TVLM 513-46546	P	Star	15:01:08.2	+22:50:02	10.7 pc	-43.8	-64.0	...		152
P198	CU Vir	P	Star	14:12:15.8	+2:24:34	71.8 pc	-42.6	-26.7	...		153
P199	2MASS J0532+8246	P	Star	5:32:54.4	+82:46:45	24.9 pc	2038.3	-1663.7	...		154
P200	Kaptyen's Star	P	Star	5:11:40.6	-45:01:06	3.9 pc	6491.5	-5709.2	...		155
P201	Groombridge 1830	P	Star	11:52:58.8	+37:43:07	9.2 pc	4002.6	-5817.9	...		156
P202	BD -00 4470	P	Star	23:09:32.9	+0:42:40	75.1 pc	-221.3	-1295.6	...		157
P203	HD 84937	P	Star	9:48:56.1	+13:44:39	72.8 pc	373.1	-774.4	...		158
P204	HD 140283	PS	Star	15:43:03.1	-10:56:01	62.1 pc	-1114.9	-303.6	...		159
P205	HD 122563	P	Star	14:02:31.8	+9:41:10	290.4 pc	-189.7	-70.3	...		160
P206	HE 0107-5240	P	Star	1:09:29.2	-52:24:34	12.5 kpc	2.4	-3.7	...		161
P207	Mira A	P	Star, Inter-acting binary star	2:19:20.8	-2:58:39	91.7 pc	9.3	-237.4	...		162
P208	β Cep	P	Star	21:28:39.6	+70:33:39	210.1 pc	12.5	8.4	...		163
P209	γ Dor	P	Star	4:16:01.6	-51:29:12	20.5 pc	99.5	183.4	...		164
P210	UV Cet	P	Star	1:39:01.6	-17:57:01	2.7 pc	3182.7	592.1	...		165, 166
P211	V838 Mon	P	Star	7:04:04.8	-3:50:51	6.1 kpc	-0.5	0.1	...		167
P212	M67-S1236	P	Star	8:51:50.2	+11:46:07	915.8 pc	-11.2	-2.9	...		168, 169
P213	FK Com	P	Star	13:30:46.8	+24:13:58	216.9 pc	-52.0	-22.3	...		170, 171
P214	R CrB	P	Star	15:48:34.4	+28:09:24	1.3 kpc	-2.4	-11.8	...		172
P215	HD 124448	P	Star	14:14:58.6	-46:17:19	1.8 kpc	-6.9	-0.1	...		173
P216	40 Cancri	P	Star	8:40:11.5	+19:58:16	192.1 pc	-35.3	-13.6	...		174
P217	HD 149382	P	Star	16:34:23.3	-4:00:52	76.8 pc	-6.1	-5.5	...		175
P218	BD+28 4211	P	Star	21:51:11.0	+28:51:50	113.6 pc	-34.7	-56.9	...		176
P219	G77-61	P	Star	3:32:38.1	+1:58:00	78.6 pc	194.1	-749.5	...		177
P220	ζ Oph	P	Star	16:37:09.5	-10:34:02	222.0 pc	15.3	24.8	...		178
P221	HD 271791	P	Star	6:08:14.5	-71:23:07	1.1 kpc	-3.2	3.3	...		179
P222	HVS 1	P	Star	9:07:45.0	+2:45:07	110.0 kpc		180
P223	NLTT 11748	PS	Collapsed star	3:45:16.8	+17:48:09	134.0 pc	234.2	-178.3	...		181
P224	LAWD 32	P	Collapsed star	9:46:39.1	+43:54:52	34.2 pc	-2.5	286.9	...		182
P225	van Maanen 2	P	Collapsed star	0:49:09.9	+5:23:19	4.3 pc	1231.3	-2711.8	...		183
P226	Sirius B	P	Collapsed star	6:45:09.3	-16:43:01	2.7 pc	-459.7	-915.0	...		184
P227	GD50	P	Collapsed star	3:48:50.2	+0:58:32	31.2 pc	84.4	-163.0	...		185
P228	PG 1159-035	P	Collapsed star	12:01:46.0	-3:45:41	551.5 pc	-14.2	-3.3	...		186
P229	QU Vul	P	Collapsed star	20:26:45.9	+27:50:42	2.4 kpc		186

Table E2 continued

Table E2 (*continued*)

ID	Name	Samples	Phyla	RA	Dec	D_L^{eff}	μ_α	μ_δ	Θ	I17?	Refs
P230	Grw +70°8247	P	Collapsed star	19:00:10.3	+70:39:51	13.0 pc	85.8	505.1	...		187
P231	ZZ Cet	P	Collapsed star	1:36:13.6	-11:20:33	32.8 pc	460.8	-116.4	...		188
P232	Ton 124	P	Collapsed star	12:45:35.6	+42:38:25	71.0 pc	19.1	-54.1	...		189, 190
P233	1E 1207.4-5209	P	Collapsed star	12:10:00.9	-52:26:28	2.1 kpc		191
P234	Geminga	P	Collapsed star	6:33:54.2	+17:46:13	250.0 pc		192
P235	Crab pulsar	P	Collapsed star	5:34:31.9	+22:00:52	2.0 kpc		
P236	SGR 1806-20	P	Collapsed star	18:08:39.3	-20:24:40	15.1 kpc		
P237	SGR 1935+2154	PA	Collapsed star	19:34:55.7	+21:53:48	9.5 kpc		193
P238	PSR B0656+14	P	Collapsed star	6:59:48.2	+14:14:22	288.2 pc		194
P239	RX J1856.5-3754	P	Collapsed star	18:56:35.1	-37:54:30	123.0 pc	326.7	-59.1	...		
P240	PSR J0437-4715	P	Collapsed star, Stellar group	4:37:15.8	-47:15:09	120.1 pc	122.9	-71.2	...		
P241	Cygnus X-1	P	Collapsed star, Interacting binary star	19:58:21.7	+35:12:06	2.4 kpc	-3.9	-6.2	...		
P242	QV Tel Ab	P	Collapsed star	18:17:07.5	-56:01:24	343.1 pc	-3.7	-11.1	...		
P243	NGC 6946-BH1	PA	Star, Collapsed star	20:35:27.6	+60:08:08	7.7 Mpc		195
P244	Algol	P	Interacting binary star	3:08:10.1	+40:57:20	27.6 pc	3.0	-1.7	...	✓	
P245	W UMa	P	Interacting binary star	9:43:45.5	+55:57:09	51.9 pc	17.1	-29.2	...		
P246	FG Hya	P	Interacting binary star	8:27:03.9	+3:30:52	153.7 pc	3.6	-64.1	...		
P247	OO Aql	P	Interacting binary star	19:48:12.7	+9:18:32	119.2 pc	65.5	-7.2	...		
P248	CH Cyg	P	Interacting binary star	19:24:33.1	+50:14:29	183.0 pc	-8.3	-11.4	...		
P249	R Aqr	P	Interacting binary star	23:43:49.5	-15:17:04	320.3 pc	27.3	-29.9	...		
P250	RR Tel	P	Interacting binary star	20:04:18.5	-55:43:33	3.5 kpc	3.3	-3.2	...		196
P251	RS Oph	P	Interacting binary star	17:50:13.2	-6:42:28	2.3 kpc	1.2	-5.9	...		
P252	SS Cyg	P	Interacting binary star	21:42:42.8	+43:35:10	114.6 pc	112.4	33.6	...		
P253	UX UMa	P	Interacting binary star	13:36:41.0	+51:54:49	297.6 pc	-41.7	17.1	...		
P254	T Pyx	P	Interacting binary star	9:04:41.5	-32:22:48	3.2 kpc	-2.5	0.2	...		
P255	GK Per	P	Interacting binary star	3:31:12.0	+43:54:15	441.9 pc	-6.7	-17.2	...		
P256	DQ Her	P	Interacting binary star	18:07:30.3	+45:51:33	500.6 pc	-0.9	12.4	...		
P257	AE Aqr	P	Interacting binary star	20:40:09.2	+0:52:15	91.2 pc	70.6	13.1	...		
P258	AM Her	P	Interacting binary star	18:16:13.3	+49:52:05	87.8 pc	-46.0	28.0	...		
P259	AR Sco	P	Interacting binary star	16:21:47.3	-22:53:10	117.8 pc	9.7	-51.5	...		
P260	AM CVn	P	Interacting binary star	12:34:54.6	+37:37:44	298.4 pc	30.9	12.4	...		
P261	QR And	P	Interacting binary star	0:19:49.9	+21:56:52	2.0 kpc	18.5	-5.5	...		
P262	Sco X-1	P	Interacting binary star	16:19:55.1	-15:38:25	2.8 kpc	-6.8	-12.2	...		
P263	4U 1608-52	P	Interacting binary star	16:12:43.0	-52:25:23	3.3 kpc		
P264	4U 1730-335	P	Interacting binary star	17:33:24.6	-33:23:20	8.8 kpc		

Table E2 *continued*

Table E2 (continued)

ID	Name	Samples	Phyla	RA	Dec	D_L^{eff}	μ_α	μ_δ	Θ	I17?	Refs
P265	4U 1820-303	P	Interacting binary star	18:23:40.6	-30:21:41	7.6 kpc		
P266	SAX J1808.4-3658	P	Interacting binary star	18:08:27.5	-36:58:44	3.5 kpc		197
P267	PSR J1023+0038	P	Interacting binary star	10:23:47.7	+0:38:41	1.4 kpc	4.8	-17.3	...		
P268	A 0535+26	P	Interacting binary star	5:38:54.6	+26:18:57	2.0 kpc	-0.6	-2.8	...		
P269	Vela X-1	P	Interacting binary star	9:02:06.9	-40:33:17	2.6 kpc	-5.0	9.1	...		
P270	Cen X-3	P	Interacting binary star	11:21:15.1	-60:37:26	10.0 kpc	-3.1	2.1	...		
P271	V404 Cyg	P	Interacting binary star	20:24:03.8	+33:52:02	2.4 kpc		198
P272	MCW 656	P	Interacting binary star	18:18:36.4	-13:48:02	2.6 kpc	0.1	2.1	...		199
P273	GRS 1915+105	P	Interacting binary star	19:15:11.5	+10:56:45	11.0 kpc		
P274	SS433	P	Interacting binary star	19:11:49.6	+4:58:58	4.5 kpc	-2.9	-4.6	...		200
P275	M82 X-1	P	Interacting binary star	9:55:50.0	+69:40:46	3.4 Mpc		201
P276	M101 ULX-1	P	Interacting binary star	14:03:32.4	+54:21:03	6.5 Mpc		202
P277	M82 X-2	P	Interacting binary star	9:55:51.0	+69:40:45	3.4 Mpc		203
P278	γ Cas	P	Interacting binary star	0:56:42.5	+60:43:00	117.0 pc	25.6	-3.8	...		
P279	IGR J17544-2619	P	Interacting binary star	17:54:25.3	-26:19:53	3.2 kpc	-0.7	-0.5	...		
P280	WR 140	P	Interacting binary star	20:20:28.0	+43:51:16	1.7 kpc	-4.7	-2.0	...		
P281	PSR B1259-63	P	Interacting binary star	13:02:47.7	-63:50:09	2.4 kpc	-7.0	-0.4	...		
P282	PSR B1957+20	PS	Collapsed star, Interacting binary star	19:59:36.7	+20:48:15	2.5 kpc	-16.0	-26.0	...		204
P283	PSR J1417-4402	P	Interacting binary star	14:17:30.6	-44:02:57	3.1 kpc		205
P284	α Cen AB	P	Stellar group	14:39:29.7	-60:49:56	1.3 pc	-3608.0	686.0	...	✓	206
P285	T Tau	P	Stellar group	4:21:59.4	+19:32:06	144.3 pc	11.4	-14.8	...		207
P286	Luhman 16	P	Stellar group	10:49:18.9	-53:19:10	2.0 pc	-2759.0	354.0	...		208
P287	WD 0135-052	P	Stellar group	1:37:59.4	-4:59:45	12.6 pc	580.9	-350.2	...		209
P288	PSR J1719-1438	P	Stellar group	17:19:10.1	-14:38:01	1.2 kpc		210
P289	PSR B1913+16	P	Stellar group	19:15:28.0	+16:06:27	5.2 kpc		
P290	RS CVn	P	Stellar group	13:10:36.9	+35:56:06	135.9 pc	-50.0	20.6	...		
P291	YY Gem	P	Stellar group	7:34:37.4	+31:52:10	15.1 pc	-201.5	-97.1	...	✓	211
P292	ϵ Aur	P	Stellar group	5:01:58.1	+43:49:24	414.9 pc	-0.9	-2.7	...		212
P293	PSR J0737-3039	P	Stellar group	7:37:51.2	-30:39:41	1.1 kpc		213
P294	KIC 8145411	PA	Stellar group	18:50:08.0	+44:04:25		214
P295	IC 2391	P	Stellar group	8:40:32.0	-53:02:00	176.0 pc	-24.9	23.3	...		
P296	M67	P	Stellar group	8:51:18.0	+11:48:00	900.0 pc	-11.0	-2.9	...		
P297	Westerlund 1	P	Stellar group	16:47:04.0	-45:51:05	4.0 kpc	-2.3	-3.7	...		
P298	47 Tuc	P	Stellar group	0:24:05.4	-72:04:53	4.5 kpc	5.2	-2.5	...		215, 216
P299	M15	P	Stellar group	21:29:58.3	+12:10:01	10.4 kpc	-0.6	-3.8	...		217, 218
P300	NGC 6752	P	Stellar group	19:10:52.1	-59:59:04	4.0 kpc	-3.2	-4.0	...		219, 220
P301	M31-EC4	P	Stellar group	0:58:15.4	+38:03:02	785.0 kpc		221

Table E2 continued

Table E2 (continued)

ID	Name	Samples	Phyla	RA	Dec	D_L^{eff}	μ_α	μ_δ	Θ	I17?	Refs
P302	Palomar 1	P	Stellar group	3:33:20.0	+79:34:52	11.1 kpc	-0.2	0.0	...		222, 223
P303	Central Cluster	P	Stellar group	17:45:40.0	-29:00:28	8.2 kpc		224
P304	ω Cen	P	Stellar group	13:26:47.3	-47:28:46	5.2 kpc	-3.2	-6.7	...		225, 226
P305	CMa R1	P	Stellar group	7:04	-11:30	690.0 pc	$200' \times < 1^\circ$		227
P306	Cyg OB2	P	Stellar group	20:33:12.0	+41:19:00	1.5 kpc	-1.6	-4.7	...		
P307	NGC 604	PS	Stellar group, ISM	1:34:32.1	+30:47:01	809.0 kpc		228
P308	Cen A Outer Filament	P	Stellar group	13:26:28.1	-42:50:06	3.7 Mpc	$8'$		229
P309	ζ Oph cloud	P	ISM	16:37:09.0	-10:34:00	150.0 pc		230
P310	NGC 7023	P	ISM	21:01:36.9	+68:09:48	320.0 pc		231
P311	Orion A	P	ISM	5:38:14.2	-7:07:08	400.0 pc	$7^\circ \times 1^\circ$		232
P312	G028.37+00.07	P	ISM	18:42:50.6	-4:03:30	4.8 kpc	$6.3'$		233
P313	TMC-1	P	ISM	4:41:45.9	+25:41:27	140.0 pc	$15'$		234
P314	Barnard 68	P	ISM	17:22:38.2	-23:49:34	125.0 pc		235
P315	Orion hot core	P	ISM	5:35:14.5	-5:22:30	418.0 pc		236
P316	Sextans A hole	P	ISM	10:11:00.5	-4:41:30	1.4 Mpc	$3.6'$		237
P317	M42	P	ISM	5:35:17.3	-5:23:28	500.0 pc	1.7	-0.3	$5.5'$		
P318	W3(OH)	P	ISM	2:27:04.1	+61:52:22	2.0 kpc		238
P319	NGC 3603	P	ISM	11:15:18.6	-61:15:26	7.0 kpc	-5.5	2.0	...		239
P320	Arp 220	P	ISM, Galaxy	15:34:57.2	+23:30:12	80.0 Mpc	$1.3'$		240, 241
P321	HH 1	P	ISM	5:36:20.8	-6:45:13	400.0 pc		242
P322	EGO G16.59-0.05	P	ISM	18:21:09.2	-14:31:45	4.3 kpc	$46''$		243
P323	ζ Oph bow shock	P	ISM	16:37:15.0	-10:30	112.2 pc	$1'$		
P324	Red Rectangle nebula	P	ISM	6:19:58.2	-10:38:15	440.5 pc	-6.5	-22.7	...		
P325	Helix Nebula	P	ISM	22:29:38.5	-20:50:14	201.0 pc	38.9	-3.4	$13.4'$		
P326	NGC 6302	P	ISM	17:13:44.3	-37:06:11	741.0 pc	$0.7'$		
P327	IRC +10420	P	ISM	19:26:48.1	+11:21:17	1.7 kpc	-2.0	-7.4	...		
P328	Homunculus Nebula	P	ISM	10:45:03.5	-59:41:04	2.4 kpc		244
P329	S 308	P	ISM	6:54:13.0	-23:55:42	838.0 pc	-4.4	2.9	...		
P330	Cas A	P	ISM	23:23:24.0	+58:48:54	3.4 kpc	$5.0'$		
P331	Kes 75	P	ISM	18:46:25.5	-2:59:14	5.8 kpc	$3.0'$		245
P332	W44	P	ISM	18:56:10.7	+1:13:21	3.0 kpc	$35.0'$		246
P333	SN 1987A	P	ISM	5:35:28.0	-69:16:11	49.6 kpc		247
P334	Crab nebula	P	ISM	5:34:31.9	+22:00:52	2.0 kpc	$7.0'$		
P335	PSR B1957+20 bow shock	P	ISM	19:59:36.7	+20:48:15	2.5 kpc	-16.0	-26.0	...		248
P336	Geminga halo	P	ISM	6:33:55.0	+17:46:11	250.0 pc	5.5°		249
P337	R Aqr nebula	P	ISM	23:43:49.5	-15:17:04	320.3 pc		
P338	GK Per shell	P	ISM	3:31:11.9	+43:54:15	441.9 pc	$1.0'$		
P339	CAL 83 nebula	P	ISM	5:43:34.2	-68:22:22	49.6 kpc	1.6	0.5	...		250
P340	SAX J1712.6-3739 nebula	P	ISM	17:12:34.6	-37:39:00	6.9 kpc		
P341	Cygnus X-1 shell	P	ISM	19:58:15.0	+35:17	2.4 kpc	$10'$		251
P342	N159F	P	ISM	5:39:38.8	-69:44:36	49.6 kpc	1.8	0.7	...		252
P343	W50	P	ISM	19:12:20.0	+4:55:00	4.5 kpc	$120.0'$		253
P344	Cygnus Cocoon	P	ISM	20:28:39.7	+41:10:18	1.4 kpc	2°		254
P345	HVC 125+41-208	P	ISM	12:24:00.0	+75:36:00		
P346	SSA22a-LAB01	P	ISM	22:17:26.1	+0:12:32	26.5 Gpc		
P347	NGC 6166	P	Galaxy	16:28:38.2	+39:33:04	135.7 Mpc	$1.1'$		
P348	NGC 4636	P	Galaxy	12:42:49.9	+2:41:16	13.2 Mpc	$7.8'$		255
P349	M59	P	Galaxy	12:42:02.3	+11:38:49	6.2 Mpc	$5.5'$	✓	256
P350	NGC 821	P	Galaxy	2:08:21.1	+10:59:42	25.0 Mpc	$1.9'$	✓	

Table E2 continued

Table E2 (continued)

ID	Name	Samples	Phyla	RA	Dec	D_L^{eff}	μ_α	μ_δ	Θ	I17?	Refs
P351	NGC 3115	P	Galaxy	10:05:14.0	-7:43:07	9.5 Mpc	7.8'		257
P352	NGC 4260	P	Galaxy	12:19:22.2	+6:05:56	25.7 Mpc	1.9'		258
P353	M32	P	Galaxy	0:42:41.8	+40:51:55	785.0 kpc		259, 260
P354	NGC 4656 UCD-1	P	Galaxy	12:35:28.7	-3:47:21	18.1 Mpc		261
P355	NGC 205	P	Galaxy	0:40:22.1	+41:41:07	824.0 kpc	18.6'		262, 263
P356	Sculptor dSph	P	Galaxy	1:00:09.4	-33:42:32	90.0 kpc	15.3'	✓	264
P357	UMa II	P	Galaxy	8:51:30.0	+63:07:48	30.0 kpc		
P358	NGC 4431	P	Galaxy	12:27:27.4	+12:17:25	11.3 Mpc	0.9'		
P359	NGC 1277	P	Galaxy	3:19:51.5	+41:34:24	74.0 Mpc	0.7'		265
P360	MRG-M0150	P	Galaxy	1:50:21.2	-10:05:30	6.4 Gpc		266
P361	MRG-M0138	P	Galaxy	1:38:03.9	-21:55:49	2.9 Gpc		267
P362	IC 976	P	Galaxy	14:08:43.3	-1:09:42	17.8 Mpc	0.9'		
P363	NGC 404	P	Galaxy	1:09:27.1	+35:43:05	3.0 Mpc	6.0'		268
P364	M81	P	Galaxy	9:55:33.2	+69:03:55	3.7 Mpc	21.4'	✓	269
P365	M100	P	Galaxy	12:22:54.9	+15:49:20	22.6 Mpc	7.6'		
P366	D563-4	P	Galaxy	8:55:07.2	+19:45:04	50.7 Mpc	0.3'		
P367	NGC 891	P	Galaxy	2:22:32.9	+42:20:54	7.6 Mpc	12.3'		270
P368	Phoenix dwarf	P	Galaxy	1:51:06.3	-44:26:41	440.0 kpc	4.9'	✓	271
P369	NGC 5173	P	Galaxy	13:28:25.3	+46:35:30	36.9 Mpc	0.6'		272, 273
P370	IC 225	P	Galaxy	2:26:28.3	+1:09:37	22.0 Mpc	0.4'		274, 275
P371	M101	P	Galaxy	14:03:12.6	+54:20:56	6.5 Mpc	21.9'	✓	276, 277
P372	NGC 300	P	Galaxy	0:54:53.4	-37:41:03	2.1 Mpc	20.9'		278
P373	NGC 55	P	Galaxy	0:14:53.6	-39:11:48	1.8 Mpc	32.4'		279
P374	NGC 4701	P	Galaxy	12:49:11.6	+3:23:19	10.8 Mpc	0.9'		
P375	SS 16	P	Galaxy	9:47:00.1	+25:40:46	505.5 Mpc	0.9'		280, 281
P376	M99	P	Galaxy	12:18:49.6	+14:24:59	34.7 Mpc	5.1'		
P377	NGC 4631	P	Galaxy	12:42:08.0	+32:32:29	8.7 Mpc	13.5'		282
P378	NGC 6822	P	Galaxy	19:44:56.2	-14:47:51	520.0 kpc	13.8'	✓	283, 284
P379	IC 1613	P	Galaxy	1:04:54.2	+2:08:00	760.0 kpc	16.2'	✓	285
P380	NGC 3077	P	Galaxy	10:03:19.1	+68:44:02	171.5 kpc	2.4'		286, 287
P381	SGAS J143845.1+145407	P	Galaxy	14:38:45.1	+14:54:07	1.5 Gpc		288, 289
P382	Sp1149 (A1)	P	Galaxy	11:49:35.3	+22:23:46	2.3 Gpc		290, 291
P383	A68-HLS115	P	Galaxy	0:37:09.5	+9:09:04	5.5 Gpc		292, 293
P384	HLock-01 (R)	P	Galaxy	10:57:51.1	+57:30:27	8.2 Gpc		294, 295
P385	M82	P	Galaxy	9:55:52.4	+69:40:47	3.4 Mpc		296, 297
P386	Arp 236	P	Galaxy	1:07:47.2	-17:30:25	89.2 Mpc		298
P387	I Zwicky 18	P	Galaxy	9:34:02.1	+55:14:25	10.8 Mpc	2.0'		299
P388	POX 186	PS	Galaxy	13:25:48.6	-11:36:38	16.8 Mpc		
P389	Haro 2	P	Galaxy	10:32:32.0	+54:24:04	20.7 Mpc		300, 301
P390	NGC 2366	P	Galaxy	7:28:51.9	+69:12:31	1.4 Mpc	8.1'		302
P391	ID11	P	Galaxy	22:48:42.0	-44:32:28	6.7 Gpc		303, 304
P392	SL2S J02176-0513	P	Galaxy	2:17:37.1	-5:13:30	3.4 Gpc		305, 306
P393	cB 58	P	Galaxy	15:14:22.3	+36:36:26	4.1 Gpc		307, 308

Table E2 continued

Table E2 (continued)

ID	Name	Samples	Phyla	RA	Dec	D_L^{eff}	μ_α	μ_δ	Θ	I17?	Refs
P394	SMM J2135-0102	P	Galaxy	21:35:11.6	-1:02:52	3.1 Gpc		309, 310
P395	Minkowski's Object	P	Galaxy	1:25:47.0	-1:22:18	81.8 Mpc		311
P396	Malin 1	P	Galaxy	12:36:59.3	+14:19:49	377.0 Mpc	0.1'		312
P397	VCC 1287	P	Galaxy	12:30:23.8	+13:58:56	16.6 Mpc	0.8'		313, 314
P398	UGC 2162	P	Galaxy	2:40:24.6	+1:13:36	17.0 Mpc	1.4'		315
P399	HI 1232+20	P	Galaxy	12:32:00.0	+20:25:00	10.9 Mpc		316
P400	Cartwheel	P	Galaxy	0:37:41.1	-33:42:59	130.5 Mpc		
P401	NGC 4650A	P	Galaxy	12:44:49.0	-40:42:52	42.1 Mpc	0.5'		317
P402	Hoag's Object	P	Galaxy	15:17:14.4	+21:35:08	187.8 Mpc	0.3'		318
P403	M51a/b	P	Galaxy	13:29:52.7	+47:11:43	6.7 Mpc	10.0'	✓	
P404	Antennae	P	Galaxy	12:01:53.2	-18:52:38	24.6 Mpc		319
P405	Antenna TDG	P	Galaxy	12:01:25.7	-19:00:42	23.9 Mpc		
P406	3C 75	P	Galaxy, AGN	2:57:41.6	+6:01:28	100.3 Mpc	0.7'		
P407	ESO 137-001	P	Galaxy	16:13:27.3	-60:45:51	67.5 Mpc	0.4'		
P408	IC 3418	P	Galaxy	12:29:43.9	+11:24:17	409.9 Mpc	1.5'		320
P409	M51a	P	Galaxy	13:29:52.7	+47:11:43	6.7 Mpc	10.0'	✓	321
P410	NGC 7793	P	Galaxy	23:57:49.8	-32:35:28	3.2 Mpc	10.0'	✓	322
P411	NGC 4622	P	Galaxy	12:42:37.6	-40:44:39	59.6 Mpc	1.2'		
P412	M91	P	Galaxy	12:35:26.4	+14:29:47	7.1 Mpc	5.4'		
P413	NGC 1097	P	Galaxy	2:46:19.1	-30:16:30	18.1 Mpc	10.0'		
P414	M64	P	Galaxy	12:56:43.7	+21:40:58	5.8 Mpc	9.8'	✓	323
P415	NGC 2787	P	Galaxy	9:19:18.6	+69:12:12	10.0 Mpc	2.5'	✓	
P416	NGC 1365	P	Galaxy, AGN	3:33:36.5	-36:08:26	23.6 Mpc	10.7'		324
P417	NGC 6012	P	Galaxy	15:54:13.9	+14:36:04	25.8 Mpc	1.4'		
P418	NGC 1433	P	Galaxy	3:42:01.6	-47:13:19	15.4 Mpc	6.3'		
P419	NGC 5101	P	Galaxy	13:21:46.2	-27:25:50	27.0 Mpc	5.6'		
P420	NGC 3898	P	Galaxy	11:49:15.4	+56:05:04	16.9 Mpc	3.8'		
P421	UGC 7321	P	Galaxy	12:17:34.0	+22:32:23	5.9 Mpc	5.1'		325
P422	NGC 3923	P	Galaxy	11:51:01.8	-28:48:22	24.8 Mpc	6.8'		
P423	LEDA 074886	P	Galaxy	3:40:43.2	-18:38:43	19.2 Mpc	0.4'		
P424	KK 246	P	Galaxy	20:03:57.4	-31:40:53	6.1 Mpc	0.7'		
P425	ESO 243-49 HLX1	P	AGN	1:10:28.3	-46:04:22	95.9 Mpc		
P426	Sgr A*	P	AGN	17:45:40.0	-29:00:28	8.2 kpc		
P427	NGC 1052	P	AGN	2:41:04.8	-8:15:21	21.2 Mpc	2.1'	✓	
P428	NGC 4395	P	AGN	12:25:48.9	+33:32:49	4.5 Mpc	11.5'		
P429	NGC 4686	P	AGN	12:46:39.8	+54:32:03	72.7 Mpc	1.8'		
P430	NGC 7469	P	AGN	23:03:15.7	+8:52:25	68.9 Mpc	1.4'		
P431	NGC 1068	P	AGN	2:42:40.8	+0:00:48	16.4 Mpc	6.9'		
P432	I Zwicky 1	P	AGN	0:53:34.9	+12:41:36	268.9 Mpc	0.5'		
P433	NGC 2911	P	AGN	9:33:46.1	+10:09:09	46.6 Mpc	1.2'		
P434	Centaurus A	P	AGN	13:25:27.6	-43:01:09	3.7 Mpc	25.7'		326
P435	Cygnus A	P	AGN	19:59:28.4	+40:44:02	251.0 Mpc	0.6'		
P436	NGC 1265	P	AGN	3:18:15.7	+41:51:28	109.9 Mpc	1.8'		
P437	3C 403	P	AGN	19:52:15.8	+2:30:24	264.3 Mpc	0.3'		
P438	3C 286	P	AGN	13:31:08.3	+30:30:33	5.4 Gpc		
P439	PKS 1934-638	P	AGN	19:39:25.0	-63:42:46	886.4 Mpc		
P440	3C 273	P	AGN	12:29:06.7	+2:03:09	757.5 Mpc		
P441	Mrk 335	P	AGN	0:06:19.5	+20:12:11	111.1 Mpc		
P442	Cloverleaf quasar	P	AGN	14:15:46.2	+11:29:43	6.2 Gpc		327
P443	PHL 1811	P	AGN	21:55:01.5	-9:22:24	948.3 Mpc		
P444	BL Lac	P	AGN	22:02:43.3	+42:16:40	311.2 Mpc	0.0'		
P445	3C 279	P	AGN	12:56:11.2	-5:47:22	3.1 Gpc		
P446	TXS 0506+056	P	AGN	5:09:26.0	+5:41:35	1.8 Gpc	0.0'		

Table E2 continued

Table E2 (continued)

ID	Name	Samples	Phyla	RA	Dec	D_L^{eff}	μ_α	μ_δ	Θ	I17?	Refs
P447	SST24 J143644.2+350627	P	AGN	14:36:44.2	+35:06:27	14.0 Gpc		
P448	WISE 1814+3412	P	AGN	18:14:17.3	+34:12:25	19.9 Gpc		
P449	NGC 4258	P	AGN	12:18:57.6	+47:18:13	6.6 Mpc	17.8'	✓	
P450	NGC 4151	P	AGN	12:10:32.6	+39:24:21	14.0 Mpc	6.2'		
P451	NGC 6240	P	AGN	16:52:58.9	+2:24:04	106.2 Mpc	1.1'		
P452	0402+379	P	AGN	4:05:49.3	+38:03:32	243.3 Mpc	0.6'		
P453	OJ 287	P	AGN	8:54:48.9	+20:06:31	1.6 Gpc		
P454	Hanny's Voorwerp	P	AGN	9:41:03.8	+34:43:34	221.9 Mpc		328
P455	B2 0924+30	P	AGN	9:27:52.8	+29:59:09	116.6 Mpc	0.8'		
P456	Arp 294	P	Galaxy association	11:39:42.0	+31:55:00	42.4 Mpc		
P457	UGCA 319/320	P	Galaxy association	13:02:43.0	-17:19:10	10.7 Mpc		
P458	Stephan's Quintet	P	Galaxy association	22:35:57.5	+33:57:36	93.7 Mpc	3.2'		
P459	NGC 6482	P	Galaxy association	17:51:48.8	+23:04:19	56.7 Mpc	1.5'		
P460	Fornax Cluster	P	Galaxy association	3:38:30.0	-35:27:18	19.8 Mpc		
P461	Virgo Cluster	P	Galaxy association	12:26:32.1	+12:43:24	16.3 Mpc		
P462	Coma Cluster	P	Galaxy association	12:59:48.7	+27:58:50	102.1 Mpc		
P463	Perseus Cluster	P	Galaxy association	3:19:47.2	+41:30:47	77.8 Mpc		
P464	Bullet Cluster	PS	Galaxy association	6:58:29.6	-55:56:39	1.5 Gpc		
P465	SSA22	P	Galaxy association	22:17:34.7	+0:15:07	26.4 Gpc		329
P466	Abell 3667	P	Galaxy association	20:12:33.7	-56:50:26	246.6 Mpc		
P467	Coma C	P	Galaxy association	12:59:18.0	+27:47:00	100.3 Mpc		330
P468	NGC 1275 minihalo	P	Galaxy association	3:19:48.2	+41:30:42	76.3 Mpc	2.6'		
P469	1253+275	P	Galaxy association	12:55:00.0	+27:12:00	100.3 Mpc		331
P470	Leo Ring	P	LSS	10:47:46.8	+12:11:11	10.0 Mpc		332
P471	Laniakea (Great) attractor	P	LSS	14:32	-43:14	71.0 Mpc		333
P472	Dipole repeller	P	LSS	22:25	+37:15	238.6 Mpc		334
S003	Cha 110913-773444	S	Minor body	11:09:13.6	-77:34:45	165.0 pc		335, 336
S010	1SWASP J140752.03-394415.1 b	S	Minor body	14:07:52.0	-39:44:15	1.4 kpc	4.8	-0.7	...		337, 338
S016	Kepler 138b	S	Solid planetoid	19:21:31.6	+43:17:35	67.0 pc	-20.6	22.7	...		339, 340
S017	Kepler 37b	S	Solid planetoid	18:56:14.3	+44:31:05	64.0 pc	-60.5	48.7	...		341
S018	82 Eri	S	Solid planetoid	3:19:55.7	-43:04:11	6.0 pc	3038.3	726.6	...	✓	342, 343
S019	KOI 1843.03	S	Solid planetoid	19:00:03.1	+40:13:15	134.8 pc	0.7	41.2	...		344, 345
S020	TRAPPIST-1	SE	Solid plane- toid, Star	23:06:29.4	-5:02:29	12.4 pc	930.9	-479.4	...	+	346, 347
S021	HAT-P-67 b	S	Giant planet	17:06:26.6	+44:46:37	375.7 pc	9.4	-18.2	...		348, 349
S022	Kepler 51 c	S	Giant planet	19:45:55.1	+49:56:16	801.7 pc	0.0	-7.5	...		350, 351

Table E2 continued

Table E2 (*continued*)

ID	Name	Samples	Phyla	RA	Dec	D_L^{eff}	μ_α	μ_δ	Θ	I17?	Refs
S023	KELT 9 b	S	Giant planet	20:31:26.4	+39:56:20	205.7 pc	16.7	21.5	...		352, 353
S024	TrES-2 b	S	Giant planet	19:07:14.0	+49:18:59	216.7 pc	5.2	1.6	...		354, 355
S025	V830 Tau b	S	Giant planet	4:33:10.0	+24:33:43	130.6 pc	7.2	-21.2	...		356, 357
S026	PSR B1620-26 b	S	Giant planet	16:23:38.2	-26:31:54	2.2 kpc		358, 359
S027	κ And b	S	Giant planet	23:40:24.5	+44:20:02	50.1 pc	80.7	-18.7	...		360, 361
S028	σ UMa b	S	Giant planet	8:30:15.9	+60:43:05	60.5 pc	-133.8	-107.5	...		362, 363
S029	HD 208527b	S	Giant planet	21:56:24.0	+21:14:23	314.5 pc	1.2	15.0	...		364
S030	GJ 3483 B	S	Giant planet	8:07:14.7	-66:18:49	19.2 pc	340.3	-289.6	...		365
S031	HD 163269 b	S	Giant planet	17:55:54.5	-12:52:13	257.1 pc	-3.4	-11.0	...		366, 367
S032	R136 a1	S	Star	5:38:43.3	-69:06:08	49.6 kpc		368, 369, 370
S033	Feige 34	S	Star	10:39:36.7	+43:06:09	227.3 pc	12.5	-25.4	...		371, 372
S034	NML Cyg	S	Star	20:46:25.5	+40:06:59	1.6 kpc	-0.3	-0.9	...		373, 374
S035	UY Sct	S	Star	18:27:36.5	-12:27:59	1.6 kpc	-0.7	-3.0	...		375
S036	SMSS J0313-6708	S	Star	3:13:00.4	-67:08:39	10.0 kpc	7.0	1.1	...		
S037	14 Her	S	Star	16:10:24.3	+43:49:03	17.9 pc	132.0	-296.5	...	✓	376
S038	SDSS J102915+172927	S	Star	10:29:15.1	+17:29:28	1.4 kpc	-10.9	-4.1	...		
S039	S0-16	S	Star	17:45:40.0	-29:00:28	8.2 kpc		377
S040	S5-HVS1	S	Star	22:54:51.6	-51:11:44	8.6 kpc	35.3	0.6	...		378, 379
S041	S0-102	S	Star	17:45:40.0	-29:00:28	8.2 kpc	35.3	0.6	...		380
S042	SDSS J222859.93+362359.6	S	Collapsed star	22:28:59.9	+36:23:60	286.0 pc	-2.9	-2.0	...		381
S043	U Sco	S	Collapsed star	16:22:30.8	-17:52:43	12.6 kpc	0.5	-7.9	...		382
S044	LHS 4033	S	Collapsed star	23:52:31.9	-2:53:12	30.2 pc	637.8	285.1	...		383
S045	PSR J2222-0137b	S	Collapsed star	22:22:06.0	-1:37:16	267.2 pc		384
S046	RX J0439.8-6809	S	Collapsed star	4:39:49.6	-68:09:01	9.2 kpc		385, 386
S047	PG 1031+234	S	Collapsed star	10:33:49.2	+23:09:16	64.1 pc	-51.3	-11.8	...		
S048	WD 0346+246	S	Collapsed star	3:46:46.5	+24:56:03	27.8 pc	520.9	-1157.5	...		387
S049	D6-3	S	Collapsed star	18:52:01.9	+62:02:07	2.3 kpc	9.0	211.5	...		
S050	4U 1538-522	S	Collapsed star	15:42:23.4	-52:23:10	6.4 kpc	-6.7	-4.1	...		
S051	MSP J0740+6620	S	Collapsed star	7:40:45.8	+66:20:34	2.0 kpc		388
S052	PSR J0537-6910	S	Collapsed star	5:37:46.7	-69:10:17	49.6 kpc		389
S053	PSR J2144-3933	S	Collapsed star	21:44:12.1	-39:33:55	160.0 pc		390
S054	XTE J1739-285	S	Collapsed star	17:39:54.0	-28:29:47	12.0 kpc		
S055	AX J1910.7+0917	S	Collapsed star	19:10:43.6	+9:16:30	16.0 kpc		391
S056	SGR 1900+14	S	Collapsed star	19:07:13.0	+9:19:34	13.5 kpc		
S057	NS 1987A	S	Collapsed star	5:35:28.0	-69:16:11	49.6 kpc		392
S058	PSR J1748-2446ad	S	Collapsed star	17:48:04.9	-24:46:04	6.9 kpc		393
S059	PSR J0250+5854	S	Collapsed star	2:50:17.8	+58:54:01	1.6 kpc		394
S060	2MASS J05215658+4359220	S	Collapsed star	5:21:56.6	+43:59:22	3.7 kpc	-0.1	-3.7	...		
S061	HM Cnc	S	Interacting binary star	8:06:23.0	+15:27:31	50.0 pc		
S062	NGC 5907 ULX	S	Interacting binary star	15:15:58.6	+56:18:10	17.1 Mpc		395
S063	PSR J2322-2650	S	Stellar group	23:22:34.6	-26:50:58	227.3 pc	-2.4	-8.3	...		396

Table E2 *continued*

Table E2 (continued)

ID	Name	Samples	Phyla	RA	Dec	D_L^{eff}	μ_α	μ_δ	Θ	I17?	Refs
S064	ZTF J153932.16+502738.8	S	Stellar group	15:39:32.2	+50:27:39	2.3 kpc	-3.4	-3.8	...		397, 398
S065	65 UMa	S	Stellar group	11:55:05.7	+46:28:37	86.8 pc	22.7	-19.4	...		399
S066	IRS 13E	SA	Stellar group	17:45:39.7	-29:00:30	8.2 kpc		400
S067	NGC 7252 W3	S	Stellar group	22:20:43.9	-24:40:38	64.4 Mpc		
S068	Be 17	S	Stellar group	5:20:37.4	+30:35:24	2.7 kpc	2.6	-0.3	...		
S069	NGC 6791	S	Stellar group	19:20:53.0	+37:46:18	6.9 kpc	-0.4	-2.3	...		401
S070	G1	S	Stellar group	0:32:46.5	+39:34:40	785.0 kpc		402, 403
S071	(GC) 037-B327	S	Stellar group	0:41:35.0	+41:14:55	785.0 kpc		404
S072	M85-HCC 1	S	Stellar group	12:25:22.8	+18:10:54	15.8 Mpc		405, 406
S073	Kim 3	S	Stellar group	13:22:45.2	-30:36:04	15.1 kpc		407
S074	NGC 6522	S	Stellar group	18:03:34.1	-30:02:02	7.7 kpc	2.6	-6.4	...		408, 409
S075	ESO 280-SC06	S	Stellar group	18:09:06.0	-46:25:24	21.4 kpc	-0.5	-2.8	...		410
S076	NGC 6528	S	Stellar group	18:04:49.6	-30:03:21	7.9 kpc	-2.2	-5.5	...		411, 412
S077	Boomerang Nebula	S	ISM	12:44:46.1	-54:31:13	197.8 pc	-2.9	-1.6	1.4'		
S078	Sgr B2	S	ISM	17:47:20.4	-28:23:07	8.2 kpc		413
S079	Sgr B2(N) AN01	S	ISM	17:47:19.9	-28:22:18	8.2 kpc		414
S080	30 Dor	S	ISM	5:38:36.0	-69:05:11	49.6 kpc	40.0'		415
S081	W49N	S	ISM	19:10:13.2	+9:06:12	11.1 kpc		416
S082	Segue 2	S	Galaxy	2:19:16.0	+20:10:31	30.0 kpc		
S083	Segue 1	S	Galaxy	10:07:03.2	+16:04:25	20.0 kpc		
S084	IC 1101	S	Galaxy, AGN	15:10:56.1	+5:44:41	353.6 Mpc	0.9'		
S085	OGC 21	S	Galaxy	12:22:05.3	+45:18:11	1.3 Gpc	0.3'		
S086	LEDA 088678	S	Galaxy	12:59:22.5	-4:11:46	389.1 Mpc	0.5'		
S087	M59-UCD3	S	Galaxy	12:42:11.0	+11:38:41	15.3 Mpc		417, 418
S088	SPT 0346-52	S	Galaxy	3:46:41.2	-52:05:06	22.9 Gpc		419, 420
S089	WISE J101326.25+611220.1	S	Galaxy	10:13:26.2	+61:12:20	32.7 Gpc		421
S090	Antlia 2	S	Galaxy	9:35:32.8	-36:46:02	132.0 kpc		422
S091	Reticulum II	S	Galaxy	3:35:42.1	-54:02:57	30.0 kpc		
S092	GN-z11	S	Galaxy	12:36:25.5	+62:14:31	116.9 Gpc		423, 424
S093	MACS0647-JD	S	Galaxy	6:47:55.7	+70:14:36	31.1 Gpc		425, 426
S094	ZF-COSMOS-20115	S	Galaxy	10:00:14.8	+2:22:43	32.9 Gpc		
S095	AGC 229385	S	Galaxy	12:32:10.3	+20:25:24	10.9 Mpc	1.6'		427, 428
S096	J0811+4730	S	Galaxy	8:11:52.1	+47:30:26	197.0 Mpc		429
S097	IRAS 14070+0525	S	Galaxy	14:09:30.7	+5:11:31	1.3 Gpc		430
S098	SS 14	S	Galaxy	9:57:27.0	+8:35:02	1.3 Gpc		431, 432
S099	SS 03	S	Galaxy	16:39:46.0	+46:09:06	1.2 Gpc	0.3'		433, 434
S100	A1689B11	S	Galaxy	13:11:33.3	-1:21:07	20.8 Gpc		435
S101	SPT-CLJ2344-4243 Arc	S	Galaxy	23:44:46.5	-42:43:06	1.4 Gpc		436, 437
S102	The Snake	S	Galaxy	12:06:10.8	-8:48:01	772.5 Mpc		438, 439
S103	RGG 118	S	AGN	15:23:03.8	+11:45:45	106.1 Mpc		
S104	Holm 15A	S	AGN	0:41:50.5	-9:18:11	247.3 Mpc	0.6'		
S105	HS 1946+7658	S	AGN	19:44:54.9	+77:05:53	26.0 Gpc		
S106	SMSS 2157-36	S	AGN	21:57:28.2	-36:02:15	44.0 Gpc		440

Table E2 continued

Table E2 (*continued*)

ID	Name	Samples	Phyla	RA	Dec	D_L^{eff}	μ_α	μ_δ	Θ	I17?	Refs
S107	WISE 2246-0526	S	AGN	22:46:07.6	-5:26:35	42.2 Gpc		
S108	M60-UCD1	S	AGN	12:43:36.0	+11:32:05	16.2 Mpc		441
S109	J1329+3234	S	Other	13:29:32.4	+32:34:17	67.7 Mpc		
S110	J1342+0928	S	AGN	13:42:08.1	+9:28:38	75.3 Gpc		
S111	CLASH B1938+666	S	AGN	19:38:25.3	+66:48:53	1.2 Gpc		442
S112	COSMOS 5921+0638	S	AGN	9:59:21.7	+2:06:38	252.8 Mpc		443
S113	J1420-0545	S	AGN	14:20:23.8	-5:45:28	1.6 Gpc		
S114	J0804+3607	S	AGN	8:04:31.0	+36:07:18	4.0 Gpc		
S115	HCG 54	S	Galaxy association	11:29:15.0	+20:34:42	21.1 Mpc	0.7'		
S116	Seyfert's Sextet	S	Galaxy association	15:59:11.6	+20:45:25	62.0 Mpc	1.3'		
S117	Abell 370	S	Galaxy association	2:39:50.5	-1:35:08	2.0 Gpc		
S118	MACS J0717.5+34	S	Galaxy association	7:17:36.5	+37:45:23	3.2 Gpc		
S119	Abell 665	S	Galaxy association	8:30:45.2	+65:52:55	881.2 Mpc		
S120	Phoenix Cluster	S	Galaxy association	23:44:40.9	-42:41:54	3.5 Gpc		
S121	CL J1001+0220	S	Galaxy association	10:00:57.2	+2:20:13	20.5 Gpc		
S122	A2744z8OD	S	Galaxy association	0:14:24.9	-30:22:56	85.0 Gpc		
S123	Shapley Supercluster	S	LSS	13:06:00.0	-33:04:00	204.1 Mpc		
A001	HE 0430-2457	A	Stellar group	4:33:03.8	-24:51:20	978.4 pc	3.0	0.8	...		444
A002	PSR J1911-5958A	A	Stellar group	19:11:42.8	-59:58:27	4.0 kpc		445, 446
A003	PSR J1740-5340	A	Star, Stellar group	17:40:44.6	-53:40:41	2.3 kpc		447
A004	S0-2	A	Star	17:45:40.0	-29:00:28	8.2 kpc	-10.9	19.7	...		448, 449
A005	IRS 16C	A	Star	17:45:40.1	-29:00:28	8.2 kpc	-9.0	7.8	...		450, 451
A006	G2	A	ISM	17:45:40.0	-29:00:28	8.2 kpc		452
A007	ASASSN -14jb	A	Collapsed star	0:00:00.0	+0:00:00		
A008	HVGC-1	A	Stellar group	12:30:54.7	+12:40:59	16.5 Mpc		453, 454
A009	3C 186	A	AGN	7:44:17.5	+37:53:17	7.2 Gpc		
A010	SDSS J113323.97+550415.9	A	AGN	11:33:24.0	+55:04:16	39.1 Mpc		
A013	HIP 41378f	A	Giant planet	8:26:27.8	+10:04:49	106.6 pc	-48.1	0.1	...		455, 456
A014	Przybylski's Star	A	Star	11:37:37.0	-46:42:35	108.8 pc	-46.8	34.0	...		457
A015	HD 106038	A	Star	12:12:01.4	+13:15:41	134.8 pc	-218.5	-439.6	...		458
A016	HD 135485	A	Star	15:15:45.3	-14:41:35	231.9 pc	-0.3	-35.0	...		459
A017	LS IV-14 116	A	Star	20:57:38.9	-14:25:44	420.3 pc	7.5	-128.0	...		460, 461
A018	M67-S1063	A	Star	8:51:13.4	+11:51:40	847.7 pc	-11.0	-2.8	...		462, 463
A019	[SBD2011] 5	A	Star	11:15:07.0	-61:15:26	7.0 kpc		464, 465
A020	1E 1613-5055	A	Collapsed star	16:17:33.0	-51:02:00	3.2 kpc		
A021	DWD 2220+2146	HS	Stellar group	22:23:01.6	+22:01:31	70.6 pc		466
A022	NGC 1277*	A	AGN	3:19:51.5	+41:34:24	74.0 Mpc	0.7'		
A023	Was 49b	A	AGN	12:14:17.8	+29:31:43	285.3 Mpc		
A024	ASASSN -15lh	A	Unknown	22:02:15.4	-61:39:35	1.2 Gpc		

Table E2 *continued*

Table E2 (continued)

ID	Name	Samples	Phyla	RA	Dec	D_L^{eff}	μ_α	μ_δ	Θ	I17?	Refs
A025	CMB Cold Spot	A	LSS	3:13:00.0	-20:30:00		
A027	Boyajian's Star	A	Minor body, Star	20:06:15.5	+44:27:25	450.8 pc	-10.4	-10.3	...	+	467
A028	HD 139139	A	Minor body	15:37:06.2	-19:08:33	107.6 pc	-67.6	-92.5	...	+	468
A029	VVV-WIT-07	A	Minor body	17:26:29.4	-35:40:56		
A030	ASASSN-V J060000.76- 310027.83	A	Star	6:00:00.7	-31:00:28	156.0 pc		469
A031	WISEA 0615-1247	A	Star	6:15:43.6	-12:47:22	38.6 pc	450.3	-415.9	...		
A032	ASASSN-V J190917.06+182837.36	A	Star	19:09:17.1	+18:28:37	1.4 kpc	-0.7	-4.9	...		
A033	ASASSN-V J213939.3-702817.4	A	Star	21:39:39.3	-70:28:17	1.2 kpc	13.7	-13.1	...		
A034	NGC 3021- CANDIDATE 1	A	Star	9:50:55.4	+33:33:14	27.3 Mpc		470
A035	PTF 14jg	A	Star	2:40:30.1	+60:52:46		
A036	Landstreet's Star	A	Star	5:40:56.4	-1:30:26	437.5 pc	2.8	1.7	...		471
A037	YZ CMi	A	Star	7:44:40.2	+3:33:09	6.0 pc	-348.1	-445.9	...	✓	472
A038	DDE 168	A	Unknown	13:05:14.6	-49:18:60	125.0 pc	-30.2	-16.4	...		473
A039	UMi dSph	A	Galaxy	15:09:11.3	+67:12:52	60.0 kpc	32.2'	✓	474
A040	NGC 247	A	Galaxy	0:47:08.6	-20:45:37	3.7 Mpc	20.4'		475
A041	Leoncino Dwarf	A	Galaxy	9:43:32.4	+33:26:58	8.0 Mpc	8.1''		476, 477
A042	Spikey	A	AGN	19:18:45.6	+49:37:56	6.0 Gpc		
A043	GSN 069	A	AGN	1:19:08.7	-34:11:31	78.7 Mpc	0.3'		
A044	MCG+00-09-070	A	AGN	3:22:08.7	+0:50:11	160.8 Mpc	0.5'		
A045	3C 141	A	Unknown	5:26:42.6	+32:49:58		
A046	3C 125	A	Unknown	4:46:17.8	+39:45:03		
A047	3C 431	A	Unknown	21:18:52.5	+49:36:59		
A048	PMN J1751-2524	A	Unknown	17:51:51.3	-25:24:00		
A049	Galactic Center Ra- dio Arc	A	Unknown	17:46:16.9	-28:48:52	8.2 kpc	1.9	-3.0	...		478
A050	3FGL J1539.2-3324	A	Unknown	15:39:11.6	-33:22:06		
A051	3FGL J1231.6-5113	A	Unknown	12:31:36.5	-51:13:16		
A052	TeV J2032+4130	A	Unknown	20:32:06.0	+41:34:00		
A053	HESS J1745-303	A	Unknown	17:45:11.3	-30:11:56		
A054	LWAT 171018	A	Unknown	3:04	+2		479
A055	ILT J225347+862146	A	Unknown	22:53:47.1	+86:21:46		
A056	TGSSADR J183304.4-384046	A	Unknown	18:33:04.5	-38:40:46	0.8'		
A057	J103916.2+585124	A	Unknown	10:39:16.2	+58:51:24		
A058	WJN J1443+3439	A	Unknown	14:43:22.0	+34:39:00		
A059	FIRST J141918.9+394036	A	Unknown	14:19:18.9	+39:40:36		
A060	RT 19920826	A	Unknown	21:36:22.0	+41:59:20		
A061	GCRT J1745-3009	A	Unknown	17:45:05.0	-30:09:54		
A062	FRB 121102	A	Unknown	5:32:09.6	+33:05:13	941.4 Mpc		480
A063	FRB 180916.J0158+65	A	Unknown	1:58:00.8	+65:43:00	148.2 Mpc		481
A064	VVV-WIT-02	A	Unknown	17:53:02.1	-24:51:59		
A065	OTS 1809+31	A	Unknown	18:11:00.0	+31:24:00		
A066	PTF 11agg	A	Unknown	8:22:17.2	+21:37:38		
A067	MASTER OT J051515.25+223945.7	A	Unknown	5:15:15.2	+22:39:46		
A068	USNO-B1.0 1084- 0241525	AE	Unknown	14:57:36.6	+18:25:02		

Table E2 continued

Table E2 (*continued*)

ID	Name	Samples	Phyla	RA	Dec	D_L^{eff}	μ_α	μ_δ	Θ	I17?	Refs
A069	SN 2008S	A	Unknown	20:34:45.3	+60:05:58	7.7 Mpc		482
A070	PTF 09dav	A	Unknown	22:46:55.1	+21:37:34	158.1 Mpc		483
A071	AT 2018cow	A	Unknown	16:16:00.3	+22:16:05	61.3 Mpc		484
A072	Dougie	A	Unknown	12:08:47.9	+43:01:21	932.0 Mpc		485
A073	XRT 000519	A	Unknown	12:25:31.6	+13:03:59	17.1 Mpc		486
A074	CDF-S XT1	A	Unknown	3:32:38.8	-27:51:34		
A075	CXOU J124839.0-054750	A	Unknown	12:48:39.0	-5:47:50	12.4 Mpc		487
A076	M86 tULX-1	A	Unknown	12:26:02.3	+12:59:51	17.1 Mpc		488
A077	Swift J195509.6+261406	A	Unknown	19:55:09.6	+26:14:07		
A078	IceCube neutrino multiplet	A	Unknown	1:42:48.0	+39:36:00		489
A079	KIC 2856960	A	Stellar group	19:29:31.5	+38:04:36	800.4 pc	-10.6	-10.4	...		
A080	AAE-061228	A	Unknown	18:48:34.0	+20:19:50		490
A081	AAE-141220	A	Unknown	3:23:08.0	+38:39:18		491
A082	AAC-150108	A	Unknown	11:25:48.0	+16:18:00		492
E001	IRAS 16406-1406	E	Star	16:43:27.3	-14:12:00		
E002	IRAS 20331+4024	E	Star	20:34:55.7	+40:35:06		
E003	IRAS 20369+5131	E	Star	20:38:26.0	+51:41:41		
E004	IRAS 04287+6444	E	Stellar group	4:33:28.0	+64:50:53		
E005	UW CMi	E	Star	7:45:16.1	+1:10:56	961.5 pc	-3.0	-2.0	...		
E006	WISE J224436.12+372533.6	E	Galaxy	22:44:36.1	+37:25:34		
E007	UGC 3097	E	Galaxy	4:35:48.5	+2:15:30	52.0 Mpc	0.5'		493
E008	NGC 814	E	Galaxy	2:10:37.6	-15:46:25	23.3 Mpc	0.7'		
E009	ESO 400-28	E	Galaxy	20:28:25.3	-33:04:29	53.1 Mpc	0.7'		
E010	MCG+02-60-017	E	Galaxy	23:47:09.2	+15:35:48	114.2 Mpc	0.6'		
E011	TYC 6111-1162-1	E	Star	12:50:54.4	-16:52:05	174.0 pc	-76.0	-7.8	...		494
E012	UGC 5394	E	Galaxy	10:01:47.9	+36:29:55	18.7 Mpc	1.1'		
E013	NGC 4502	E	Galaxy	12:32:03.4	+16:41:16	23.2 Mpc	0.6'		495
E014	NGC 4698	E	Galaxy	12:48:22.9	+8:29:15	14.8 Mpc	3.1'		496
E015	IC 3877	E	Galaxy	12:54:48.7	+19:10:42	13.1 Mpc	0.7'		
E016	AGC 470027	E	Galaxy	7:03:26.8	-48:59:43	187.5 Mpc	0.3'		
E017	HR 6171	E	Star	16:36:21.4	-2:19:29	9.9 pc	456.4	-309.3	...	✓	
E018	GJ 1019	E	Star	0:43:35.6	+28:26:41	20.9 pc	-127.1	-1064.1	...		
E019	GJ 299	E	Star	8:11:57.6	+8:46:23	6.9 pc	1078.9	-5096.2	...		497
E020	HD 220077	E	Star	23:20:52.9	+16:42:39	177.7 pc	33.7	-76.2	...		498
E021	HIP 107359	E	Star	21:44:41.9	-16:31:37	770.3 pc	-59.2	-31.6	...		499
E022	TYC 3010-1024-1	E	Star	11:04:19.8	+40:10:42	164.6 pc	-55.2	-10.7	...		
E023	Wow! Signal (A)	E	Unknown	19:25:28.0	-26:56:50		500
E024	Wow! Signal (B)	E	Unknown	19:28:17.0	-26:56:50		501
E025	5.13h +2.1	E	Unknown	5:07:48.0	+2:06		502
E026	08.00h -08.50	E	Unknown	8:01	-8:32		503
E027	03.10h +58.0	E	Unknown	3:07	+58:02		504
E028	11.03.91	E	Unknown	16:39:16.0	+30:31:04		505
E029	WISE 0735-5946	E	Unknown	7:35:04.8	-59:46:12		
E030	IRAS 16329+8252	E	Unknown	16:27:22.5	+82:45:46		
C001	CSL-1	C	Galaxy association	12:23:30.5	-12:38:57	2.6 Gpc		506
C002	GRB 090709A	C	Other	19:19:46.7	+60:43:41	13.7 Gpc		
C003	GW100916 (A)	C	Not real	7:23:55.0	-27:31:48		507
C004	GW100916 (B)	C	Not real	7:19:26.0	-27:34:12		508
C005	HD 117043	C	Star	13:25:59.9	+63:15:41	20.9 pc	-392.5	220.9	...	✓	
C006	HIP 114176	C	Not real	23:07:19.4	-32:16:06		
C007	KIC 5520878	C	Star	19:10:23.6	+40:46:05	4.5 kpc	-5.2	-3.4	...		

Table E2 *continued*

Table E2 (*continued*)

ID	Name	Samples	Phyla	RA	Dec	D_L^{eff}	μ_α	μ_δ	Θ	I17?	Refs
C008	KIC 9832227	C	Stellar group	19:29:16.0	+46:37:20	595.1 pc	-9.8	-5.8	...		
C009	KOI 6705.01	C	Star	18:56:57.6	+41:49:09	85.8 pc	-148.9	-128.0	...		509
C010	Perseus Flasher	C	Not real	3:13:39.0	+32:14:37		
C011	PSR B1829-10	C	Collapsed star	18:32:40.9	-10:21:33	4.7 kpc		
C012	OT 060420	C	Not real	13:40	-11:40		510
C013	SSSPM J1549-3544	C	Star	15:48:40.2	-35:44:26	95.9 pc	-597.8	-535.9	...		511
C014	Swift Trigger 954840	C	Not real	10:54:30.0	-49:34:52		512

NOTE—**Samples** – All samples a target is in. P: Prototype, S: Superlative, A: non-SETI Anomaly, E: SETI Anomaly, C: Control.

D_L^{eff} – effective luminosity distance of target, after taking into account lensing magnification.

μ_α, μ_δ – Proper motion in RA and declination, respectively.

Θ – Angular size of the target.

I17? – \checkmark : source is part of I17 sample; \dagger : source is not part of I17 sample but has been observed in Breakthrough Listen campaign.

Table E3. Relationships of *Exotica Catalog* targets

Object	ID	Relationship	Partner	Partner IDs
<i>Within Exotica Catalog</i>				
NGC 7293 central star	P071	IN	Helix Nebula	P325
Proxima b	P078	BOUND	α Cen AB	P284
Luhman 16B	P128	IN	Luhman 16	P286
		MUTUAL_ORBIT	Luhman 16B	P128
Luhman 16A	P129	IN	Luhman 16	P286
		MUTUAL_ORBIT	Luhman 16A	P129
61 Cyg B	P137	MUTUAL_ORBIT	61 Cyg A	P138
61 Cyg A	P138	MUTUAL_ORBIT	61 Cyg B	P137
κ CrB	P154	IN	Cygnus Cocoon	P344
		ADJACENT	Cyg OB2, TeV J2032+4130	P306, A052
HD 44179	P169	IN	Red Rectangle nebula	P324
ι Ori	P182	IN	Orion A	P311
		ADJACENT	M42	P317
EZ CMa	P188	IN	S 308	P329
η Car	P193	IN	Homunculus Nebula	P328
ζ Oph	P220	IN	ζ Oph cloud, ζ Oph bow shock	P309, P323
Geminga	P234	IN	Geminga halo	P336
Crab pulsar	P235	IN	Crab nebula	P334
Cygnus X-1	P241	IN	Cygnus X-1 shell	P341
NGC 6946-BH1	P243	ADJACENT	SN 2008S	A069
R Aqr	P249	IN	R Aqr nebula	P337
GK Per	P255	IN	GK Per shell	P338
SS433	P274	IN	W50	P343
M82 X-1	P275	IN	M82	P385
		ADJACENT	M82 X-2	P277
M101 ULX-1	P276	IN	M101	P371
M82 X-2	P277	IN	M82	P385
		ADJACENT	M82 X-1	P275
PSR B1957+20	P282	IN	PSR B1957+20 bow shock	P335
α Cen AB	P284	SHARED_SYSTEM	Proxima b	P078
Luhman 16	P286	GROUP_OF	Luhman 16A, Luhman 16B	P129, P128
M67	P296	CONTAINS	M67-S1063	A018
M31-EC4	P301	ADJACENT	(GC) 037-B327, M32, G1, NGC 205	S071, P353, S070, P355
Central Cluster	P303	CONTAINS	G2, IRS 13E, IRS 16C, S0-2, S0-16, S0-102, Sgr A*	A006, S066, A005, A004, S039, S041, P426

Table E3 *continued*

Table E3 (*continued*)

Object	ID	Relationship	Partner	Partner IDs
Cyg OB2	P306	IN	Cygnus Cocoon	P344
		ADJACENT	TeV J2032+4130	A052
Cen A Outer Filament	P308	IN	Centaurus A	P434
ζ Oph cloud	P309	CONTAINS	ζ Oph bow shock, ζ Oph	P323, P220
Orion A	P311	CONTAINS	ι Ori, M42, Orion hot core	P182, P317, P315
Orion hot core	P315	IN	Orion A, M42	P311, P317
M42	P317	IN	Orion A	P311
		ADJACENT	ι Ori	P182
		CONTAINS	Orion hot core	P315
NGC 3603	P319	CONTAINS	[SBD2011] 5	A019
ζ Oph bow shock	P323	IN	ζ Oph bow shock	P323
		CONTAINS	ζ Oph	P220
Red Rectangle nebula	P324	CONTAINS	HD 44179	P169
Helix Nebula	P325	CONTAINS	NGC 7293 central star	P071
NGC 6302	P326	CONTAINS	EZ CMa	P188
Homunculus Nebula	P328	CONTAINS	η Car	P193
S 308	P329	CONTAINS	EZ CMa	P188
SN 1987A	P333	CONTAINS	NS 1987A	S057
		ADJACENT	30 Dor, CAL 83 nebula, N159F, PSR J0537-6910, R136 a1	S080, P339, P342, S052, S032
Crab nebula	P334	CONTAINS	Crab pulsar	P235
PSR B1957+20 bow shock	P335	CONTAINS	PSR B1957+20	P282
Geminga halo	P336	CONTAINS	Geminga	P234
R Aqr nebula	P337	CONTAINS	R Aqr	P249
GK Per shell	P338	CONTAINS	GK Per	P255
CAL 83 nebula	P339	ADJACENT	30 Dor, N159F, NS 1987A, PSR J0537-6910, R136 a1, SN 1987A	S080, P342, S057, S052, S032, P333
Cygnus X-1 shell	P341	CONTAINS	Cygnus X-1	P241
N159F	P342	ADJACENT	30 Dor, CAL 83 nebula, R136 a1, NS 1987A, SN 1987A	S080, P339, S032, S057, P333
W50	P343	CONTAINS	SS433	P274
Cygnus Cocoon	P344	CONTAINS	Cyg OB2, TeV J2032+4130	P306, A052
SSA22a-LAB01	P346	IN	SSA22	P465
NGC 4636	P348	IN	Virgo Cluster	P461
M59	P349	BOUND	M59-UCD3	S087
		IN	Virgo Cluster	P461
M32	P353	ADJACENT	(GC) 037-B327, M31-EC4, G1, NGC 205	S071, P301, S070, P355
NGC 205	P355	ADJACENT	(GC) 037-B327, M31-EC4, M32, G1	S071, P301, P353, S070
NGC 4431	P358	IN	Virgo Cluster	P461
NGC 1277	P359	CONTAINS	NGC 1277*	A022
		IN	Perseus Cluster	P463
		ADJACENT	NGC 1265, NGC 1275 minihalo	P436, P468
M101	P371	CONTAINS	M101 ULX-1	P276
M82	P385	CONTAINS	M82 X-1, M82 X-2	P275, P277
VCC 1287	P397	IN	Virgo Cluster	P461
HI 1232+20	P399	CONTAINS	AGC 229385	S095
M51a/b	P403	CONTAINS	M51a	P409
Antennae	P404	ADJACENT	Antenna TDG	P405
Antenna TDG	P405	ADJACENT	Antennae	P404
M51a	P409	IN	M51a/b	P403
M91	P412	IN	Virgo Cluster	P461
NGC 1365	P416	IN	Fornax Cluster	P460
UGC 7321	P421	IN	Virgo Cluster	P461
Sgr A*	P426	IN	Central Cluster	P303
		HOSTS	G2, IRS 13E, IRS 16C, S0-2, S0-16, S0-102	A006, S066, A005, A004, S039, S041

Table E3 *continued*

Table E3 (continued)

Object	ID	Relationship	Partner	Partner IDs
Centaurus A	P434	CONTAINS	Cen A Outer Filament	P308
NGC 1265	P436	IN	Perseus Cluster	P463
		ADJACENT	NGC 1275 minihalo, NGC 1277	P468, P359
Fornax Cluster	P460	CONTAINS	NGC 1365	P416
Virgo Cluster	P461	CONTAINS	HVGC-1, M59, M59-UCD3, M85-HCC 1, M86 tULX-1, M91, UGC 7321, VCC 1287, XRT 000519	A008, P349, S087, S072, A076, P412, P421, P397, A073
Coma Cluster	P462	CONTAINS	Coma C	P467
Perseus Cluster	P463	CONTAINS	NGC 1265, NGC 1275 minihalo, NGC 1277, NGC 1277*	P436, P468, P359, A022
SSA22	P465	CONTAINS	SSA22a-LAB01	P346
Coma C	P467	IN	Coma Cluster	P462
NGC 1275 minihalo	P468	IN	Perseus Cluster	P463
1253+275	P469	IN	Coma Cluster	P462
R136 a1	S032	IN	30 Dor	S080
		ADJACENT	CAL 83 nebula, N159F, NS 1987A, PSR J0537- 6910, SN 1987A	P339, P342, S057, S052, P333
S0-16	S039	IN	Central Cluster	P303
		ORBITS	Sgr A*	P426
		ADJACENT	G2, IRS 13E, IRS 16C, S0-2, S0-102	A006, S066, A005, A004, S041
S0-102	S041	IN	Central Cluster	P303
		ORBITS	Sgr A*	P426
		ADJACENT	G2, IRS 13E, IRS 16C, S0-2, S0-16	A006, S066, A005, A004, S039
PSR J0537-6910	S052	ADJACENT	30 Dor, CAL 83 nebula, N159F, NS 1987A, R136 a1, SN 1987A	S080, P339, P342, S057, S032, P333
NS 1987A	S057	IN	SN 1987A	P333
		ADJACENT	30 Dor, CAL 83 nebula, N159F, PSR J0537-6910, R136 a1	S080, P339, P342, S052, S032
IRS 13E	S066	IN	Central Cluster	P303
		ORBITS	Sgr A*	P426
		ADJACENT	G2, IRS 16C, S0-2, S0-16, S0-102	A006, A005, A004, S039, S041
G1	S070	ADJACENT	(GC) 037-B327, M31-EC4, M32, NGC 205	S071, P301, P353, P355
(GC) 037-B327	S071	ADJACENT	M31-EC4, M32, G1, NGC 205	P301, P353, S070, P355
M85-HCC 1	S072	IN	Virgo Cluster	P461
Sgr B2	S078	CONTAINS	Sgr B2(N) AN01	S079
Sgr B2(N) AN01	S079	IN	Sgr B2	S078
30 Dor	S080	CONTAINS	R136 a1	S032
		ADJACENT	CAL 83 nebula, NS 1987A, PSR J0537-6910, SN 1987A	P339, S057, S052, P333
M59-UCD3	S087	BOUND	M59	P349
		IN	Virgo Cluster	P461
AGC 229385	S095	IN	HI 1232+20	P399
SPT-CLJ2344-4243 Arc	S101	IN	Phoenix Cluster	S120
M60-UCD1	S108	IN	Virgo Cluster	P461
Phoenix Cluster	S120	CONTAINS		
S0-2	A004	IN	Central Cluster	P303
		ORBITS	Sgr A*	P426
		ADJACENT	G2, S0-16, S0-102	A006, S039, S041
IRS 16C	A005	IN	Central Cluster	P303
		ORBITS	Sgr A*	P426
		ADJACENT	G2, IRS 13E, S0-2, S0-16, S0-102	A006, S066, A004, S039, S041
G2	A006	IN	Central Cluster	P303
		ORBITS	Sgr A*	P426
		ADJACENT	IRS 13E, IRS 16C, S0-2, S0-16, S0-102	S066, A005, A004, S039, S041
HVGC-1	A008	IN	Virgo Cluster	P461
M67-S1063	A018	IN	M67	P296

Table E3 continued

Table E3 (*continued*)

Object	ID	Relationship	Partner	Partner IDs
[SBD2011] 5	A019	IN	NGC 3603	P319
NGC 1277*	A022	IN	NGC 1277, Perseus Cluster	P359, P463
TeV J2032+4130	A052	IN	Cygnus Cocoon	P344
		ADJACENT	Cyg OB2	P306
SN 2008S	A069	ADJACENT	NGC 6946-BH1	P243
XRT 000519	A073	IN	Virgo Cluster	P461
M86 tULX-1	A076	IN	Virgo Cluster	P461
NGC 4502	E013	IN	Virgo Cluster	P461
NGC 4698	E014	IN	Virgo Cluster	P461
Wow! Signal (A)	E023	ADJACENT	Wow! Signal (B)	E024
Wow! Signal (B)	E024	ADJACENT	Wow! Signal (A)	E023
GW100916 (A)	C003	ADJACENT	GW100916 (B)	C004
GW100916 (B)	C004	ADJACENT	GW100916 (A)	C003

With I17 targets				
ϵ Ind Bb	P127	BOUND	GJ845A	...
MSX SMC 055	P181	IN	SMC	...
UV Cet	P210	MUTUAL_ORBIT	GJ 65A	...
Sirius B	P226	MUTUAL_ORBIT	Sirius A	...
NGC 6946-BH1	P243	IN	NGC 6946	...
YY Gem	P291	BOUND	Castor AB	...
M31-EC4	P301	BOUND	M31	...
NGC 604	P307	IN	M33	...
Sextans A hole	P316	IN	Sextans A	...
SN 1987A	P333	IN	LMC	...
CAL 83 nebula	P339	IN	LMC	...
N159F	P342	IN	LMC	...
M32	P353	BOUND	M31	...
NGC 205	P355	BOUND	M31	...
M51a/b	P403	CONTAINS	NGC 5195	...
M51a	P409	ADJACENT	NGC 5195	...
Virgo Cluster	P461	CONTAINS	NGC 4489, NGC 4486B, M87, M49, NGC 4478, M86, NGC 4473, NGC 4660, M60, M87, M84, NGC 4564, NGC 4551, NGC 4387, NGC 4239, NGC 4458	...
R136 a1	S032	IN	LMC	...
PSR J0537-6910	S052	IN	LMC	...
NS 1987A	S057	IN	LMC	...
G1	S070	BOUND	M31	...
(GC) 037-B327	S071	BOUND	M31	...
30 Dor	S080	IN	LMC	...
M60-UCD1	S108	BOUND	M60	...
SN 2008S	A069	IN	NGC 6946	...
XRT 000519	A073	IN	M86	...
M86 tULX-1	A076	IN	M86	...

NOTE—**Relationships** – ADJACENT: object’s sky location is projected within same parent object as partner.

BOUND: gravitationally bound with, orbital motion of either partner too slow to detect.

CONTAINS: partner’s sky location is projected within boundaries of object.

GROUP_OF: object consists entirely of collection of listed objects.

HOSTS: partner orbits object, object’s motion too small to detect astrometrically.

IN: object’s sky location is within bounds of other object.

MUTUAL_ORBIT: object and partner bound, both with astrometrically detectable orbital motion.

SHARED_SYSTEM: object is part of same gravitationally bound system, although given object is small subcomponent of object’s partner.

ORBITS: object orbits partner, partner’s motion too small to detect astrometrically.

REFERENCES

- Aartsen, M. G., Ackermann, M., Adams, J., et al. 2017, *Astroparticle Physics*, 92, 30, doi: [10.1016/j.astropartphys.2017.05.002](https://doi.org/10.1016/j.astropartphys.2017.05.002)
- . 2020, *ApJ*, 892, 53, doi: [10.3847/1538-4357/ab791d](https://doi.org/10.3847/1538-4357/ab791d)

- Abbot, D. S., & Switzer, E. R. 2011, *ApJL*, 735, L27, doi: [10.1088/2041-8205/735/2/L27](https://doi.org/10.1088/2041-8205/735/2/L27)
- Abbott, B. P., Abbott, R., Abbott, T. D., et al. 2016, *PhRvL*, 116, 061102, doi: [10.1103/PhysRevLett.116.061102](https://doi.org/10.1103/PhysRevLett.116.061102)
- Abbott, B. P., et al. 2019a, *ApJ*, 875, 161, doi: [10.3847/1538-4357/ab0e8f](https://doi.org/10.3847/1538-4357/ab0e8f)
- . 2019b, *Physical Review X*, 9, 031040, doi: [10.1103/PhysRevX.9.031040](https://doi.org/10.1103/PhysRevX.9.031040)
- Abdalla, H., Adam, R., Aharonian, F., et al. 2019, *Nature*, 575, 464, doi: [10.1038/s41586-019-1743-9](https://doi.org/10.1038/s41586-019-1743-9)
- Abdo, A. A., Ackermann, M., Ajello, M., et al. 2011, *Science*, 331, 739, doi: [10.1126/science.1199705](https://doi.org/10.1126/science.1199705)
- Abell, G. O., Corwin, Harold G., J., & Olowin, R. P. 1989, *ApJS*, 70, 1, doi: [10.1086/191333](https://doi.org/10.1086/191333)
- Abeyssekara, A. U., Archambault, S., Archer, A., et al. 2016, *ApJL*, 818, L33, doi: [10.3847/2041-8205/818/2/L33](https://doi.org/10.3847/2041-8205/818/2/L33)
- Abeyssekara, A. U., Alfaro, R., Alvarez, C., et al. 2017, *ApJ*, 843, 116, doi: [10.3847/1538-4357/aa789f](https://doi.org/10.3847/1538-4357/aa789f)
- Abramov, O., & Mojszis, S. J. 2011, *Icarus*, 213, 273, doi: [10.1016/j.icarus.2011.03.003](https://doi.org/10.1016/j.icarus.2011.03.003)
- Acciari, V. A., Beilicke, M., Blaylock, G., et al. 2008, *ApJ*, 679, 397, doi: [10.1086/587458](https://doi.org/10.1086/587458)
- Acciari, V. A., Aliu, E., Arlen, T., et al. 2009, *ApJL*, 706, L275, doi: [10.1088/0004-637X/706/2/L275](https://doi.org/10.1088/0004-637X/706/2/L275)
- Acero, F., Donato, D., Ojha, R., et al. 2013, *ApJ*, 779, 133, doi: [10.1088/0004-637X/779/2/133](https://doi.org/10.1088/0004-637X/779/2/133)
- Ackermann, M., Ajello, M., Allafort, A., et al. 2011, *Science*, 334, 1103, doi: [10.1126/science.1210311](https://doi.org/10.1126/science.1210311)
- Ackermann, M., Ajello, M., Albert, A., et al. 2016, *ApJL*, 823, L2, doi: [10.3847/2041-8205/823/1/L2](https://doi.org/10.3847/2041-8205/823/1/L2)
- Adam, T., Agafonova, N., Aleksandrov, A., et al. 2012, *Journal of High Energy Physics*, 2012, 93, doi: [10.1007/JHEP10\(2012\)093](https://doi.org/10.1007/JHEP10(2012)093)
- Adams, F. C., & Laughlin, G. 1997, *Reviews of Modern Physics*, 69, 337, doi: [10.1103/RevModPhys.69.337](https://doi.org/10.1103/RevModPhys.69.337)
- Adams, S. M., Kochanek, C. S., Gerke, J. R., Stanek, K. Z., & Dai, X. 2017, *MNRAS*, 468, 4968, doi: [10.1093/mnras/stx816](https://doi.org/10.1093/mnras/stx816)
- Adrián-Martínez, S., et al. 2016, *PhRvD*, 93, 122010, doi: [10.1103/PhysRevD.93.122010](https://doi.org/10.1103/PhysRevD.93.122010)
- Agol, E., Hogan, C. J., & Plotkin, R. M. 2006, *PhRvD*, 73, 087302, doi: [10.1103/PhysRevD.73.087302](https://doi.org/10.1103/PhysRevD.73.087302)
- Aguilera-Gómez, C., Ramírez, I., & Chanamé, J. 2018, *A&A*, 614, A55, doi: [10.1051/0004-6361/201732209](https://doi.org/10.1051/0004-6361/201732209)
- Aharonian, F., Akhperjanian, A., Beilicke, M., et al. 2002, *A&A*, 393, L37, doi: [10.1051/0004-6361:20021171](https://doi.org/10.1051/0004-6361:20021171)
- Aharonian, F., Akhperjanian, A. G., Barres de Almeida, U., et al. 2008, *A&A*, 477, 353, doi: [10.1051/0004-6361:20078516](https://doi.org/10.1051/0004-6361:20078516)
- Ahn, C. P., Alexandroff, R., Allende Prieto, C., et al. 2012, *ApJS*, 203, 21, doi: [10.1088/0067-0049/203/2/21](https://doi.org/10.1088/0067-0049/203/2/21)
- Airy, G. B. 1846, *MNRAS*, 7, 121, doi: [10.1093/mnras/7.9.121](https://doi.org/10.1093/mnras/7.9.121)
- Alam, S., Albareti, F. D., Allende Prieto, C., et al. 2015, *ApJS*, 219, 12, doi: [10.1088/0067-0049/219/1/12](https://doi.org/10.1088/0067-0049/219/1/12)
- Aliu, E., Aune, T., Behera, B., et al. 2014, *ApJ*, 783, 16, doi: [10.1088/0004-637X/783/1/16](https://doi.org/10.1088/0004-637X/783/1/16)
- Alpar, M. A., Cheng, A. F., Ruderman, M. A., & Shaham, J. 1982, *Nature*, 300, 728, doi: [10.1038/300728a0](https://doi.org/10.1038/300728a0)
- Anantharamaiah, K. R., Pedlar, A., Ekers, R. D., & Goss, W. M. 1991, *MNRAS*, 249, 262, doi: [10.1093/mnras/249.2.262](https://doi.org/10.1093/mnras/249.2.262)
- Andersson, N., Antonopoulou, D., Espinoza, C. M., Haskell, B., & Ho, W. C. G. 2018, *ApJ*, 864, 137, doi: [10.3847/1538-4357/aad6eb](https://doi.org/10.3847/1538-4357/aad6eb)
- Andreasen, D. T., Sousa, S. G., Tsantaki, M., et al. 2017, *A&A*, 600, A69, doi: [10.1051/0004-6361/201629967](https://doi.org/10.1051/0004-6361/201629967)
- Andrews, J. J., Agüeros, M., Brown, W. R., et al. 2016, *ApJ*, 828, 38, doi: [10.3847/0004-637X/828/1/38](https://doi.org/10.3847/0004-637X/828/1/38)
- Angerhausen, D., DeLarme, E., & Morse, J. A. 2015, *PASP*, 127, 1113, doi: [10.1086/683797](https://doi.org/10.1086/683797)
- Anguita, T., Faure, C., Kneib, J. P., et al. 2009, *A&A*, 507, 35, doi: [10.1051/0004-6361/200912091](https://doi.org/10.1051/0004-6361/200912091)
- Ann, H. B., Seo, M., & Ha, D. K. 2015, *ApJS*, 217, 27, doi: [10.1088/0067-0049/217/2/27](https://doi.org/10.1088/0067-0049/217/2/27)
- Annis, J. 1999a, *Journal of the British Interplanetary Society*, 52, 19. <https://arxiv.org/abs/astro-ph/9901322>
- . 1999b, *Journal of the British Interplanetary Society*, 52, 33
- Aoki, T., Tanaka, T., Niinuma, K., et al. 2014, *ApJ*, 781, 10, doi: [10.1088/0004-637X/781/1/10](https://doi.org/10.1088/0004-637X/781/1/10)
- Archambault, S., Beilicke, M., Benbow, W., et al. 2013, *ApJ*, 779, 150, doi: [10.1088/0004-637X/779/2/150](https://doi.org/10.1088/0004-637X/779/2/150)
- Arp, H. 1966, *ApJS*, 14, 1, doi: [10.1086/190147](https://doi.org/10.1086/190147)
- Atwood, W. B., Abdo, A. A., Ackermann, M., et al. 2009, *ApJ*, 697, 1071, doi: [10.1088/0004-637X/697/2/1071](https://doi.org/10.1088/0004-637X/697/2/1071)
- Bañados, E., Venemans, B. P., Mazzucchelli, C., et al. 2018, *Nature*, 553, 473, doi: [10.1038/nature25180](https://doi.org/10.1038/nature25180)
- Baan, W. A., Rhoads, J., Fisher, K., Altschuler, D. R., & Haschick, A. 1992, *ApJL*, 396, L99, doi: [10.1086/186526](https://doi.org/10.1086/186526)
- Backer, D. C., Kulkarni, S. R., Heiles, C., Davis, M. M., & Goss, W. M. 1982, *Nature*, 300, 615, doi: [10.1038/300615a0](https://doi.org/10.1038/300615a0)
- Bahcall, N. A. 1977, *ARA&A*, 15, 505, doi: [10.1146/annurev.aa.15.090177.002445](https://doi.org/10.1146/annurev.aa.15.090177.002445)
- Bai, Y., Zou, H., Liu, J., & Wang, S. 2015, *ApJS*, 220, 6, doi: [10.1088/0067-0049/220/1/6](https://doi.org/10.1088/0067-0049/220/1/6)
- Bailes, M., Lyne, A. G., & Shemar, S. L. 1991, *Nature*, 352, 311, doi: [10.1038/352311a0](https://doi.org/10.1038/352311a0)

- Balanutsa, P., Lipunov, V., Denisenko, D., et al. 2015, *The Astronomer's Telegram*, 6918, 1
- Baldassare, V. F., Reines, A. E., Gallo, E., & Greene, J. E. 2015, *ApJL*, 809, L14, doi: [10.1088/2041-8205/809/1/L14](https://doi.org/10.1088/2041-8205/809/1/L14)
- Ball, C., Cannon, J. M., Leisman, L., et al. 2018, *AJ*, 155, 65, doi: [10.3847/1538-3881/aaa156](https://doi.org/10.3847/1538-3881/aaa156)
- Barbier, D., & Morguleff, N. 1962, *ApJ*, 136, 315, doi: [10.1086/147382](https://doi.org/10.1086/147382)
- Barclay, T., Rowe, J. F., Lissauer, J. J., et al. 2013, *Nature*, 494, 452, doi: [10.1038/nature11914](https://doi.org/10.1038/nature11914)
- Bardelli, S., Zucca, E., Vettolani, G., et al. 1994, *MNRAS*, 267, 665, doi: [10.1093/mnras/267.3.665](https://doi.org/10.1093/mnras/267.3.665)
- Baron, D., & Poznanski, D. 2017, *MNRAS*, 465, 4530, doi: [10.1093/mnras/stw3021](https://doi.org/10.1093/mnras/stw3021)
- Baross, J. A., Benner, S. A., Cody, G. D., et al. 2007, *The limits of organic life in planetary systems* (National Academies Press)
- Barucci, M. A., Belskaya, I. N., Fulchignoni, M., & Birlan, M. 2005, *AJ*, 130, 1291, doi: [10.1086/431957](https://doi.org/10.1086/431957)
- Barvainis, R., & Antonucci, R. 2005, *ApJL*, 628, L89, doi: [10.1086/432666](https://doi.org/10.1086/432666)
- Barvainis, R., & Ivison, R. 2002, *ApJ*, 571, 712, doi: [10.1086/340096](https://doi.org/10.1086/340096)
- Batalha, N. M., Rowe, J. F., Bryson, S. T., et al. 2013, *ApJS*, 204, 24, doi: [10.1088/0067-0049/204/2/24](https://doi.org/10.1088/0067-0049/204/2/24)
- Bauer, F. E., Treister, E., Schawinski, K., et al. 2017, *MNRAS*, 467, 4841, doi: [10.1093/mnras/stx417](https://doi.org/10.1093/mnras/stx417)
- Bayliss, M. B., McDonald, M., Sharon, K., et al. 2020, *Nature Astronomy*, 4, 159, doi: [10.1038/s41550-019-0888-7](https://doi.org/10.1038/s41550-019-0888-7)
- Beech, M. 1990, *Earth Moon and Planets*, 49, 177, doi: [10.1007/BF00053979](https://doi.org/10.1007/BF00053979)
- Belczyński, K., Mikołajewska, J., Munari, U., Ivison, R. J., & Friedjung, M. 2000, *A&AS*, 146, 407, doi: [10.1051/aas:2000280](https://doi.org/10.1051/aas:2000280)
- Bell Burnell, S. J. 1977, in *Annals of the New York Academy of Sciences*, Vol. 302, Eighth Texas Symposium on Relativistic Astrophysics, ed. M. D. Papagiannis, 685, doi: [10.1111/j.1749-6632.1977.tb37085.x](https://doi.org/10.1111/j.1749-6632.1977.tb37085.x)
- Bellazzini, M., Ferraro, F. R., Origlia, L., et al. 2002, *AJ*, 124, 3222, doi: [10.1086/344794](https://doi.org/10.1086/344794)
- Benford, J. 2019, *AJ*, 158, 150, doi: [10.3847/1538-3881/ab3e35](https://doi.org/10.3847/1538-3881/ab3e35)
- Bensby, T., Feltzing, S., & Oey, M. S. 2014, *A&A*, 562, A71, doi: [10.1051/0004-6361/201322631](https://doi.org/10.1051/0004-6361/201322631)
- Bernkopf, J., Chini, R., Buda, L. S., et al. 2012, *MNRAS*, 425, 1308, doi: [10.1111/j.1365-2966.2012.21534.x](https://doi.org/10.1111/j.1365-2966.2012.21534.x)
- Bialy, S., & Loeb, A. 2018, *ApJL*, 868, L1, doi: [10.3847/2041-8213/aaeda8](https://doi.org/10.3847/2041-8213/aaeda8)
- Bidelman, W. P. 2005, *Astronomical Society of the Pacific Conference Series*, Vol. 336, *Tc and Other Unstable Elements in Przybylski's Star*, ed. I. Barnes, Thomas G. & F. N. Bash, 309
- Blair, D. G., Norris, R. P., Troup, E. R., et al. 1992, *MNRAS*, 257, 105, doi: [10.1093/mnras/257.1.105](https://doi.org/10.1093/mnras/257.1.105)
- Blanton, M. R., & Roweis, S. 2007, *AJ*, 133, 734, doi: [10.1086/510127](https://doi.org/10.1086/510127)
- Bochenek, C. D., Ravi, V., Belov, K. V., et al. 2020, arXiv e-prints, arXiv:2005.10828, <https://arxiv.org/abs/2005.10828>
- Bohigas, J. 2017, *MNRAS*, 466, 1412, doi: [10.1093/mnras/stw3187](https://doi.org/10.1093/mnras/stw3187)
- Bonafede, A., Feretti, L., Giovannini, G., et al. 2009, *A&A*, 503, 707, doi: [10.1051/0004-6361/200912520](https://doi.org/10.1051/0004-6361/200912520)
- Bond, H. E., Nelan, E. P., VandenBerg, D. A., Schaefer, G. H., & Harmer, D. 2013, *ApJL*, 765, L12, doi: [10.1088/2041-8205/765/1/L12](https://doi.org/10.1088/2041-8205/765/1/L12)
- Borovicka, J., & Hudec, R. 1989, *Bulletin of the Astronomical Institutes of Czechoslovakia*, 40, 170
- Borra, E. F. 2013, *ApJ*, 774, 142, doi: [10.1088/0004-637X/774/2/142](https://doi.org/10.1088/0004-637X/774/2/142)
- Borra, E. F., & Trottier, E. 2016, *PASP*, 128, 114201, doi: [10.1088/1538-3873/128/969/114201](https://doi.org/10.1088/1538-3873/128/969/114201)
- Borucki, W. J., Koch, D. G., Basri, G., et al. 2011, *ApJ*, 728, 117, doi: [10.1088/0004-637X/728/2/117](https://doi.org/10.1088/0004-637X/728/2/117)
- Bower, G. C., Saul, D., Bloom, J. S., et al. 2007, *ApJ*, 666, 346, doi: [10.1086/519831](https://doi.org/10.1086/519831)
- Bowyer, S., Lampton, M., Korpela, E., et al. 2016, arXiv e-prints, arXiv:1607.00440, <https://arxiv.org/abs/1607.00440>
- Boyajian, T. S., LaCourse, D. M., Rappaport, S. A., et al. 2016, *MNRAS*, 457, 3988, doi: [10.1093/mnras/stw218](https://doi.org/10.1093/mnras/stw218)
- Boyajian, T. S., Alonso, R., Ammerman, A., et al. 2018, *ApJL*, 853, L8, doi: [10.3847/2041-8213/aaa405](https://doi.org/10.3847/2041-8213/aaa405)
- Brin, G. D. 1983, *QJRAS*, 24, 283
- Brinchmann, J., Charlot, S., White, S. D. M., et al. 2004, *MNRAS*, 351, 1151, doi: [10.1111/j.1365-2966.2004.07881.x](https://doi.org/10.1111/j.1365-2966.2004.07881.x)
- Broadhurst, T., Umetsu, K., Medezinski, E., Oguri, M., & Rephaeli, Y. 2008, *ApJL*, 685, L9, doi: [10.1086/592400](https://doi.org/10.1086/592400)
- Brown, M. E., & Schaller, E. L. 2007, *Science*, 316, 1585, doi: [10.1126/science.1139415](https://doi.org/10.1126/science.1139415)
- Brzycki, B., Siemion, A., Croft, S., et al. 2019, *Research Notes of the American Astronomical Society*, 3, 147, doi: [10.3847/2515-5172/ab4bd6](https://doi.org/10.3847/2515-5172/ab4bd6)
- Buldgen, G., Farnir, M., Pezzotti, C., et al. 2019, *A&A*, 630, A126, doi: [10.1051/0004-6361/201936126](https://doi.org/10.1051/0004-6361/201936126)

- Burgasser, A. J., Geballe, T. R., Leggett, S. K., Kirkpatrick, J. D., & Golimowski, D. A. 2006, *ApJ*, 637, 1067, doi: [10.1086/498563](https://doi.org/10.1086/498563)
- Burns, J. A. 1986, in *Satellites*, 1–38
- Bus, S. J., & Binzel, R. P. 2002, *Icarus*, 158, 146, doi: [10.1006/icar.2002.6856](https://doi.org/10.1006/icar.2002.6856)
- Buta, R. J., Sheth, K., Athanassoula, E., et al. 2015, *ApJS*, 217, 32, doi: [10.1088/0067-0049/217/2/32](https://doi.org/10.1088/0067-0049/217/2/32)
- Caballero, J. A. 2018, *Geosciences*, 8, 362, doi: [10.3390/geosciences8100362](https://doi.org/10.3390/geosciences8100362)
- Caffau, E., Bonifacio, P., François, P., et al. 2011, *Nature*, 477, 67, doi: [10.1038/nature10377](https://doi.org/10.1038/nature10377)
- Caffau, E., Bonifacio, P., Oliva, E., et al. 2019, *A&A*, 622, A68, doi: [10.1051/0004-6361/201834318](https://doi.org/10.1051/0004-6361/201834318)
- Caldwell, N., Strader, J., Romanowsky, A. J., et al. 2014, *ApJL*, 787, L11, doi: [10.1088/2041-8205/787/1/L11](https://doi.org/10.1088/2041-8205/787/1/L11)
- Campante, T. L., Barclay, T., Swift, J. J., et al. 2015, *ApJ*, 799, 170, doi: [10.1088/0004-637X/799/2/170](https://doi.org/10.1088/0004-637X/799/2/170)
- Cappellari, M. 2013, *ApJL*, 778, L2, doi: [10.1088/2041-8205/778/1/L2](https://doi.org/10.1088/2041-8205/778/1/L2)
- Carrigan, Jr., R. A. 2009, *ApJ*, 698, 2075, doi: [10.1088/0004-637X/698/2/2075](https://doi.org/10.1088/0004-637X/698/2/2075)
- Castro-Tirado, A. J., de Ugarte Postigo, A., Gorosabel, J., et al. 2008, *Nature*, 455, 506, doi: [10.1038/nature07328](https://doi.org/10.1038/nature07328)
- Cayrel de Strobel, G., Soubiran, C., & Ralite, N. 2001, *A&A*, 373, 159, doi: [10.1051/0004-6361:20010525](https://doi.org/10.1051/0004-6361:20010525)
- Cenadelli, D., & Bernagozzi, A. 2015, *European Physical Journal H*, 40, doi: [10.1140/epjh/e2015-60041-5](https://doi.org/10.1140/epjh/e2015-60041-5)
- Lenko, S. B., Butler, N. R., Ofek, E. O., et al. 2010, *AJ*, 140, 224, doi: [10.1088/0004-6256/140/1/224](https://doi.org/10.1088/0004-6256/140/1/224)
- Lenko, S. B., Kulkarni, S. R., Horesh, A., et al. 2013, *ApJ*, 769, 130, doi: [10.1088/0004-637X/769/2/130](https://doi.org/10.1088/0004-637X/769/2/130)
- Chambers, K. C., Magnier, E. A., Metcalfe, N., et al. 2016, arXiv e-prints, arXiv:1612.05560. <https://arxiv.org/abs/1612.05560>
- Chan, B. M. Y., Broadhurst, T., Lim, J., et al. 2017, *ApJ*, 835, 44, doi: [10.3847/1538-4357/835/1/44](https://doi.org/10.3847/1538-4357/835/1/44)
- Chardin, G., & Gerbier, G. 1989, *A&A*, 210, 52
- Chatterjee, S., Law, C. J., Wharton, R. S., et al. 2017, *Nature*, 541, 58, doi: [10.1038/nature20797](https://doi.org/10.1038/nature20797)
- Chennamangalam, J., Siemion, A. P. V., Lorimer, D. R., & Werthimer, D. 2015, *NewA*, 34, 245, doi: [10.1016/j.newast.2014.07.011](https://doi.org/10.1016/j.newast.2014.07.011)
- Chiaberge, M., Tremblay, G. R., Capetti, A., & Norman, C. 2018, *ApJ*, 861, 56, doi: [10.3847/1538-4357/aac48b](https://doi.org/10.3847/1538-4357/aac48b)
- Chiaberge, M., Ely, J. C., Meyer, E. T., et al. 2017, *A&A*, 600, A57, doi: [10.1051/0004-6361/201629522](https://doi.org/10.1051/0004-6361/201629522)
- CHIME/FRB Collaboration, Amiri, M., Bandura, K., et al. 2018, *ApJ*, 863, 48, doi: [10.3847/1538-4357/aad188](https://doi.org/10.3847/1538-4357/aad188)
- Choi, J., McCarthy, C., Marcy, G. W., et al. 2013, *ApJ*, 764, 131, doi: [10.1088/0004-637X/764/2/131](https://doi.org/10.1088/0004-637X/764/2/131)
- Chon, G., Böhringer, H., & Zaroubi, S. 2015, *A&A*, 575, L14, doi: [10.1051/0004-6361/201425591](https://doi.org/10.1051/0004-6361/201425591)
- Chu, D. S., Do, T., Hees, A., et al. 2018, *ApJ*, 854, 12, doi: [10.3847/1538-4357/aaa3eb](https://doi.org/10.3847/1538-4357/aaa3eb)
- Cigan, P., Matsuura, M., Gomez, H. L., et al. 2019, *ApJ*, 886, 51, doi: [10.3847/1538-4357/ab4b46](https://doi.org/10.3847/1538-4357/ab4b46)
- Čirković, M. M. 2009, *Serbian Astronomical Journal*, 178, 1, doi: [10.2298/SAJ0978001C](https://doi.org/10.2298/SAJ0978001C)
- . 2018, *The Great Silence: Science and Philosophy of Fermi's Paradox*
- Čirković, M. M. 2018, *Acta Astronautica*, 152, 289, doi: [10.1016/j.actaastro.2018.07.051](https://doi.org/10.1016/j.actaastro.2018.07.051)
- Čirković, M. M., & Bradbury, R. J. 2006, *NewA*, 11, 628, doi: [10.1016/j.newast.2006.04.003](https://doi.org/10.1016/j.newast.2006.04.003)
- Čirković, M. M., & Vukotić, B. 2008, *Origins of Life and Evolution of the Biosphere*, 38, 535, doi: [10.1007/s11084-008-9149-y](https://doi.org/10.1007/s11084-008-9149-y)
- Clanton, C., & Gaudi, B. S. 2014, *ApJ*, 791, 91, doi: [10.1088/0004-637X/791/2/91](https://doi.org/10.1088/0004-637X/791/2/91)
- Clark, J. S., Najarro, F., Negueruela, I., et al. 2012, *A&A*, 541, A145, doi: [10.1051/0004-6361/201117472](https://doi.org/10.1051/0004-6361/201117472)
- Cocozza, G., Ferraro, F. R., Possenti, A., & D'Amico, N. 2006, *ApJL*, 641, L129, doi: [10.1086/504040](https://doi.org/10.1086/504040)
- Coe, D., Zitrin, A., Carrasco, M., et al. 2013, *ApJ*, 762, 32, doi: [10.1088/0004-637X/762/1/32](https://doi.org/10.1088/0004-637X/762/1/32)
- Colomb, F., Hurrell, E., Lemarchand, G., & Olald, J. 1995, in *Astronomical Society of the Pacific Conference Series*, Vol. 74, *Progress in the Search for Extraterrestrial Life.*, ed. G. S. Shostak, 345
- Comerón, S., Salo, H., Laurikainen, E., et al. 2014, *A&A*, 562, A121, doi: [10.1051/0004-6361/201321633](https://doi.org/10.1051/0004-6361/201321633)
- Corbet, R. H. D. 1997, *Journal of the British Interplanetary Society*, 50, 253. <https://arxiv.org/abs/1609.00330>
- Cordes, E. e. a. 2006, *Memo 85: Discovery and Understanding with the SKA, Square Kilometre Array*. https://www.skatelescope.org/uploaded/18720_memo.85.pdf
- Cordes, J. 1993, in *Astronomical Society of the Pacific Conference Series*, Vol. 47, *Third Decennial US-USSR Conference on SETI*, ed. G. S. Shostak, 257–266
- Cordiner, M. A., Boogert, A. C. A., Charnley, S. B., et al. 2016, *ApJ*, 828, 51, doi: [10.3847/0004-637X/828/1/51](https://doi.org/10.3847/0004-637X/828/1/51)
- Corso, G. J., Harris, R. W., & Ringwald, F. A. 1987, *A&A*, 183, L9
- Cosens, M., Maire, J., Wright, S. A., et al. 2018, in *Society of Photo-Optical Instrumentation Engineers (SPIE) Conference Series*, Vol. 10702, *Proc. SPIE*, 107025H, doi: [10.1117/12.2314252](https://doi.org/10.1117/12.2314252)

- Coughlin, J. L., Mullally, F., Thompson, S. E., et al. 2016, *ApJS*, 224, 12, doi: [10.3847/0067-0049/224/1/12](https://doi.org/10.3847/0067-0049/224/1/12)
- Cowley, C. R., Bidelman, W. P., Hubrig, S., Mathys, G., & Bord, D. J. 2004, *A&A*, 419, 1087, doi: [10.1051/0004-6361:20035726](https://doi.org/10.1051/0004-6361:20035726)
- Cox, D. P. 2005, *ARA&A*, 43, 337, doi: [10.1146/annurev.astro.43.072103.150615](https://doi.org/10.1146/annurev.astro.43.072103.150615)
- Creevey, O. L., Thévenin, F., Berio, P., et al. 2015, *A&A*, 575, A26, doi: [10.1051/0004-6361/201424310](https://doi.org/10.1051/0004-6361/201424310)
- Croft, S., Bower, G. C., Keating, G., et al. 2011, *ApJ*, 731, 34, doi: [10.1088/0004-637X/731/1/34](https://doi.org/10.1088/0004-637X/731/1/34)
- Croft, S. K. 1992, *Icarus*, 99, 402, doi: [10.1016/0019-1035\(92\)90156-2](https://doi.org/10.1016/0019-1035(92)90156-2)
- Cromartie, H. T., Fonseca, E., Ransom, S. M., et al. 2020, *Nature Astronomy*, 4, 72, doi: [10.1038/s41550-019-0880-2](https://doi.org/10.1038/s41550-019-0880-2)
- Crowther, P. A. 2019, *Galaxies*, 7, 88, doi: [10.3390/galaxies7040088](https://doi.org/10.3390/galaxies7040088)
- Crowther, P. A., Schnurr, O., Hirschi, R., et al. 2010, *MNRAS*, 408, 731, doi: [10.1111/j.1365-2966.2010.17167.x](https://doi.org/10.1111/j.1365-2966.2010.17167.x)
- Crowther, P. A., Caballero-Nieves, S. M., Bostroem, K. A., et al. 2016, *MNRAS*, 458, 624, doi: [10.1093/mnras/stw273](https://doi.org/10.1093/mnras/stw273)
- Cruz, M., Martínez-González, E., Vielva, P., & Cayón, L. 2005, *MNRAS*, 356, 29, doi: [10.1111/j.1365-2966.2004.08419.x](https://doi.org/10.1111/j.1365-2966.2004.08419.x)
- Cruz, M., Martínez-González, E., Vielva, P., et al. 2008, *MNRAS*, 390, 913, doi: [10.1111/j.1365-2966.2008.13812.x](https://doi.org/10.1111/j.1365-2966.2008.13812.x)
- Cunningham, C. J., Marsden, B. G., & Orchiston, W. 2011, *Journal for the History of Astronomy*, 42, 283, doi: [10.1177/002182861104200301](https://doi.org/10.1177/002182861104200301)
- Currie, T., Muto, T., Kudo, T., et al. 2014, *ApJL*, 796, L30, doi: [10.1088/2041-8205/796/2/L30](https://doi.org/10.1088/2041-8205/796/2/L30)
- Currie, T., Brandt, T. D., Uyama, T., et al. 2018, *AJ*, 156, 291, doi: [10.3847/1538-3881/aae9ea](https://doi.org/10.3847/1538-3881/aae9ea)
- Dahn, C. C., Bergeron, P., Liebert, J., et al. 2004, *ApJ*, 605, 400, doi: [10.1086/382208](https://doi.org/10.1086/382208)
- Davenport, J. R. A. 2019, arXiv e-prints, arXiv:1907.04443. <https://arxiv.org/abs/1907.04443>
- Davies, P. 2010, *The Eerie Silence: Are We Alone in the Universe?* (Penguin UK)
- de la Fuente Marcos, C., & de la Fuente Marcos, R. 2019, *Research Notes of the American Astronomical Society*, 3, 106, doi: [10.3847/2515-5172/ab346c](https://doi.org/10.3847/2515-5172/ab346c)
- . 2020, *MNRAS*, 494, L6, doi: [10.1093/mnras/slaa027](https://doi.org/10.1093/mnras/slaa027)
- De Luca, A., Caraveo, P. A., Mereghetti, S., Tiengo, A., & Bignami, G. F. 2006, *Science*, 313, 814, doi: [10.1126/science.1129185](https://doi.org/10.1126/science.1129185)
- de Luca, A., Esposito, P., Israel, G. L., et al. 2010, *MNRAS*, 402, 1870, doi: [10.1111/j.1365-2966.2009.16012.x](https://doi.org/10.1111/j.1365-2966.2009.16012.x)
- de Vaucouleurs, G., de Vaucouleurs, A., Corwin, Herold G., J., et al. 1991, *Third Reference Catalogue of Bright Galaxies*
- Deka-Szymankiewicz, B., Niedzielski, A., Adamczyk, M., et al. 2018, *A&A*, 615, A31, doi: [10.1051/0004-6361/201731696](https://doi.org/10.1051/0004-6361/201731696)
- Dekany, I., Minniti, D., & Saito, R. K. 2014, *The Astronomer's Telegram*, 5954, 1
- DeMeo, F. E., & Carry, B. 2014, *Nature*, 505, 629, doi: [10.1038/nature12908](https://doi.org/10.1038/nature12908)
- Demers, S., & Battinelli, P. 2001, *A&A*, 377, 425, doi: [10.1051/0004-6361:20011128](https://doi.org/10.1051/0004-6361:20011128)
- Denisenko, D. 2019, *The Astronomer's Telegram*, 12638, 1
- Di Stefano, R., & Ray, A. 2016, *ApJ*, 827, 54, doi: [10.3847/0004-637X/827/1/54](https://doi.org/10.3847/0004-637X/827/1/54)
- Dick, S. J. 2003, *International Journal of Astrobiology*, 2, 65, doi: [10.1017/S147355040300137X](https://doi.org/10.1017/S147355040300137X)
- . 2013, *Discovery and Classification in Astronomy*
- Dicke, R. H., Peebles, P. J. E., Roll, P. G., & Wilkinson, D. T. 1965, *ApJ*, 142, 414, doi: [10.1086/148306](https://doi.org/10.1086/148306)
- Dieterich, S. B., Henry, T. J., Jao, W.-C., et al. 2014, *AJ*, 147, 94, doi: [10.1088/0004-6256/147/5/94](https://doi.org/10.1088/0004-6256/147/5/94)
- Dixon, R. S. 1985, in *IAU Symposium*, Vol. 112, *The Search for Extraterrestrial Life: Recent Developments*, ed. M. D. Papagiannis, 305–314
- Djorgovski, S. 2000, *Astronomical Society of the Pacific Conference Series*, Vol. 213, *Generalized SETI in a Virtual Observatory*, ed. G. Lemarchand & K. Meech, 519
- Djorgovski, S. G., Mahabal, A., Drake, A., Graham, M., & Donalek, C. 2013, *Sky Surveys*, ed. T. D. Oswalt & H. E. Bond, 223, doi: [10.1007/978-94-007-5618-2_5](https://doi.org/10.1007/978-94-007-5618-2_5)
- Djorgovski, S. G., Mahabal, A. A., Brunner, R. J., et al. 2001, *Astronomical Society of the Pacific Conference Series*, Vol. 225, *Searches for Rare and New Types of Objects*, ed. R. J. Brunner, S. G. Djorgovski, & A. S. Szalay, 52
- Do, T., Kerzendorf, W., Konopacky, Q., et al. 2018, *ApJL*, 855, L5, doi: [10.3847/2041-8213/aaac3](https://doi.org/10.3847/2041-8213/aaac3)
- Donati, J. F., Moutou, C., Malo, L., et al. 2016, *Nature*, 534, 662, doi: [10.1038/nature18305](https://doi.org/10.1038/nature18305)
- Dong, S., Katz, B., & Socrates, A. 2014, *ApJL*, 781, L5, doi: [10.1088/2041-8205/781/1/L5](https://doi.org/10.1088/2041-8205/781/1/L5)
- Dong, S., Shappee, B. J., Prieto, J. L., et al. 2016, *Science*, 351, 257, doi: [10.1126/science.aac9613](https://doi.org/10.1126/science.aac9613)
- Drake, F. D. 1962, *Intelligent life in space*.
- Dubus, G. 2013, *A&A Rv*, 21, 64, doi: [10.1007/s00159-013-0064-5](https://doi.org/10.1007/s00159-013-0064-5)
- Dullo, B. T., Graham, A. W., & Knapen, J. H. 2017, *MNRAS*, 471, 2321, doi: [10.1093/mnras/stx1635](https://doi.org/10.1093/mnras/stx1635)

- Durbala, A., del Olmo, A., Yun, M. S., et al. 2008, *AJ*, 135, 130, doi: [10.1088/0004-6256/135/1/130](https://doi.org/10.1088/0004-6256/135/1/130)
- Dyson, F. J. 1963, in *Interstellar Communication*, ed. A. G. W. Cameron, 115–120
- Dyson, F. J. 2003, *International Journal of Astrobiology*, 2, 103, doi: [10.1017/S1473550403001538](https://doi.org/10.1017/S1473550403001538)
- Ebeling, H., Ma, C. J., Kneib, J. P., et al. 2009, *MNRAS*, 395, 1213, doi: [10.1111/j.1365-2966.2009.14502.x](https://doi.org/10.1111/j.1365-2966.2009.14502.x)
- Eggleton, P. P., & Tokovinin, A. A. 2008, *MNRAS*, 389, 869, doi: [10.1111/j.1365-2966.2008.13596.x](https://doi.org/10.1111/j.1365-2966.2008.13596.x)
- Elbaz, D., Dickinson, M., Hwang, H. S., et al. 2011, *A&A*, 533, A119, doi: [10.1051/0004-6361/201117239](https://doi.org/10.1051/0004-6361/201117239)
- Elliot, J. L., Person, M. J., Zuluaga, C. A., et al. 2010, *Nature*, 465, 897, doi: [10.1038/nature09109](https://doi.org/10.1038/nature09109)
- Elmegreen, D. M., & Elmegreen, B. G. 1982, *MNRAS*, 201, 1021, doi: [10.1093/mnras/201.4.1021](https://doi.org/10.1093/mnras/201.4.1021)
- Elmegreen, D. M., Elmegreen, B. G., Rubin, D. S., & Schaffer, M. A. 2005, *ApJ*, 631, 85, doi: [10.1086/432502](https://doi.org/10.1086/432502)
- Enriquez, J. E., Siemion, A., Foster, G., et al. 2017, *ApJ*, 849, 104, doi: [10.3847/1538-4357/aa8d1b](https://doi.org/10.3847/1538-4357/aa8d1b)
- Enriquez, J. E., Siemion, A., Lazio, T. J. W., et al. 2018, *Research Notes of the American Astronomical Society*, 2, 9, doi: [10.3847/2515-5172/aaa6c9](https://doi.org/10.3847/2515-5172/aaa6c9)
- Enriquez, J. E., Siemion, A., Dana, R., et al. 2019, *International Journal of Astrobiology*, 18, 33, doi: [10.1017/S1473550417000465](https://doi.org/10.1017/S1473550417000465)
- Esteves, L. J., De Mooij, E. J. W., & Jayawardhana, R. 2015, *ApJ*, 804, 150, doi: [10.1088/0004-637X/804/2/150](https://doi.org/10.1088/0004-637X/804/2/150)
- Evans, P. A., Fridriksson, J. K., Gehrels, N., et al. 2012, *ApJS*, 203, 28, doi: [10.1088/0067-0049/203/2/28](https://doi.org/10.1088/0067-0049/203/2/28)
- Ewen, H. I., & Purcell, E. M. 1951, *Nature*, 168, 356, doi: [10.1038/168356a0](https://doi.org/10.1038/168356a0)
- Fajardo-Acosta, S. B., Kirkpatrick, J. D., Schneider, A. C., et al. 2016, *ApJ*, 832, 62, doi: [10.3847/0004-637X/832/1/62](https://doi.org/10.3847/0004-637X/832/1/62)
- Falanga, M., Bozzo, E., Lutovinov, A., et al. 2015, *A&A*, 577, A130, doi: [10.1051/0004-6361/201425191](https://doi.org/10.1051/0004-6361/201425191)
- Fan, L., Gao, Y., Knudsen, K. K., & Shu, X. 2018, *ApJ*, 854, 157, doi: [10.3847/1538-4357/aaaaae](https://doi.org/10.3847/1538-4357/aaaaae)
- Fanaroff, B. L., & Riley, J. M. 1974, *MNRAS*, 167, 31P, doi: [10.1093/mnras/167.1.31P](https://doi.org/10.1093/mnras/167.1.31P)
- Farihi, J., Wood, P. R., & Stalder, B. 2005, *ApJL*, 627, L41, doi: [10.1086/432158](https://doi.org/10.1086/432158)
- Feltzing, S., & Gonzalez, G. 2001, *A&A*, 367, 253, doi: [10.1051/0004-6361:20000477](https://doi.org/10.1051/0004-6361:20000477)
- Filho, M. E., & Sánchez Almeida, J. 2018, *MNRAS*, 478, 2541, doi: [10.1093/mnras/sty1130](https://doi.org/10.1093/mnras/sty1130)
- Forgan, D. H., & Nichol, R. C. 2011, *International Journal of Astrobiology*, 10, 77, doi: [10.1017/S1473550410000236](https://doi.org/10.1017/S1473550410000236)
- Forward, R. L. 1980, *Dragon's Egg* (Ballantine)
- Frail, D. A., Kulkarni, S. R., Ofek, E. O., Bower, G. C., & Nakar, E. 2012, *ApJ*, 747, 70, doi: [10.1088/0004-637X/747/1/70](https://doi.org/10.1088/0004-637X/747/1/70)
- Freitas, R. A., J. 1985, *Icarus*, 62, 518, doi: [10.1016/0019-1035\(85\)90192-7](https://doi.org/10.1016/0019-1035(85)90192-7)
- Frey, K., & Accomazzi, A. 2018, *ApJS*, 236, 24, doi: [10.3847/1538-4365/aab760](https://doi.org/10.3847/1538-4365/aab760)
- Fritz, T. K., Gillessen, S., Dodds-Eden, K., et al. 2010, *ApJ*, 721, 395, doi: [10.1088/0004-637X/721/1/395](https://doi.org/10.1088/0004-637X/721/1/395)
- Fulchignoni, M., Belskaya, I., Barucci, M. A., de Sanctis, M. C., & Doressoundiram, A. 2008, *Transneptunian Object Taxonomy*, ed. M. A. Barucci, H. Boehnhardt, D. P. Cruikshank, A. Morbidelli, & R. Dotson, 181
- Fulton, B. J., Petigura, E. A., Howard, A. W., et al. 2017, *AJ*, 154, 109, doi: [10.3847/1538-3881/aa80eb](https://doi.org/10.3847/1538-3881/aa80eb)
- Gaia Collaboration, Brown, A. G. A., Vallenari, A., et al. 2018, *A&A*, 616, A1, doi: [10.1051/0004-6361/201833051](https://doi.org/10.1051/0004-6361/201833051)
- Gaidos, E., Mann, A. W., & Ansdell, M. 2016, *ApJ*, 817, 50, doi: [10.3847/0004-637X/817/1/50](https://doi.org/10.3847/0004-637X/817/1/50)
- Gajjar, V., Siemion, A. P. V., Price, D. C., et al. 2018, *ApJ*, 863, 2, doi: [10.3847/1538-4357/aad005](https://doi.org/10.3847/1538-4357/aad005)
- Galle, J. G. 1846, *MNRAS*, 7, 153, doi: [10.1093/mnras/7.9.153](https://doi.org/10.1093/mnras/7.9.153)
- Garrett, M., Siemion, A., & van Cappellen, W. 2017, arXiv e-prints, arXiv:1709.01338. <https://arxiv.org/abs/1709.01338>
- Garrett, M. A. 2015, *A&A*, 581, L5, doi: [10.1051/0004-6361/201526687](https://doi.org/10.1051/0004-6361/201526687)
- Gaudi, B. S., Stassun, K. G., Collins, K. A., et al. 2017, *Nature*, 546, 514, doi: [10.1038/nature22392](https://doi.org/10.1038/nature22392)
- Geha, M., Willman, B., Simon, J. D., et al. 2009, *ApJ*, 692, 1464, doi: [10.1088/0004-637X/692/2/1464](https://doi.org/10.1088/0004-637X/692/2/1464)
- Gerke, J. R., Kochanek, C. S., & Stanek, K. Z. 2015, *MNRAS*, 450, 3289, doi: [10.1093/mnras/stv776](https://doi.org/10.1093/mnras/stv776)
- Gertz, J. 2016, *Journal of the British Interplanetary Society*, 69, 88. <https://arxiv.org/abs/1609.04635>
- . 2019, *Journal of the British Interplanetary Society*, 72, 386. <https://arxiv.org/abs/2001.00673>
- Ghez, A. M., Salim, S., Hornstein, S. D., et al. 2005, *ApJ*, 620, 744, doi: [10.1086/427175](https://doi.org/10.1086/427175)
- Ghez, A. M., Duchêne, G., Matthews, K., et al. 2003, *ApJL*, 586, L127, doi: [10.1086/374804](https://doi.org/10.1086/374804)
- Ghisellini, G., Tavecchio, F., Foschini, L., & Ghirland a, G. 2011, *MNRAS*, 414, 2674, doi: [10.1111/j.1365-2966.2011.18578.x](https://doi.org/10.1111/j.1365-2966.2011.18578.x)
- Giles, D., & Walkowicz, L. 2019, *MNRAS*, 484, 834, doi: [10.1093/mnras/sty3461](https://doi.org/10.1093/mnras/sty3461)
- Gillessen, S., Genzel, R., Fritz, T. K., et al. 2012, *Nature*, 481, 51, doi: [10.1038/nature10652](https://doi.org/10.1038/nature10652)

- Gillon, M., Triaud, A. H. M. J., Demory, B.-O., et al. 2017, *Nature*, 542, 456, doi: [10.1038/nature21360](https://doi.org/10.1038/nature21360)
- Gladman, B., Marsden, B. G., & Vanlaerhoven, C. 2008, *Nomenclature in the Outer Solar System*, ed. M. A. Barucci, H. Boehnhardt, D. P. Cruikshank, A. Morbidelli, & R. Dotson, 43
- Glazebrook, K., Schreiber, C., Labbé, I., et al. 2017, *Nature*, 544, 71, doi: [10.1038/nature21680](https://doi.org/10.1038/nature21680)
- Golenetskii, S., Aptekar, R., Mazets, E., et al. 2009, *GRB Coordinates Network*, 9647, 1
- Gonzales, E. C., Faherty, J. K., Gagné, J., et al. 2019, *ApJ*, 886, 131, doi: [10.3847/1538-4357/ab48fc](https://doi.org/10.3847/1538-4357/ab48fc)
- Gonzalez, A. H., Zabludoff, A. I., Zaritsky, D., & Dalcanton, J. J. 2000, *ApJ*, 536, 561, doi: [10.1086/308985](https://doi.org/10.1086/308985)
- Gonzalez, G., Wallerstein, G., & Saar, S. H. 1999, *ApJL*, 511, L111, doi: [10.1086/311847](https://doi.org/10.1086/311847)
- Gopka, V. F., Yushchenko, A. V., Yushchenko, V. A., Panov, I. V., & Kim, C. 2008, *Kinematics and Physics of Celestial Bodies*, 24, 89, doi: [10.3103/S0884591308020049](https://doi.org/10.3103/S0884591308020049)
- Gordon, M. S., & Humphreys, R. M. 2019, *Galaxies*, 7, 92, doi: [10.3390/galaxies7040092](https://doi.org/10.3390/galaxies7040092)
- Gorham, P. W., Rotter, B., Allison, P., et al. 2018, *PhRvL*, 121, 161102, doi: [10.1103/PhysRevLett.121.161102](https://doi.org/10.1103/PhysRevLett.121.161102)
- Gotz, D., Mereghetti, S., von Kienlin, A., & Beck, M. 2009, *GRB Coordinates Network*, 9649, 1
- Gowanlock, M. G. 2016, *ApJ*, 832, 38, doi: [10.3847/0004-637X/832/1/38](https://doi.org/10.3847/0004-637X/832/1/38)
- Graham, A. W. 2019, *MNRAS*, 487, 4995, doi: [10.1093/mnras/stz1623](https://doi.org/10.1093/mnras/stz1623)
- Graham, A. W., Durré, M., Savorgnan, G. A. D., et al. 2016, *ApJ*, 819, 43, doi: [10.3847/0004-637X/819/1/43](https://doi.org/10.3847/0004-637X/819/1/43)
- Graham, A. W., & Guzmán, R. 2003, *AJ*, 125, 2936, doi: [10.1086/374992](https://doi.org/10.1086/374992)
- Gray, R. H. 2015, *Astrobiology*, 15, 195, doi: [10.1089/ast.2014.1247](https://doi.org/10.1089/ast.2014.1247)
- Gray, R. H., & Ellingsen, S. 2002, *ApJ*, 578, 967, doi: [10.1086/342646](https://doi.org/10.1086/342646)
- Gray, R. H., & Mooley, K. 2017, *AJ*, 153, 110, doi: [10.3847/1538-3881/153/3/110](https://doi.org/10.3847/1538-3881/153/3/110)
- Green, E. M., Guvenen, B., O'Malley, C. J., et al. 2011, *ApJ*, 734, 59, doi: [10.1088/0004-637X/734/1/59](https://doi.org/10.1088/0004-637X/734/1/59)
- Greenstreet, S. 2020, *MNRAS*, doi: [10.1093/mnras/slaa025](https://doi.org/10.1093/mnras/slaa025)
- Griffith, R. L., Wright, J. T., Maldonado, J., et al. 2015, *ApJS*, 217, 25, doi: [10.1088/0067-0049/217/2/25](https://doi.org/10.1088/0067-0049/217/2/25)
- Groh, J. H., Hillier, D. J., Damineli, A., et al. 2009, *ApJ*, 698, 1698, doi: [10.1088/0004-637X/698/2/1698](https://doi.org/10.1088/0004-637X/698/2/1698)
- Gropp, J. D., Siegel, M. H., & Neil Gehrels Swift Observatory Team. 2020, *GRB Coordinates Network*, 27008, 1
- Gudennavar, S. B., Bubbly, S. G., Preethi, K., & Murthy, J. 2012, *ApJS*, 199, 8, doi: [10.1088/0067-0049/199/1/8](https://doi.org/10.1088/0067-0049/199/1/8)
- Guillot, S., Pavlov, G. G., Reyes, C., et al. 2019, *ApJ*, 874, 175, doi: [10.3847/1538-4357/ab0f38](https://doi.org/10.3847/1538-4357/ab0f38)
- Guillot, T., Burrows, A., Hubbard, W. B., Lunine, J. I., & Saumon, D. 1996, *ApJL*, 459, L35, doi: [10.1086/309935](https://doi.org/10.1086/309935)
- Guseva, N. G., Papaderos, P., Izotov, Y. I., Noeske, K. G., & Fricke, K. J. 2004, *A&A*, 421, 519, doi: [10.1051/0004-6361:20035949](https://doi.org/10.1051/0004-6361:20035949)
- Guzik, P., Drahus, M., Rusek, K., et al. 2020, *Nature Astronomy*, 4, 53, doi: [10.1038/s41550-019-0931-8](https://doi.org/10.1038/s41550-019-0931-8)
- Habibi, M., Gillessen, S., Martins, F., et al. 2017, *ApJ*, 847, 120, doi: [10.3847/1538-4357/aa876f](https://doi.org/10.3847/1538-4357/aa876f)
- Habing, H. J., & Israel, F. P. 1979, *ARA&A*, 17, 345, doi: [10.1146/annurev.aa.17.090179.002021](https://doi.org/10.1146/annurev.aa.17.090179.002021)
- Hachisu, I., & Kato, M. 2001, *ApJ*, 558, 323, doi: [10.1086/321601](https://doi.org/10.1086/321601)
- Hagen, H. J., Cordis, L., Engels, D., et al. 1992, *A&A*, 253, L5
- Haisch, B. M., & Glampapa, M. S. 1985, *PASP*, 97, 340, doi: [10.1086/131541](https://doi.org/10.1086/131541)
- Hall, A. 1878, *MNRAS*, 38, 205, doi: [10.1093/mnras/38.4.205](https://doi.org/10.1093/mnras/38.4.205)
- Halliday, I., Feldman, P. A., & Blackwell, A. T. 1987, *ApJL*, 320, L153, doi: [10.1086/184993](https://doi.org/10.1086/184993)
- Hankins, T. H., Kern, J. S., Weatherall, J. C., & Eilek, J. A. 2003, *Nature*, 422, 141, doi: [10.1038/nature01477](https://doi.org/10.1038/nature01477)
- Hansen, C. J., Jofré, P., Koch, A., McWilliam, A., & Sneden, C. S. 2017, *A&A*, 598, A54, doi: [10.1051/0004-6361/201629628](https://doi.org/10.1051/0004-6361/201629628)
- Hao, C.-N., Kennicutt, R. C., Johnson, B. D., et al. 2011, *ApJ*, 741, 124, doi: [10.1088/0004-637X/741/2/124](https://doi.org/10.1088/0004-637X/741/2/124)
- Harp, G. R., Ackermann, R. F., Astorga, A., et al. 2018, *ApJ*, 869, 66, doi: [10.3847/1538-4357/aaeb98](https://doi.org/10.3847/1538-4357/aaeb98)
- Hart, M. H. 1975, *QJRAS*, 16, 128
- Harwit, M. 1981, *Cosmic discovery. The search, scope, and heritage of astronomy*
- . 1984, *Cosmic Discovery* (The MIT Press), 346
- Hayakawa, T., Torii, K., Enokiya, R., Amano, T., & Fukui, Y. 2012, *PASJ*, 64, 8, doi: [10.1093/pasj/64.1.8](https://doi.org/10.1093/pasj/64.1.8)
- Heber, U. 2016, *PASP*, 128, 082001, doi: [10.1088/1538-3873/128/966/082001](https://doi.org/10.1088/1538-3873/128/966/082001)
- Heger, A., Fryer, C. L., Woosley, S. E., Langer, N., & Hartmann, D. H. 2003, *ApJ*, 591, 288, doi: [10.1086/375341](https://doi.org/10.1086/375341)
- Heiter, U., Jofré, P., Gustafsson, B., et al. 2015, *A&A*, 582, A49, doi: [10.1051/0004-6361/201526319](https://doi.org/10.1051/0004-6361/201526319)
- Heller, R., & Pudritz, R. E. 2016, *Astrobiology*, 16, 259, doi: [10.1089/ast.2015.1358](https://doi.org/10.1089/ast.2015.1358)

- Hermes, J. J., Montgomery, M. H., Gianninas, A., et al. 2013, *MNRAS*, 436, 3573, doi: [10.1093/mnras/stt1835](https://doi.org/10.1093/mnras/stt1835)
- Hessels, J. W. T., Ransom, S. M., Stairs, I. H., et al. 2006, *Science*, 311, 1901, doi: [10.1126/science.1123430](https://doi.org/10.1126/science.1123430)
- Hewish, A., Bell, S. J., Pilkington, J. D. H., Scott, P. F., & Collins, R. A. 1968, *Nature*, 217, 709, doi: [10.1038/217709a0](https://doi.org/10.1038/217709a0)
- Heyl, J. S. 2005, *PhRvD*, 72, 107302, doi: [10.1103/PhysRevD.72.107302](https://doi.org/10.1103/PhysRevD.72.107302)
- Hickson, P. 1993, *Astrophysical Letters and Communications*, 29, 1
- Hickson, P., Mendes de Oliveira, C., Huchra, J. P., & Palumbo, G. G. 1992, *ApJ*, 399, 353, doi: [10.1086/171932](https://doi.org/10.1086/171932)
- Hillenbrand, L. A., Miller, A. A., Carpenter, J. M., et al. 2019, *ApJ*, 874, 82, doi: [10.3847/1538-4357/ab06c8](https://doi.org/10.3847/1538-4357/ab06c8)
- Hinkel, N. R., Timmes, F. X., Young, P. A., Pagano, M. D., & Turnbull, M. C. 2014, *AJ*, 148, 54, doi: [10.1088/0004-6256/148/3/54](https://doi.org/10.1088/0004-6256/148/3/54)
- Hinkel, N. R., Mamajek, E. E., Turnbull, M. C., et al. 2017, *ApJ*, 848, 34, doi: [10.3847/1538-4357/aa8b0f](https://doi.org/10.3847/1538-4357/aa8b0f)
- Hippke, M., & Angerhausen, D. 2018, *ApJL*, 854, L11, doi: [10.3847/2041-8213/aaab44](https://doi.org/10.3847/2041-8213/aaab44)
- Hippke, M., Learned, J. G., Zee, A., et al. 2015, *ApJ*, 798, 42, doi: [10.1088/0004-637X/798/1/42](https://doi.org/10.1088/0004-637X/798/1/42)
- Hoffman, Y., Pomarède, D., Tully, R. B., & Courtois, H. M. 2017, *Nature Astronomy*, 1, 0036, doi: [10.1038/s41550-016-0036](https://doi.org/10.1038/s41550-016-0036)
- Holmberg, J., Nordström, B., & Andersen, J. 2007, *A&A*, 475, 519, doi: [10.1051/0004-6361:20077221](https://doi.org/10.1051/0004-6361:20077221)
- Horner, J., Müller, T. G., & Lykawka, P. S. 2012, *MNRAS*, 423, 2587, doi: [10.1111/j.1365-2966.2012.21067.x](https://doi.org/10.1111/j.1365-2966.2012.21067.x)
- Horowitz, P., & Sagan, C. 1993, *ApJ*, 415, 218, doi: [10.1086/173157](https://doi.org/10.1086/173157)
- Howard, A. W., Horowitz, P., Wilkinson, D. T., et al. 2004, *ApJ*, 613, 1270, doi: [10.1086/423300](https://doi.org/10.1086/423300)
- Hsieh, H. H., Fitzsimmons, A., Joshi, Y., Christian, D., & Pollacco, D. L. 2010, *MNRAS*, 407, 1784, doi: [10.1111/j.1365-2966.2010.17016.x](https://doi.org/10.1111/j.1365-2966.2010.17016.x)
- Hu, B. X., D'Orazio, D. J., Haiman, Z., et al. 2020, *MNRAS*, 495, 4061, doi: [10.1093/mnras/staa1312](https://doi.org/10.1093/mnras/staa1312)
- Huang, C., Wu, Y., & Triaud, A. H. M. J. 2016, *ApJ*, 825, 98, doi: [10.3847/0004-637X/825/2/98](https://doi.org/10.3847/0004-637X/825/2/98)
- Hubble, E. P. 1926, *ApJ*, 64, 321, doi: [10.1086/143018](https://doi.org/10.1086/143018)
- Hudec, R., Peresty, R., & Motch, C. 1990, *A&A*, 235, 174
- Hughes, A. M., Duchêne, G., & Matthews, B. C. 2018, *ARA&A*, 56, 541, doi: [10.1146/annurev-astro-081817-052035](https://doi.org/10.1146/annurev-astro-081817-052035)
- Hui, C. Y., Yeung, P. K. H., Ng, C. W., et al. 2016, *MNRAS*, 457, 4262, doi: [10.1093/mnras/stw209](https://doi.org/10.1093/mnras/stw209)
- Hyman, S. D., Lazio, T. J. W., Kassim, N. E., et al. 2005, *Nature*, 434, 50, doi: [10.1038/nature03400](https://doi.org/10.1038/nature03400)
- Icecube Collaboration, Aartsen, M. G., Ackermann, M., et al. 2017, *A&A*, 607, A115, doi: [10.1051/0004-6361/201730620](https://doi.org/10.1051/0004-6361/201730620)
- Inoue, M., & Yokoo, H. 2011, *Journal of the British Interplanetary Society*, 64, 59
- Isaacson, H., Siemion, A. P. V., Marcy, G. W., et al. 2019, *PASP*, 131, 014201, doi: [10.1088/1538-3873/aaeae0](https://doi.org/10.1088/1538-3873/aaeae0)
- Isaacson, H., Siemion, A. P. V., Marcy, G. W., et al. 2017, *PASP*, 129, 054501, doi: [10.1088/1538-3873/aa5800](https://doi.org/10.1088/1538-3873/aa5800)
- Ishigaki, M., Ouchi, M., & Harikane, Y. 2016, *ApJ*, 822, 5, doi: [10.3847/0004-637X/822/1/5](https://doi.org/10.3847/0004-637X/822/1/5)
- Israel, G. L., Hummel, W., Covino, S., et al. 2002, *A&A*, 386, L13, doi: [10.1051/0004-6361:20020314](https://doi.org/10.1051/0004-6361:20020314)
- Israel, G. L., Belfiore, A., Stella, L., et al. 2017, *Science*, 355, 817, doi: [10.1126/science.aai8635](https://doi.org/10.1126/science.aai8635)
- Izotov, Y. I., Thuan, T. X., Guseva, N. G., & Liss, S. E. 2018, *MNRAS*, 473, 1956, doi: [10.1093/mnras/stx2478](https://doi.org/10.1093/mnras/stx2478)
- Jaeger, T. R., Hyman, S. D., Kassim, N. E., & Lazio, T. J. W. 2012, *AJ*, 143, 96, doi: [10.1088/0004-6256/143/4/96](https://doi.org/10.1088/0004-6256/143/4/96)
- Janowiecki, S., Leisman, L., Józsa, G., et al. 2015, *ApJ*, 801, 96, doi: [10.1088/0004-637X/801/2/96](https://doi.org/10.1088/0004-637X/801/2/96)
- Jansky, K. G. 1933, *Popular Astronomy*, 41, 548
- Jarrett, T. H., Cluver, M. E., Brown, M. J. I., et al. 2019, *ApJS*, 245, 25, doi: [10.3847/1538-4365/ab521a](https://doi.org/10.3847/1538-4365/ab521a)
- Jayasinghe, T., Stanek, K. Z., Kochanek, C. S., et al. 2019, *The Astronomer's Telegram*, 12836, 1
- Jeffery, C. S. 2008, *Astronomical Society of the Pacific Conference Series*, Vol. 391, *Hydrogen-Deficient Stars: An Introduction*, ed. A. Werner & T. Rauch, 3
- Jester, S., Schneider, D. P., Richards, G. T., et al. 2005, *AJ*, 130, 873, doi: [10.1086/432466](https://doi.org/10.1086/432466)
- Jewitt, D., & Luu, J. 1993, *Nature*, 362, 730, doi: [10.1038/362730a0](https://doi.org/10.1038/362730a0)
- Johnson, J. A., Winn, J. N., Albrecht, S., et al. 2009, *PASP*, 121, 1104, doi: [10.1086/644604](https://doi.org/10.1086/644604)
- Jonas, J. L. 2009, *IEEE Proceedings*, 97, 1522, doi: [10.1109/JPROC.2009.2020713](https://doi.org/10.1109/JPROC.2009.2020713)
- Jones, S., Röpkke, F. K., Pakmor, R., et al. 2016, *A&A*, 593, A72, doi: [10.1051/0004-6361/201628321](https://doi.org/10.1051/0004-6361/201628321)
- Jonker, P. G., Glennie, A., Heida, M., et al. 2013, *ApJ*, 779, 14, doi: [10.1088/0004-637X/779/1/14](https://doi.org/10.1088/0004-637X/779/1/14)
- Kaaret, P., Feng, H., & Roberts, T. P. 2017, *ARA&A*, 55, 303, doi: [10.1146/annurev-astro-091916-055259](https://doi.org/10.1146/annurev-astro-091916-055259)
- Kaaret, P., Prieskorn, Z., in 't Zand, J. J. M., et al. 2007, *ApJL*, 657, L97, doi: [10.1086/513270](https://doi.org/10.1086/513270)
- Kahabka, P., & van den Heuvel, E. P. J. 1997, *ARA&A*, 35, 69, doi: [10.1146/annurev.astro.35.1.69](https://doi.org/10.1146/annurev.astro.35.1.69)

- Kaplan, D. L., Marsh, T. R., Walker, A. N., et al. 2014a, *ApJ*, 780, 167, doi: [10.1088/0004-637X/780/2/167](https://doi.org/10.1088/0004-637X/780/2/167)
- Kaplan, D. L., Boyles, J., Dunlap, B. H., et al. 2014b, *ApJ*, 789, 119, doi: [10.1088/0004-637X/789/2/119](https://doi.org/10.1088/0004-637X/789/2/119)
- Karachentsev, I. D., Makarov, D. I., & Kaisina, E. I. 2013, *AJ*, 145, 101, doi: [10.1088/0004-6256/145/4/101](https://doi.org/10.1088/0004-6256/145/4/101)
- Karakas, A. I., & Lattanzio, J. C. 2014, *PASA*, 31, e030, doi: [10.1017/pasa.2014.21](https://doi.org/10.1017/pasa.2014.21)
- Kardashev, N. S. 1964, *Soviet Ast.*, 8, 217
- Kasliwal, M. M., Cenko, S. B., Kulkarni, S. R., et al. 2008, *ApJ*, 678, 1127, doi: [10.1086/526407](https://doi.org/10.1086/526407)
- Kasliwal, M. M., Kulkarni, S. R., Gal-Yam, A., et al. 2012, *ApJ*, 755, 161, doi: [10.1088/0004-637X/755/2/161](https://doi.org/10.1088/0004-637X/755/2/161)
- Katz, B., Driscoll, D., Millyard, K., et al. 1986, *ApJL*, 307, L33, doi: [10.1086/184723](https://doi.org/10.1086/184723)
- Keller, S. C., Bessell, M. S., Frebel, A., et al. 2014, *Nature*, 506, 463, doi: [10.1038/nature12990](https://doi.org/10.1038/nature12990)
- Kellermann, K. I., Sramek, R., Schmidt, M., Shaffer, D. B., & Green, R. 1989, *AJ*, 98, 1195, doi: [10.1086/115207](https://doi.org/10.1086/115207)
- Kelly, P. L., Diego, J. M., Rodney, S., et al. 2018, *Nature Astronomy*, 2, 334, doi: [10.1038/s41550-018-0430-3](https://doi.org/10.1038/s41550-018-0430-3)
- Kennicutt, R. C., J., & Hodge, P. W. 1986, *ApJ*, 306, 130, doi: [10.1086/164326](https://doi.org/10.1086/164326)
- Kenworthy, M. A., Lacour, S., Kraus, A., et al. 2015, *MNRAS*, 446, 411, doi: [10.1093/mnras/stu2067](https://doi.org/10.1093/mnras/stu2067)
- Kiefer, F. 2019, *A&A*, 632, L9, doi: [10.1051/0004-6361/201936942](https://doi.org/10.1051/0004-6361/201936942)
- Kilic, M., Thorstensen, J. R., Kowalski, P. M., & Andrews, J. 2012, *MNRAS*, 423, L132, doi: [10.1111/j.1745-3933.2012.01271.x](https://doi.org/10.1111/j.1745-3933.2012.01271.x)
- Kipping, D. M., & Spiegel, D. S. 2011, *MNRAS*, 417, L88, doi: [10.1111/j.1745-3933.2011.01127.x](https://doi.org/10.1111/j.1745-3933.2011.01127.x)
- Kirby, E. N., Boylan-Kolchin, M., Cohen, J. G., et al. 2013, *ApJ*, 770, 16, doi: [10.1088/0004-637X/770/1/16](https://doi.org/10.1088/0004-637X/770/1/16)
- Kirkpatrick, J. D. 2005, *ARA&A*, 43, 195, doi: [10.1146/annurev.astro.42.053102.134017](https://doi.org/10.1146/annurev.astro.42.053102.134017)
- Kirkpatrick, J. D., Henry, T. J., & McCarthy, Donald W., J. 1991, *ApJS*, 77, 417, doi: [10.1086/191611](https://doi.org/10.1086/191611)
- Kirsch, M. G., Briel, U. G., Burrows, D., et al. 2005, *Society of Photo-Optical Instrumentation Engineers (SPIE) Conference Series*, Vol. 5898, Crab: the standard x-ray candle with all (modern) x-ray satellites, ed. O. H. W. Siegmund, 22–33, doi: [10.1117/12.616893](https://doi.org/10.1117/12.616893)
- Klebesadel, R. W., Strong, I. B., & Olson, R. A. 1973, *ApJL*, 182, L85, doi: [10.1086/181225](https://doi.org/10.1086/181225)
- Kocevski, D. D., & Ebeling, H. 2006, *ApJ*, 645, 1043, doi: [10.1086/503666](https://doi.org/10.1086/503666)
- Koposov, S. E., Boubert, D., Li, T. S., et al. 2020, *MNRAS*, 491, 2465, doi: [10.1093/mnras/stz3081](https://doi.org/10.1093/mnras/stz3081)
- Kormendy, J., & Bender, R. 2012, *ApJS*, 198, 2, doi: [10.1088/0067-0049/198/1/2](https://doi.org/10.1088/0067-0049/198/1/2)
- Kormendy, J., Fisher, D. B., Cornell, M. E., & Bender, R. 2009, *ApJS*, 182, 216, doi: [10.1088/0067-0049/182/1/216](https://doi.org/10.1088/0067-0049/182/1/216)
- Koss, M., Blecha, L., Mushotzky, R., et al. 2014, *MNRAS*, 445, 515, doi: [10.1093/mnras/stu1673](https://doi.org/10.1093/mnras/stu1673)
- Kovacs, G., Hartman, J. D., & Bakos, G. Á. 2019, *A&A*, 631, A126, doi: [10.1051/0004-6361/201936207](https://doi.org/10.1051/0004-6361/201936207)
- Krauss, L. M., & Starkman, G. D. 2000, *ApJ*, 531, 22, doi: [10.1086/308434](https://doi.org/10.1086/308434)
- Krimm, H. A., Holland, S. T., Corbet, R. H. D., et al. 2013, *ApJS*, 209, 14, doi: [10.1088/0067-0049/209/1/14](https://doi.org/10.1088/0067-0049/209/1/14)
- Kurtz, M. J., Eichhorn, G., Accomazzi, A., et al. 2000, *A&AS*, 143, 41, doi: [10.1051/aas:2000170](https://doi.org/10.1051/aas:2000170)
- La Palombara, N., Mereghetti, S., Esposito, P., & Tiengo, A. 2019, *A&A*, 626, A29, doi: [10.1051/0004-6361/201935339](https://doi.org/10.1051/0004-6361/201935339)
- Lacki, B. C. 2016a, ArXiv e-prints. <https://arxiv.org/abs/1609.05931>
- . 2016b, ArXiv e-prints. <https://arxiv.org/abs/1604.07844>
- Lada, C. J. 1987, in *IAU Symposium*, Vol. 115, Star Forming Regions, ed. M. Peimbert & J. Jugaku, 1
- Lam, D., Bouwens, R. J., Coe, D., et al. 2019, arXiv e-prints, arXiv:1903.08177. <https://arxiv.org/abs/1903.08177>
- Laporte, N., Ellis, R. S., Boone, F., et al. 2017, *ApJL*, 837, L21, doi: [10.3847/2041-8213/aa62aa](https://doi.org/10.3847/2041-8213/aa62aa)
- Latham, D. W. 2012, *NewAR*, 56, 16, doi: [10.1016/j.newar.2011.06.003](https://doi.org/10.1016/j.newar.2011.06.003)
- Latham, D. W., Mazeh, T., Stefanik, R. P., Mayor, M., & Burki, G. 1989, *Nature*, 339, 38, doi: [10.1038/339038a0](https://doi.org/10.1038/339038a0)
- Lattimer, J. M. 2019, *Universe*, 5, 159, doi: [10.3390/universe5070159](https://doi.org/10.3390/universe5070159)
- Laughlin, G., Bodenheimer, P., & Adams, F. C. 1997, *ApJ*, 482, 420, doi: [10.1086/304125](https://doi.org/10.1086/304125)
- Law, C. J., Gaensler, B. M., Metzger, B. D., Ofek, E. O., & Sironi, L. 2018, *ApJL*, 866, L22, doi: [10.3847/2041-8213/aae5f3](https://doi.org/10.3847/2041-8213/aae5f3)
- Law, N. M., Fors, O., Ratzloff, J., et al. 2015, *PASP*, 127, 234, doi: [10.1086/680521](https://doi.org/10.1086/680521)
- Learned, J. G., Kudritzki, R.-P., Pakvasa, S., & Zee, A. 2008, arXiv e-prints, arXiv:0809.0339. <https://arxiv.org/abs/0809.0339>
- Lebofsky, M., Croft, S., Siemion, A. P. V., et al. 2019, *PASP*, 131, 124505, doi: [10.1088/1538-3873/ab3e82](https://doi.org/10.1088/1538-3873/ab3e82)
- Lee, B. C., Han, I., & Park, M. G. 2013, *A&A*, 549, A2, doi: [10.1051/0004-6361/201220301](https://doi.org/10.1051/0004-6361/201220301)
- Leloudas, G., Fraser, M., Stone, N. C., et al. 2016, *Nature Astronomy*, 1, 0002, doi: [10.1038/s41550-016-0002](https://doi.org/10.1038/s41550-016-0002)

- Leroy, A. K., Walter, F., Martini, P., et al. 2015, *ApJ*, 814, 83, doi: [10.1088/0004-637X/814/2/83](https://doi.org/10.1088/0004-637X/814/2/83)
- Levison, H. F. 1996, *Astronomical Society of the Pacific Conference Series*, Vol. 107, *Comet Taxonomy*, ed. T. Rettig & J. M. Hahn, 173–191
- Libby-Roberts, J. E., Berta-Thompson, Z. K., Désert, J.-M., et al. 2020, *AJ*, 159, 57, doi: [10.3847/1538-3881/ab5d36](https://doi.org/10.3847/1538-3881/ab5d36)
- Licquia, T. C., Newman, J. A., & Brinchmann, J. 2015, *ApJ*, 809, 96, doi: [10.1088/0004-637X/809/1/96](https://doi.org/10.1088/0004-637X/809/1/96)
- Liebert, J., Bergeron, P., & Holberg, J. B. 2005, *ApJS*, 156, 47, doi: [10.1086/425738](https://doi.org/10.1086/425738)
- Lingam, M., Ginsburg, I., & Bialy, S. 2019, *ApJ*, 877, 62, doi: [10.3847/1538-4357/ab1b2f](https://doi.org/10.3847/1538-4357/ab1b2f)
- Lingam, M., & Loeb, A. 2017, *ApJL*, 837, L23, doi: [10.3847/2041-8213/aa633e](https://doi.org/10.3847/2041-8213/aa633e)
- . 2020, *ApJ*, 894, 36, doi: [10.3847/1538-4357/ab7dc7](https://doi.org/10.3847/1538-4357/ab7dc7)
- Lipman, D., Isaacson, H., Siemion, A. P. V., et al. 2019, *PASP*, 131, 034202, doi: [10.1088/1538-3873/aafe86](https://doi.org/10.1088/1538-3873/aafe86)
- Lipunov, V., Gorbovskoy, E., Kornilov, V., et al. 2020, *GRB Coordinates Network*, 27007, 1
- Litke, K. C., Marrone, D. P., Spilker, J. S., et al. 2019, *ApJ*, 870, 80, doi: [10.3847/1538-4357/aaf057](https://doi.org/10.3847/1538-4357/aaf057)
- Liu, C., Peng, E. W., Toloba, E., et al. 2015, *ApJL*, 812, L2, doi: [10.1088/2041-8205/812/1/L2](https://doi.org/10.1088/2041-8205/812/1/L2)
- Lo, K. Y. 2005, *ARA&A*, 43, 625, doi: [10.1146/annurev.astro.41.011802.094927](https://doi.org/10.1146/annurev.astro.41.011802.094927)
- Loeb, A., Batista, R. A., & Sloan, D. 2016, *JCAP*, 2016, 040, doi: [10.1088/1475-7516/2016/08/040](https://doi.org/10.1088/1475-7516/2016/08/040)
- Lopez, B., Schneider, J., & Danchi, W. C. 2005, *ApJ*, 627, 974, doi: [10.1086/430416](https://doi.org/10.1086/430416)
- Lorenz, R. D., Lunine, J. I., & McKay, C. P. 1997, *Geophys. Res. Lett.*, 24, 2905, doi: [10.1029/97GL52843](https://doi.org/10.1029/97GL52843)
- Lorimer, D. R., Bailes, M., McLaughlin, M. A., Narkevic, D. J., & Crawford, F. 2007, *Science*, 318, 777, doi: [10.1126/science.1147532](https://doi.org/10.1126/science.1147532)
- Loubser, S. I., & Sánchez-Blázquez, P. 2011, *MNRAS*, 410, 2679, doi: [10.1111/j.1365-2966.2010.17666.x](https://doi.org/10.1111/j.1365-2966.2010.17666.x)
- Luhman, K. L. 2014, *ApJL*, 786, L18, doi: [10.1088/2041-8205/786/2/L18](https://doi.org/10.1088/2041-8205/786/2/L18)
- Luhman, K. L., Adame, L., D’Alessio, P., et al. 2005, *ApJL*, 635, L93, doi: [10.1086/498868](https://doi.org/10.1086/498868)
- Lyne, A. G., & Bailes, M. 1992, *Nature*, 355, 213, doi: [10.1038/355213b0](https://doi.org/10.1038/355213b0)
- Ma, J., Gonzalez, A. H., Vieira, J. D., et al. 2016, *ApJ*, 832, 114, doi: [10.3847/0004-637X/832/2/114](https://doi.org/10.3847/0004-637X/832/2/114)
- Machalski, J., Koziel-Wierzbowska, D., Jamrozy, M., & Saikia, D. J. 2008, *ApJ*, 679, 149, doi: [10.1086/586703](https://doi.org/10.1086/586703)
- Mackey, A. D., & van den Bergh, S. 2005, *MNRAS*, 360, 631, doi: [10.1111/j.1365-2966.2005.09080.x](https://doi.org/10.1111/j.1365-2966.2005.09080.x)
- MacMahon, D. H. E., Price, D. C., Lebofsky, M., et al. 2018, *PASP*, 130, 044502, doi: [10.1088/1538-3873/aa80d2](https://doi.org/10.1088/1538-3873/aa80d2)
- Madau, P., & Dickinson, M. 2014, *ARA&A*, 52, 415, doi: [10.1146/annurev-astro-081811-125615](https://doi.org/10.1146/annurev-astro-081811-125615)
- Maíz-Apellániz, J., Pérez, E., & Mas-Hesse, J. M. 2004, *AJ*, 128, 1196, doi: [10.1086/422925](https://doi.org/10.1086/422925)
- Maley, P. D. 1987, *ApJL*, 317, L39, doi: [10.1086/184909](https://doi.org/10.1086/184909)
- Mamajek, E. E., Quillen, A. C., Pecaut, M. J., et al. 2012, *AJ*, 143, 72, doi: [10.1088/0004-6256/143/3/72](https://doi.org/10.1088/0004-6256/143/3/72)
- Marcote, B., Nimmo, K., Salafia, O. S., et al. 2019, *ApJL*, 876, L14, doi: [10.3847/2041-8213/ab1aad](https://doi.org/10.3847/2041-8213/ab1aad)
- Marcote, B., Nimmo, K., Hessels, J. W. T., et al. 2020, *Nature*, 577, 190, doi: [10.1038/s41586-019-1866-z](https://doi.org/10.1038/s41586-019-1866-z)
- Markevitch, M., & Vikhlinin, A. 2007, *PhR*, 443, 1, doi: [10.1016/j.physrep.2007.01.001](https://doi.org/10.1016/j.physrep.2007.01.001)
- Markwardt, C. B., Gavriil, F. P., Palmer, D. M., Baumgartner, W. H., & Barthelmy, S. D. 2009, *GRB Coordinates Network*, 9645, 1
- Marsh, T. R., Armstrong, D. J., & Carter, P. J. 2014, *MNRAS*, 445, 309, doi: [10.1093/mnras/stu1733](https://doi.org/10.1093/mnras/stu1733)
- Marshall, F. E., Gotthelf, E. V., Zhang, W., Middleditch, J., & Wang, Q. D. 1998, *ApJL*, 499, L179, doi: [10.1086/311381](https://doi.org/10.1086/311381)
- Martel, A. R., Sparks, W. B., Macchetto, D., et al. 1998, *AJ*, 115, 1348, doi: [10.1086/300293](https://doi.org/10.1086/300293)
- Martin, N. F., de Jong, J. T. A., & Rix, H.-W. 2008, *ApJ*, 684, 1075, doi: [10.1086/590336](https://doi.org/10.1086/590336)
- Maselli, A., Massaro, F., Cusumano, G., et al. 2016, *MNRAS*, 460, 3829, doi: [10.1093/mnras/stw1222](https://doi.org/10.1093/mnras/stw1222)
- Massaro, F., D’Abrusco, R., Landoni, M., et al. 2015, *ApJS*, 217, 2, doi: [10.1088/0067-0049/217/1/2](https://doi.org/10.1088/0067-0049/217/1/2)
- Masuda, K., Kawahara, H., Latham, D. W., et al. 2019, *ApJL*, 881, L3, doi: [10.3847/2041-8213/ab321b](https://doi.org/10.3847/2041-8213/ab321b)
- Mateo, M. L. 1998, *ARA&A*, 36, 435, doi: [10.1146/annurev.astro.36.1.435](https://doi.org/10.1146/annurev.astro.36.1.435)
- Mathieu, R. D., van den Berg, M., Torres, G., et al. 2003, *AJ*, 125, 246, doi: [10.1086/344944](https://doi.org/10.1086/344944)
- Matsuoka, M., Kawasaki, K., Ueno, S., et al. 2009, *PASJ*, 61, 999, doi: [10.1093/pasj/61.5.999](https://doi.org/10.1093/pasj/61.5.999)
- Mayor, M., & Queloz, D. 1995, *Nature*, 378, 355, doi: [10.1038/378355a0](https://doi.org/10.1038/378355a0)
- . 2012, *NewAR*, 56, 19, doi: [10.1016/j.newar.2011.06.005](https://doi.org/10.1016/j.newar.2011.06.005)
- McConnachie, A. W. 2012, *AJ*, 144, 4, doi: [10.1088/0004-6256/144/1/4](https://doi.org/10.1088/0004-6256/144/1/4)
- McDonald, M., Bayliss, M., Benson, B. A., et al. 2012, *Nature*, 488, 349, doi: [10.1038/nature11379](https://doi.org/10.1038/nature11379)
- Medezinski, E., Umetsu, K., Nonino, M., et al. 2013, *ApJ*, 777, 43, doi: [10.1088/0004-637X/777/1/43](https://doi.org/10.1088/0004-637X/777/1/43)
- Meech, K. J., Weryk, R., Micheli, M., et al. 2017, *Nature*, 552, 378, doi: [10.1038/nature25020](https://doi.org/10.1038/nature25020)

- Mehrgan, K., Thomas, J., Saglia, R., et al. 2019, *ApJ*, 887, 195, doi: [10.3847/1538-4357/ab5856](https://doi.org/10.3847/1538-4357/ab5856)
- Melnick, J. 1980, *A&A*, 86, 304
- Messerschmitt, D. G. 2015, *Acta Astronautica*, 107, 20, doi: [10.1016/j.actaastro.2014.11.007](https://doi.org/10.1016/j.actaastro.2014.11.007)
- Meyer, L., Ghez, A. M., Schödel, R., et al. 2012, *Science*, 338, 84, doi: [10.1126/science.1225506](https://doi.org/10.1126/science.1225506)
- Meza, N., Prieto, J. L., Clocchiatti, A., et al. 2019, *A&A*, 629, A57, doi: [10.1051/0004-6361/201834972](https://doi.org/10.1051/0004-6361/201834972)
- Micheli, M., Farnocchia, D., Meech, K. J., et al. 2018, *Nature*, 559, 223, doi: [10.1038/s41586-018-0254-4](https://doi.org/10.1038/s41586-018-0254-4)
- Michilli, D., Seymour, A., Hessels, J. W. T., et al. 2018, *Nature*, 553, 182, doi: [10.1038/nature25149](https://doi.org/10.1038/nature25149)
- Mikulášek, Z., Krtička, J., Shultz, M. E., et al. 2019, arXiv e-prints, arXiv:1912.04121. <https://arxiv.org/abs/1912.04121>
- Miniutti, G., Saxton, R. D., Giustini, M., et al. 2019, *Nature*, 573, 381, doi: [10.1038/s41586-019-1556-x](https://doi.org/10.1038/s41586-019-1556-x)
- Molnar, L. A., Van Noord, D. M., Kinemuchi, K., et al. 2017, *ApJ*, 840, 1, doi: [10.3847/1538-4357/aa6ba7](https://doi.org/10.3847/1538-4357/aa6ba7)
- Montalto, M., Riffeser, A., Hopp, U., Wilke, S., & Carraro, G. 2008, *A&A*, 479, L45, doi: [10.1051/0004-6361:20079130](https://doi.org/10.1051/0004-6361:20079130)
- Montet, B. T., & Simon, J. D. 2016, *ApJL*, 830, L39, doi: [10.3847/2041-8205/830/2/L39](https://doi.org/10.3847/2041-8205/830/2/L39)
- Morgan, W. W., & Keenan, P. C. 1973, *ARA&A*, 11, 29, doi: [10.1146/annurev.aa.11.090173.000333](https://doi.org/10.1146/annurev.aa.11.090173.000333)
- Moskovitz, N. A., Lawrence, S., Jedicke, R., et al. 2008, *ApJL*, 682, L57, doi: [10.1086/591030](https://doi.org/10.1086/591030)
- Mucciarelli, A., Salaris, M., Lanzoni, B., et al. 2013, *ApJL*, 772, L27, doi: [10.1088/2041-8205/772/2/L27](https://doi.org/10.1088/2041-8205/772/2/L27)
- Murphy, T., Kaplan, D. L., Croft, S., et al. 2017, *MNRAS*, 466, 1944, doi: [10.1093/mnras/stw3087](https://doi.org/10.1093/mnras/stw3087)
- Nakashima, J.-i., Deguchi, S., Imai, H., Kembell, A., & Lewis, B. M. 2011, *ApJ*, 728, 76, doi: [10.1088/0004-637X/728/2/76](https://doi.org/10.1088/0004-637X/728/2/76)
- Naslim, N., Jeffery, C. S., Behara, N. T., & Hibbert, A. 2011, *MNRAS*, 412, 363, doi: [10.1111/j.1365-2966.2010.17909.x](https://doi.org/10.1111/j.1365-2966.2010.17909.x)
- Nemiroff, R. J. 1994, *Comments on Astrophysics*, 17, 189. <https://arxiv.org/abs/astro-ph/9402012>
- Nemiroff, R. J., & Shamir, L. 2006, *GRB Coordinates Network*, 4998, 1
- Niinuma, K., Asuma, K., Kuniyoshi, M., et al. 2007, *ApJL*, 657, L37, doi: [10.1086/512970](https://doi.org/10.1086/512970)
- Norris, R. P. 2017, *PASA*, 34, e007, doi: [10.1017/pasa.2016.63](https://doi.org/10.1017/pasa.2016.63)
- Ochsenbein, F., Bauer, P., & Marcout, J. 2000, *A&AS*, 143, 23, doi: [10.1051/aas:2000169](https://doi.org/10.1051/aas:2000169)
- Oesch, P. A., Brammer, G., van Dokkum, P. G., et al. 2016, *ApJ*, 819, 129, doi: [10.3847/0004-637X/819/2/129](https://doi.org/10.3847/0004-637X/819/2/129)
- Ofir, A., & Dreizler, S. 2013, *A&A*, 555, A58, doi: [10.1051/0004-6361/201219877](https://doi.org/10.1051/0004-6361/201219877)
- Ogle, P. M., Lanz, L., Appleton, P. N., Helou, G., & Mazzarella, J. 2019, *ApJS*, 243, 14, doi: [10.3847/1538-4365/ab21c3](https://doi.org/10.3847/1538-4365/ab21c3)
- Ogle, P. M., Lanz, L., Nader, C., & Helou, G. 2016, *ApJ*, 817, 109, doi: [10.3847/0004-637X/817/2/109](https://doi.org/10.3847/0004-637X/817/2/109)
- Ohno, M., Iwakiri, W., Suzuki, M., et al. 2009, *GRB Coordinates Network*, 9653, 1
- Olausen, S. A., & Kaspi, V. M. 2014, *ApJS*, 212, 6, doi: [10.1088/0067-0049/212/1/6](https://doi.org/10.1088/0067-0049/212/1/6)
- Orosz, J. A., & van Kerkwijk, M. H. 2003, *A&A*, 397, 237, doi: [10.1051/0004-6361:20021468](https://doi.org/10.1051/0004-6361:20021468)
- Ortiz, J. L., Duffard, R., Pinilla-Alonso, N., et al. 2015, *A&A*, 576, A18, doi: [10.1051/0004-6361/201424461](https://doi.org/10.1051/0004-6361/201424461)
- Osaki, Y. 1996, *PASP*, 108, 39, doi: [10.1086/133689](https://doi.org/10.1086/133689)
- Osmanov, Z. 2016, *International Journal of Astrobiology*, 15, 127, doi: [10.1017/S1473550415000257](https://doi.org/10.1017/S1473550415000257)
- Osterbrock, D. E. 1977, *ApJ*, 215, 733, doi: [10.1086/155407](https://doi.org/10.1086/155407)
- 'Oumuamua ISSI Team, Bannister, M. T., Bhandare, A., et al. 2019, *Nature Astronomy*, 3, 594, doi: [10.1038/s41550-019-0816-x](https://doi.org/10.1038/s41550-019-0816-x)
- Padovani, P., Alexander, D. M., Assef, R. J., et al. 2017, *A&A Rv*, 25, 2, doi: [10.1007/s00159-017-0102-9](https://doi.org/10.1007/s00159-017-0102-9)
- Page, D., Beznogov, M. V., Garibay, I., et al. 2020, arXiv e-prints, arXiv:2004.06078. <https://arxiv.org/abs/2004.06078>
- Pandey-Pommier, M., Richard, J., Combes, F., et al. 2013, *A&A*, 557, A117, doi: [10.1051/0004-6361/201321809](https://doi.org/10.1051/0004-6361/201321809)
- Papagiannis, M. D. 1978, *QJRAS*, 19, 277
- Patterson, J. 1994, *PASP*, 106, 209, doi: [10.1086/133375](https://doi.org/10.1086/133375)
- Paumard, T., Genzel, R., Martins, F., et al. 2006, *ApJ*, 643, 1011, doi: [10.1086/503273](https://doi.org/10.1086/503273)
- Pearl, J. C., Conrath, B. J., Hanel, R. A., Pirraglia, J. A., & Coustenis, A. 1990, *Icarus*, 84, 12, doi: [10.1016/0019-1035\(90\)90155-3](https://doi.org/10.1016/0019-1035(90)90155-3)
- Penny, A. J. 2013, *European Physical Journal H*, 38, 535, doi: [10.1140/epjh/e2012-30052-6](https://doi.org/10.1140/epjh/e2012-30052-6)
- Penzias, A. A., & Wilson, R. W. 1965, *ApJ*, 142, 419, doi: [10.1086/148307](https://doi.org/10.1086/148307)
- Perley, R. A., & Butler, B. J. 2017, *ApJS*, 230, 7, doi: [10.3847/1538-4365/aa6df9](https://doi.org/10.3847/1538-4365/aa6df9)
- Perryman, M. A. C., Lindegren, L., Kovalevsky, J., et al. 1997, *A&A*, 500, 501
- Peterson, B. M. 1997, *An Introduction to Active Galactic Nuclei*
- Petroff, E., Keane, E. F., Barr, E. D., et al. 2015, *MNRAS*, 451, 3933, doi: [10.1093/mnras/stv1242](https://doi.org/10.1093/mnras/stv1242)

- Petrovich, C., & Tremaine, S. 2016, *ApJ*, 829, 132, doi: [10.3847/0004-637X/829/2/132](https://doi.org/10.3847/0004-637X/829/2/132)
- Phifer, K., Do, T., Meyer, L., et al. 2013, *ApJL*, 773, L13, doi: [10.1088/2041-8205/773/1/L13](https://doi.org/10.1088/2041-8205/773/1/L13)
- Phinney, E. S., & Hansen, B. M. S. 1993, in *Astronomical Society of the Pacific Conference Series*, Vol. 36, *Planets Around Pulsars*, ed. J. A. Phillips, S. E. Thorsett, & S. R. Kulkarni, 371–390
- Pihlström, Y. M., Baan, W. A., Darling, J., & Klöckner, H. R. 2005, *ApJ*, 618, 705, doi: [10.1086/426098](https://doi.org/10.1086/426098)
- Pinchuk, P., Margot, J.-L., Greenberg, A. H., et al. 2019, *AJ*, 157, 122, doi: [10.3847/1538-3881/ab0105](https://doi.org/10.3847/1538-3881/ab0105)
- Piro, A. L., & Vissapragada, S. 2020, *AJ*, 159, 131, doi: [10.3847/1538-3881/ab7192](https://doi.org/10.3847/1538-3881/ab7192)
- Platts, E., Weltman, A., Walters, A., et al. 2019, *PhR*, 821, 1, doi: [10.1016/j.physrep.2019.06.003](https://doi.org/10.1016/j.physrep.2019.06.003)
- Plewa, P. M., Gillessen, S., Pfuhl, O., et al. 2017, *ApJ*, 840, 50, doi: [10.3847/1538-4357/aa6e00](https://doi.org/10.3847/1538-4357/aa6e00)
- Podsiadlowski, P. 1993, in *Astronomical Society of the Pacific Conference Series*, Vol. 36, *Planets Around Pulsars*, ed. J. A. Phillips, S. E. Thorsett, & S. R. Kulkarni, 149–165
- Porco, C. C., Baker, E., Barbara, J., et al. 2005, *Science*, 307, 1237, doi: [10.1126/science.1107981](https://doi.org/10.1126/science.1107981)
- Prentice, S. J., Maguire, K., Smartt, S. J., et al. 2018, *ApJL*, 865, L3, doi: [10.3847/2041-8213/aadd90](https://doi.org/10.3847/2041-8213/aadd90)
- Price, D. C., MacMahon, D. H. E., Lebofsky, M., et al. 2018, *PASA*, 35, 41, doi: [10.1017/pasa.2018.36](https://doi.org/10.1017/pasa.2018.36)
- Price, D. C., Foster, G., Geyer, M., et al. 2019a, *MNRAS*, 486, 3636, doi: [10.1093/mnras/stz958](https://doi.org/10.1093/mnras/stz958)
- Price, D. C., Croft, S., DeBoer, D., et al. 2019b, *Research Notes of the American Astronomical Society*, 3, 19, doi: [10.3847/2515-5172/ab010b](https://doi.org/10.3847/2515-5172/ab010b)
- Price, D. C., Enriquez, J. E., Brzycki, B., et al. 2020, *AJ*, 159, 86, doi: [10.3847/1538-3881/ab65f1](https://doi.org/10.3847/1538-3881/ab65f1)
- Prieto, J. L., Kistler, M. D., Thompson, T. A., et al. 2008, *ApJL*, 681, L9, doi: [10.1086/589922](https://doi.org/10.1086/589922)
- Proust, D., Quintana, H., Carrasco, E. R., et al. 2006, *A&A*, 447, 133, doi: [10.1051/0004-6361:20052838](https://doi.org/10.1051/0004-6361:20052838)
- Przybylski, A. 1961, *Nature*, 189, 739, doi: [10.1038/189739a0](https://doi.org/10.1038/189739a0)
- Pursimo, T., Galindo-Guil, F., Dennefeld, M., et al. 2019, *The Astronomer's Telegram*, 12911, 1
- Ramirez, R. M., & Kaltenecker, L. 2016, *ApJ*, 823, 6, doi: [10.3847/0004-637X/823/1/6](https://doi.org/10.3847/0004-637X/823/1/6)
- Rampadarath, H., Morgan, J. S., Tingay, S. J., & Trott, C. M. 2012, *AJ*, 144, 38, doi: [10.1088/0004-6256/144/2/38](https://doi.org/10.1088/0004-6256/144/2/38)
- Randall, S. K., Bagnulo, S., Ziegerer, E., Geier, S., & Fontaine, G. 2015, *A&A*, 576, A65, doi: [10.1051/0004-6361/201425251](https://doi.org/10.1051/0004-6361/201425251)
- Rappaport, S., Sanchis-Ojeda, R., Rogers, L. A., Levine, A., & Winn, J. N. 2013, *ApJL*, 773, L15, doi: [10.1088/2041-8205/773/1/L15](https://doi.org/10.1088/2041-8205/773/1/L15)
- Rappaport, S., Vanderburg, A., Kristiansen, M. H., et al. 2019, *MNRAS*, 488, 2455, doi: [10.1093/mnras/stz1772](https://doi.org/10.1093/mnras/stz1772)
- Reach, W. T., Vaubaillon, J., Lisse, C. M., Holloway, M., & Rho, J. 2010, *Icarus*, 208, 276, doi: [10.1016/j.icarus.2010.01.020](https://doi.org/10.1016/j.icarus.2010.01.020)
- Rees, M. J. 1977, *Nature*, 266, 333, doi: [10.1038/266333a0](https://doi.org/10.1038/266333a0)
- Reig, P. 2011, *Ap&SS*, 332, 1, doi: [10.1007/s10509-010-0575-8](https://doi.org/10.1007/s10509-010-0575-8)
- Relaño, M., & Kenicutt, Robert C., J. 2009, *ApJ*, 699, 1125, doi: [10.1088/0004-637X/699/2/1125](https://doi.org/10.1088/0004-637X/699/2/1125)
- Renzini, A., & Peng, Y.-j. 2015, *ApJL*, 801, L29, doi: [10.1088/2041-8205/801/2/L29](https://doi.org/10.1088/2041-8205/801/2/L29)
- Reynolds, T. M., Fraser, M., & Gilmore, G. 2015, *MNRAS*, 453, 2885, doi: [10.1093/mnras/stv1809](https://doi.org/10.1093/mnras/stv1809)
- Ribas, I., Tuomi, M., Reiners, A., et al. 2018, *Nature*, 563, 365, doi: [10.1038/s41586-018-0677-y](https://doi.org/10.1038/s41586-018-0677-y)
- Roberts, M. S. E. 2013, in *IAU Symposium*, Vol. 291, *Neutron Stars and Pulsars: Challenges and Opportunities after 80 years*, ed. J. van Leeuwen, 127–132, doi: [10.1017/S174392131202337X](https://doi.org/10.1017/S174392131202337X)
- Rodriguez, D. R., Zuckerman, B., Melis, C., & Song, I. 2011, *ApJL*, 732, L29, doi: [10.1088/2041-8205/732/2/L29](https://doi.org/10.1088/2041-8205/732/2/L29)
- Rogers, L. A. 2015, *ApJ*, 801, 41, doi: [10.1088/0004-637X/801/1/41](https://doi.org/10.1088/0004-637X/801/1/41)
- Roy, S., Hyman, S. D., Pal, S., et al. 2010, *ApJL*, 712, L5, doi: [10.1088/2041-8205/712/1/L5](https://doi.org/10.1088/2041-8205/712/1/L5)
- Russell, C. T., Raymond, C. A., Ammannito, E., et al. 2016, *Science*, 353, 1008, doi: [10.1126/science.aaf4219](https://doi.org/10.1126/science.aaf4219)
- Rutledge, R. E. 1998, *PASP*, 110, 754, doi: [10.1086/316184](https://doi.org/10.1086/316184)
- Sagan, C. 1994, *Pale blue dot : a vision of the human future in space Sagan*.
- Sagan, C., & Salpeter, E. E. 1976, *ApJS*, 32, 737, doi: [10.1086/190414](https://doi.org/10.1086/190414)
- Sagan, C., Thompson, W. R., Carlson, R., Gurnett, D., & Hord, C. 1993, *Nature*, 365, 715, doi: [10.1038/365715a0](https://doi.org/10.1038/365715a0)
- Sahai, R., & Nyman, L.-Å. 1997, *ApJL*, 487, L155, doi: [10.1086/310897](https://doi.org/10.1086/310897)
- Sahlholdt, C. L., Feltzing, S., Lindegren, L., & Church, R. P. 2019, *MNRAS*, 482, 895, doi: [10.1093/mnras/sty2732](https://doi.org/10.1093/mnras/sty2732)
- Saito, R. K., Minniti, D., Ivanov, V. D., et al. 2019, *MNRAS*, 482, 5000, doi: [10.1093/mnras/sty3004](https://doi.org/10.1093/mnras/sty3004)
- Salim, S. 2014, *Serbian Astronomical Journal*, 189, 1, doi: [10.2298/SAJ1489001S](https://doi.org/10.2298/SAJ1489001S)

- Salvetti, D., Mignani, R. P., De Luca, A., et al. 2017, *MNRAS*, 470, 466, doi: [10.1093/mnras/stx1247](https://doi.org/10.1093/mnras/stx1247)
- Sánchez-Monge, Á., Schilke, P., Schmiedeke, A., et al. 2017, *A&A*, 604, A6, doi: [10.1051/0004-6361/201730426](https://doi.org/10.1051/0004-6361/201730426)
- Sanders, D. B., Mazzarella, J. M., Kim, D. C., Surace, J. A., & Soifer, B. T. 2003, *AJ*, 126, 1607, doi: [10.1086/376841](https://doi.org/10.1086/376841)
- Sandoval, M. A., Vo, R. P., Romanowsky, A. J., et al. 2015, *ApJL*, 808, L32, doi: [10.1088/2041-8205/808/1/L32](https://doi.org/10.1088/2041-8205/808/1/L32)
- Santerne, A., Malavolta, L., Kosiarek, M. R., et al. 2019, arXiv e-prints, arXiv:1911.07355. <https://arxiv.org/abs/1911.07355>
- Sato, B., Izumiura, H., Toyota, E., et al. 2007, *ApJ*, 661, 527, doi: [10.1086/513503](https://doi.org/10.1086/513503)
- Savage, B. D., Massa, D., Meade, M., & Wesselius, P. R. 1985, *ApJS*, 59, 397, doi: [10.1086/191078](https://doi.org/10.1086/191078)
- Sazhin, M., Longo, G., Capaccioli, M., et al. 2003, *MNRAS*, 343, 353, doi: [10.1046/j.1365-8711.2003.06568.x](https://doi.org/10.1046/j.1365-8711.2003.06568.x)
- Schaefer, B. E. 2010, *ApJS*, 187, 275, doi: [10.1088/0067-0049/187/2/275](https://doi.org/10.1088/0067-0049/187/2/275)
- . 2016, *ApJL*, 822, L34, doi: [10.3847/2041-8205/822/2/L34](https://doi.org/10.3847/2041-8205/822/2/L34)
- Schaefer, B. E., Barber, M., Brooks, J. J., et al. 1987, *ApJ*, 320, 398, doi: [10.1086/165552](https://doi.org/10.1086/165552)
- Schawinski, K., Urry, C. M., Simmons, B. D., et al. 2014, *MNRAS*, 440, 889, doi: [10.1093/mnras/stu327](https://doi.org/10.1093/mnras/stu327)
- Scheffer, L. K. 1994, *QJRAS*, 35, 157
- Schmidt, G. A., & Frank, A. 2019, *International Journal of Astrobiology*, 18, 142, doi: [10.1017/S1473550418000095](https://doi.org/10.1017/S1473550418000095)
- Schmidt, G. D., West, S. C., Liebert, J., Green, R. F., & Stockman, H. S. 1986, *ApJ*, 309, 218, doi: [10.1086/164593](https://doi.org/10.1086/164593)
- Schmidt, M. 1963, *Nature*, 197, 1040, doi: [10.1038/1971040a0](https://doi.org/10.1038/1971040a0)
- Schmiedeke, A., Schilke, P., Möller, T., et al. 2016, *A&A*, 588, A143, doi: [10.1051/0004-6361/201527311](https://doi.org/10.1051/0004-6361/201527311)
- Schneider, J., Dedieu, C., Le Sidaner, P., Savalle, R., & Zolotukhin, I. 2011, *A&A*, 532, A79, doi: [10.1051/0004-6361/201116713](https://doi.org/10.1051/0004-6361/201116713)
- Scholz, P., & Chime/Frb Collaboration. 2020, *The Astronomer's Telegram*, 13681, 1
- Scholz, R. D., Lehmann, I., Matute, I., & Zinnecker, H. 2004, *A&A*, 425, 519, doi: [10.1051/0004-6361:20041059](https://doi.org/10.1051/0004-6361:20041059)
- Schreiber, C., Labbé, I., Glazebrook, K., et al. 2018, *A&A*, 611, A22, doi: [10.1051/0004-6361/201731917](https://doi.org/10.1051/0004-6361/201731917)
- Sequist, E. R., & Odegard, N. 1991, *ApJ*, 369, 320, doi: [10.1086/169764](https://doi.org/10.1086/169764)
- Secrest, N. J., Schmitt, H. R., Blecha, L., Rothberg, B., & Fischer, J. 2017, *ApJ*, 836, 183, doi: [10.3847/1538-4357/836/2/183](https://doi.org/10.3847/1538-4357/836/2/183)
- Semiz, İ., & Oğur, S. 2015, arXiv e-prints, arXiv:1503.04376. <https://arxiv.org/abs/1503.04376>
- Seth, A. C., van den Bosch, R., Mieske, S., et al. 2014, *Nature*, 513, 398, doi: [10.1038/nature13762](https://doi.org/10.1038/nature13762)
- Shamir, L., & Nemiroff, R. J. 2006, *PASP*, 118, 1180, doi: [10.1086/506989](https://doi.org/10.1086/506989)
- Shara, M. M., Prialnik, D., Hillman, Y., & Kovetz, A. 2018, *ApJ*, 860, 110, doi: [10.3847/1538-4357/aabfbd](https://doi.org/10.3847/1538-4357/aabfbd)
- Sheikh, S. Z. 2019, arXiv e-prints, arXiv:1908.02683. <https://arxiv.org/abs/1908.02683>
- Sheikh, S. Z., Siemion, A., Enriquez, J. E., et al. 2020, arXiv e-prints, arXiv:2002.06162. <https://arxiv.org/abs/2002.06162>
- Shen, K. J., Boubert, D., Gänsicke, B. T., et al. 2018, *ApJ*, 865, 15, doi: [10.3847/1538-4357/aad55b](https://doi.org/10.3847/1538-4357/aad55b)
- Shostak, S. 2004, in *IAU Symposium, Vol. 213, Bioastronomy 2002: Life Among the Stars*, ed. R. Norris & F. Stootman, 409
- Shostak, S., Ekers, R., & Vaile, R. 1996, *AJ*, 112, 164, doi: [10.1086/117996](https://doi.org/10.1086/117996)
- Sidoli, L., Israel, G. L., Esposito, P., Rodríguez Castillo, G. A., & Postnov, K. 2017, *MNRAS*, 469, 3056, doi: [10.1093/mnras/stx1105](https://doi.org/10.1093/mnras/stx1105)
- Siemion, A., Von Korff, J., McMahon, P., et al. 2010, *Acta Astronautica*, 67, 1342, doi: [10.1016/j.actaastro.2010.01.016](https://doi.org/10.1016/j.actaastro.2010.01.016)
- Siemion, A. P. V., Bower, G. C., Foster, G., et al. 2012, *ApJ*, 744, 109, doi: [10.1088/0004-637X/744/2/109](https://doi.org/10.1088/0004-637X/744/2/109)
- Sigurdsson, S., & Thorsett, S. E. 2005, *Astronomical Society of the Pacific Conference Series, Vol. 328, Update on Pulsar B1620-26 in M4: Observations, Models, and Implications*, ed. F. A. Rasio & I. H. Stairs, 213
- Simon, J. D. 2019, *ARA&A*, 57, 375, doi: [10.1146/annurev-astro-091918-104453](https://doi.org/10.1146/annurev-astro-091918-104453)
- Simon, J. D., Drlica-Wagner, A., Li, T. S., et al. 2015, *ApJ*, 808, 95, doi: [10.1088/0004-637X/808/1/95](https://doi.org/10.1088/0004-637X/808/1/95)
- Sivakoff, G. R., Sarazin, C. L., & Jordán, A. 2005, *ApJL*, 624, L17, doi: [10.1086/430374](https://doi.org/10.1086/430374)
- Skrutskie, M. F., Cutri, R. M., Stiening, R., et al. 2006, *AJ*, 131, 1163, doi: [10.1086/498708](https://doi.org/10.1086/498708)
- Smette, A. 2006, *GRB Coordinates Network*, 4997, 1
- Smiljanic, R., Pasquini, L., Primas, F., et al. 2008, *MNRAS*, 385, L93, doi: [10.1111/j.1745-3933.2008.00440.x](https://doi.org/10.1111/j.1745-3933.2008.00440.x)
- Smith, K. L., Mushotzky, R. F., Boyd, P. T., et al. 2018, *ApJ*, 857, 141, doi: [10.3847/1538-4357/aab88d](https://doi.org/10.3847/1538-4357/aab88d)
- Snowden, S. L., Cox, D. P., McCammon, D., & Sanders, W. T. 1990, *ApJ*, 354, 211, doi: [10.1086/168680](https://doi.org/10.1086/168680)
- Socia, Q. J., Welsh, W. F., Short, D. R., et al. 2018, *ApJL*, 864, L32, doi: [10.3847/2041-8213/aad0d](https://doi.org/10.3847/2041-8213/aad0d)

- Sokolovsky, K. V., Aydi, E., Chomiuk, L., et al. 2019, *The Astronomer's Telegram*, 13377, 1
- Solarz, A., Bilicki, M., Gromadzki, M., et al. 2017, *A&A*, 606, A39, doi: [10.1051/0004-6361/201730968](https://doi.org/10.1051/0004-6361/201730968)
- Song, X., Walton, D. J., Lansbury, G. B., et al. 2020, *MNRAS*, 491, 1260, doi: [10.1093/mnras/stz3036](https://doi.org/10.1093/mnras/stz3036)
- Soubiran, C., Le Campion, J.-F., Brouillet, N., & Chemin, L. 2016, *A&A*, 591, A118, doi: [10.1051/0004-6361/201628497](https://doi.org/10.1051/0004-6361/201628497)
- Speagle, J. S., Steinhardt, C. L., Capak, P. L., & Silverman, J. D. 2014, *ApJS*, 214, 15, doi: [10.1088/0067-0049/214/2/15](https://doi.org/10.1088/0067-0049/214/2/15)
- Spezzi, L., Beccari, G., De Marchi, G., et al. 2011, *ApJ*, 731, 1, doi: [10.1088/0004-637X/731/1/1](https://doi.org/10.1088/0004-637X/731/1/1)
- Spitler, L. G., Scholz, P., Hessels, J. W. T., et al. 2016, *Nature*, 531, 202, doi: [10.1038/nature17168](https://doi.org/10.1038/nature17168)
- Stanek, K. Z., Kochanek, C. S., Bersier, D., et al. 2019, *The Astronomer's Telegram*, 12794, 1
- Stefanescu, A., Kanbach, G., Słowikowska, A., et al. 2008, *Nature*, 455, 503, doi: [10.1038/nature07308](https://doi.org/10.1038/nature07308)
- Stern, S. A., Grundy, W. M., McKinnon, W. B., Weaver, H. A., & Young, L. A. 2018, *ARA&A*, 56, 357, doi: [10.1146/annurev-astro-081817-051935](https://doi.org/10.1146/annurev-astro-081817-051935)
- Stevenson, D. J. 1999, *Nature*, 400, 32, doi: [10.1038/21811](https://doi.org/10.1038/21811)
- Stewart, A. J., Fender, R. P., Broderick, J. W., et al. 2016, *MNRAS*, 456, 2321, doi: [10.1093/mnras/stv2797](https://doi.org/10.1093/mnras/stv2797)
- Stock, S., Reffert, S., & Quirrenbach, A. 2018, *A&A*, 616, A33, doi: [10.1051/0004-6361/201833111](https://doi.org/10.1051/0004-6361/201833111)
- Strateva, I., Ivezić, Ž., Knapp, G. R., et al. 2001, *AJ*, 122, 1861, doi: [10.1086/323301](https://doi.org/10.1086/323301)
- Struve, O. 1952, *The Observatory*, 72, 199
- Su, M., Slatyer, T. R., & Finkbeiner, D. P. 2010, *ApJ*, 724, 1044, doi: [10.1088/0004-637X/724/2/1044](https://doi.org/10.1088/0004-637X/724/2/1044)
- Sullivan, M., Kasliwal, M. M., Nugent, P. E., et al. 2011, *ApJ*, 732, 118, doi: [10.1088/0004-637X/732/2/118](https://doi.org/10.1088/0004-637X/732/2/118)
- Swihart, S. J., Garcia, E. V., Stassun, K. G., et al. 2017, *AJ*, 153, 16, doi: [10.3847/1538-3881/153/1/16](https://doi.org/10.3847/1538-3881/153/1/16)
- Szapudi, I., Kovács, A., Granett, B. R., et al. 2015, *MNRAS*, 450, 288, doi: [10.1093/mnras/stv488](https://doi.org/10.1093/mnras/stv488)
- Tachihara, K., Gratier, P., Sano, H., et al. 2018, *PASJ*, 70, S52, doi: [10.1093/pasj/psy020](https://doi.org/10.1093/pasj/psy020)
- Takeda, G., Ford, E. B., Sills, A., et al. 2007, *ApJS*, 168, 297, doi: [10.1086/509763](https://doi.org/10.1086/509763)
- Tan, C. M., Bassa, C. G., Cooper, S., et al. 2018, *ApJ*, 866, 54, doi: [10.3847/1538-4357/aade88](https://doi.org/10.3847/1538-4357/aade88)
- Tarter, J. 2001, *ARA&A*, 39, 511, doi: [10.1146/annurev.astro.39.1.511](https://doi.org/10.1146/annurev.astro.39.1.511)
- Tavani, M., Bulgarelli, A., Vittorini, V., et al. 2011, *Science*, 331, 736, doi: [10.1126/science.1200083](https://doi.org/10.1126/science.1200083)
- Taylor, B. J. 2006, *MNRAS*, 368, 1880, doi: [10.1111/j.1365-2966.2006.10267.x](https://doi.org/10.1111/j.1365-2966.2006.10267.x)
- Teague, R., Bae, J., Bergin, E. A., Birnstiel, T., & Foreman-Mackey, D. 2018, *ApJL*, 860, L12, doi: [10.3847/2041-8213/aac6d7](https://doi.org/10.3847/2041-8213/aac6d7)
- Tedesco, E. F., Williams, J. G., Matson, D. L., et al. 1989, *AJ*, 97, 580, doi: [10.1086/115007](https://doi.org/10.1086/115007)
- The CHIME/FRB Collaboration, Amiri, M., Andersen, B. C., et al. 2020, arXiv e-prints, arXiv:2001.10275, <https://arxiv.org/abs/2001.10275>
- Tholen, D. J. 1984, PhD thesis, University of Arizona, Tucson
- Thompson, C. 2017, *ApJ*, 844, 162, doi: [10.3847/1538-4357/aa7845](https://doi.org/10.3847/1538-4357/aa7845)
- Thompson, T. A., Kochanek, C. S., Stanek, K. Z., et al. 2019, *Science*, 366, 637, doi: [10.1126/science.aau4005](https://doi.org/10.1126/science.aau4005)
- Tiengo, A., Mignani, R. P., de Luca, A., et al. 2011, *MNRAS*, 412, L73, doi: [10.1111/j.1745-3933.2011.01009.x](https://doi.org/10.1111/j.1745-3933.2011.01009.x)
- Tingay, S. J., Tremblay, C., Walsh, A., & Urquhart, R. 2016, *ApJL*, 827, L22, doi: [10.3847/2041-8205/827/2/L22](https://doi.org/10.3847/2041-8205/827/2/L22)
- Tingay, S. J., Tremblay, C. D., & Croft, S. 2018a, *ApJ*, 856, 31, doi: [10.3847/1538-4357/aab363](https://doi.org/10.3847/1538-4357/aab363)
- Tingay, S. J., Goeke, R., Bowman, J. D., et al. 2013, *PASA*, 30, e007, doi: [10.1017/pasa.2012.007](https://doi.org/10.1017/pasa.2012.007)
- Tingay, S. J., Kaplan, D. L., Lenc, E., et al. 2018b, *ApJ*, 857, 11, doi: [10.3847/1538-4357/aab359](https://doi.org/10.3847/1538-4357/aab359)
- Tisserand, P., Le Guillou, L., Afonso, C., et al. 2007, *A&A*, 469, 387, doi: [10.1051/0004-6361:20066017](https://doi.org/10.1051/0004-6361:20066017)
- Titov, O., Jauncey, D. L., Johnston, H. M., Hunstead, R. W., & Christensen, L. 2011, *AJ*, 142, 165, doi: [10.1088/0004-6256/142/5/165](https://doi.org/10.1088/0004-6256/142/5/165)
- Toba, Y., Wang, W.-H., Nagao, T., et al. 2020, *ApJ*, 889, 76, doi: [10.3847/1538-4357/ab616d](https://doi.org/10.3847/1538-4357/ab616d)
- Tokovinin, A. 2018, *ApJS*, 235, 6, doi: [10.3847/1538-4365/aaa1a5](https://doi.org/10.3847/1538-4365/aaa1a5)
- Torrealba, G., Belokurov, V., Koposov, S. E., et al. 2019, *MNRAS*, 488, 2743, doi: [10.1093/mnras/stz1624](https://doi.org/10.1093/mnras/stz1624)
- Tramper, F., Straal, S. M., Sanyal, D., et al. 2015, *A&A*, 581, A110, doi: [10.1051/0004-6361/201425390](https://doi.org/10.1051/0004-6361/201425390)
- Trevisan, M., Barbay, B., Eriksson, K., et al. 2011, *A&A*, 535, A42, doi: [10.1051/0004-6361/201016056](https://doi.org/10.1051/0004-6361/201016056)
- Trujillo, C. A., & Sheppard, S. S. 2014, *Nature*, 507, 471, doi: [10.1038/nature13156](https://doi.org/10.1038/nature13156)
- Trujillo, I., Ferré-Mateu, A., Balcels, M., Vazdekis, A., & Sánchez-Blázquez, P. 2014, *ApJL*, 780, L20, doi: [10.1088/2041-8205/780/2/L20](https://doi.org/10.1088/2041-8205/780/2/L20)
- Trundle, C., Dufton, P. L., Rolleston, W. R. J., et al. 2001, *MNRAS*, 328, 291, doi: [10.1046/j.1365-8711.2001.04872.x](https://doi.org/10.1046/j.1365-8711.2001.04872.x)
- Tsai, C.-W., Eisenhardt, P. R. M., Jun, H. D., et al. 2018, *ApJ*, 868, 15, doi: [10.3847/1538-4357/aae698](https://doi.org/10.3847/1538-4357/aae698)

- Tucker, W., Blanco, P., Rappoport, S., et al. 1998, *ApJL*, 496, L5, doi: [10.1086/311234](https://doi.org/10.1086/311234)
- Tully, R. B., Courtois, H., Hoffman, Y., & Pomarède, D. 2014, *Nature*, 513, 71, doi: [10.1038/nature13674](https://doi.org/10.1038/nature13674)
- Turnbull, M. C., & Tarter, J. C. 2003, *ApJS*, 145, 181, doi: [10.1086/345779](https://doi.org/10.1086/345779)
- Umetsu, K., Broadhurst, T., Zitrin, A., Medezinski, E., & Hsu, L.-Y. 2011, *ApJ*, 729, 127, doi: [10.1088/0004-637X/729/2/127](https://doi.org/10.1088/0004-637X/729/2/127)
- Urry, C. M., & Padovani, P. 1995, *PASP*, 107, 803, doi: [10.1086/133630](https://doi.org/10.1086/133630)
- Uson, J. M., Boughn, S. P., & Kuhn, J. R. 1991, *ApJ*, 369, 46, doi: [10.1086/169737](https://doi.org/10.1086/169737)
- van de Kamp, P. 1963, *AJ*, 68, 515, doi: [10.1086/109001](https://doi.org/10.1086/109001)
- van den Bergh, S. 1976, *ApJ*, 206, 883, doi: [10.1086/154452](https://doi.org/10.1086/154452)
- van den Bosch, R. C. E., Gebhardt, K., Gültekin, K., et al. 2012, *Nature*, 491, 729, doi: [10.1038/nature11592](https://doi.org/10.1038/nature11592)
- van Haften, L. M., Maccarone, T. J., Rhode, K. L., Kundu, A., & Zepf, S. E. 2019, *MNRAS*, 483, 3566, doi: [10.1093/mnras/sty3221](https://doi.org/10.1093/mnras/sty3221)
- van Haarlem, M. P., Wise, M. W., Gunst, A. W., et al. 2013, *A&A*, 556, A2, doi: [10.1051/0004-6361/201220873](https://doi.org/10.1051/0004-6361/201220873)
- van Kerkwijk, M. H., Breton, R. P., & Kulkarni, S. R. 2011, *ApJ*, 728, 95, doi: [10.1088/0004-637X/728/2/95](https://doi.org/10.1088/0004-637X/728/2/95)
- van Weeren, R. J., de Gasperin, F., Akamatsu, H., et al. 2019, *SSRv*, 215, 16, doi: [10.1007/s11214-019-0584-z](https://doi.org/10.1007/s11214-019-0584-z)
- van Weeren, R. J., Röttgering, H. J. A., Brügger, M., & Cohen, A. 2009, *A&A*, 508, 75, doi: [10.1051/0004-6361/200912501](https://doi.org/10.1051/0004-6361/200912501)
- VandenBerg, D. A., Bond, H. E., Nelan, E. P., et al. 2014, *ApJ*, 792, 110, doi: [10.1088/0004-637X/792/2/110](https://doi.org/10.1088/0004-637X/792/2/110)
- Varghese, S. S., Obenberger, K. S., Dowell, J., & Taylor, G. B. 2019, *ApJ*, 874, 151, doi: [10.3847/1538-4357/ab07c6](https://doi.org/10.3847/1538-4357/ab07c6)
- VERITAS Collaboration, Acciari, V. A., Aliu, E., et al. 2009, *Nature*, 462, 770, doi: [10.1038/nature08557](https://doi.org/10.1038/nature08557)
- Vidal, C. 2011, arXiv e-prints, arXiv:1104.4362. <https://arxiv.org/abs/1104.4362>
- Vilenius, E., Stansberry, J., Müller, T., et al. 2018, *A&A*, 618, A136, doi: [10.1051/0004-6361/201732564](https://doi.org/10.1051/0004-6361/201732564)
- Villarroel, B., Imaz, I., & Bergstedt, J. 2016, *AJ*, 152, 76, doi: [10.3847/0004-6256/152/3/76](https://doi.org/10.3847/0004-6256/152/3/76)
- Villarroel, B., Soodla, J., Comerón, S., et al. 2020, *AJ*, 159, 8, doi: [10.3847/1538-3881/ab570f](https://doi.org/10.3847/1538-3881/ab570f)
- Vinkó, J., Yuan, F., Quimby, R. M., et al. 2015, *ApJ*, 798, 12, doi: [10.1088/0004-637X/798/1/12](https://doi.org/10.1088/0004-637X/798/1/12)
- Vogt, S. S., Radovan, M., Kibrick, R., et al. 2014, *PASP*, 126, 359, doi: [10.1086/676120](https://doi.org/10.1086/676120)
- Voros, J. 2014, ArXiv e-prints. <https://arxiv.org/abs/1412.4011>
- Vos, J., Zorotovic, M., Vučković, M., Schreiber, M. R., & Østensen, R. 2018, *MNRAS*, 477, L40, doi: [10.1093/mnrasl/sly050](https://doi.org/10.1093/mnrasl/sly050)
- Wagner-Kaiser, R., De Maio, T., Sarajedini, A., & Chakrabarti, S. 2014, *MNRAS*, 443, 3260, doi: [10.1093/mnras/stu1327](https://doi.org/10.1093/mnras/stu1327)
- Walborn, N. R., Howarth, I. D., Lennon, D. J., et al. 2002, *AJ*, 123, 2754, doi: [10.1086/339831](https://doi.org/10.1086/339831)
- Walker, G. A. H. 2012, *NewAR*, 56, 9, doi: [10.1016/j.newar.2011.06.001](https://doi.org/10.1016/j.newar.2011.06.001)
- Wang, Q. D., Li, J., Russell, C. M. P., & Cuadra, J. 2020, *MNRAS*, 492, 2481, doi: [10.1093/mnras/stz3624](https://doi.org/10.1093/mnras/stz3624)
- Wang, T., Elbaz, D., Daddi, E., et al. 2016, *ApJ*, 828, 56, doi: [10.3847/0004-637X/828/1/56](https://doi.org/10.3847/0004-637X/828/1/56)
- Way, Z., Stanek, K. Z., Kochanek, C. S., et al. 2019a, *The Astronomer's Telegram*, 13346, 1
- Way, Z., Jayasinghe, T., Stanek, K. Z., et al. 2019b, *The Astronomer's Telegram*, 13106, 1
- Weekes, T. C., Badran, H., Biller, S. D., et al. 2002, *Astroparticle Physics*, 17, 221, doi: [10.1016/S0927-6505\(01\)00152-9](https://doi.org/10.1016/S0927-6505(01)00152-9)
- Weinreb, S., Barrett, A. H., Meeks, M. L., & Henry, J. C. 1963, *Nature*, 200, 829, doi: [10.1038/200829a0](https://doi.org/10.1038/200829a0)
- Weiss, L. M., & Marcy, G. W. 2014, *ApJL*, 783, L6, doi: [10.1088/2041-8205/783/1/L6](https://doi.org/10.1088/2041-8205/783/1/L6)
- Wenger, M., Ochsenbein, F., Egret, D., et al. 2000, *A&AS*, 143, 9, doi: [10.1051/aas:2000332](https://doi.org/10.1051/aas:2000332)
- Werner, K., & Rauch, T. 2015, *A&A*, 584, A19, doi: [10.1051/0004-6361/201527261](https://doi.org/10.1051/0004-6361/201527261)
- Wesson, P. S. 1990, *QJRAS*, 31, 161
- Whitmire, D. P., & Wright, D. P. 1980, *Icarus*, 42, 149, doi: [10.1016/0019-1035\(80\)90253-5](https://doi.org/10.1016/0019-1035(80)90253-5)
- Wickramasinghe, D. T., & Ferrario, L. 2000, *PASP*, 112, 873, doi: [10.1086/316593](https://doi.org/10.1086/316593)
- Wilkinson, P. 2016, in *Astronomical Society of the Pacific Conference Series*, Vol. 502, *Frontiers in Radio Astronomy and FAST Early Sciences Symposium 2015*, ed. L. Qain & D. Li, 87
- Wilkinson, P. N., Kellermann, K. I., Ekers, R. D., Cordes, J. M., & W. Lazio, T. J. 2004, *NewAR*, 48, 1551, doi: [10.1016/j.newar.2004.09.036](https://doi.org/10.1016/j.newar.2004.09.036)
- Williams, R. E., Blacker, B., Dickinson, M., et al. 1996, *AJ*, 112, 1335, doi: [10.1086/118105](https://doi.org/10.1086/118105)
- Wilson-Hodge, C. A., Cherry, M. L., Case, G. L., et al. 2011, *ApJL*, 727, L40, doi: [10.1088/2041-8205/727/2/L40](https://doi.org/10.1088/2041-8205/727/2/L40)
- Wing, R. F. 2009, *Astronomical Society of the Pacific Conference Series*, Vol. 412, *The Biggest Stars of All*, ed. D. G. Luttermoser, B. J. Smith, & R. E. Stencel, 113
- Wing, R. F., Peimbert, M., & Spinrad, H. 1967, *PASP*, 79, 351, doi: [10.1086/128496](https://doi.org/10.1086/128496)

- Wittkowski, M., Arroyo-Torres, B., Marcaide, J. M., et al. 2017, *A&A*, 597, A9, doi: [10.1051/0004-6361/201629349](https://doi.org/10.1051/0004-6361/201629349)
- Wolf, C., Bian, F., Onken, C. A., et al. 2018, *PASA*, 35, e024, doi: [10.1017/pasa.2018.22](https://doi.org/10.1017/pasa.2018.22)
- Wolszczan, A. 2012, *NewAR*, 56, 2, doi: [10.1016/j.newar.2011.06.002](https://doi.org/10.1016/j.newar.2011.06.002)
- Wolszczan, A., & Frail, D. A. 1992, *Nature*, 355, 145, doi: [10.1038/355145a0](https://doi.org/10.1038/355145a0)
- Woosley, S. E., & Heger, A. 2015, *ApJ*, 810, 34, doi: [10.1088/0004-637X/810/1/34](https://doi.org/10.1088/0004-637X/810/1/34)
- Worden, S. P., Drew, J., Siemion, A., et al. 2017, *Acta Astronautica*, 139, 98, doi: [10.1016/j.actaastro.2017.06.008](https://doi.org/10.1016/j.actaastro.2017.06.008)
- Wordsworth, R. D. 2016, *Annual Review of Earth and Planetary Sciences*, 44, 381, doi: [10.1146/annurev-earth-060115-012355](https://doi.org/10.1146/annurev-earth-060115-012355)
- Wright, J. T. 2018a, *Research Notes of the American Astronomical Society*, 2, 16, doi: [10.3847/2515-5172/aaa83e](https://doi.org/10.3847/2515-5172/aaa83e)
- . 2018b, *International Journal of Astrobiology*, 17, 96, doi: [10.1017/S1473550417000143](https://doi.org/10.1017/S1473550417000143)
- Wright, J. T., Cartier, K. M. S., Zhao, M., Jontof-Hutter, D., & Ford, E. B. 2016, *ApJ*, 816, 17, doi: [10.3847/0004-637X/816/1/17](https://doi.org/10.3847/0004-637X/816/1/17)
- Wright, J. T., Kanodia, S., & Lubar, E. 2018, *AJ*, 156, 260, doi: [10.3847/1538-3881/aae099](https://doi.org/10.3847/1538-3881/aae099)
- Wright, J. T., & Sigurdsson, S. 2016, *ApJL*, 829, L3, doi: [10.3847/2041-8205/829/1/L3](https://doi.org/10.3847/2041-8205/829/1/L3)
- Wu, J., Evans, Neal J., I., Shirley, Y. L., & Knez, C. 2010, *ApJS*, 188, 313, doi: [10.1088/0067-0049/188/2/313](https://doi.org/10.1088/0067-0049/188/2/313)
- Wyder, T. K., Martin, D. C., Schiminovich, D., et al. 2007, *ApJS*, 173, 293, doi: [10.1086/521402](https://doi.org/10.1086/521402)
- Yates, J. S., Palmer, P. I., Biller, B., & Cockell, C. S. 2017, *ApJ*, 836, 184, doi: [10.3847/1538-4357/836/2/184](https://doi.org/10.3847/1538-4357/836/2/184)
- Yuan, T., Richard, J., Gupta, A., et al. 2017, *ApJ*, 850, 61, doi: [10.3847/1538-4357/aa951d](https://doi.org/10.3847/1538-4357/aa951d)
- Yusef-Zadeh, F., Morris, M., & Chance, D. 1984, *Nature*, 310, 557, doi: [10.1038/310557a0](https://doi.org/10.1038/310557a0)
- Zackrisson, E., Calissendorff, P., Asadi, S., & Nyholm, A. 2015, *ApJ*, 810, 23, doi: [10.1088/0004-637X/810/1/23](https://doi.org/10.1088/0004-637X/810/1/23)
- Zackrisson, E., Korn, A. J., Wehrhahn, A., & Reiter, J. 2018, *ApJ*, 862, 21, doi: [10.3847/1538-4357/aac386](https://doi.org/10.3847/1538-4357/aac386)
- Zhang, B., Reid, M. J., Menten, K. M., Zheng, X. W., & Brunthaler, A. 2012, *A&A*, 544, A42, doi: [10.1051/0004-6361/201219587](https://doi.org/10.1051/0004-6361/201219587)
- Zhang, Y. G., Won, K. H., Son, S. W., Siemion, A., & Croft, S. 2019, arXiv e-prints, arXiv:1901.04636. <https://arxiv.org/abs/1901.04636>
- Zhou, G., Bakos, G. Á., Hartman, J. D., et al. 2017, *AJ*, 153, 211, doi: [10.3847/1538-3881/aa674a](https://doi.org/10.3847/1538-3881/aa674a)
- Zuckerman, B., & Song, I. 2004, *ARA&A*, 42, 685, doi: [10.1146/annurev.astro.42.053102.134111](https://doi.org/10.1146/annurev.astro.42.053102.134111)